1974

Sediment transport processes in a salt marsh drainage system

John Daniel Boon III
College of William and Mary - Virginia Institute of Marine Science

SEDIMENT TRANSPORT PROCESSES IN A SALT MARSH DRAINAGE SYSTEM

A Dissertation

Presented to

The Faculty of the School of Marine Science

The College of William and Mary in Virginia

In Partial Fulfillment

Of the Requirements for the Degree of

Doctor of Philosophy

---

by

John D. Boon, III, M.A.

1973

APPROVAL SHEET

This dissertation is submitted in partial fulfillment of the requirements for the degree of

Doctor of Philosophy

John D. Boon, III
Author

Approved, December 1973

Robert J. Byrne

John M. Zeigler

Maynard M. Nichols

Albert Y. Kuo

Paul V. Hyer

Christopher S. Welch

John B. Thomas
Geology Dept., College of
William & Mary

Marvin L. Wass

TABLE OF CONTENTS

ACKNOWLEDGMENTS

Special thanks are given to Dr. Robert J. Byrne, the author's principal advisor, who, through his patient rendering of advice and guidance during the past three years, is largely responsible for whatever success this paper may enjoy. The author is also indebted to Drs. Bick, Harrison, Hyer, Kuo, Nichols, Wass, Welch, and Zeigler for their help and constructive criticism during the initial planning of the work at the Virginia Institute of Marine Science (VIMS).

Dr. Blair Kinsman of the Smithsonian Institution suggested the use of recent Fast Fourier Transform procedures in the analysis of tidal data; Dr. Christopher Welch of VIMS kindly assisted the author in implementing the analysis and in interpreting the results.

Laboratory analyses of water samples were conducted by Mrs. Jean Watkinson of Wachapreague, Virginia. Appreciation is expressed to Mr. Michael Castagna, scientist-in-charge of VIMS Eastern Shore Laboratory, for making the necessary facilities available in Wachapreague, in addition to sharing his extensive knowledge of the local environment.

The onerous task of intensive sample collecting during long hours in the marsh was shared by the following persons

to whom the author is indeed grateful, both for their assistance and for their cheerful company: C. Hobbs, D. Tyler, G. Anderson, E. Hogge, D. Byrd, S. Byrd, M. Holt, J. Sovich, D. Stauble, A. Sallenger, J. DeAlteris, and P. Rosen.

Funds for the support of this work were provided by the Research Applied to National Needs (RANN) program of the National Science Foundation (NSF) through grant GI 29909, Virginia Institute of Marine Science, FY 1972 and grant GI 34869, Chesapeake Research Consortium, Inc., FY 1973. Additional support was provided in part by NSF Doctoral Dissertation Grant GA 28545 during the period May, 1971, through October, 1972.

LIST OF TABLES

LIST OF FIGURES

LIST OF FIGURES (Cont'd.)

LIST OF FIGURES (Cont'd.)

ABSTRACT

Transport of fine-grained suspended solids of both organic and inorganic origin occurs in salt marsh drainage systems through the action of tidally-induced open channel flow. The movement of this material is of importance to geologists who wish to understand how marshes may have evolved and to biologists investigating the production and export of marsh detritus as a source of food for organisms. The complex nature of this type of transport system makes difficult the interpretation of those patterns and mechanisms of transport which result in net movement of materials into or out of the marsh proper. Consequently, a detailed study has been undertaken in a typical salt marsh creek near Wachapreague, Virginia, with a twofold purpose: (1) to determine with some accuracy the flux of material past a stream cross-section at the entrance to a closed channel network draining a definable area of marsh, (2) to investigate those processes which tend to cause a residual transport of suspended solids during various times of the year in marsh channels.

Results indicate that fairly detailed sampling in both space and time is required to obtain more than casual estimates of residual transport, even as regards the direction, in small marsh creeks. Among the most important factors governing the level of transport are: (1) the annual water temperature cycle which modulates the amount of erosion and turbulent suspension of cohesive bottom sediments, (2) an annual cycle in steric sea level which produces significant variations in the frequency of occurrence of the higher discharge volumes entering and leaving the marsh (an index of flushing activity), (3) wind stress effects. Other factors considered important in terms of residual transport are: (1) observed asymmetries in time-varying current speed maxima caused primarily by marsh and channel topographic form and, to a lesser extent, shallow water tides, (2) heat exchange processes on the marsh during individual tidal cycles, (3) advective processes acting between marshes and adjacent bays and tidal flats.

The tentative interpretation made of the data at hand holds that the small channels incising the marsh are, on balance, a conveyance for net removal of sediment having a fairly consistent composition, 10-15% of which is combustible organic material. The source of most of the sediment

is to be found at the heads of the first-order channel segments while some deposition does occur along the main channel levees. Other avenues of transport, for example along the outer marsh perimeter, should be explored to account for the continuing vertical growth of the marsh. In addition, the effects of storm related events remain open to question.

SEDIMENT TRANSPORT PROCESSES IN A SALT MARSH DRAINAGE SYSTEM

INTRODUCTION

The purpose of this study is to investigate a number of the dynamic processes operating in a typical salt marsh drainage system and to evaluate their importance in terms of sediment transport. This type of drainage network forms a basic transportation link for sediments moving between the marsh proper, itself a creation of sedimentary processes, and the larger bodies of water adjacent to the marsh. Since the alternating tidal flow within marsh channels transports particulate matter of both organic and inorganic origin in both inner (flood) and outer (ebb) directions relative to the marsh, some of the basic questions which confront the investigator are:

1) What processes act to achieve a net transport of sediment in either direction via the channel network; i.e., which are marsh constructive and which are marsh destructive?

2) Where are sediments most likely to be deposited within a marsh; where are they most likely to erode?

3) What is the composition of the material in transit in terms of organic and inorganic constituents? How do these constituents respond to the transport process when considered separately?

4) What seasonal or long-term trends can be observed in patterns of marsh sediment transport? What are the implications regarding the evolution of the marsh?

Answers to these questions are as yet incomplete. Because of the complex nature of water and sediment movement in and around marshes, it is difficult to model the behavior of any isolated segment of the transport system. On a given day, the marsh drainage system may appear as a common example of an open channel flow regime at one stage of the tide and an example of an inundated flood plain at another stage.

In this work, the author's main objective has been that of obtaining answers to questions (1) through (4) by undertaking a detailed study of sediments and sediment transport processes in a single, closed-channel drainage network; i.e., one whose uppermost tributaries end on the marsh within a drainage basin of discernible form at all but the highest stages of the tide. Examples of this type of system are fairly common in marsh environments and the results obtained should have general applicability.

The assumption is made that most of the sediment in transit within the region of study is carried in suspension and not as bedload in view of the cohesive nature of the sediments in the marsh channels. Interparticle bonds in fine, cohesive sediments normally yield only to tractive forces that are sufficient to place individual particles or their aggregates directly into suspension.

The primary measurements required to achieve the stated objectives are those necessary to compute suspended sediment flux (dry mass per unit time) past a stream cross section at

the entrance to the marsh drainage network. The flux at any point in time will be obtained as the product of cross-sectional average current speed, cross-sectional average suspended sediment concentration, and cross-sectional area. Time-integration of the curve of suspended sediment flux over complete tidal cycles then yields the residual (non-tidal) transport as the difference between flood and ebb suspended sediment transport. Residual transports, having magnitude and direction (into or out of the marsh), are an important factor in the sedimentary budget of the marsh.

In practice, the success of the above procedure depends heavily on proper instrumentation and methods used in measuring current speed and suspended sediment concentration. Care must be exercised both in obtaining these measures and in computing their space-time averages in the stream cross-section. The instrumentation and methods adopted by the present author are therefore described in a separate section. Error analysis and experimental design are discussed in an adjoining section.

REVIEW OF PREVIOUS STUDIES

Development of Salt Marshes and Salt Marsh Drainage Channels

Salt marshes are characterized by fine sediment accumulations in protected shallow-water marine environments with limited river inflow and an associated biota attuned to varying degrees of salt water submergence (Chapman, 1960). Guilcher (1958) described the detailed history of marshes as "extremely complicated" but observed that they often derive their form from deposition in areas drowned by transgressing seas. A key feature was observed by Mudge (in Johnson, 1925); namely, that relatively great thicknesses of marsh peat of the variety formed by plants growing at or near high water level must indicate a progressive submergence and accompanying buildup of the marsh facies.

Redfield (1965), in a classic paper, presented a detailed study of an isolated salt marsh in Cape Cod, Massachusetts. According to him, the process of marsh development begins with a protected embayment having a shallow, sandy bottom and proceeds to a stage where mud flats accumulate along the periphery due to siltation at a rate equal to or in excess of submergence. The mud flats are eventually elevated above low tide level and migrating drainage basins are formed in them where local depressions

exist. Once sufficient periods of subaerial exposure are achieved, pioneer vegetation (in this case Spartina alterniflora) takes root in scattered areas and causes accelerated deposition due to the tendency of the roots and stems to trap sediments and reduce the erosive power of currents. This zone of vegetation extends over the upper two-thirds of the intertidal region and is designated low marsh. The initial colonies of plants exist in isolated patches but these later converge through lateral growth into continuous marsh cover. Behind the advance of low marsh, deposition in the established areas results in vertical growth so that succeeding plants (Spartina patens, Distichlis spicata and others) form the high marsh zone of vegetation near the level of mean high tide. High marsh zones are characterized by a flat and level appearance and may have considerable extent. Living high marsh vegetation is only intermittently covered by the higher tides.

A number of investigators have described processes by which marsh channels may form and develop. Although common elements in these processes were recognized, general agreement on their importance has not been reached.

Redfield (1965, pp. 113-114) observed that tidal flat embayments contained drainage channels that were more or less free to meander in the unconsolidated fine sands and muds of the flats, but that marsh vegetation tended to advance over these flats and converge on the channel so that they eventually attained an essentially fixed areal

configuration within the marsh.

Chapman (1960, pp. 29-32) and Steers (1964, pp. 518, 523) noted a similar origin for marsh channels and creeks in the British Isles, but also mentioned that these channels may become blocked through bank undercutting to form stagnant channel pans or may actually grow headward by a process of erosion. However, Steers (1964, p. 525) concluded that such erosion was "... in the opinion of the writer, a distinctly secondary process in creek formation as compared with the upward building on developing marshes."

Chapman (1960, p. 31) described three separate phases of creek development: 1) an active youthful phase when head erosion may occur concomitant with rapid marsh accretion and creek deepening, 2) a mature phase with further accretion accompanied by extensive lateral erosion through undercutting, 3) a senile phase when vegetation predominates and portions are successively cut from the head of the creek to form pans, or may cover the creek entirely so that drainage runs underground (small tributaries only; main creeks remaining open).

A recent study of marsh drainage systems in the Lower San Francisco Bay area by Pestrong (1965) described a distinctive difference in flow relationships between the upper and lower tributaries. Small upper tributaries were observed to have unidirectional flow suggestive of terrestrial streams whereas the larger seaward channels demonstrated an alternating flow typical of tidal regimes.

The underlying cause of this effect seems unclear. Pestrong concluded that the small channels have geomorphic characteristics similar to those of terrestrial streams and gullies including, it is presumed, headward erosion toward higher elevations.

Concerning the vertical growth caused by sediment accumulation on marshes, Chapman (1960, pp. 35-44) and Steers (1964, pp. 526-535) obtained measurements showing that different portions of English marshes possessed a distinctive variety of growth rates. Typically, sedimentation rates were highest on low marshes and lowest on high marshes, with maximum rates occurring near large creeks and minimal rates occurring along the highest portions of the marsh. This differentiation was attributed to the tendency of a marsh to accumulate sediments slowly until a thick spread of vegetation had been established, then to progress vertically at a rapid rate until the amount of tidal flooding falls off and a much reduced accumulation ensues.

Chapman (1960, p. 43), from studies of a marsh near Boston, Massachusetts, estimated that 490 years were required for a 5 ft. section of low marsh to accumulate whereas 600 years were required for a 1.5 ft. section of high marsh peat to accumulate.

Transport Processes in Marsh and Tidal Flat Environments

Among the most noted studies dealing with processes of suspended sediment transport were those carried out in the Dutch Wadden Sea by Postma (1954, 1961, 1967) and by

Van Straaten and Kuenen (1957, 1958). The principle concern of these investigators was the identification of the source of large volumes of fine sediment deposited within the extensive intertidal regions of this body. A gradient in the concentration of fine-grained suspended matter, decreasing from the inner portions of the Wadden Sea towards the North Sea tidal inlets, was observed which was maintained in the face of strong tidal flushing and which could not be explained by marsh or tidal flat erosion or river inflow. Thus, for the gradient to be maintained, a net landward transport of suspended sediment from the North Sea was required.

A mechanism for net suspended sediment transport landward in the Wadden Sea was put forth by the above authors incorporating the effects of settling lag and scouring lag. Briefly, the mechanism may be explained by following a hypothetical water mass during a tidal cycle. As the water mass moves landward at the onset of flood current, sediment moves with it, maintained in suspension by the turbulence associated with the flow. When the velocity decreases near the end of flood, a point is reached at which the sediment particles will begin to settle; however, the particles do not reach bottom immediately, but continue landward some distance before deposition (settling lag). At the onset of ebb, a significantly greater velocity is required to resuspend the particles than to maintain suspension, whereupon there is a delay in entrainment

(scouring lag) and the unit water mass which eventually carries the particles seaward is not the original mass but one that has come from farther landward than the original. The combined effect is augmented by an assumed linear decrease in average tidal current strength landward.

Groen (1967, p. 565) pointed out several shortcomings in the settling lag - scouring lag concept, primarily noting that one cannot treat individual water masses and sediment particles as being constrained in their behavior by the mean water velocity at any point. In reality, the statistical behavior of a large population of suspended particles is determined by the mean current speed and attendant levels of turbulence. Groen then developed a mathematical model of suspended sediment transport in alternating tidal flows which took note of the observed distortion in flow curves as compared to the nearly sinusoidal shape of the tide curve. The main consequence of this distortion was that maximum flow velocities were not evenly distributed within the tidal cycle; i.e., an asymmetry exists in the position of these maxima with respect to the times of slack water. Groen's model was intended for tidal flat channels in which maximum current strengths occur shortly before and after the low water slack portion of the cycle. Given simulated flow curves and a quadratic formula for sediment load as a function of velocity, the model predicted that the onset of flood would be immediately preceded by a period of higher current velocities (with higher turbulence and suspended

load) than would precede the onset of ebb, resulting in a net landward transport of suspended sediment over the complete tidal cycle. Groen stated that differences of as much as 38% between flood and ebb transport might occur with no net discharge of water.

It is apparently not the case, however, that all tidal channels demonstrate a current asymmetry which would favor landward transport as in Groen's analysis. Velocity curves for marsh creeks entering the Potomac River in Virginia (Myrick and Leopold, 1963, p. B12) and in the San Francisco Bay area (Pestrong, 1965, p. 19) show asymmetries in which the ebb phase is preceded by higher velocities, maximum current strengths occurring one to two hours before and after the high water stage.

Apart from phenomenological descriptions of concentration and velocity (e.g., the various "lag" effects), there have been few field studies to date that involve actual measurements of suspended solids transport in marshes. De La Cruz (1965), in a study of particulate organic detritus in the salt marshes of Georgia, calculated the transport of this material in a small tidal creek. Although primarily an ecological study, his work represents perhaps the first attempt at quantifying net transport per tidal cycle. Regrettably, there is little description of hydraulic factors in the study and the results are seemingly compromised by this omission.

DESCRIPTION OF STUDY AREA

The area selected for study is situated in the marshland adjacent to Wachapreague, Virginia, on the seaward side of the Delmarva Peninsula (Figure 1). The area is covered by USGS Wachapreague Quadrangle Map N 3730-W75. The general physiography of the region consists of barrier islands fronting the Atlantic Ocean, behind which are lagoons consisting of shallow bays and mud flats dissected by tidal channels, and marshes which are drained by a large number of tidal creeks. The barrier islands are broken by a regular series of tidal inlets which connect to the main tidal channels landward. The lagoons are met by low-lying uplands to the west.

The Holocene geologic history of the Wachapreague area was treated in papers by Newman and Rusnak (1965) and Newman and Munsart (1968). Briefly, it can be stated that the Wachapreague lagoonal complex was probably formed some 5,100 years ago and has undergone varying rates of submergence up to the present. Newman and Munsart (op. cit., p. 98) noted that either crustal downwarping or decreased sedimentation rates may have caused a delay in marsh development until about 1,000 years B.P. in contrast to New England areas where marsh development began some 3,000

Figure 1. Location map, Wachapreague area, showing location of study creek and tide stations.

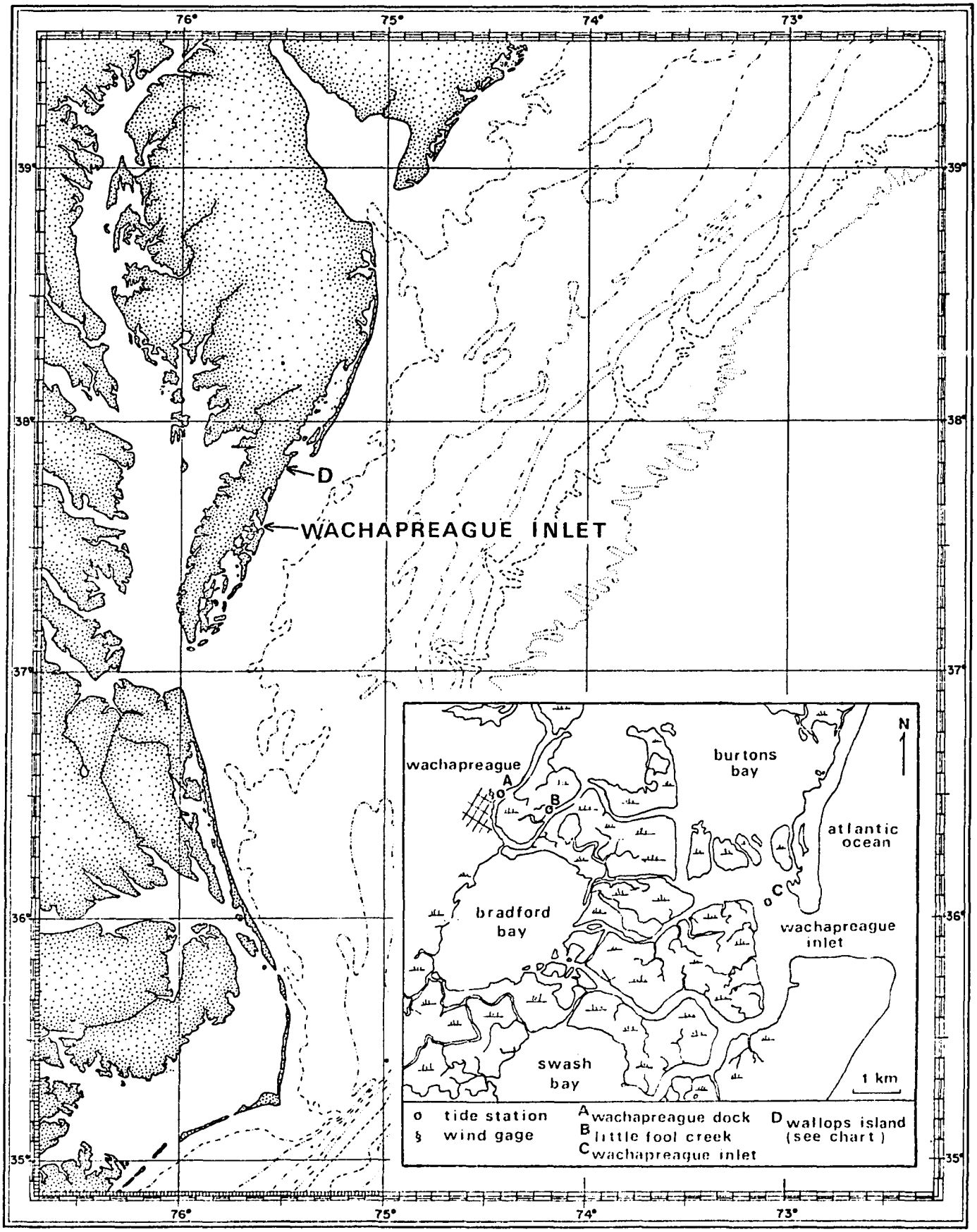

years B.P. Harrison and others (1965, p. 227) have postulated that late Pleistocene uplift occurred in the vicinity of the present Virginia Capes from about 15,000 to 8,000 years B.P., followed by crustal downwarping from 6,000 to 2,000 years B.P. with a resumption of uplift from then until the present time. At present, sea level rise relative to the land is about 0.011 feet (3.4 mm) per year (Hicks and Shofnos, 1965).

Modification of the natural state of the marshes, tidal channels and creeks has been minimal compared to other areas. With the exception of those main channel segments belonging to the intracoastal waterway, little dredging has been conducted here and the bulk of the interior channels appear quite stable as evidenced by a comparison of old and recent aerial photographs. There are no major sources of fresh water inflow anywhere in the area.

The site selected for study was a small marsh channel near the town of Wachapreague, Virginia (Figure 1), which has been designated Little Fool Creek. Several small tributaries, each of which originates on the upper marsh surface, are joined to the main channel of this creek. The entire network comprises a single closed system which drains a well-defined area of marsh. The creek is perhaps intermediate in size compared to the hundreds of similar channels which enter the marshes, having a width of 12 m near the mouth where the depth is a little more than 1 m below the creek banks. Three bridges were built across the

creek at selected locations to provide measurement platforms.

INSTRUMENTATION AND METHODS

Ducted Current Speed Sensor

Current speeds were measured using a fast-response, ducted-impeller type sensor. A detailed description of this instrument has been presented elsewhere (Byrne and Boon, 1973). Calibration of the instrument indicated a highly linear response to axial flows in the range 0-150 cm/sec with a threshold speed of about 1.5 cm/sec, making this a very suitable instrument for use in small tidal creeks where bidirectional, nonsteady flows often contain sharp temporal and spatial gradients.

Normally, an array of sensors was used to make simultaneous measurements of flow speed in the channel cross-section while rigidly mounted in a supporting apparatus.

Suspended Sediment Sampler

A streamlined tube of approximately 400 ml capacity was used to obtain water samples for suspended sediment analyses. The sampler is rigidly mounted to a support frame and features an air-operated valve which is actuated by remote control to obtain the sample *in situ* (Figure 2). The sampler, which has design characteristics similar to a Prandtl tube, collects water at a rate that is proportional

Figure 2. Schematic drawing of gas-operated water sampler showing method of deployment in a tidal stream.

DISCHARGE-SUSPENDED SEDIMENT SAMPLER

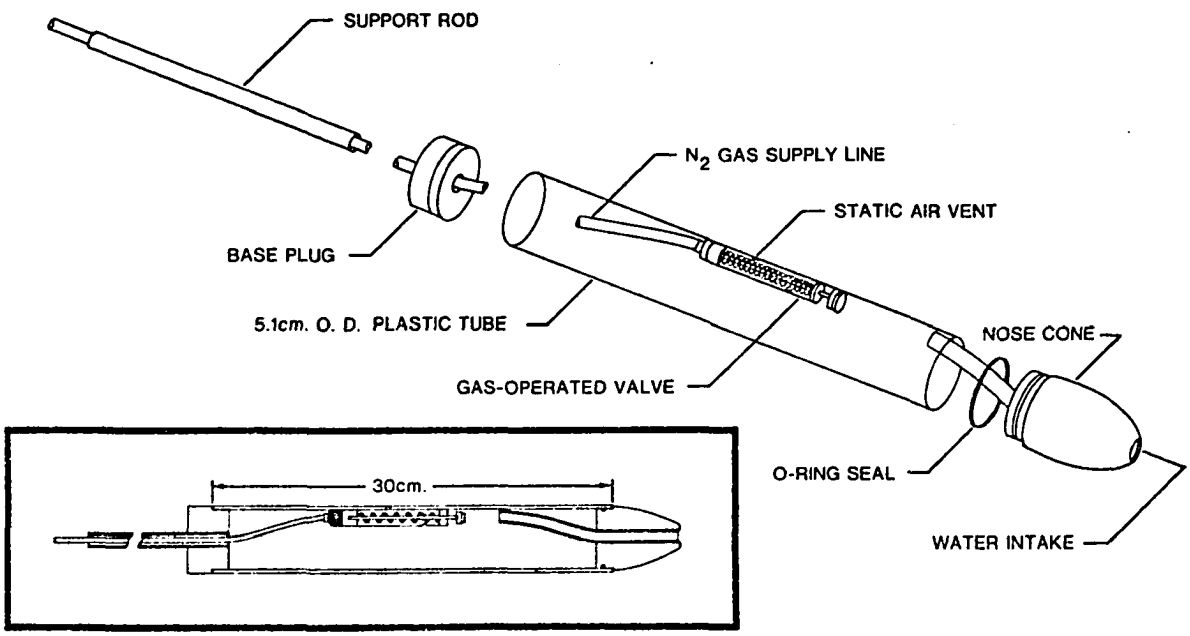

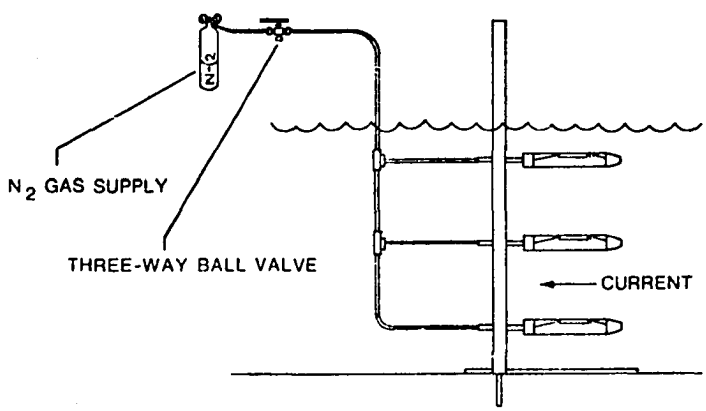

to the free stream velocity. An array of the samplers could be operated simultaneously in the cross-section to collect point water samples during an interval of about 100 seconds. Samples were transferred to pint Mason jars and stored under refrigeration at the end of each experiment.

Laboratory Analyses

Water samples were filtered *in toto* using preweighed General Electric Nuclepore filters having a pore-size of 0.6μ. The filters and sediments were dried at 80°C, then weighed on a Cahn DTL Millibalance capable of rapid measurement to the nearest 0.1 mg. Concentrations were then computed as the dry weight of sediment divided by the volume of water filtered, expressed in mg/1.

To test the precision of the method, duplicate analyses were initially performed using paired subsamples of about 400 ml each, taken from a large carboy of creek water. The subsample pairs were obtained as splits of 800 ml samples of the creek water using a Folsom sample splitter. Results indicated an average analytical error of 3.1% for five pairs of subsamples having a mean concentration of 29.4 mg/1.

Ashing of the samples to determine the amount of combustible material in each was done in a Thermolyne series 1600 furnace at 550°C. Sediment and filter were weighed, then placed in aluminum foil liners molded to fit inside small covered porcelain crucibles. Blank liners and crucibles were heated along with those containing the

samples for a period of one hour. After heating, the liners were allowed to cool, then weighed again. Use of these liners allowed the more sensitive scale of the millibalance to be utilized in obtaining the combustibles weight as the difference in liner plus contents weight before and after heating. The blank liners showed no weight changes in excess of 0.1 mg.

Dessicants were not used in any of the above procedures due to the rapid gain in moisture content of dessicated samples upon removal from their containers (Eaton, et al., 1969). The room in which weighing was done was equipped with a dehumidifier to give some uniformity to moisture levels in the samples. Static electricity effects were reduced through the use of a Staticmaster (alpha-emitting polonium source, Nuclear Products Co.).

Marsh Topographic Survey

To define the topographic relief and hypsometry of the marsh and drainage channel network comprising Little Fool Creek, a combined photogrammetric-plane table survey was made. Near-vertical aerial photographs were taken at various tidal stages using 35 mm black and white infrared film. The pictures were taken from a light plane at a 2,000 ft. (610 m) altitude.

Black and white infrared photographs show even very shallow areas of water as a black expanse. Waterlines within the marshes themselves can thus be fairly well

defined (Figures 11, 13 and 14). Three measured baselines within the study area (between the bridges, Figure 11) allowed scale and distortion effects to be evaluated in each photograph whose water areas could then be obtained by planimetry. The time at which each photograph was taken could be matched with records of tidal height data to obtain height above mean low water corresponding to a given measurement of area.

A plane table survey using a K & E self-leveling alidade provided both the baseline lengths on the ground and several check points of ground elevation that could be identified in the photographs to verify water surface heights. All elevations are given in terms of MLW datum which was transferred to a tide staff on the bridge nearest the mouth of the creek (Little Fool No. 1) using the method of simultaneous comparisons (Boon and Lynch, 1972, pp. 20-25).

MEASUREMENT ERROR ANALYSIS AND EXPERIMENTAL DESIGN

Transport at a Stream Cross-Section

If the distributions of longitudinal current speed (u) and suspended sediment concentration (c) were both steady and completely uniform throughout a cross-section of the flow having fixed dimensions, the transport of suspended matter (mass per unit time) could be easily determined using the equation

$$q_s = uc \times \text{area of cross-section}$$

In reality, all three terms on the right side of this equation are variables; the first two vary both spatially and temporally, the area varying only with time at one location. The usual practice is then to take averages of these quantities. This should be done first of all with a proper sampling design containing enough sample points to attain accurate estimates of each variable average. In addition, there are constraints on the manner in which the averages are used. This is particularly important as regards the transport per unit area, uc, as will now be shown.

Both u and c may be represented at any point in the cross-section at some instant by the local values

$$u = [u] - u'$$

$$c = [c] - c'$$

where the brackets denote a spatial average for a finite number of points and the primes denote the local deviation from the average. Taking the product

$$uc = [u]\,[c] - u'[c] - c'[u] + u'c'$$

and averaging over all points,

$$[uc] = [u]\,[c] + [u'c'] \qquad (1)$$

since $[u'], [c'] = 0$. The last expression reveals that the average of uc in the cross-section is equal to the product of u and c, each averaged separately, only if the correlation term, $[u'c']$, is zero. If significant spatial gradients exist in both the u and the c distributions, this will not be the case and $[u'c']$ may be considered to be the spatial correlation error when using $[u]\,[c]$ as an approximation of $[uc]$.

In a similar fashion, the instantaneous values of $[u]$ and $[c]$ may be given as

$$[u] = \overline{[u]} - [u]'$$

$$[c] = \overline{[c]} - [c]'$$

where the bars denote time averages for a finite number of points in time and the primes signify deviations of the spatial averages from the space-time means. Substitution

in Equation (1) gives

$$[uc] = (\overline{[u]} - [u]')\,(\overline{[c]} - [c]') + [u'c']$$

Averaging over all time points,

$$\overline{[uc]} = \overline{[u]}\;\overline{[c]} = \overline{[u]'[c]'} + \overline{[u'c']} \qquad (2)$$

so that a time correlation term, $\overline{[u]'[c]'}$, appears in addition to the average spatial correlation term, $\overline{[u'c']}$.

Equation (2) illustrates the following fact: If, during a given tidal cycle, one measured the concentration of some constituent and determined its space-time average in some way for the entire cycle, this average could not be multiplied by the average discharge for the cycle (the tidal prism divided by the cycle duration) without risking errors due to both space and time correlation effects.

To determine the possible extent of these various errors, the author conducted a presurvey of simultaneous u and c distributions in the stream cross-section at Bridge 1, Little Fool Creek. The results of the presurvey have been given in a previous report (Boon, 1972) which will be treated here as a detailed summary.

Vertical Distribution of Current Speed

A series of measurements of longitudinal current speed were made using seven current meters arranged at different depths in the channel center on a fixed vertical support. Resulting current profiles appeared logarithmic for fully

developed flow in the lower half of the water column, the current usually decreasing above this point toward the surface. This type of profile is typical of open-channel flows in which the depression of the point of maximum speed is due to the action of secondary currents (Henderson, 1966, p. 88).

Average current speeds were determined from 48 separate profiles by integrating their curves from surface to bottom. Speeds occurring at 0.2, 0.6, and 0.8 of the depth below the surface were then picked from each curve to be used as single point and two point estimates of mean speed, computed as $u_{0.6}$ and $\frac{1}{2}(u_{0.2} + u_{0.8})$ respectively. Using single point estimates, the deviations from the integrated means were often higher than 20% for speeds less than 10 cm/sec but usually less than 10% for greater speeds. Two point estimates were about 10% off for the lower speeds and no more than 5% off at speeds higher than 10 cm/sec. Experience indicates that the latter are likely to be the more significant speeds in terms of total discharge except during neap tide conditions.

Transverse Distribution of Current Speed

As a basis for sampling, the author chose to adopt Harlacher's method (see Troskolansky, 1960, p. 56) which divides the flow section into several vertical compartments each having a width b and a height h. The total rate of flow is then computed as

$$q = \sum u_{im} h_i b_i$$

where u_{im} is the mean flow in the ith compartment. The average speed for the entire cross-section is then

$$[u] = \frac{q}{\Sigma h_i b_i}$$

Guided by this type of sampling design, the stream was divided into one, two, and four compartments. Transverse current speed profiles were determined using seven current meters placed at equal intervals across the stream at about 0.2 of the depth below the surface. Speed estimates were then picked off the profiles at the mid-point of each compartment. Using these values as approximations of u_{im}, estimates of [u] were computed by the above formulas. Comparing these estimates with the corresponding means derived by integrating the profiles, the following difference percentages were obtained (average of 6 runs):

one compartment - 12.4%

two compartment - 8.7%

four compartment - 2.7%

These data serve to show the improvement realized by sampling at more than one point in the transverse flow profile. The conclusion reached was that, during transport runs, a total of eight current meters should be used, two in each of four compartments at the 0.2, 0.8 depths. Since the compartmenting procedure is actually a form of stratified sampling, which is conducive of reduced sampling error, the

overall error estimate placed on significant magnitudes of [u] is taken to be about the same as that of an individual two-point average in the vertical, roughly 5%.

Vertical Distribution of Concentration

Theoretical formulations such as Rouse's equation (see Graf, 1971) consider that suspended sediment distributions in steady flow represent a balance between gravitational settling and turbulent diffusion expressed as

$$v_s c = -\epsilon_s \frac{\partial c}{\partial y} \qquad (3)$$

where v_s is particle settling velocity and ϵ_s is a mass transfer coefficient. The difficulty in using this approach is twofold: Firstly, cohesive marsh sediments consist of complex soil aggregates and organic detritus. Concentrations (dry mass per unit volume) are not as consistent as those which would be found for ideal particles of uniform size, shape and density. Secondly, the variation of ϵ_s with depth is not well known for flows having nonuniform turbulence distributions.

Measured concentration profiles were plotted on semilog paper with normalized depths, y/h, being entered on the abscissa (normal) axis. These plots, except for a certain amount of random scattering, appeared to be linear in each of sixteen runs using seven samplers distributed evenly from near the surface to within 5 cm of the bottom. This kind of distribution suggests a log-linear relationship of the form

$$\ln c = b(y/h) + \ln a$$

or

$$c = a e^{b(y/h)} \qquad (4)$$

where a and b are constants representing the ordinate axis intercept and the curve slope, respectively. Equation (4) may be derived from Equation (3) by integration wherein $b = -v_s/\epsilon_s$ and $a = c_o$, the concentration expected at the intercept.

In most turbulent flows, ϵ_s is a function of depth. Equation (4) is not strictly valid in such instances because its derivation depends on the ratio v_s/ϵ_s being constant. But fine-grained suspended sediments have low v_s values which may themselves vary with depth, little being known of the particle size, shape, and density distributions in marsh creeks. The data seem to justify the use of Equation (4) in place of more complex formulations in describing vertical distributions of c in the present case.

It can be shown that, for slopes less than 0.5, the average concentration for a vertical distribution given by Equation (4) will be found near mid-depth. Since a simple formula like Equation (4) easily lends itself to least squares methods of curve fitting, concentration measurements taken at various known depths can be used to determine the curve of best fit and the average concentration obtained from this curve at mid-depth. Selecting three water

samplers evenly spaced in the water column, out of the seven used to determine the profile, the above method produced error estimates for mean concentration of about 5%.

Transverse Distribution of Concentration

Several runs were made to determine the extent of transverse concentration gradients. In each case, the observed concentrations were nearly uniform across the channel except for those very near the channel walls. Three samplers placed with the current meters in each of the four compartments previously mentioned should then give an estimate of [c] of 5% or less.

Spatial Correlation Effects

Vertical and transverse profiles from simultaneous concentration and current speed runs were used to estimate the spatial correlation error term [u'c']. The errors were found to be less than 2% for the vertical and less than 1% for the transverse direction, due to the relative uniformity of the concentrations. The flux, q_s, at any given time could then be computed as $\sum_{i=1}^{4} [u]_i [c]_i h_i b_i$ for the whole cross-section without appreciable correlation error.

Temporal Distributions of u and c

Measurements of [u] and [c], closely spaced in time, were impossible to obtain. Time series measurements of u and c at a fixed point in the cross-section were made

instead. The water sampler required approximately 100 seconds to operate while various time intervals could be applied in obtaining a current speed reading. The principle of operation of both devices is such that an integrated average of current speed and concentration is obtained. This type of average then applies as a discrete measurement value at the time central to the integration interval.

Temporal sampling errors were investigated by picking values at discrete intervals of time (the sampling interval) and comparing their averages as the sampling interval was increased from 2 to 60 minutes over a six hour period (half tidal cycle). Using this arrangement, a marked change was noted for current averages obtained with a sampling interval greater than about 40 minutes. The optimum interval appeared to be around 30 minutes. Averages for this interval differed by about 3% from the averages using 2 minute intervals. Concentration averages were less consistent but did not indicate more than a 7% change for sampling intervals varying between 5 and 30 minutes. See Run 6, Appendix A, for an example of discharge measures using both a 15-minute and a 30-minute sampling interval.

Temporal Correlation Effects

Since both current speed and concentration can be as easily determined at the same points in time as through any other means, there is little reason to compute total transport as $\overline{[u]}\ \overline{[c]}$ (Eq. 2). Experience indicates that sharp increases in both [c] and [u] often occur during

periods of maximum discharge, hence the temporal correlation error, $\overline{[u]'[c]'}$, is probably significant during most runs. Clearly the most expedient answer is to obtain temporal transport averages as $\overline{[u]\,[c]}$, i.e., the time-average of the product of spatial averages for u and c, which eliminates temporal correlation error.

Combined Error Propagation

If an error estimate of 5% is placed on both [u] and [c], the error of their product may be found as

$$E = \sqrt{(.05)^2 + (.05)^2}$$
$$= 0.07 \text{ or } 7\%$$

provided that the contributing estimates involve only random errors. The latter assumption is probably valid here since the estimates were obtained by synoptic sampling amid changing spatial distributions of u and c. Furthermore, if the time-varying product, [u] [c], could be considered as an example of a random, stationary process, then the space-time transport mean, $\overline{[u]\,[c]}$, would have a 7% error reduced by the factor $1/\sqrt{N}$ where N is the number of measurements made through time. Tidal flows are not stationary, however, and any reduction of the 7% estimate would be difficult to justify by formal means.

Assuming no error associated with the measurement of cross-sectional area, the error estimates for total transport of water and sediment during a given tidal phase are

placed at 5% and 7%, respectively.

Final Experimental Design

Based on the above findings, the final sampling configuration at the cross-section of Bridge 1 is as shown in Figure 3. Here the cross-section is dimensioned by a grid system whose origin occurs in the lower left corner of the figure (flood flow comes out of the plane of the paper). The surface reference for this grid is a level string attached at fixed points under the bridge, from which depth measurements were made. These measurements, along with tidal height data, were transferred to an arbitrary datum a set distance below the string. From this datum, all height measurements appear as positive coordinate values. The samples obtained are identifiable as items in a sample matrix whose actual positions are given in terms of grid coordinates.

The advantage to this type of measurement configuration is realized through computerized data processing techniques. Field personnel were supplied with special IBM coding forms on which all the necessary field measurement information was entered with a minimum risk of operator error. A similar form was issued to laboratory personnel whose analyses were also standardized. The only element in common on the two forms were the sample bottle numbers which permitted matching of all forms of data in the computer. Printouts of velocity and discharge values could usually be obtained one or two days after each run, transport values requiring about

Figure 3. Sampling configuration used at Bridge 1, Little Fool Creek.

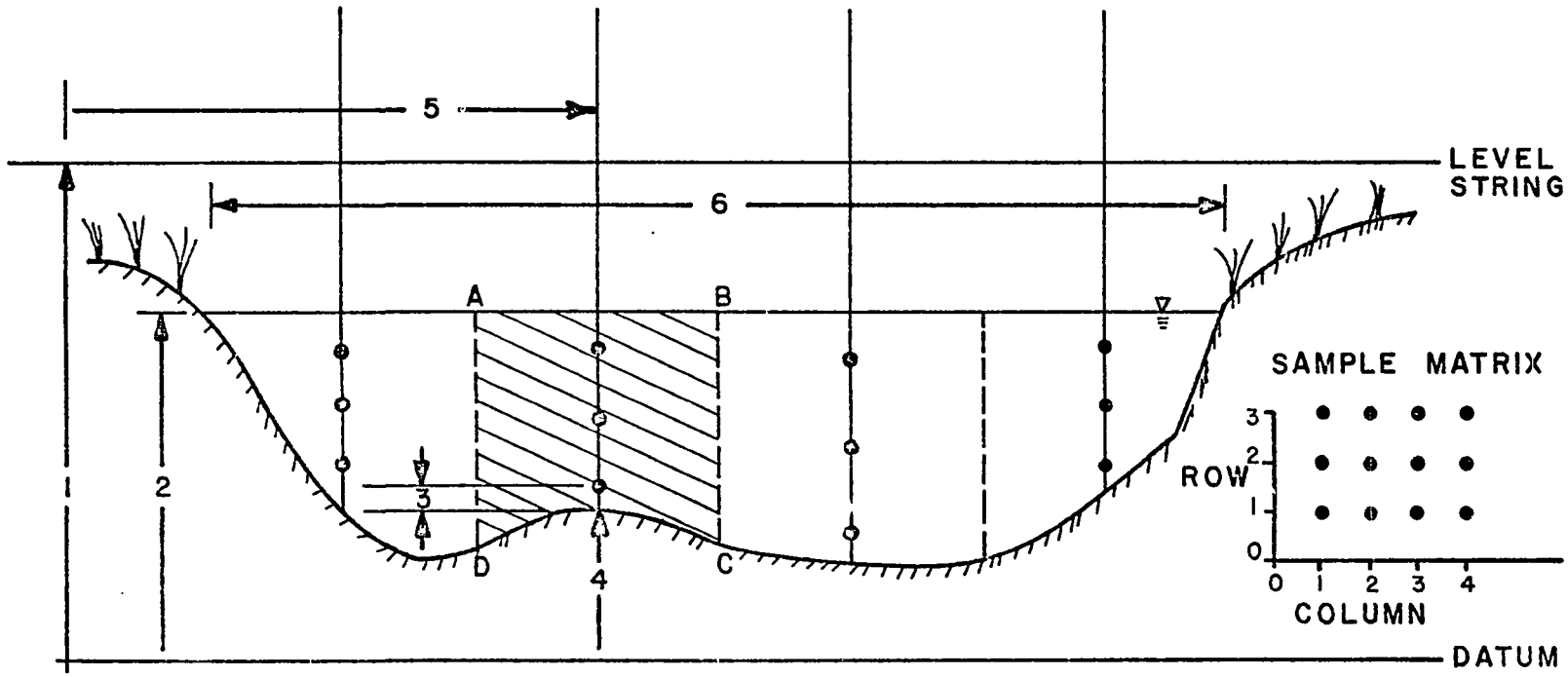

1-HEIGHT OF LEVEL STRING ABOVE DATUM (1000 cm.)
2-HEIGHT OF WATER SURFACE ABOVE DATUM
3-ELEVATION OF SAMPLE IN ITH COLUMN, JTH ROW, ABOVE BOTTOM
4-HEIGHT OF BOTTOM ABOVE DATUM AT TRANSVERSE DISTANCE X
5-TRANSVERSE DISTANCE TO ITH COLUMN OF SAMPLES
6-MAXIMUM WIDTH OF LONGITUDINAL CONVEYANCE IN CHANNEL (1050 cm.)

SECTION A,B,C,D- AREA OVER WHICH ITH COLUMN SAMPLE AVERAGE APPLIES

two weeks longer. The computer used was an IBM 1130 with disk operating system.

Curve Fitting Technique

Initial processing runs produced data in the form of spatial averages of discharge, sediment flux, current speed, and suspended sediment concentration at discrete intervals of time. Curves were fitted to the plotted time values with a computerized method known as the spline fit. Numerical integration of these curves gave highly objective estimates of such quantities as the total discharge (m^3) during each tidal phase, plus the residual discharge, if any. A description of the spline fit method is given in Appendix B, along with the program and subroutines used for the computations (Program INTEFIT, subroutines SLIC and SPLIN).

TIDES

Introduction

This section includes a discussion of some important aspects of basic tidal theory. Tides provide the driving force behind the mechanisms of transport of both water and sediment in salt marsh creeks which is the principal subject of interest in this work. In view of this importance, it is well worth examining at this point some of the salient features of the observed tide in the area of study. A number of useful tools are available to aid one in this type of study, including numerical methods such as that of spectral analysis.

When the heights of the tide are measured at some fixed location at regularly spaced intervals of time, the resultant series of data appear as a recurring sinusoid which can be viewed as a composite of a number of simple cosine waves differing only in amplitude, period, and phase. A single cosine constituent may be written

$$h(t) = R \cos (\omega t - \phi) \qquad (5)$$

where

h = height as a function of time

ϕ = the phase of the constituent relative to some time origin

R = the amplitude of the constituent

$\omega = 2\pi/T$, the angular speed of the constituent

T = period (in hours)

t = time (in hours)

Main Tidal Constituents

Due to the gravitational attractions and periodic motions of the earth-moon-sun system, quite a number of the tidal constituents making up the observed tide may be linked to celestial origins. Familiar diagrams of revolving tidal "bulges" are seen in many texts which illustrate Newton's Equilibrium Tidal Theory. This is a static theory, however, and thus fails to consider the motion of water in tidal waves traveling over varying terrestrial configurations as does the more advanced dynamic theory proposed by LaPlace. The dynamic theory allows one to consider tidal motions as having periods equal to those of the astronomic forces which produce them, whereupon the amplitude and phase of any constituent tide at a given locality is found empirically by harmonic analysis of long-term tidal measurements. The periods and theoretical amplitudes of the major tide producing forces are shown in Table 1.

The observed amplitudes of the tides vary widely in different parts of the world. The three main classes of tide are based, for example, on the computed ratio $(K_1 + O_1) \div (M_2 + S_2)$ in which the symbols stand for the amplitudes of the constituents indicated (see Table 1).

TABLE 1

THE MAIN CONSTITUENTS OF THE ASTRONOMIC TIDE
(after Defant, 1958, p. 48)

Type	Symbol	Period (solar hours)	Amplitude (M_2 = 100)	Description
Semidiurnal	M_2	12.42	100.0	Main Lunar Constituent
Semidiurnal	S_2	12.00	46.6	Main Solar Constituent
Semidiurnal	N_2	12.66	19.1	Lunar Constituent Due to Variation in Distance
Semidiurnal	K_2	11.97	12.7	Soli-Lunar Constituent Due to Declinational Change
Diurnal	K_1	23.93	58.4	Soli-Lunar Constituent
Diurnal	O_1	25.82	41.5	Diurnal Lunar Constituent
Diurnal	P_1	24.07	19.3	Diurnal Solar Constituent
Long-Period	M_f	327.86	17.2	Moon's Fortnightly Constituent

If the ratio is less than 0.25, the tide is classed as the daily (semidiurnal) type, if it is between 0.25 and 1.50, the tide is classed as mixed, and if greater than 1.50, it is classed as the daily (diurnal) variety. On the U. S. Atlantic Coast, tides are of the semidiurnal type. Mixed tides commonly occur on the U. S. Pacific Coast while diurnal tides occur in some parts of the U. S. Gulf Coast area.

Shallow-Water Tides

A frequently important addition to the main tidal components occurs within shallow-water areas; e.g., coastal embayments and estuaries (Doodson, 1941). Away from continental landmasses, tides are propagated in the progressive wave form with celerity

$$c = \sqrt{gh}$$

where

c = rate of travel of a point in the wave form relative to the bottom

g = gravitational acceleration

h = mean water depth

However, upon entering a channel, the rate of advance of a point in the wave form becomes, according to Doodson (1941, p. 151),

$$c = \sqrt{g(h + 3y)}$$

in which y is the elevation of the point above (or below)

mean water level. The resulting wave form is a distorted one in which the crest of the wave is advanced while the trough is held back. It can be shown that the distorted wave consists of a "pure" cosine wave to which one or more higher harmonic waves (waves whose periods are one-half, one-third, etc., of the parent wave period) of lesser amplitude have been added. The additional components are called shallow-water tides or "overtides." If the parent wave is designated M_2 (semidiurnal), then the first harmonic is designated M_4 (quarterdiurnal), the second M_6 (sixth-diurnal), and so on. Before examining shallow-water tides more closely, the interaction of the progressive tidal wave with its reflected wave form must be considered.

The progressive wave entering a channel closed at one end may be reflected in such a manner as to reinforce other incoming waves and produce a standing oscillation. The fundamental resonant period of a channel of length $\underline{L}$ and depth $\underline{h}$ (neglecting friction) is

$$T = \frac{2L}{\sqrt{gh}}$$

Although such a channel would have to be rather long to achieve internal resonance with semidiurnal tidal oscillations (some 383 km for a channel 30 m deep), there are clear indications in a great many coastal areas that the incoming tidal waves are strongly influenced by reflected tidal waves. For example, standing oscillations have

associated oscillatory flows that are out of phase by one-quarter wavelength, i.e., slack waters occur at the high and low water stages. This type of reversing flow pattern is approximated inside many coastal inlets and tidal channels. However, as indicated by progressively later times of arrival of high and low waters as one proceeds inland along these waterways, there is still a progressive aspect to the resultant wave forms. This would logically be so due to frictional effects which attenuate reflected progressive waves to a greater extent than incoming ones.

Doodson (1941, p. 64) discusses the distortion of standing tidal waves in shallow water and states that if the parent wave is of the form of Equation (5), then the first harmonic will be proportional to

$$\cos (2\ \omega t - 2\phi\ ) \text{ or } \cos (2\ \omega t - 2\phi - 180°)$$

where ϕ = phase of the parent wave. By comparison, progressive waves produce a first harmonic proportional to

$$\cos (2\ \omega t - 2\phi + 90°)$$

One may then suppose that a shallow-water wave intermediate between standing and progressive will give rise to a first harmonic constituent with a phase lag somewhere between $2\phi - 90°$ and $2\phi + 180°$ with respect to the fundamental phase.

Figure 4 contains two examples of resultant tidal wave forms derived from hypothetical M_2 and M_4 components having a small phase difference ϕ. When ϕ is positive, the duration of rising tide is noticeably longer than the duration of

Figure 4. Wave forms resulting from semidiurnal (M_2) and quarter-diurnal (M_4) constituents having a phase difference $\pm\phi$ which is (a) negative, (b) positive.

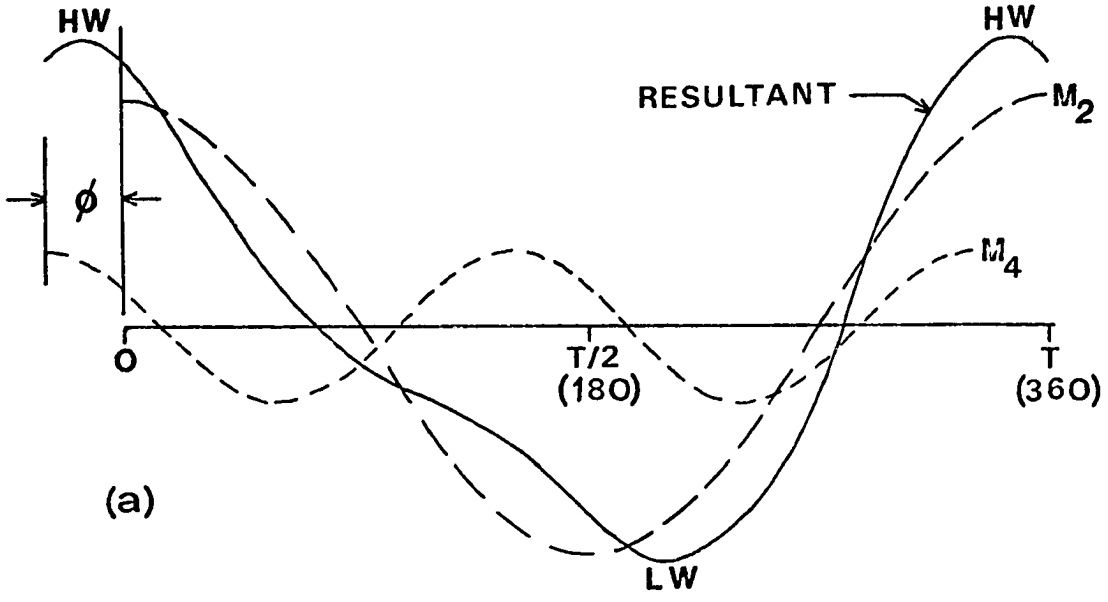

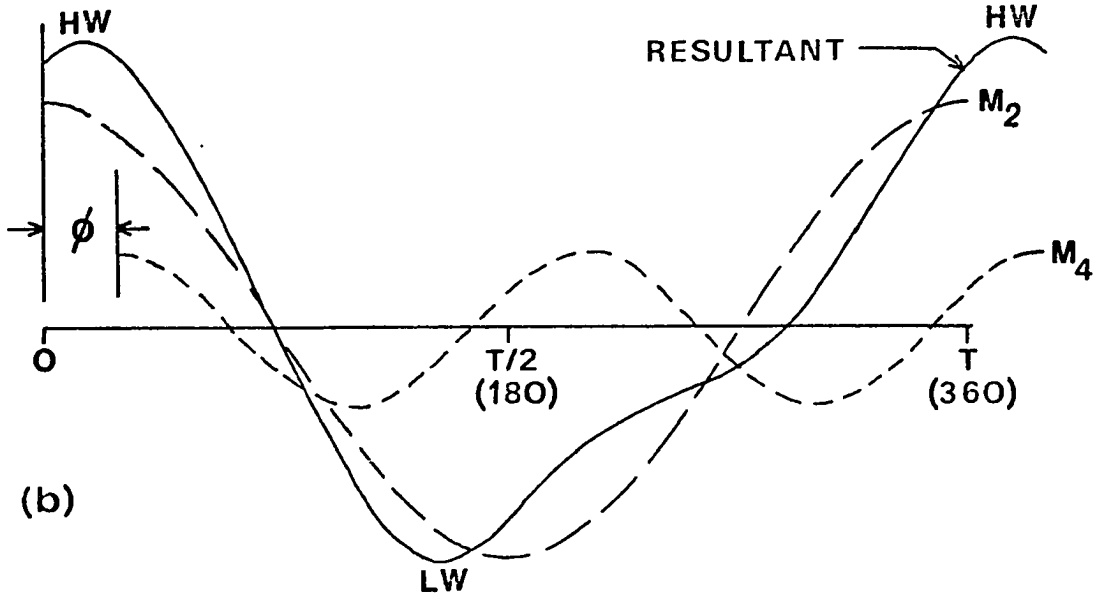

falling tide, the reverse being true when ϕ is negative. It should be noted as well that the period of the resultant wave is exactly the same as that of the fundamental (M_2) harmonic. This simplified illustration omits higher harmonics and other tidal constituents present in actual tides, but shows clearly the mechanism by which duration asymmetries arise. The asymmetry may be significant in terms of sediment transport because of the possible effect on tidal flow and tidal discharge curves (Groen, 1965; Mota Olivera, 1971). One such result is that the maximum strengths of ebb and flood flow will tend to be unequal due to the duration asymmetry even though the total ebb and total flood discharge volumes remain equal. Tidal discharge relationships are the principal subject of a later section.

Before proceeding, the amplitude relationship of various species of shallow-water tides will be briefly discussed. Doodson (1941) has shown that the amplitude of any M_4 wave varies approximately as the square of the amplitude of its parent M_2 wave; similarly, the amplitude of an M_6 wave varies approximately as the cube of the M_2 amplitude. This means that the effect of wave distortion by overtides is amplitude dependent. A spring tide curve will therefore exhibit a greater degree of duration asymmetry than will a neap tide curve having the same fundamental period, ignoring other factors for the moment.

TIDAL ANALYSIS

Tide Gauges

The records of four recording tide gauges in and adjacent to the study area were available to the author. The main tide station at the Virginia Institute of Marine Science dock in Wachapreague, Virginia, has been in continuous operation since November 1, 1969. Another VIMS gauge just inside Wachapreague Inlet has been in intermittant operation since November 4, 1970, while a third VIMS gauge was operated during a 43-day period in the fall of 1972 in Little Fool Creek, the marsh channel selected for intensive study in the present work. All of the above stations are shown in Figure 1. A fourth station operated on the ocean side at the National Aeronautics and Space Administration's facility at Wallops Island, Virginia, has been in operation intermittantly over a number of years. All of the tide gauges used at the above stations were Bristol Recording Bubbler Gauges (Bristol Company, Waterbury, Connecticut).

Rise and Fall Durations

The Wachapreague Dock and Wallops Island tide records were reduced to times and heights of high and low waters to obtain long series of this type of information. Tables 2

through 4 utilize a three-year segment of this data to show monthly mean rise and fall durations at Wachapreague Dock. Table 5 shows the same information for one year of Wallops Island data.

In all of the above tables, the yearly average sum of rise and fall durations is 12.42 hours, the period of the M_2 constituent (Table 1). But at Wachapreague Dock, the data show fairly consistent monthly and yearly averages of the difference between rise and fall durations of about 0.4 hour favoring rise durations. Wallops Island, on the other hand, has a mixed monthly average difference which is about zero for the yearly average. The data clearly show a duration asymmetry for Wachapreague Dock (some three miles inland on a major tidal channel) which is not present on the ocean side of Wallops Island. A few months data from Wachapreague Inlet show essentially the same duration asymmetries as at Wachapreague Dock and need not be included here.

Figure 5 shows how the daily variations in rise and fall durations appear during a typical month. The month of June was chosen because weather effects are normally not so severe at this time. But, to give weather it due, the spike to right in the figure coincides with tropical storm Agnes which occurred June 22, 1972 (peak NE winds 47 MPH), and shows that the effect can be considerable. Elsewhere during the month, a saw-tooth pattern and a fortnightly "beat" can be discerned which is due to diurnal inequalities

TABLE 2

MONTHLY MEANS OF RISE AND FALL DURATIONS IN HOURS AT WACHAPREAGUE DOCK, 1970

Month	Duration of Rise	Duration of Fall	Difference	Sum
1	6.52	5.91	0.61	12.43
2	6.45	5.96	0.49	12.41
3	6.44	5.99	0.45	12.43
4	6.38	6.04	0.34	12.42
5	6.39	6.03	0.36	12.42
6	6.36	6.04	0.32	12.40
7	6.42	6.00	0.42	12.42
8	6.43	5.98	0.45	12.41
9	6.42	6.00	0.42	12.42
10	6.45	5.98	0.47	12.43
11	6.33	6.10	0.23	12.43
12	6.42	6.00	0.42	12.42
Mean	6.42	6.00	0.42	12.42

TABLE 3

MONTHLY MEANS OF RISE AND FALL DURATIONS IN HOURS AT WACHAPREAGUE DOCK, 1971

Month	Duration of Rise	Duration of Fall	Difference	Sum
1	6.36	6.05	0.31	12.41
2	6.42	6.00	0.42	12.42
3	6.40	6.01	0.39	12.41
4	6.35	6.06	0.29	12.42
5	6.30	6.12	0.18	12.42
6	6.36	6.05	0.31	12.41
7	6.41	6.01	0.40	12.42
8	6.37	6.05	0.32	12.42
9	6.38	6.05	0.33	12.43
10	6.39	6.03	0.36	12.42
11	6.38	6.05	0.33	12.43
12	6.52	5.29	0.60	12.44
Mean	6.39	6.03	0.36	12.42

TABLE 4

MONTHLY MEANS OF RISE AND FALL DURATIONS IN HOURS AT WACHAPREAGUE DOCK, 1972

Month	Duration of Rise	Duration of Fall	Difference	Sum
1	6.39	6.04	0.35	12.43
2	6.46	5.96	0.50	12.42
3	6.46	5.96	0.50	12.42
4	6.42	5.97	0.45	12.39
5	6.36	6.05	0.31	12.41
6	6.47	5.95	0.52	12.42
7	6.42	6.00	0.42	12.42
8	6.42	6.02	0.40	12.44
9	6.40	6.03	0.37	12.43
10	6.40	6.03	0.37	12.43
11	6.47	5.94	0.53	12.41
12	6.50	5.90	0.60	12.40
Mean	6.43	5.99	0.44	12.42

TABLE 5

MONTHLY MEANS OF RISE AND FALL DURATIONS IN HOURS AT WALLOPS ISLAND, 1969-70

Month	Duration of Rise	Duration of Fall	Difference	Sum
11 (69)	6.10	6.33	- 0.23	12.43
12 (69)	6.25	6.17	0.08	12.42
1 (70)	6.34	6.09	0.25	12.43
2	6.21	6.19	0.02	12.40
3	6.23	6.19	0.04	12.42
4	6.10	6.31	- 0.21	12.41
5	6.17	6.25	- 0.08	12.42
6	6.09	6.34	- 0.25	12.43
7	6.10	6.32	- 0.22	12.42
8	6.12	6.28	- 0.16	12.40
9	6.14	6.27	- 0.13	12.41
10	6.16	6.25	- 0.09	12.41
Mean	6.17	6.25	- 0.08	12.42

Figure 5. Daily rise and fall durations, June 1972, Wachapreague Dock.

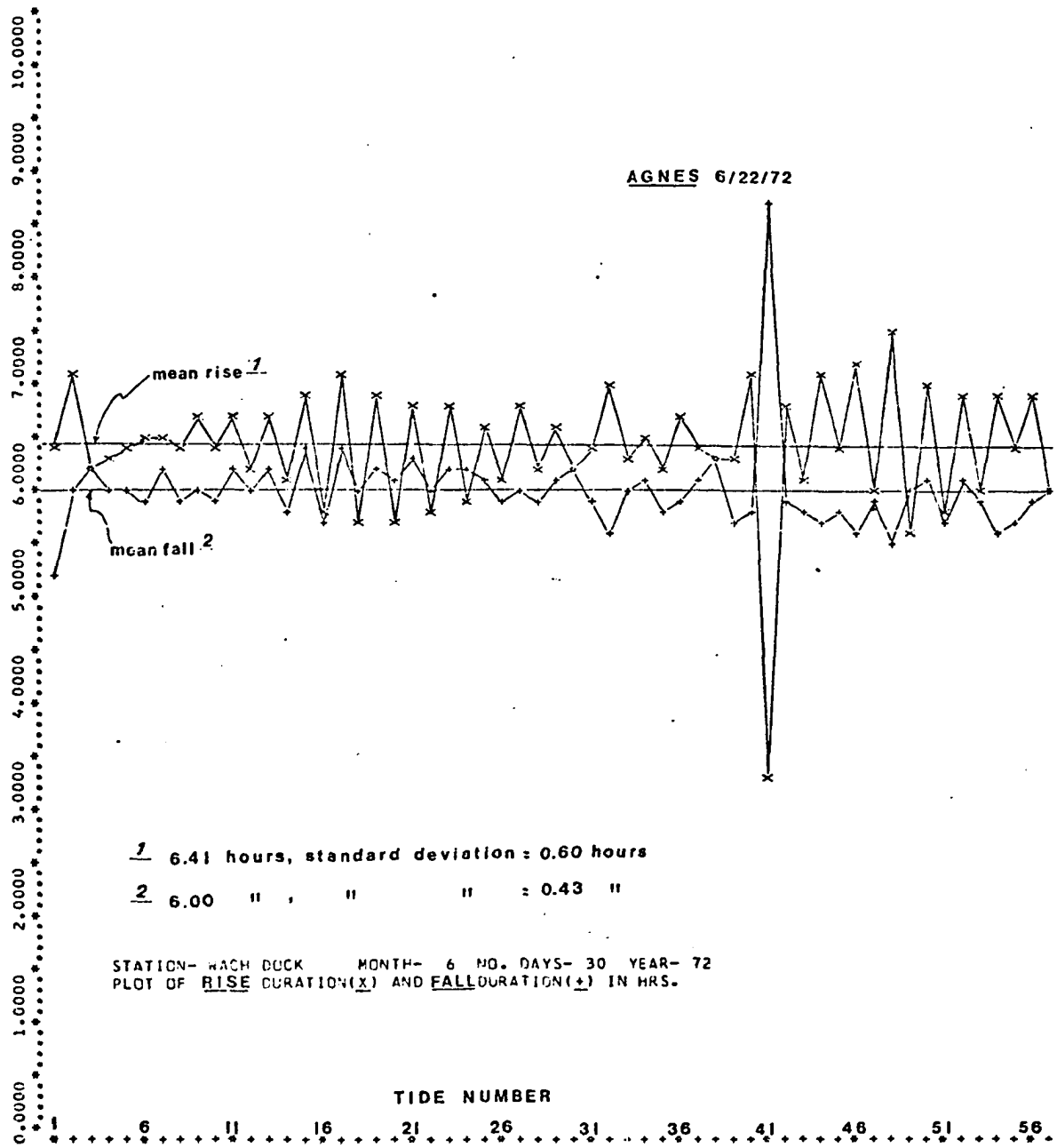

1 6.41 hours, standard deviation : 0.60 hours

2 6.00 " , " " : 0.43 "

STATION- WASH DOCK MONTH- 6 NO. DAYS- 30 YEAR- 72
PLOT OF RISE DURATION(X) AND FALLDURATION(+) IN HRS.

in times of the tides that are related to the familiar diurnal inequalities in heights. Diurnal inequality of both quantities is present in most semidiurnal tides. This is a consequence of the moon's fortnightly declinational cycle, perhaps more instructively viewed as an interaction of the main semidiurnal (M_2, S_2) constituents and the main diurnal (K_1, O_1) constituents. These constituents, like all astronomic constituents, have different angular speeds and hence periodically reinforce and oppose one another as they pass in and out of phase. Only the higher harmonic shallow-water constituents can effect a long-term net duration asymmetry because only they have angular speeds which are exact multiples of those of their parent oscillations and therefore have more or less constant phase lags with respect to those oscillations. Hence, tides inside the Wachapreague marsh-lagoon complex have net duration asymmetries while those of the open ocean typically do not. But as is quite evident in Figure 5, a given day may contain values totally unrelated to the long term result.

The above analyses provide information concerning distorted tidal waves which is essentially qualitative. Further investigation of the constituents causing the distortion will now be reported using the results of spectral analyses performed on the data. This will provide amplitude and phase information necessary to model this aspect of the tide's behavior in the area of study.

SPECTRAL ANALYSIS

The Fourier Model

The sum of one or more harmonic constituents may be represented by a finite Fourier series

$$h(t) = R_o + 2 \sum_{m=1}^{n-1} R_m \cos (m\,\omega t + \phi_m) + R_n \cos n\,\omega t \quad (6)$$

where

R_o = mean value of h

$2R_m$ = amplitude of the mth constituent

R_n = amplitude of the nth constituent

with the other symbols as defined for Equation (5). Equation (6), however, denotes harmonic terms with $\omega = 2\pi/T$ where T is taken as the fundamental period of the series and in the model is set equal to the length of the record observed. To fit data to this type of model, one must obtain $N = T/\Delta t$ discrete data observations where Δt is the sampling interval. The number of harmonic constituents found by this method is equal to one-half of the data points used ($n = N/2$).

The "fit" of the model is achieved by setting $t' = t/\Delta t$ and solving for the Fourier coefficients

$$A_m = \frac{1}{N} \sum_{t'=o}^{N-1} h(t') \cos \frac{2\pi mt'}{N}$$

$$B_m = \frac{1}{N} \sum_{t'=o}^{N-1} h(t') \sin \frac{2\pi mt'}{N}$$

after which R_m and ϕ_m are computed as

$$R_m = \sqrt{A_m^2 + B_m^2}$$

$$\phi_m = \text{ARCTAN} - \frac{B_m}{A_m}$$

This procedure involves a great many calculations for the kind of record lengths required and was therefore costly to run even for large computers until the recent advent of the Fast Fourier Transform (FFT) which greatly reduces the necessary running times. Detailed descriptions of the FFT and its usage may be found in most recent texts on spectral analysis (Jenkins and Watts, 1968; Bendat and Piersol, 1971).

Before applying this type of model, it is to be noted that Equation (6) describes a true periodic function; i.e., all of its harmonic constituents have angular speeds ($m\omega$) which are integral multiples of the fundamental speed ($\omega = 2\pi/T$). In most recorded series, none of the primary tidal constituents are so related, hence resultant tidal

curves are not, in the finite sense, periodic.[1] This shortcoming is overcome through the use of special data analysis methods.

The Periodogram

The mean square value of a periodic function $h(t')$, $t' = 0, 1, 2, \ldots, N-1$, can be decomposed into mean square values associated with each harmonic term in Equation (6), or

$$\frac{1}{N} \sum_{t'=0}^{N-1} h(t')^2 = R_o^2 + 2 \sum_{m=1}^{n-1} R_m^2 + R_n^2$$

which is attributable to Parseval's Theorem (Jenkins and Watts, 1968, p. 21). The above equation can also be expressed in terms of the mean square value about the mean; i.e., the variance

$$\sigma^2 = \frac{1}{N} \sum_{t'=0}^{N-1} \left[h(t')-R_o\right]^2 = 2 \sum_{m=1}^{n-1} R_m^2 + R_n^2 \qquad (7)$$

This expression provides a means of estimating the average power or variance within selected regions (bands) of the frequency spectrum. Based on N data points, a graph showing the frequency distribution of the variance can be

---

[1] They would be essentially periodic only if the record lengths were equal to the fundamental tidal period of 18.6 years.

constructed covering the range of frequencies between the fundamental frequency, $f_f = 1/N\Delta T$, and a "cutoff" frequency, $f_c = 1/2\Delta t$. This range may be subdivided into P number of bands, each containing the variance contributed from L terms in Equation (7) so that $P = N/2L$. Thus, the average power or variance arising from those harmonic constituents whose frequencies fall within a given band may be represented by a variance estimate at the midpoint of that band at the frequency

$$f_k = \frac{(2K-1)L+1}{2N\Delta t}, \quad K = 1, 2, \ldots, P.$$

For example, the midpoint of the first band in a series where $N = 24$, $L = 4$, $\Delta t = 0.5$ hr is found at $f_1 = 5/24$ CPH where the variance estimate within the band is $2(R_1^2 + R_2^2 + R_3^2 + R_4^2)$.

The above procedure results in what is called the raw periodogram. In dealing with a finite series, such a periodogram will be distorted by power "leakage;" i.e., power which should occur at one frequency only is distributed at adjacent frequencies to a greater or lesser extent as well. This distribution can be expressed by a mathematical formula known as a window function, which in turn can be modified by various treatments of the data that reduce the "end" effects arising in a finite series. The treatment, called a data window, may include tapering the ends of the series through a cosine attentuation

function. This has the effect, then, of reducing leakage so that more of the energy in the modified periodogram falls within the appropriate band.

Finally, it is desirable to carry out frequency smoothing within the modified periodogram. Using FFT procedures, this involves selecting the proper band width to include enough R_m^2 terms to obtain a precise enough average for any given band. Since bandwidth is equal to $L/N\Delta t$, one maintains a small bandwidth (necessary for good resolution) and averages more R_m^2 terms, L, (necessary for good precision) by increasing the length of the series, $N\Delta t$. This can be done by either increasing the number of observations, N, or the sampling interval, Δt. However, there is a limitation on the sampling interval; the cutoff frequency $f_c = 1/2\Delta t$ must be greater than the highest frequency component likely to be significant in terms of amplitude in the data in order to avoid aliasing or "folding" of energy back into the lower frequency regions.

A computer program for accomplishing spectral analysis of tidal data (SATIDE), written by the author for the IBM 360, may be found in Appendix B. This program utilizes a cosine-taper data window and system 360 scientific subroutines for FFT computations.

Results of Spectral Analysis

Tidal records for the four stations available were analyzed using program SATIDE. Record lengths of 43 days

with observations taken at a sampling interval of ½-hour were used at each station. The results are shown in Figures 6, 7, 8, and 9, which indicate the station names and the dates covered in each case. Bandwidths of .1872 cycles per day were selected using 8 coefficient terms per band. Variance estimates within each band are distributed as a chi-square variable with approximately 16 degrees of freedom; the range of expected values calculated at the 80% level of confidence is shown in the lower right corner of each figure. Plotting the log of variance on the ordinate axis permits the error estimate to be displayed as a band of constant width which is applicable at all points in the graph.

In each figure, a semidiurnal peak is dominant at a frequency of 2.0 cycles per day (CPD). The principal diurnal constituents, K_1 and O_1, are also present in every case, although the bandwidths used are insufficient to resolve the two peaks which occur at 1.003 and 0.929 CPD, respectively. Similarly, the S_2 constituent (2.000 CPD) merges with the M_2 constituent (1.932 CPD). It is not necessary, however, that these constituents be resolved for present purposes.

Several examples of the shallow water tides also appear in figures 6-9, the main ones being M_4 and M_6. Other shallow-water tides are indicated, some of which may be of diurnal origin (one peak to the left of M_4, one to the left of M_6), others representing interactions between

Figure 6. Fourier periodogram, Wallops Island, July 27 to September 7, 1970.

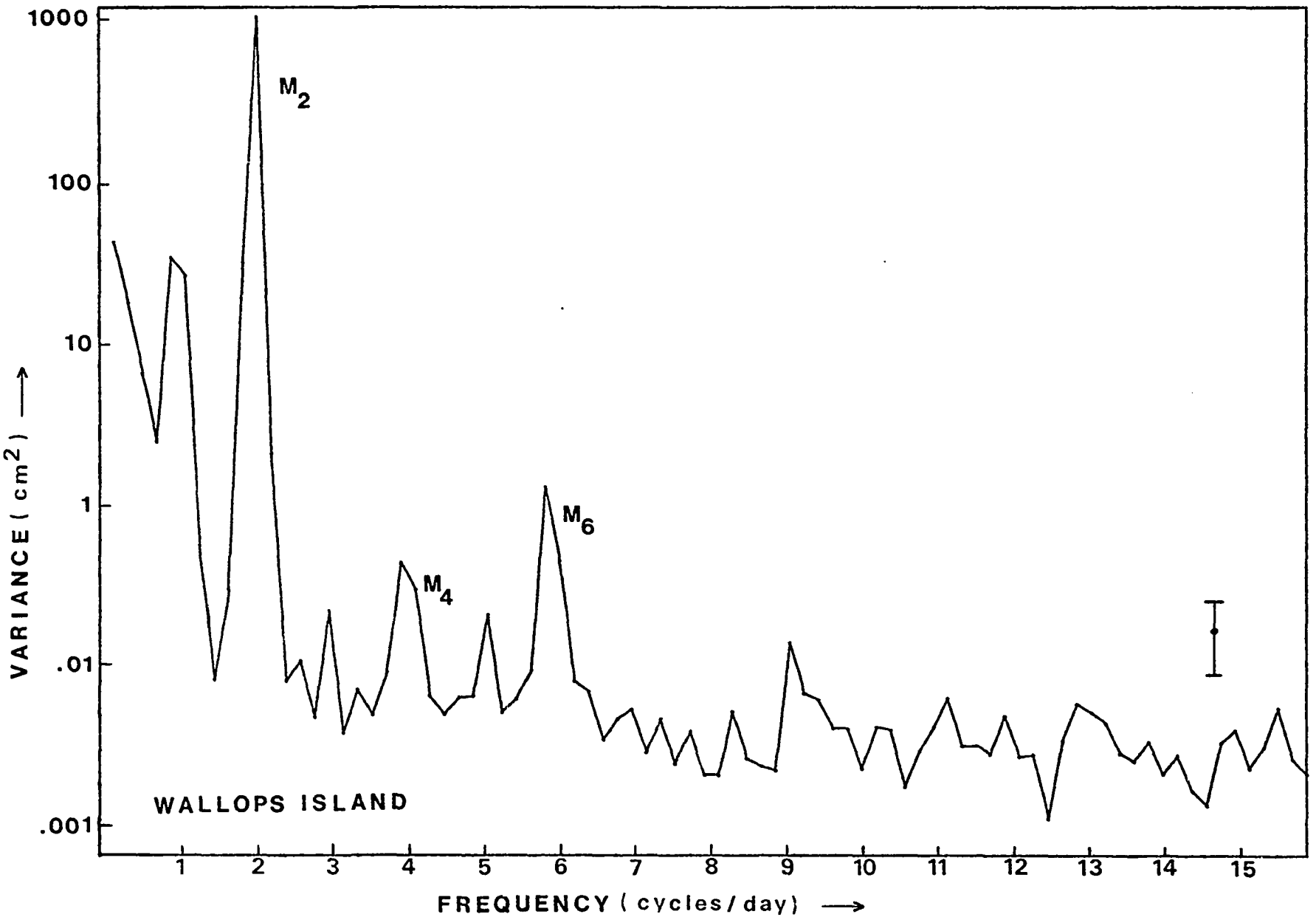

Figure 7. Fourier periodogram, Wachapreague Inlet, Oct. 30 to Dec. 11, 1972.

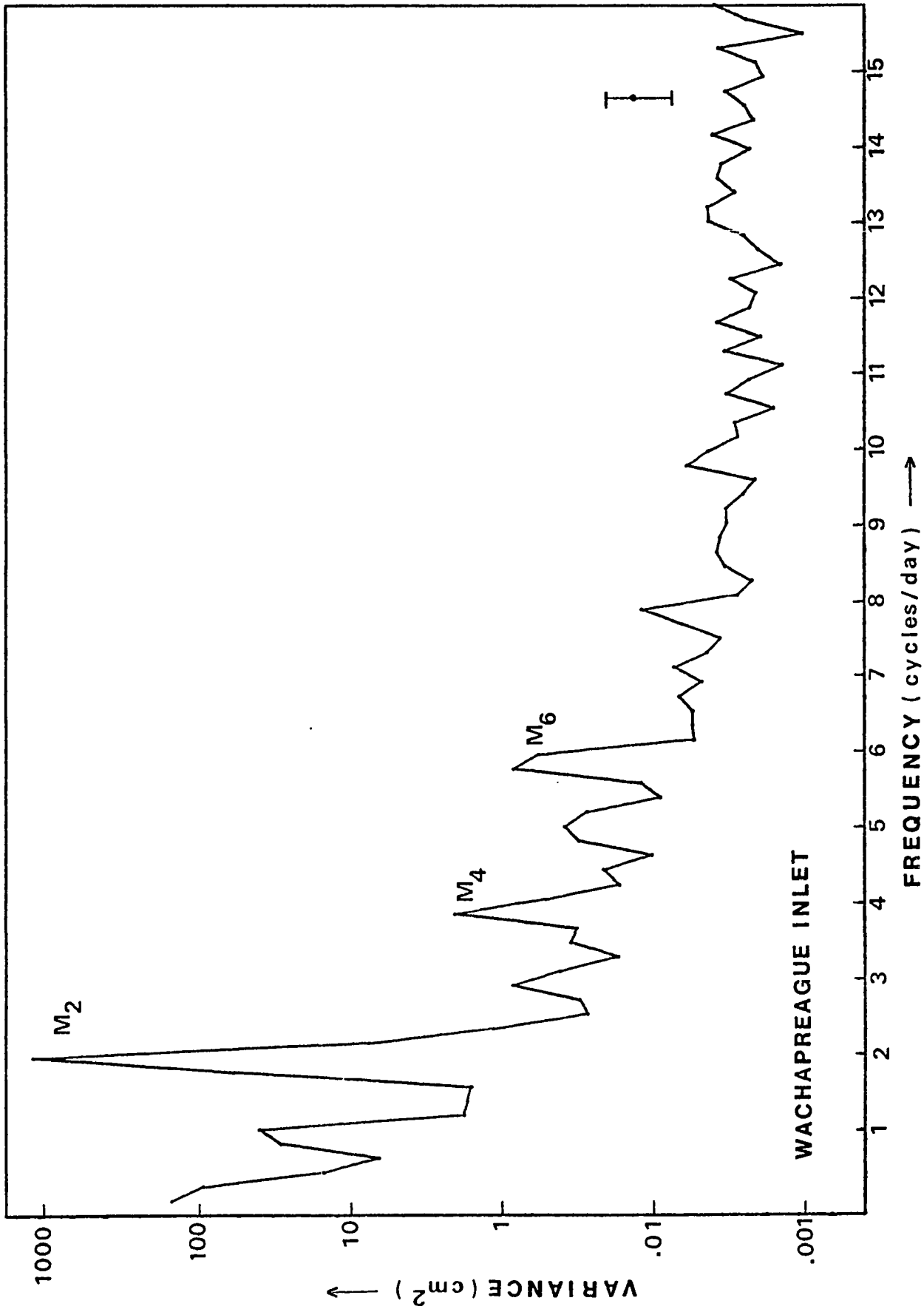

Figure 8. Fourier periodogram, Wachapreague Dock, Oct. 15 to Nov. 26, 1972.

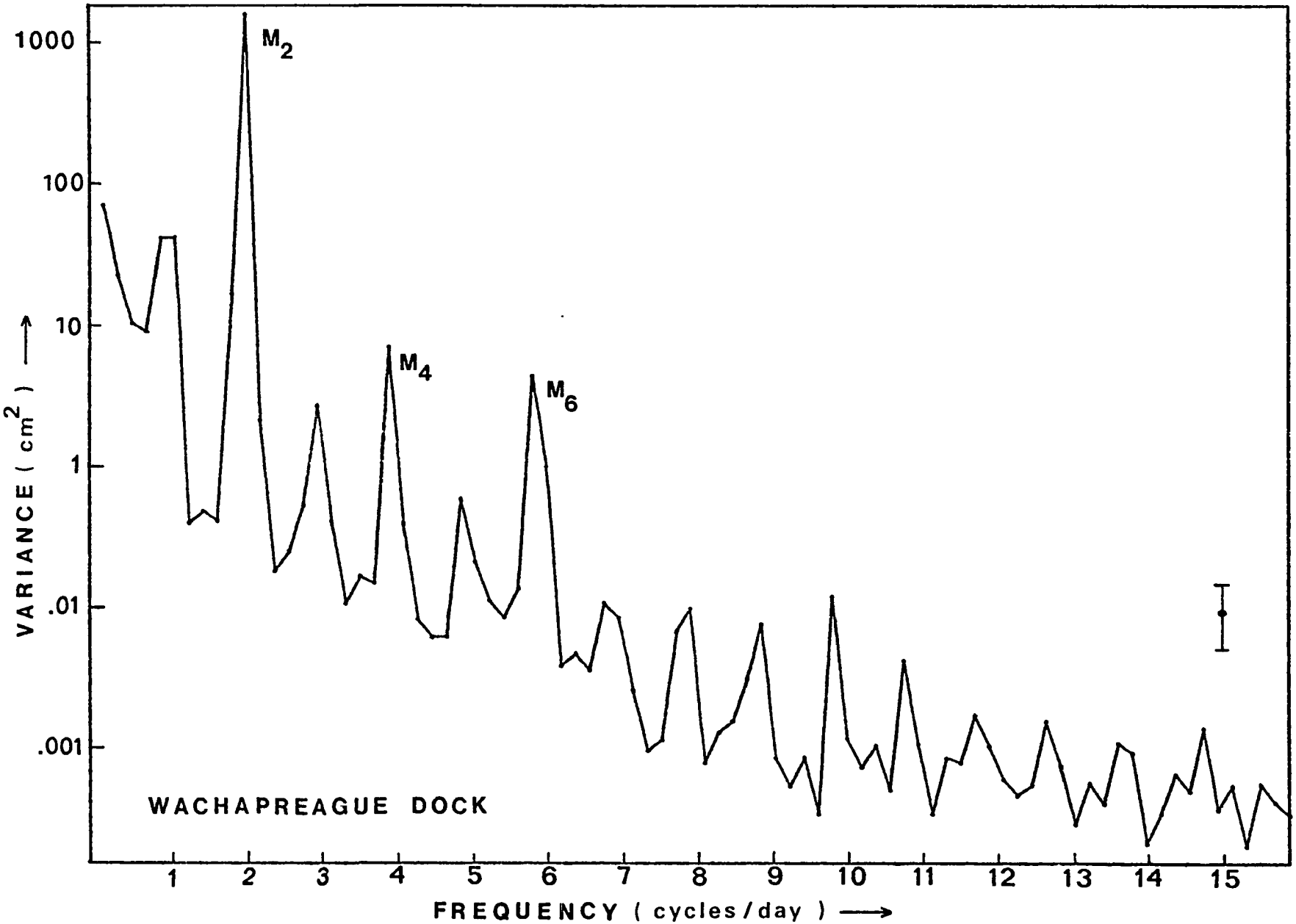

Figure 9. Fourier periodogram, Little Fool Creek, Oct. 15 to Nov. 26, 1972.

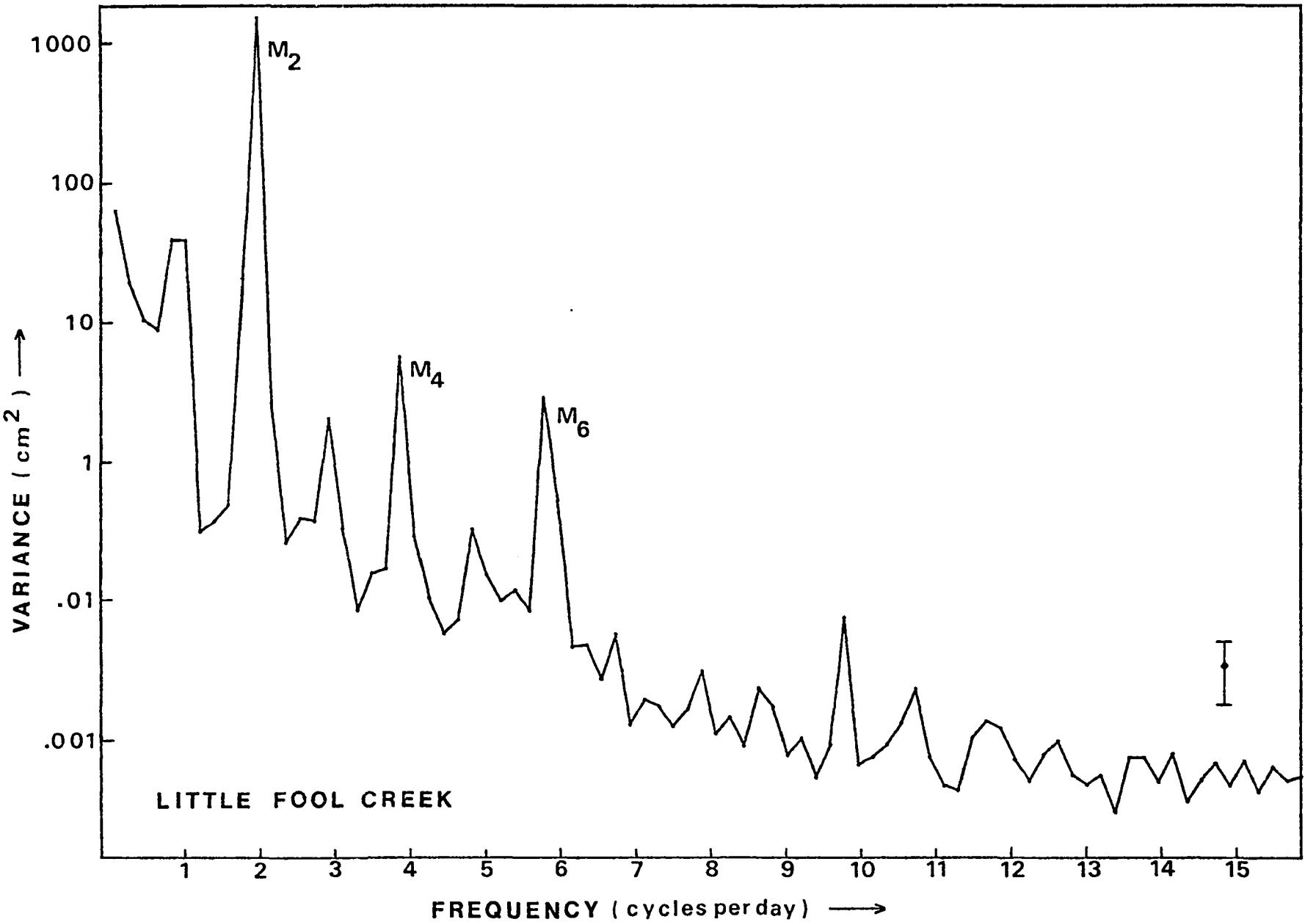

the major constituents. Restricting attention to the M_4 and M_6 constituents (which are by no means exhaustive of the shallow-water tidal content) one notices that the M_4 peak in particular is enhanced relative to the M_2 peak at Wachapreague Inlet (Fig. 7) as compared to Wallops Island (Fig. 6). Still further enhancement in both the M_4 and the M_6 peaks is seen at Wachapreague Dock (Fig. 8) and Little Fool Creek (Fig. 9). The increase in M_4, M_6 amplitudes at the inland stations is probably due to a combination of shallow-water effects and the slightly greater range of tide found inland.

Quantitative comparison of the major constituents is provided by additional output from program SATIDE as summarized in Table 6, in which the amplitudes are expressed as fractions of the mean amplitude of the observed tide for the series in question. The relative amplitude for the M_4 component, though small in comparison to M_2, is about double in value at Wachapreague Dock as compared to Wallops Island. The increase in M_4, along with the somewhat smaller increase in M_6, is sufficient in itself to account for the net duration asymmetry observed at Wachapreague. This will now be demonstrated by the use of a model.

Tide Model

For a given day, let the semidiurnal tide curve covering a single cycle be simulated by

$$h(t) = R_o + 2R_1 \cos \omega t + 2R_2 \cos(2\omega t - \phi_1) + 2R_3 \cos(3\omega t - \phi_2)$$

TABLE 6

PERCENTAGES OF TOTAL VARIANCE AND RELATIVE* AMPLITUDES FOR THE MAIN TIDAL CONSTITUENTS AND THE OVERTIDES M_4 AND M_6

Station	Constituents	% Variance	Rel. Amplitude
Wallops Is.	$K_1 + O_1$	4.97	0.223
	$M_2 + S_2$	88.47	0.941
	M_4	0.06	0.025
	M_6	0.14	0.033
	TOTAL	93.64	
Wach. Inlet	$K_1 + O_1$	4.22	0.206
	$M_2 + S_2$	77.82	0.882
	M_4	0.13	0.036
	M_6	0.09	0.030
	TOTAL	82.26	
Wach. Dock	$K_1 + O_1$	4.61	0.215
	$M_2 + S_2$	87.86	0.937
	M_4	0.38	0.063
	M_6	0.24	0.049
	TOTAL	93.09	
Little Fool	$K_1 + O_1$	4.64	0.215
	$M_2 + S_2$	87.15	0.939
	M_4	0.34	0.061
	M_6	0.20	0.045
	TOTAL	92.33	

*Relative to mean amplitude of observed tide.

where

R_o = mean level above datum

$2R_1$ = fundamental semidiurnal amplitude

$2R_2$ = first harmonic amplitude

$2R_3$ = second harmonic amplitude

ϕ_1, ϕ_2 = phase lags relative to fundamental

ω = $2\pi/T$, T = 12.42 hours.

By restricting the use of the model to a single tidal cycle, $2R_1$ can be viewed as a single constituent whose amplitude represents various combinations of the actual semidiurnal amplitudes, M_2 and S_2. For example, setting $2R_1 = M_2 + S_2$ simulates a spring tide, $2R_1 = M_2 - S_2$ a neap tide, and $2R_1 = M_2$ an average tide.

Recalling that the amplitude of a quarter-diurnal constituent varies as the square of the semidiurnal constituent,

$$2R_2 = K_1(2R_1)^2 \quad ; K_1 \text{ a constant}$$

Similarly,

$$2R_3 = K_2(2R_1)^3 \quad ; K_2 \text{ a constant}$$

and by defining dimensionless amplitudes $R_1' = 2R_1/H$, $R_2' = 2R_2/H$, $R_3' = 2R_3/H$, where H = resultant tidal amplitude, or one-half the observed tidal range, the model becomes

$$h(t) = R_o + R_1'H \cos \omega t + K_1 R_1'^2 H^2 \cos(2\omega t - \phi_1) + K_2 R_1'^3 H^3 \cos(3\omega t - \phi_2) \quad (8)$$

Using the Little Fool Creek data, $R_1' = 0.94$ (Table 6), $K_1 = 0.10\ m^{-1}$, $K_2 = 0.11\ m^{-2}$. The phase lags ϕ_1 and ϕ_2 were determined from a weighted average of the squares of the basic fourier coefficients, A_m^2 and B_m^2, in the region of the known frequencies for M_2, M_4, and M_6. The weighting was done using a cosine-taper window function (Bendat and Piersol, 1971, p. 325) centered at each frequency; the results were $\phi_1 = 37.0°$ and $\phi_2 = -16.6°$.

A simulated curve for a normal tide (H = 0.61 m) at Little Fool Creek is shown in Figure 10. The difference between the rise and fall durations of this curve is 0.48 hour. For a spring tide (H = 0.72 m), the difference increases to 0.52 hour and for a neap tide (H = 0.45 m), the difference decreases to 0.40 hour. These differences are within range of the monthly and yearly average differences found nearby at Wachapreague Dock (Tables 2-4). The model thus depicts a typical semidiurnal oscillation, including the distortion which appears in the long run due to overtides, at the study site.

Figure 10. Model tide curve based on Equation (8), using H = 0.61 m.

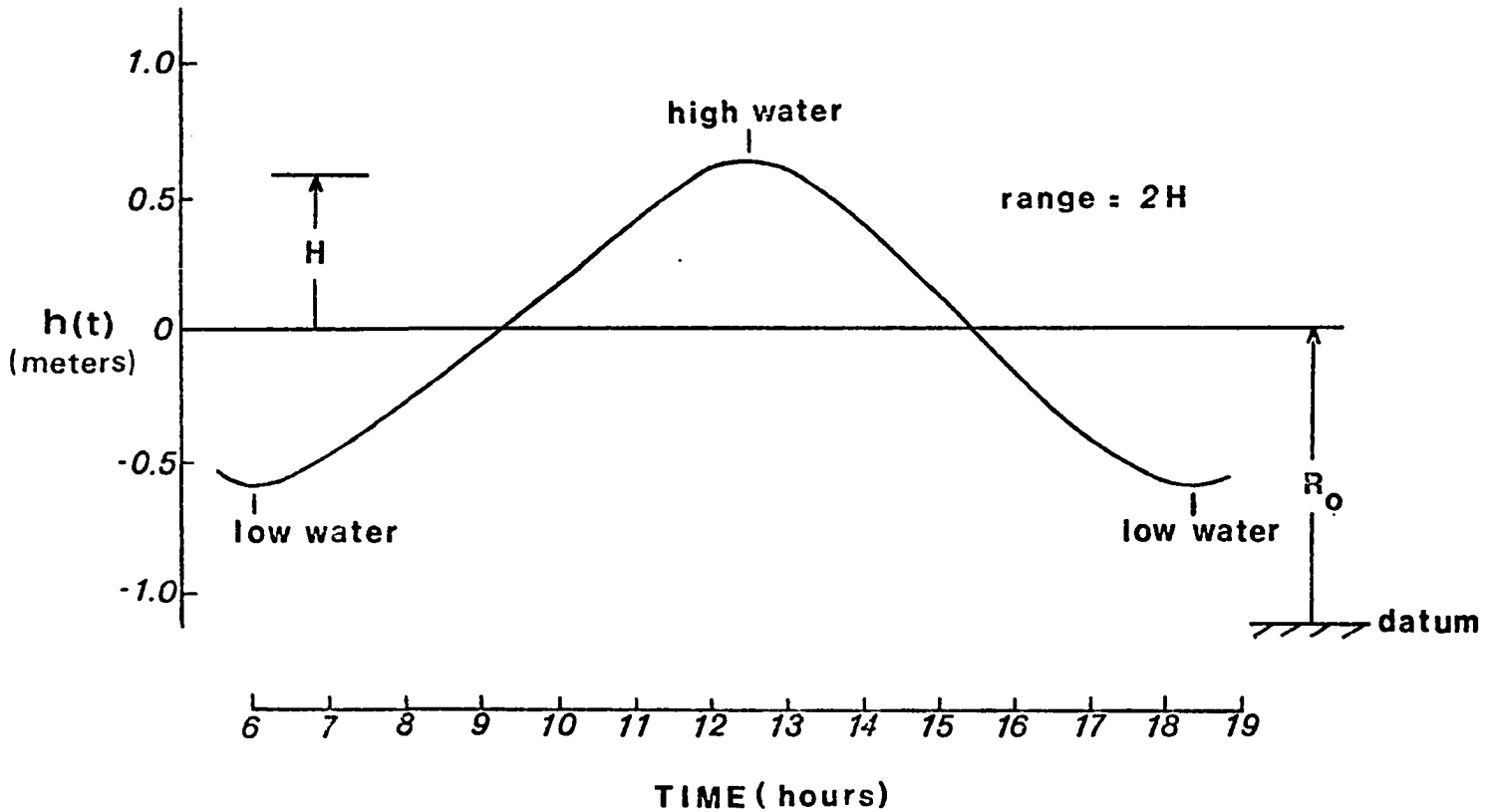

TIDAL DISCHARGE RELATIONSHIPS IN MARSH CREEKS

Introduction

In the previous section, a model of the tide was presented, representing the study area, but considered here to be typical of many shallow marsh-lagoon environments in terms of their tendency to generate shallow-water tides. One other relationship is needed before an investigation of discharge relationships in marsh creeks can be made. This is the tidal storage relationship which defines the volumes of water which must undergo transport to and from the marsh for any combination of tides. From the two principal factors of tide and storage, the time-varying discharge will emerge for the conveyance channels handling the discharge. It is necessary to begin with a discussion of tidal channel characteristics and the morphology of marsh drainage basins.

Strahler's (1952) version of Horton's (1945) classification of stream segments in terms of stream order will be followed in this study. The smallest channel segments, those which terminate on the marsh, will be designated first order; where two such segments join, the resultant seaward

segment will be termed second-order, second-order segments giving rise to third-order segments, and so on. Although subject to some interpretation, a typical marsh channel system will be fairly low in order; i.e., the trunk channel formed by coalescing smaller segments will usually be of third or fourth-order. The system selected for intensive study, Little Fool Creek, is shown in Figure 11.

The model to be developed in this section is intended to apply in general to any of the low-order drainage channels commonly found in tidal marshes. Specifically, a model is sought which will simulate the time-varying tidal discharge past a cross-section near the mouth of the trunk channel, considered here to be the dividing point between the marsh drainage network proper and the main conveyance channels that ultimately join with the ocean, as at Wachapreague Inlet (Fig. 1).

Essential to the model is the assumption that marsh channels form a closed system; i.e., each channel, along with each of its tributaries, ends on the marsh. This assumption is questionable for channels that appear continuous all the way through the marsh (from one bay or large tributary to the next) and for certain periods of complete marsh flooding. However, the marshes under study near Wachapreague contain few such open-ended channels which are not, in fact, two distinct channel systems straddling a common drainage divide. In broader terms, one usually finds distinct drainage areas on the marshes

Figure 11. Black and white infrared photograph of Little Fool Creek pictured at low tide, April 6, 1973 (water areas appear black; distance between middle and lower bridges across creek is about 143 m, or 469 ft).

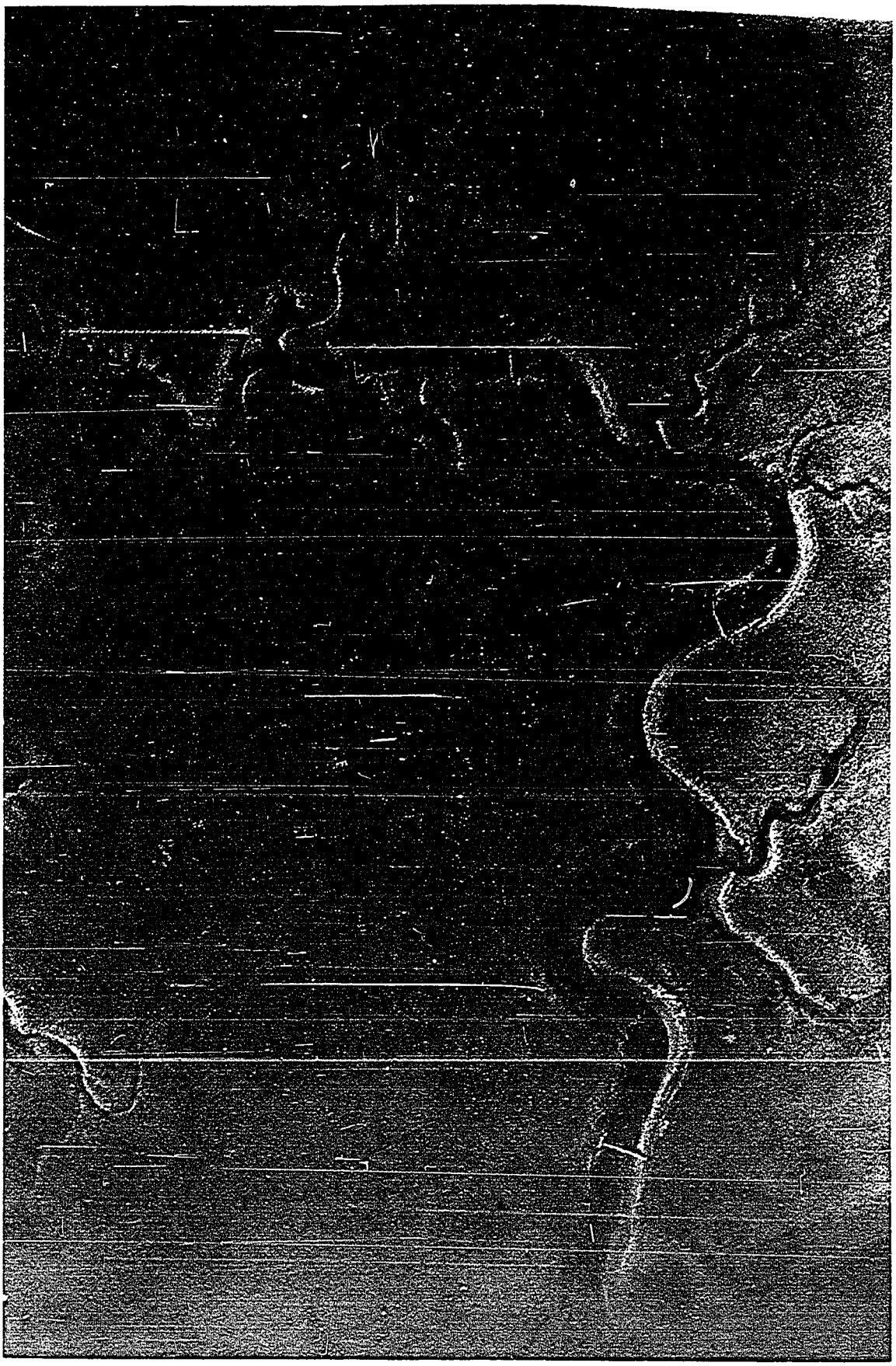

associated with a channel network leading to a single trunk channel conveying most of the flow. Moreover, net exchange of water volumes between such areas is probably minimal, except during those periods of extreme flooding most often accompanied by high winds.

Discharge Model

Consider a frictionless marsh channel closed at one end (Figure 12).

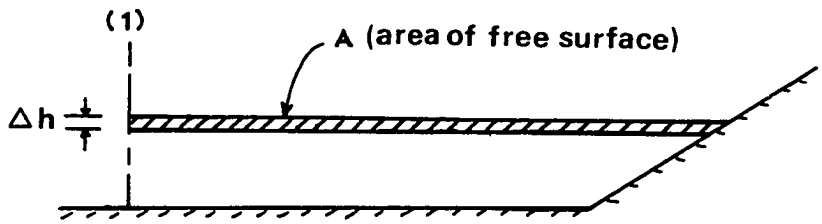

Figure 12. Longitudinal section, idealized channel.

A flow of water past section (1) in the longitudinal direction will cause a volume change, $\Delta V = A\Delta h$ where A is the free surface area, Δh is the change in height during some interval Δt. The continuity equation for discharge at section (1) can then be written

$$q = A \frac{dh}{dt} \tag{9}$$

where q has the dimensions of volume per unit time.

The above equation may be expected to hold in small channels where tidally-induced free surface slopes are not appreciable in view of the short channel length as compared to the tidal wavelength. It is to be noted, however, that this model is intended to depict the ideal behavior of the discharge and is therefore subject to such errors as may arise due to local variations in slope within the channel, due to wind stress and frictional effects.

Integration of Equation (9) produces an equation useful in obtaining the total volume of water transported during some time interval, Δt. If $\Delta t = t_2 - t_1$, while $\Delta h = h_2 - h_1$, then

$$Q = \int_{t_1}^{t_2} q\,dt = \int_{h_1}^{h_2} A\,dh \qquad (10)$$

where Q has the dimensions of volume only.

There will now follow a development of the factors in equations (9) and (10) leading to transport models which can be tested against field data. Beginning with Equation (10), the total discharge in a half tidal cycle (the flood or ebb prism) can be developed at the study site from a knowledge of the height-area relationship to be found there.

Height-Area Relationship

The relationship between the height of the tide and the free surface area within a marsh is clearly a function of drainage basin morphology. As the tide rises, the water's edge is at first restricted within well-defined channels,

but soon begins to conform to ever-widening, pear-shaped contours at the heads of the first-order channels (Figure 13). As the waters reach the maximum elevations on the marsh, the appearance of the free surface is a roughly circular outline at the moment of merger with the waters from adjacent drainage systems. Contained within the circular outline and last to be covered are the channel levees which border the high-order channels, including the main thoroughfare (lower right corner, Fig. 11) leading to the ocean.

The subject of height-area (hypsometric) relationships in terrestrial drainage basins has been given thorough treatment by Strahler (1952), who conducted a mathematical analysis dealing with land area above a given contour, determined at regularly-spaced contour intervals and expressed as a fraction of the total area in the basin. Strahler's hypsometric formulas permit both height and area to be cast as dimensionless variables. The function used to describe the relationship is

$$y = \left[\frac{d-x}{x} \cdot \frac{a}{d-a} \right]^{z}$$

where d and a are constants representing maximum and minimum area respectively, x and y are variables representing area and relative height respectively, and z is an exponential constant. Strahler demonstrated that a wide variety of terrestrial drainage basins could be described

Figure 13. Black and white infrared photograph of Little Fool Creek pictured during the initial stage of marsh flooding (MLW + 1.00 m or 3.28 ft).

hypsometrically by the above formula which generates a large family of curves dependent on one's choice of z and the factor r = a/d, a constant controlling the degree of curvature.

In the present case, it is not land area but water area that is required. The latter is easily obtained at any given height as the difference between unflooded land area and the total area of the basin. The author therefore chooses to adopt a formula which in essence describes the inverse of Strahler's hypsometric relationship, namely

$$h' = 1 - \left[\frac{Amax-A}{A} \cdot \frac{Amin}{Amax-Amin} \right]^{z} \qquad (11)$$

where h' = dimensionless tidal height and A_{max}, A_{min} are the extreme free surface areas produced by the tide in a given basin. The dimensionless height, h', is further defined as

$$h' = \frac{h-h_{min}}{h_{max}-h_{min}}$$

Here it is considered that h_{max}, h_{min} are the limiting heights corresponding to the extremes of free surface area that are associated with a particular drainage system. In the Little Fool Creek system and others that the author has observed, A_{max} occurs at an h_{max} which produces complete, or nearly complete flooding of the marsh. At this point there is general contact with the free surface areas of the adjacent drainage systems and little exposed land remains,

with the exception of a few scattered levees along the trunk channel (Figure 14). At the other extreme, A_{min} occurs at h_{min} below which there is little change in area. Referencing heights to a MLW datum, h_{min} will usually be a negative value corresponding to an extreme low. In practice, the exact level at which h_{min}, A_{min} are found is not especially critical in terms of the overall distribution of area, although a restriction of Equation (11) is that A_{min} must be greater than zero. Figure 14 shows that at a level of about 0.2 m below MLW, A_{min} converges to the area of several pools of trapped water.

Equation (11), as written, is not convenient for determining area as a function of height, as will be required in this investigation. Defining $r = A_{min}/A_{max}$ and the dimensionless area as $A' = (A - A_{min})/(A_{max}-A_{min})$, a more suitable form is

$$A' = \frac{r(1-G)}{r + G(1-r)} \; ; \; G = (1-h')^{1/z} \qquad (12)$$

Figure 15 shows a hypsographic curve based on Equation (12) that was fitted to height-area data obtained for Little Fool Creek using photogrammetric methods (see instrumentation and methods section). The parameters used are listed in Table 7.

Figure 14. Black and white infrared photograph of Little Fool Creek pictured during the maximum flooding stage (MLW + 1.20 m or 3.94 ft).

Figure 15. Hypsographic curve based on area-height data obtained for Little Fool Creek. Data points for the Duplin River, Georgia, are from Ragotzkie and Bryson (1955).

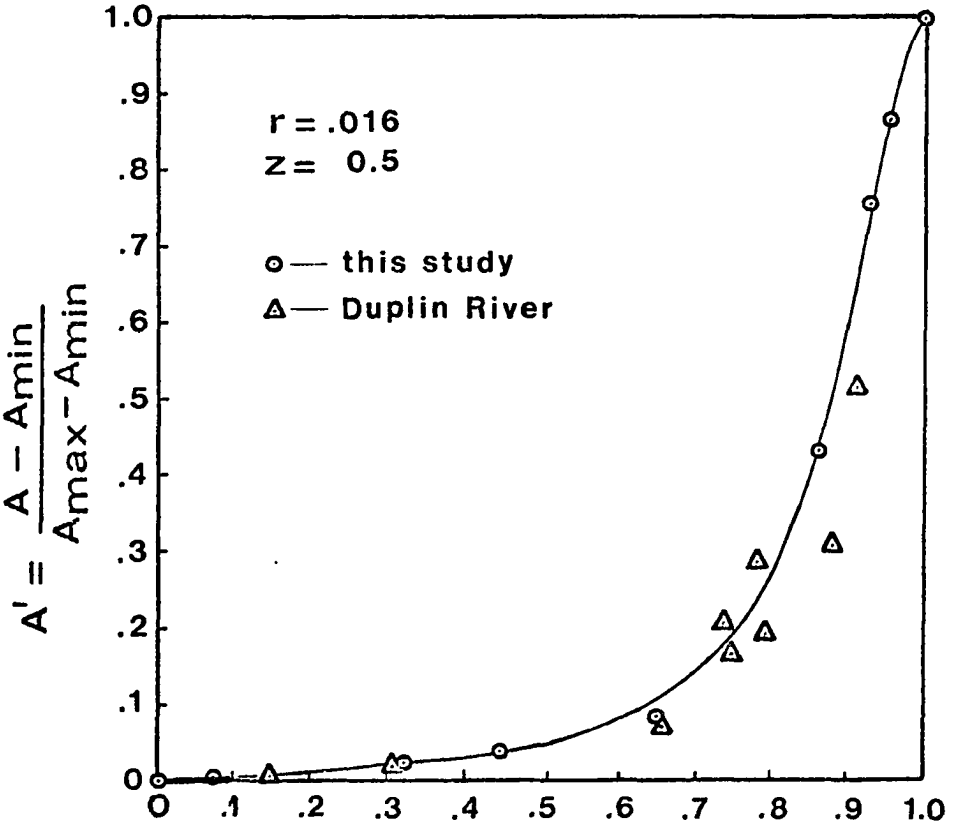

TABLE 7

LIST OF HYPSOMETRIC PARAMETERS FOR LITTLE FOOL CREEK

A_{max} = 80,200 m^2, A_{min} = 1,310 m^2

h_{max} = 1.20 m, h_{min} = -0.20 m

z = 0.50, r = 0.016

As it happens, few data are available to test the validity of the present technique in other salt marsh areas, with the exception of a study by Ragotzkie and Bryson (1955) conducted for the Duplin River at Sapelo Island, Georgia. Using U.S.C. and G.S. charts and measuring slope angles of the river bank, these authors were able to derive area-height data which are shown in Figure 12 of their paper. Using the data contained in their figure, the author calculated dimensionless heights and areas by taking the lowest height (MLW) and area ($1.7 \times 10^6 m^2$) reported as h_{min} and A_{min} respectively, and extrapolating the area from their curve corresponding to the highest tide observed by them, namely $1.83 \times 10^7 m^2$ at 3.2 m, for A_{max} and h_{max}. The authors state (p. 309) that the marshes adjacent to the Duplin were completely inundated at the latter height. Although the Duplin River data lack precision owing to the methods employed, there is a surprising agreement in form (Fig. 13) with the hypsographic curve derived for Little Fool Creek, a system more than two orders of magnitude smaller in terms of both tidal height and free surface area.

Further field investigation of this important relationship is needed.

Tidal Prisms

After constructing a hypsographic curve such as the one shown in Figure 15, it is a simple matter to obtain the total volume of discharge, or tidal prism, for any combination of high and low water values transformed into dimensionless form. Recalling Equation (10), one simply measures the area underneath the hypsographic curve between these values. To convert to true volume, the formula

$$Q = (A_{max} - A_{min})(h_{max} - h_{min})Q' + A_{min}(H_{max} - h_{min})\Delta h'$$

is used where Q = true volume, Q' = dimensionless volume, $\Delta h'$ = dimensionless range, and the other values are as previously defined. Any "overmarsh" volumes are accounted for by considering the area to be constant ($A' = 1.0$ when $h' \geq 1.0$). Volume changes below the minimum stage can normally be neglected ($A' = 0$ when $h' \leq 0$).

A computer program for the IBM 1130 is given in Appendix B which performs the integrations numerically for any given tidal cycle beginning with low water.

Figure 15 is also helpful in visualizing the process by which a particular combination of tidal factors, such as mean tide level and range of tide during an individual cycle, correspond to a particular tidal prism. For example, a spring tide may produce large flood and ebb prisms because of a large range. An equally large set of prisms could

result for a tide having much less range but a higher average tide level perhaps due to setup caused by a storm. This is the reason why tidal creeks are not amenable to stream gauging (stage vs. discharge) techniques as applied to inland rivers. As pointed out by Myrick and Leopold (1963), in their study of a small tidal estuary, a given stage of tide may be accompanied by an unlimited number of discharges. This is so because prisms which provide the discharge are determined by various combinations of range and stage.

A comparison of the prisms predicted by the hypsometric model using Equation (10) and actual tide data was made against prisms derived from current measurements at Little Fool Creek for those same tides. The reader is referred to the section on instrumentation and methods for details of the measurement procedures. The results are shown in Table 8.

The generally good agreement between measured and predicted prisms evidenced in these results supports the principal assumptions inherent in the model:

1. Coherent marsh drainage system with conveyance largely confined to high-order channels.
2. Height-area relationship according to a modified form of Strahler's hypsometric formula.
3. Approximately level free surface over the drainage area.

A discrepancy which does appear in Table 8 is the slight ebb residual in measured prisms beyond any predicted

TABLE 8

A COMPARISON OF TIDAL PRISM VALUES (m^3)
DERIVED BY THE HYPSOMETRIC MODEL
AND BY FLOW MEASUREMENTS AT THE
ENTRANCE TO LITTLE FOOL CREEK

Run	Phase	Model	Measured	Tide[1] (m)
1	Flood	46,224	44,661	-.12 to 1.52
(5/16/72)	Ebb	46,119	45,979	1.52 to -.06
	Residual	+ 105	-1,318	
	% of GA[2]	0.2	2.9	
2				
(6/30/72)	Flood	26,468	27,871	0.15 to 1.28
	Ebb	26,595	29,982	1.28 to 0.09
	Residual	- 127	-2,111	
	% of GA	0.5	7.3	
3	Flood	38,965	40,624	-.09 to 1.43
(8/1/72)	Ebb	38,741	42,269	1.43 to 0.03
	Residual	+ 224	-1,645	
	% of GA	0.6	4.0	
4	Flood	19,140	21,433	0.21 to 1.19
(8/31/72)	Ebb	19,340	22,542	1.19 to 0.12
	Residual	- 200	-1,109	
	% of GA	1.0	5.0	
5	Flood	7,034	7,184	0.17 to 0.97
(10/16/72)	Ebb	7,105	7,347	0.97 to 0.14
	Residual	- 71	-163	
	% of GA	1.0	2.2	

[1]Tidal heights (m) are referenced to MLW as determined by method of simultaneous comparisons (Marmer, 1951; Boon and Lynch, 1972). Other constants include MN = 1.22 m (4.0 ft), MTL = 0.61 m (2.0 ft).

[2]GA = gross average of flood and ebb prisms.

TABLE 8. COMPARISON OF TIDAL PRISMS (Cont'd.)

Run	Phase	Model	Measured	Tide (m)
6	Flood	37,613	37,288	0.44 to 1.43
(11/12/72)	Ebb	37,613	37,679	1.43 to 0.44
	Residual	0	- 391	
	% of GA	0	1.0	
7	Flood	28,909	30,201	0.41 to 1.32
(11/30/72)	Ebb	29,608	32,232	1.32 to 0.18
	Residual	- 698	-2,031	
	% of GA	2.4	6.5	
8	Flood	22,575	24,530	0.10 to 1.23
(12/11/72)	Ebb	22,449	24,048	1.23 to 0.16
	Residual	+ 125	+ 482	
	% of GA	0.6	2.0	
9	Flood	47,889	41,986	-.47 to 1.54
(12/20/72)	Ebb	47,889	44,962	1.54 to -.20
	Residual	0	2,976	
	% of GA	0	6.8	
10	Flood	6,569	6,201	-.02 to 0.94
(1/24/73)	Ebb	6,695	6,992	0.94 to -.10
	Residual	- 126	- 790	
	% of GA	1.9	12.0	
11	Flood	28,641	26,275	-.35 to 1.30
(3/19/73)	Ebb	28,580	28,405	1.30 to -.13
	Residual	+ 60	-2,130	
	% of GA	0.2	7.8	

by the model in the case of unequal low waters. This may be real (a possible violation in part of assumption 1.), or due to a systematic error in the discharge measurements. However, the precision estimate for discharge measurements (about 5%, see measurement error analysis section, p. 21) is not greatly exceeded by most of these residuals, expressed as a percentage of the average flood and ebb discharge. Moreover, the model itself is subject to certain errors, primarily those involved with the measurement of tides and assumption 3.

In addition to tide gauge errors and quantization errors incurred while digitizing analog records, perturbations do exist in the real tide curve. The author investigated the possible extent of the error from these sources by conducting a simultaneous comparison of tides for two tide stations a short distance apart in the area, Wachapreague Dock and Little Fool Creek. Supposing that either station could provide tidal heights for the model in Little Fool Creek, the differences found in corresponding high and low water heights for both stations were used to obtain error estimates which were found to be approximately ± 4 cm for high tides and ± 6 cm for low tides based on a comparison of 89 tides. Introducing various combinations of these errors into the model revealed little change for low water variations but high water variations produced prism errors of about 7% for the larger volumes ($> 40{,}000\ m^3$). The sample of measurement runs obtained

appear to fall well within these limits of the model which seem appropriate for individual runs. The one exception is that of the flood prism for run 9, the maximum prism predicted (47,889 m^3) and the highest tide reached (1.54 m). At these levels, the conveyance onto the marsh may bypass the main creek to some extent, accounting for the low measured prism (41,986 m^3).

Frequency Distribution of Prisms

One of the advantages to having a numerical model for tidal prisms is that of hindcasting prism values for the observed tides and determining their frequency of occurrence at various magnitude levels. This type of information may have applicability in any closed marsh drainage system which can be hypsometrically typed and for which tides are available. The resultant distributions may, for example, be used as an index of the flushing characteristics of the marsh at various times of the year. The information is also likely to be important to geomorphologists who have traditionally utilized discharge-frequency relationships to explain river channel characteristics, particularly hydraulic geometry (Leopold and Maddock, 1953; Wolman and Miller, 1960; Langbein, 1964). In terms of the erosion and transport of suspended sediment in tidal channels, the prism is also a measure of the energy available to do work in a given semidiurnal interval (Langbein, 1963; in Myrick and Leopold, 1963).

Although the prisms simulated by the present model have an obvious dependence on tidal range and some characteristic stage (be it high water, low water, or mean water level for any cycle), there does not appear to be any formulative means of relating any combination of tidal parameters to given values of the prism, owing to the nonlinearity in the hypsometric formula. A glance at Figure 15 would indicate, however, that given reasonably small variations in range, a positive trend should exist to some degree between prism and high water stage. This is, in fact, the case as can be seen in Figure 16 which is a plot of simulated prisms and their corresponding high water stages observed over a four-month period.

The question then centers on the trends in high water stage observed during the year. These can be seen in Figure 17 which shows monthly mean high water levels for a three-year period at Wachapreague Dock.

As indicated in Figure 17, there is an apparent annual cycle in which the lowest mean high water levels are commonly found in January and February, and the highest in September, October and November. This type of cycle for monthly mean high water conforms to the well known cycle of oscillation for monthly mean sea level in many parts of the world that has been shown to correspond to monthly variations in steric sea level (Pattullo, et al, 1955). At Hampton Roads in Chesapeake Bay, 20-year averages of monthly mean sea level show noticeably higher values for

Figure 16. A plot of tidal prisms, simulated by the height-area model, versus high water stage. Actual tides from Wachapreague Dock were used for the months of January, February, September and October, 1972. Actual prisms measured at Little Fool Creek are included for comparison.

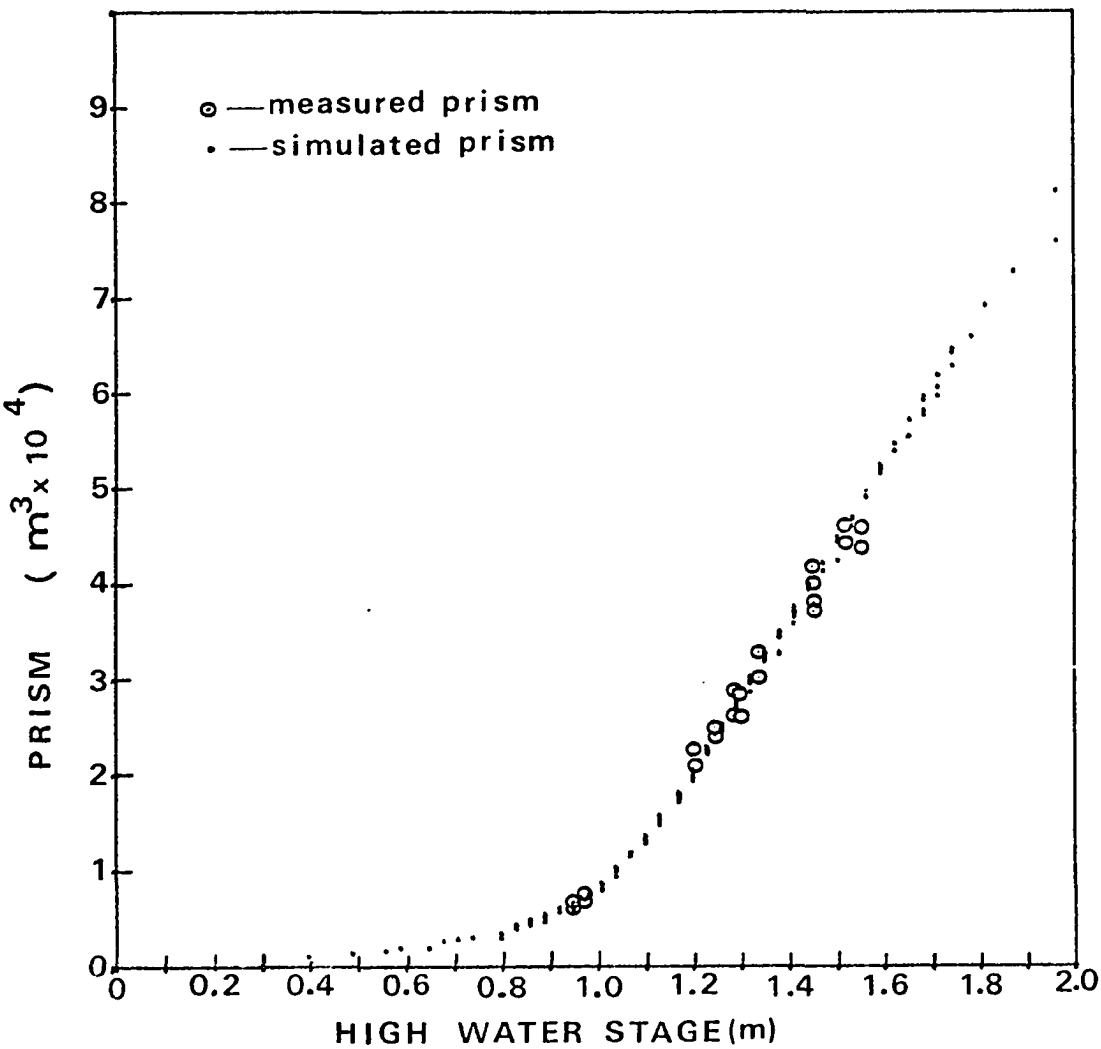

Figure 17. Monthly mean high water at Wachapreague Dock, November 1969 through October, 1972.

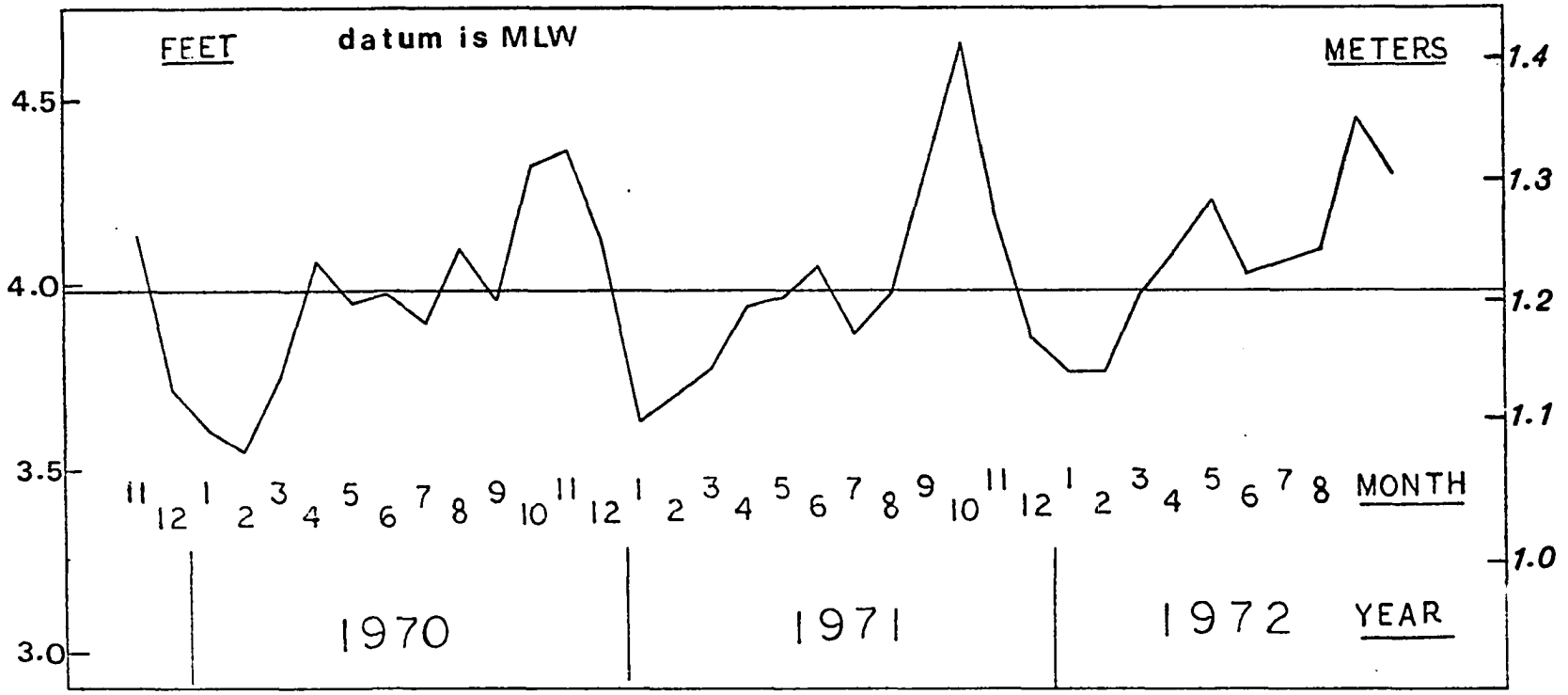

the period August through October while the lowest values occur during the period December through March (Pattullo, op. cit., p. 129). This seasonal trend being evident in Figure 17, it would seem fruitful to use some of this data to test for a seasonal effect in tidal prisms in the study basin.

Using the hypsometric model, prisms were calculated for each tide occurring in the months of September, October, January and February, 1972. The results were used to compute frequency of occurrence of prisms arranged in classes at intervals of 5000 m^3. These data are shown in Figure 18a. As expected, prisms for the test creek have significantly higher mean and median values during September and October as compared to January and February. Moreover, these extreme seasonal differences appear consistent at all but the highest prism levels, in addition to those of the mean and median; i.e., a 10,000 m^3 prism is exceeded more often in September than in January, as is a 40,000 m^3 prism, etc. Arranging the data on a quarterly basis (Figure 18b), the seasonal trend would seem to consist of a sequence of progressively greater mean and median prisms, beginning with the January-March quarter and ending with the October-December quarter. Although only one year of data has been presented, the fairly obvious connection with a well established tidal phenomena renders a high degree of certainty to the conclusion that this trend will persist year after year. The field researcher conducting hydraulic

Figure 18. Distribution of simulated tidal prisms in Little Fool Creek showing a. extreme monthly distributions, b. quarterly distributions.

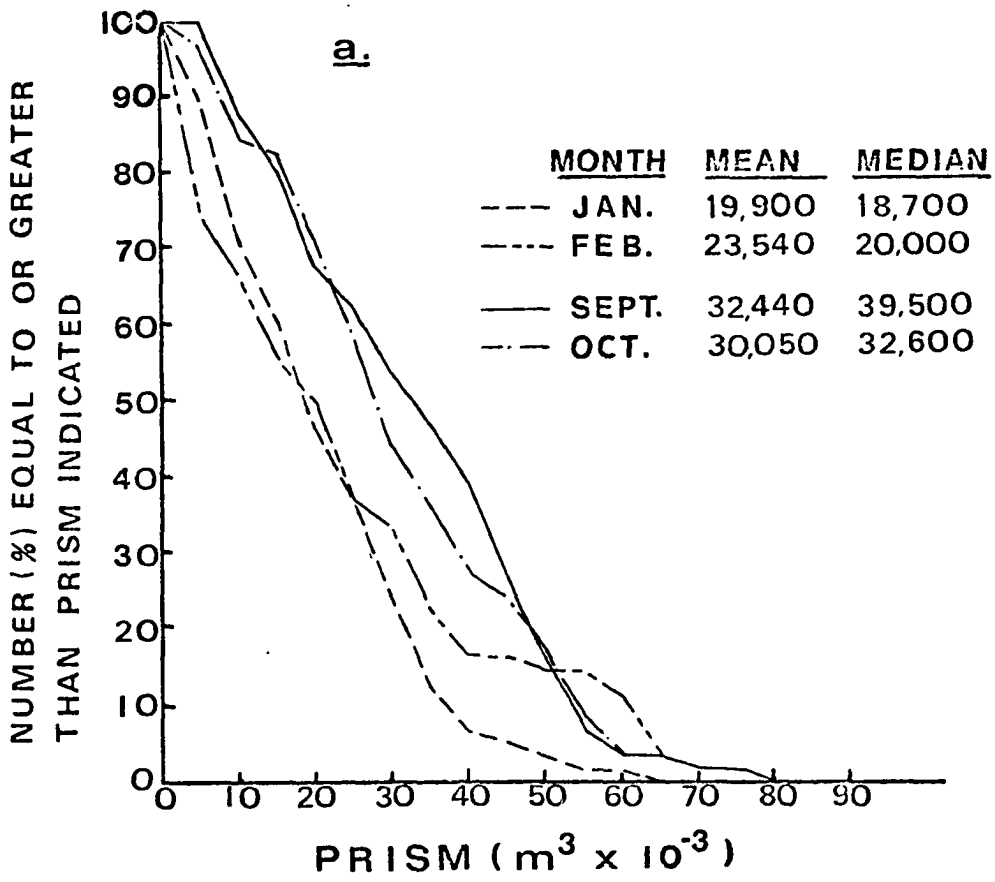

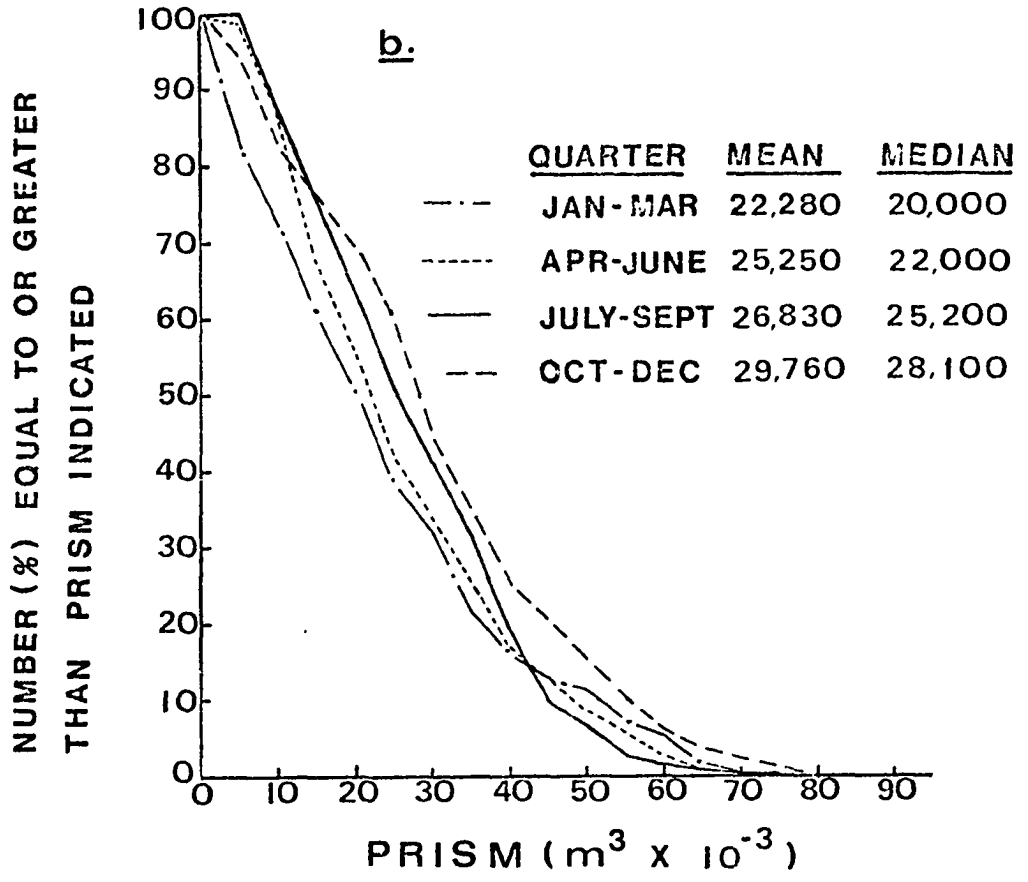

experiments of various kinds in a tidal marsh drainage system should therefore keep two points in mind regarding semidiurnal discharge volumes: (1) the relationship of the experiments to the seasonal effects produced by the tide, (2) the variability inherent in single experiments conducted over one tidal cycle as compared to the seasonal norm in prisms.

Time-Varying Tidal Discharge

In developing models that simulate the tidal prism in a drainage system, one obtains as a consequence the average discharge rate (m^3/sec) if the duration of flow is known. In reversing flows characteristic of most small tidal creeks, the flood and ebb durations correspond for all practical purposes to the rise and fall durations, whose average values have already been presented for the Wachapreague area (Tables 4-6). But on the basis of this information alone, one cannot determine what the discharge curve looks like through time, nor what the maximum rates are likely to be, or where the maxima will occur in the cycle. It is safe to say that a knowledge of sediment transport processes in the system of interest will remain limited without some understanding of the temporal aspects involved. More will be said about this matter in the section dealing with suspended sediment transport.

Recalling Equation (9), the time-varying discharge was given from continuity considerations as

$$q = A \frac{dh}{dt} \tag{9}$$

where A is now understood to be a function of tidal height according to the hypsometric formula [Eq. (7)]. Tidal height, in turn, is given by the tidal model [Eq. (4)] which also gives

$$\frac{dh}{dt} = -R_1 'H\, \omega \sin \omega t - 2K_1 R_1 '^2 H^2 \omega \sin (2\omega t - \phi_1) - 3K_2 R_1 '^3 H^3 \omega \sin(3\omega t - \phi_2) \tag{13}$$

Note that the amplitude coefficients of the first and second harmonic terms have doubled and tripled respectively in relation to the fundamental amplitude in Equation (13) as a result of differentiation.

Using the models for tide and area, Equation (9) is now a suitable model in itself for simulating discharge as a function of time at the entrance to the marsh drainage system. The three assumptions made previously for the prism model [Eq. (10)] will also apply here.

Equation (9) immediately implies that the maximum discharge occurs at those points in the tidal cycle for which the product of free surface area and slope of the tide curve is at a maximum. The hypsometric formula [Eq. (12)] portrays a bounded area whose maximum is attained at h_{max} = 1.2 m above MLW in the study area, but which increases most rapidly with height just before reaching h_{max}. The slope term, of course, is modified by the harmonic input in

Equation (13) to a greater or lesser extent depending on the mean tidal amplitude, H.

Figure 19 contains three examples of discharge curves simulated by the model for three different values of H (the mean water level, R_o, is constant). The time scale is fixed by the choice of origin in Equations (8) and (13); high waters occur at the zero crossings indicated in mid-scale. These examples approximate what would be classed as neap, mean, and spring tide conditions in Little Fool Creek, ignoring the longer period tidal fluctuations and diurnal inequalities. To see the effect of the shallow-water tides, each curve based on all three terms of Equation (13), shown as a solid line, is also compared with a similar curve computed without the higher harmonics and shown as a dashed line. Figure 19 reveals that the shallow-water tides are of little importance when the tidal amplitude is small (H = 0.45 m), as a consequence of the overtide dependency on parent wave amplitude (p. 36). However, for the larger amplitude (H = 0.72 m), the shallow-water constituents add approximately 20% to the maximum discharge values, in addition to shifting the times of occurrence for the latter. Hence, the shallow-water contribution appears to be significant, even though the most important factor with respect to the peak asymmetry in the higher amplitude curves is the factor of the drainage basin morphology which fixes the value of A for a given tide level.

Figure 19. Simulated tidal discharge curves for three different values of mean tidal amplitude, H, at Little Fool Creek. Solid lines include shallow-water harmonic terms of Equation (8), dashed lines include the fundamental oscillation only ($2R_1 = H$; R_2, $R_3 = 0$).

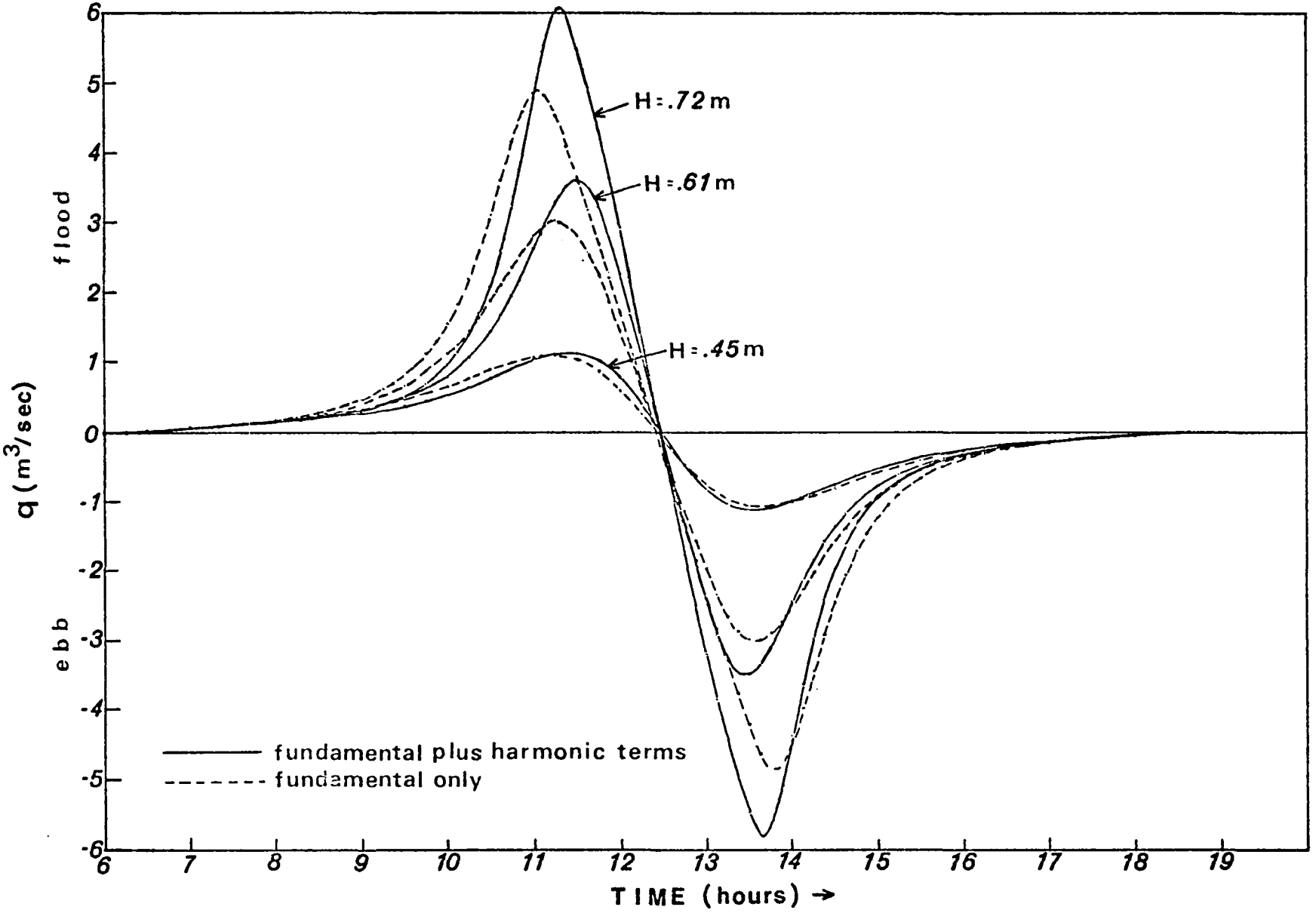

In sum, the general picture that emerges from the model is that of a highly distorted discharge curve whose peak values show a pronounced shift toward the zero crossing at high water. The peakedness of the discharge extrema increases with tidal amplitude as do the shallow-water tidal constituents which contribute significantly to the maximum values of the discharge at the higher tidal amplitudes. The conclusion which must be reached, however, is that the three assumptions made (p. 78) with regard to the model are likely to be much more critical in terms of the actual magnitudes and shape of the real discharge curve. For example, local free surface slopes caused by wind stress and frictional effects may cause changes in dh/dt at various times that equal or exceed those contributed by the tide.

Observed Tidal Discharge

The reader is referred to Appendix A for the detailed results of the measurement runs made at Little Fool Creek. The methods employed to obtain these results are discussed in the Instrumentation and Methods section. The shape of the discharge curves in Appendix A generally reflect the type of asymmetry predicted by the discharge model, with peak discharges for the higher amplitude runs (higher tidal range) occurring at about 1.2 to 1.5 hours on either side of high water slack. For convenience, the maximum values of the observed discharge peaks are listed in Table 9, along with the pertinent tidal height data.

TABLE 9

DISCHARGE MAXIMA OBSERVED AT ENTRANCE TO LITTLE FOOL CREEK. TIDE DATUM IS MLW

Run	Phase	Max. (m^3/sec)	Tide (m)
1	Flood	5.44	-.12 to 1.52
(5/16/72)	Ebb	6.04(+11%)	1.52 to -.06
2	Flood	3.60	0.15 to 1.28
(6/30/72)	Ebb	4.70(+31%)	1.28 to 0.09
3	Flood	5.00	-.09 to 1.43
(8/1/72)	Ebb	5.90(+18%)	1.43 to 0.03
4	Flood	2.85	0.21 to 1.19
(8/31/72)	Ebb	3.60(+26%)	1.19 to 0.12
5	Flood	0.66	0.17 to 0.97
(10/16/72)	Ebb	0.95(+44%)	0.97 to 0.14
6	Flood	3.80	0.44 to 1.43
(11/12/72)	Ebb	4.35(+15%)	1.43 to 0.44
7	Flood	3.65	0.41 to 1.32
(11/30/72)	Ebb	4.75(+30%)	1.32 to 0.18
8	Flood	2.84	0.10 to 1.23
(12/11/72)	Ebb	4.46(+57%)	1.23 to 0.16
9	Flood	5.44	-.47 to 1.54
(12/20/72)	Ebb	6.04(+11%)	1.54 to -.20
10	Flood	0.68	-.02 to 0.94
(1/24/73)	Ebb	0.84(+24%)	0.94 to -.10
11	Flood	3.91	-.35 to 1.30
(3/19/73)	Ebb	5.05(+29%)	1.30 to -.13

One of the most interesting features observed in this study is that, as shown in Table 9, all of the peak ebb discharge values exceed their flood peak counterparts by amounts ranging from 11 to 57%. These differences are much in excess of the residuals found for the flood and ebb prisms (Table 8) and must reflect changes in the discharge distributions within each phase. This change appears to occur in the form of greater "peakedness" and a narrower range for the higher ebb discharge values. This phenomena was also observed by Pestrong (1965, p. 18) in a San Francisco Bay marsh and was attributed by him to be due to a relationship between cross-sectional area and frictional effects during the ebb. On p. 20 he states:

> "This relationship is accentuated on the marshes, for, in addition to an increasing time lag on the marsh surface due to decreasing cross-sectional area available for [ebb] flow, considerable resistance is offered to overmarsh flow by the marsh vegetation. This would further increase the water slope and cause even greater flow velocities in the channels during the ebb cycle."

Although Pestrong is speaking of velocity in the above quote, his illustration on p. 19 shows very similar curves for both velocity and discharge.

In the present author's opinion, such an explanation of the frictional effect may be oversimplified. Certainly frictional effects operate in both the flood and the ebb directions though perhaps not to the same degree. Moreover, the onset of a typical ebb cycle follows immediately after the high water stage and most of the significant flow passes

in a short time. This behavior does not fit comfortably with simple resistance which implies a lag or "holding back" of the ebb flow. It is more likely that the purely kinematic flow field of the author's model (which takes no account of forces) is augmented to a certain extent by local hydraulic gradients which have a particular cycle of their own. To simulate these gradients adequately would require a dynamic model including friction and inertia terms. This type of model would be difficult to develop for marshes because of the nonsteady flow conditions there and the nonlinearity of the friction terms in the equations of motion. Comparing Table 9 with Figure 19 reveals that the kinematic model does indicate maximum discharge values of the right order of magnitude, which could be adjusted to reflect the observed inequality for predictive purposes.

Wind Effects

Actual measurements of the discharge through time are likely to be required wherever critical determination of transport phenomena is the objective, particularly in view of wind stress effects which are very difficult to model in the winding marsh channels, where direction as well as wind speed will be important. Thus, it is very hard to judge the contributing effects of winds during some of the measurement runs reported in this study (see Table 9, Appendix A).

Wind data were compiled for a permanent gauging station at Wachapreague Dock and summarized. In addition to reporting the winds prevailing during each run, shown on the title page for each run in Appendix A, the daily vector average wind speed and direction was computed and is shown for the months of April, 1972, through March, 1973, in Figure 20a. As a measure of the total wind activity during each day, the directionless or absolute wind values are shown in Figure 20b. Both figures show the positions of the measurement runs during their respective months.

Figure 20. Wind data, Wachapreague Dock: (a) vector average wind speed and direction, (b) absolute wind speed.

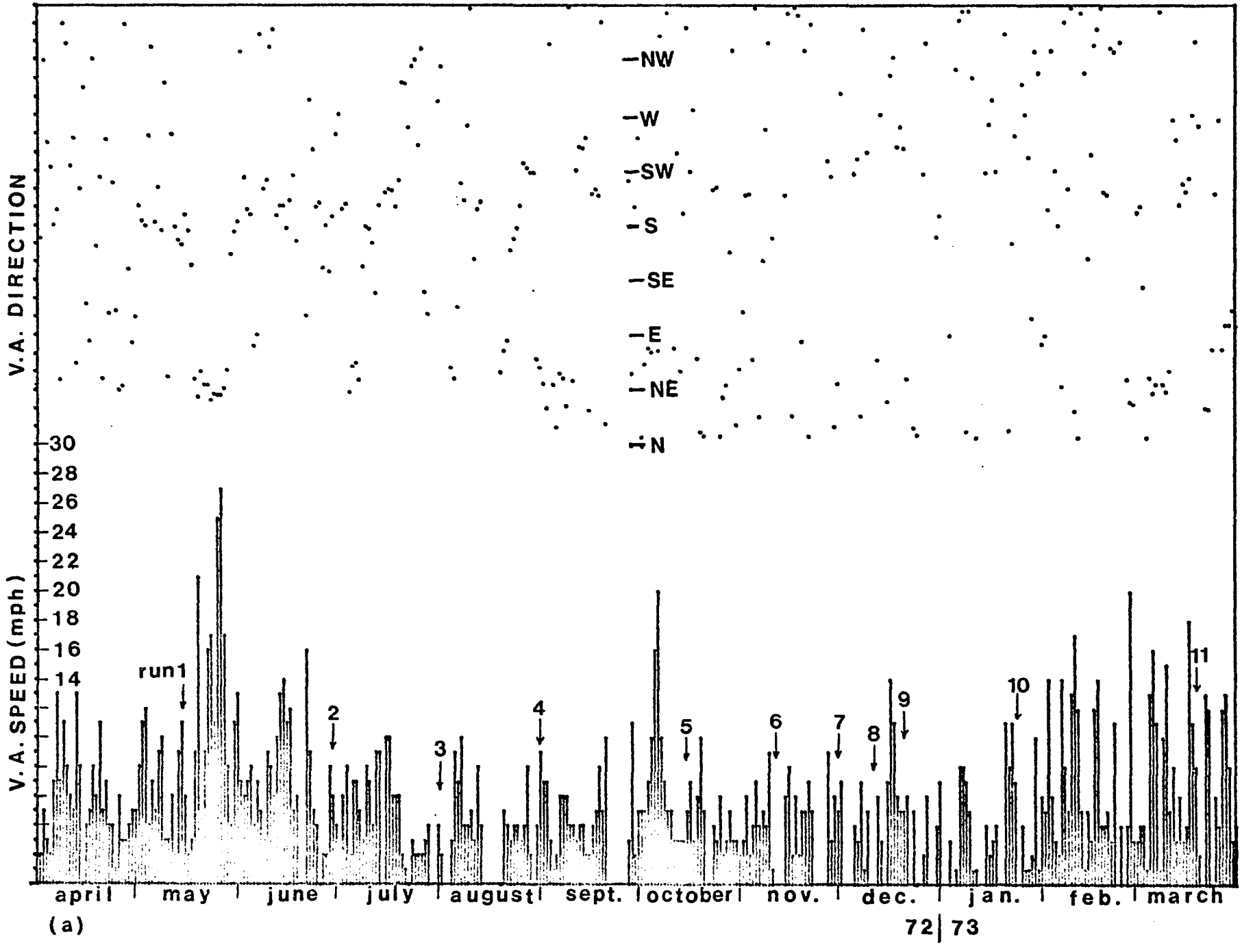

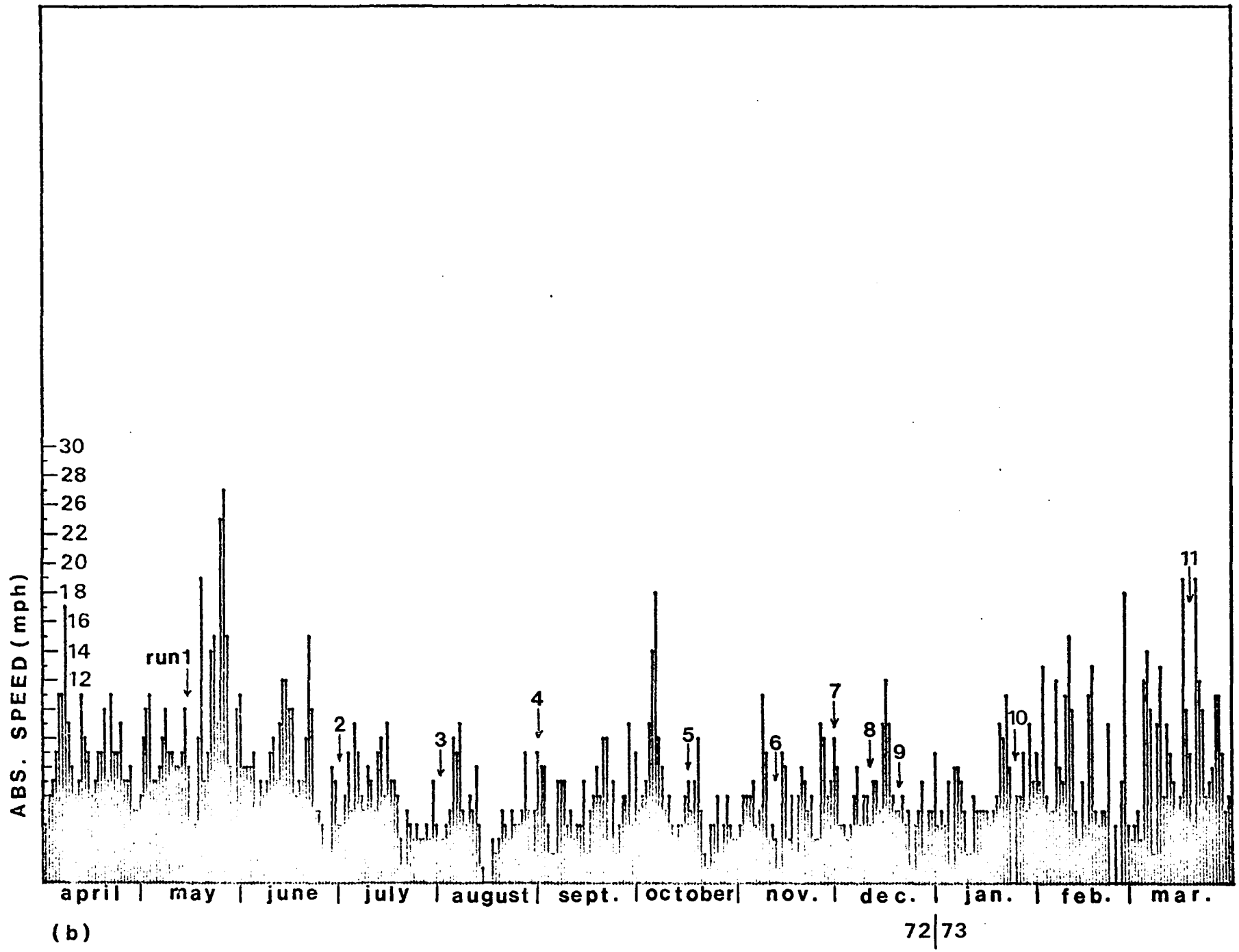

TRANSPORT OF SUSPENDED SOLIDS IN MARSH CREEKS

Introduction

Increasing attention has been given in recent years to the transport of both particulate and dissolved substances into and out of marshes via tidal flow. The biologist views the marsh as productive of various organic constituents and would like to know the extent to which the marshes retain or export these substances, either as particulate organic matter (POM) or dissolved organic matter (DOM) into adjacent biotic systems (De La Cruz, 1965; Pomeroy, et al, 1972). Geologists, on the other hand, seek information on the transport of suspended sediments to and from marshes. Since the marshes themselves are the result of local sedimentary processes, the tidal transport of suspended material (both organic and inorganic solids) must play a role in their continuing evolutionary history (Chapman, 1960; Redfield, 1965; Pestrong, 1965, 1970).

The present work will deal only with a specifically defined system, the marsh drainage network and the confined channels. This system is considered as a distinct, coherent unit which is normally easy to identify and distinguish from adjacent systems such as the larger estuaries and tidal mud

flats. To date, little has been done to investigate in detail the processes of sediment transport into and out of salt marshes and to evaluate the effects on present day marsh growth or decay.

The transport of bulk suspended solids will be dealt with in this work, differentiating only the combustible and noncombustible fractions. Questions of size distribution and the state of aggregation or agglomeration of fine-grained composite particles will not be addressed, including the very specialized question of clay floccule size equilibria in flows of varying fluid shear, sediment concentration and salinity. A review of these subjects has been presented by Swift, et al. (1972).

Transport of Suspended Solids

During a number of the runs previously described for the study site, suspended solids were collected in numerous water samples obtained simultaneously with current measurements. These data permitted the flux of suspended solids past the stream cross-section to be determined at discrete intervals of time. After graphically plotting flux versus time and passing a smooth curve through the points (an approximation to the true curve of flux through time), the total transport of solids over each portion of the tidal cycle was obtained by integrating the respective areas under the curve, as shown in Figure 21.

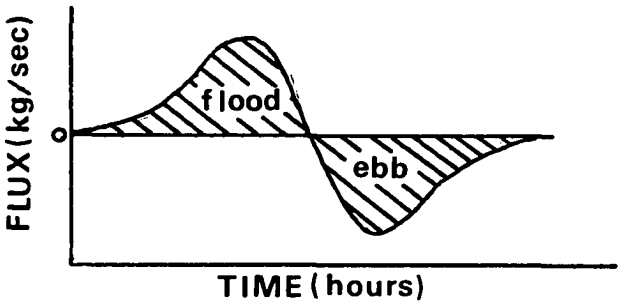

Figure 21. Flux curve and total suspended solids transport (area under curve).

Although the procedure outlined above is seemingly straightforward, a number of very basic questions arise in setting up the sampling design for the measurements involved. The questions center on the sufficiency of the spatial and temporal sampling intervals employed. These intervals must be chosen carefully to avoid introducing large errors into the transport estimates. Obviously, if one cannot ascribe an accuracy of at least 10% to either the flood or the ebb transport, then one has no basis for inferring a residual transport, even as to its direction (into or out of the marsh), that does not exceed 10%. The author has addressed these questions in a special presurvey conducted at the study creek which is presented along with a discussion of probable propagation of errors in the Measurement Error Analysis section of this paper. The final procedures employed for both laboratory and field work are given in detail in the Instrumentation and Methods section.

Of the eleven runs made at the entrance to Little Fool Creek (Little Fool No. 1), eight include measurements of suspended sediment transport. The pertinent data for these

runs may be found in Appendix A, along with computer-derived curves of the suspended solids flux. The flood and ebb transport values are summarized in Table 10 for convenience. In Table 10, it is noted that, unlike the measured prisms, the transport values have residuals which are clearly significant in terms of the measurement errors expected (about 7%). A cautious interpretation of these results, allowing for the differences among tides, is that the late spring and summer months may well be typified by higher levels of transport in association with strong ebb residuals, whereas the fall and winter months evidence much lower levels of transport and weaker flood residuals. Run 8S (3/19/73) appears to reflect an early spring renewal of high transport levels accompanied by a strong flood residual. Before speculating further, it is worthwhile to examine several associated relationships that affect transport.

Current Speed - Discharge

The methods employed in obtaining the discharge curves at the entrance to Little Fool Creek permit the computation of spatial averages for current speed through area-weighting procedures in the cross-section (p. 21). As many as eight current speed measurements, depending on the tidal stage, were obtained simultaneously within the cross-section at systematic locations, selected in accordance with the sampling design outlined in the Instrumentation and Methods section. The entire array of current meters were operated

TABLE 10

TRANSPORT OF SUSPENDED SOLIDS OBSERVED AT THE ENTRANCE TO LITTLE FOOL CREEK TIDAL DATUM IS MLW

Run	Phase	Transport (kg)	Tide (m)
1S (5/16/72)	Flood	2119	-.12 to 1.52
	Ebb	3574	1.52 to -.06
	Residual	- 1455	
	% of GA[1]	51.1	
2S (6/30/72)	Flood	890	0.15 to 1.28
	Ebb	2174	1.28 to 0.09
	Residual	- 1284	
	% of GA	83.8	
3S (8/1/72)	Flood	2065	-.09 to 1.43
	Ebb	2821	1.43 to 0.03
	Residual	- 756	
	% of GA	30.9	
4S (8/31/72)	Flood	793	0.21 to 1.19
	Ebb	1043	1.19 to 0.12
	Residual	- 250	
	% of GA	27.3	
5S (10/16/72)	Flood	276	0.17 to 0.97
	Ebb	230	0.97 to 0.14
	Residual	+ 46	
	% of GA	18.1	
6S (12/11/72)	Flood	723	0.10 to 1.23
	Ebb	548	1.23 to 0.16
	Residual	+ 175	
	% of GA	27.5	
7S (1/24/73)	Flood	101	-.02 to 0.94
	Ebb	62	0.94 to -.10
	Residual	+ 39	
	% of GA	47	

[1] GA = gross average of flood and ebb transports.

TABLE 10. TRANSPORT OF SUSPENDED SOLIDS (Cont'd.)

Run	Phase	Transport (kg)	Tide (m)
8S (3/19/73)	Flood	3054	-.35 to 1.30
	Ebb	1617	1.30 to -.13
	Residual	+ 1436	
	% of GA	61.5	

approximately once every half-hour.

Graphic plots of average current speed versus time (Appendix A) show a pronounced similarity when compared with those for the discharge except near the low water tails where discharge values taper off more rapidly due to minimal cross-sectional area available for flow. As an exception, both current speed and discharge tend to be irregular during neap tide conditions when flow rates are minimal and wind effects often dominate the system (e.g., Run 5, 10/16/72 and Run 10, 1/24/73).

Myrick and Leopold (1963) in their development of hydraulic geometry for a small tidal estuary were able to demonstrate a power function relationship between current speed and discharge at a given cross-section. The relationship is of the form

$$u = kQ^m$$

where u = speed, Q = discharge, and k, m are constants. Their figure 13 (p. B14) shows a logarithmic plot of u versus Q for flood phase which somewhat resembles half of a hysteresis loop. Very similar plots were obtained using the data of the present study, an example of which is shown in Figure 22a. Given this log-linear relationship, at least over portions of most tidal cycles, the next step is to examine the position of the maxima for u and Q for a number of different tides, as shown in Figure 22b. The latter figure suggests that the power law given above may include

Figure 22. Current speed - discharge relationship at entrance to Little Fool Creek: (a) u versus Q, (b) u_{max} versus Q_{max}.

(a)

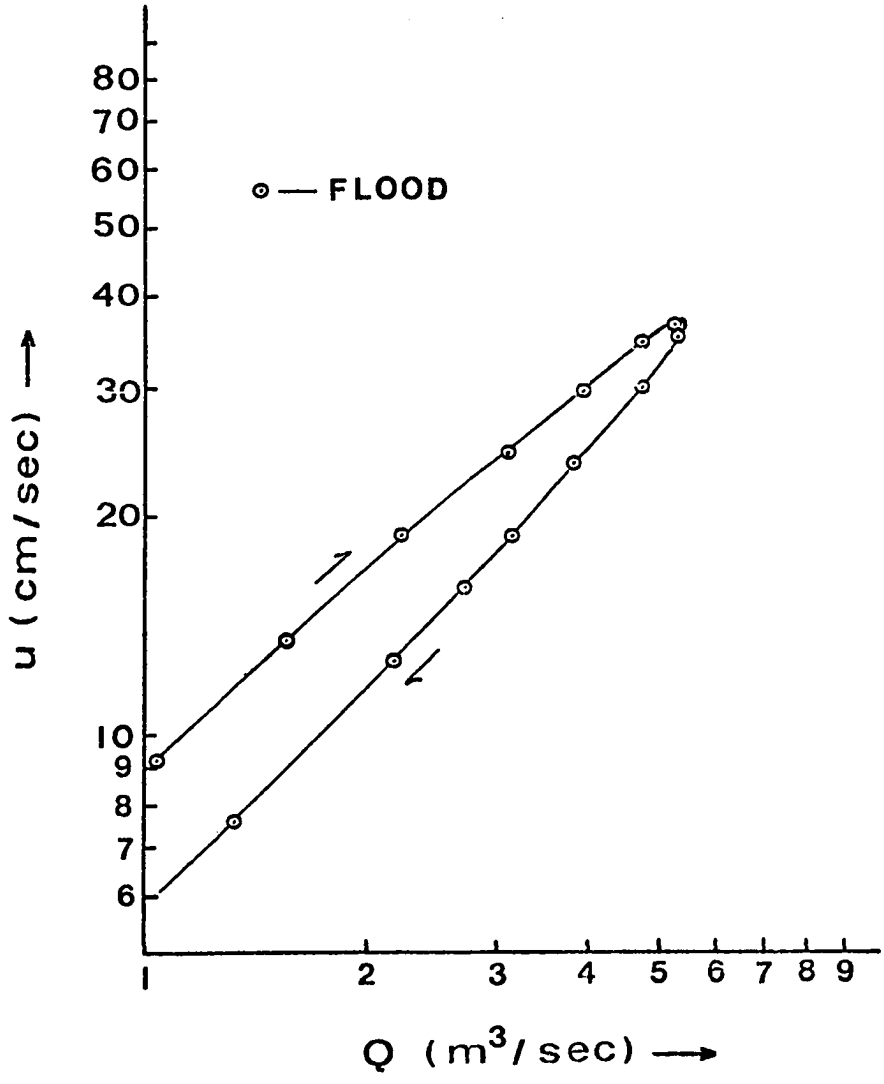

(b)

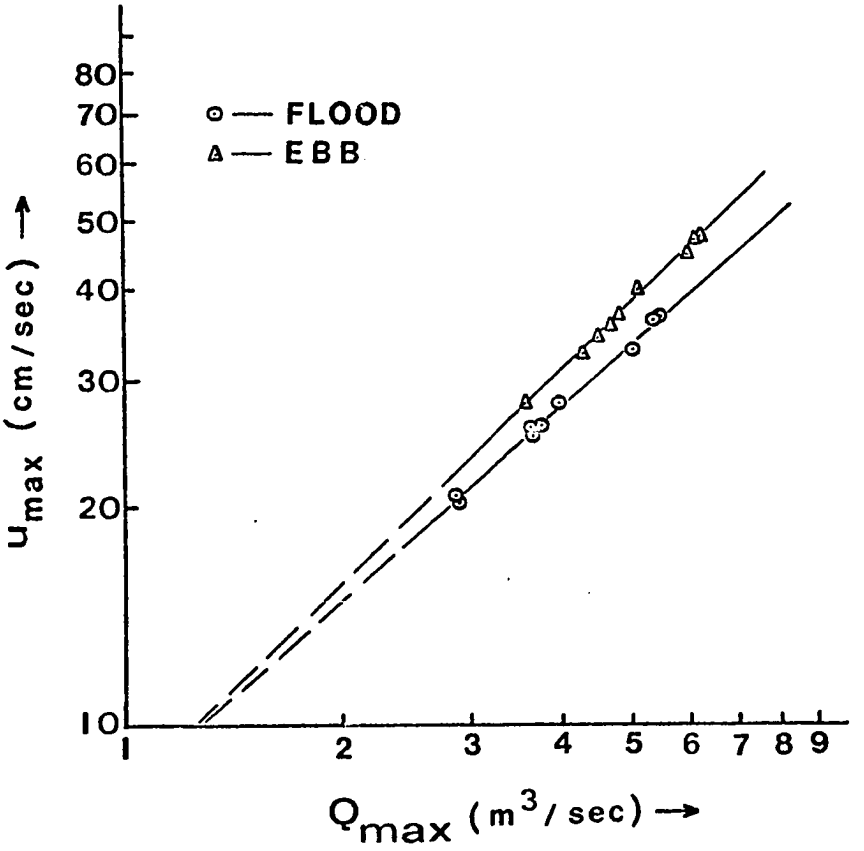

$$u_{max} = k' Q_{max}^{m'} \qquad (14)$$

where k′, m′ are the new constants relating to the maxima. Using least squares methods, the following values were obtained for the data in Figure 22b:

Flood: $m' = 0.875$, $k' = 8.28$

Ebb: $m' = 0.971$, $k' = 8.12$

As a measure of the degree of association (interdependence) of u_{max} and Q_{max}, the correlation coefficient, r, was computed and found to be 0.995 for both flood and ebb phases. Based on the 9 runs used (two neap tide runs were excluded), this value is highly significant in statistical terms and it is concluded that the relationship expressed by Equation (14) is well-founded, regardless of the tidal phase, for the ranges involved ($u_{max} \cong$ 20-50 cm/sec; $Q_{max} \cong$ 2.5 - 7.0 m^3/sec). Without further testing, it also seems apparent that the slope value, m′, for flood and ebb is distinct in each case although this is probably not true for the intercept, k′. Since both u_{max} and Q_{max} normally increase with increasing tidal prisms, the observed divergence of the lines of best fit in Figure 22b may well be a measure of the dynamic effect discussed in the section on time-varying tidal discharge.

The most significant fact revealed by the relationship shown in Figure 22b is that, for any given Q_{max}, there will be a somewhat greater u_{max} for the ebb than for the flood

phase, the magnitude of the difference depending on the magnitude of Q_{max}. This implies that the maximum currents attained during ebb flow will be more effective in initiating scour and suspension of bottom sediments. Equation (14) also suggests the feasibility of predicting maximum currents at Bridge 1, using either observed maximum discharge values or values determined by a model such as that of Equation (9).

Current Speed - Suspended Solids Concentration

Average concentration of suspended solids was determined at discrete times in essentially the same manner as the current speeds, using up to twelve water samplers (Instrumentation and Methods section) operated simultaneously with the current meters. Curves of concentration versus time are seen on the same graphs presented for average current speed (Appendix A) to facilitate comparison.

Restricting attention for the moment to the runs containing significant variation in concentration, it is evident that many of these runs show strong correlative peaks in both concentration and speed near the times of maximum discharge on either side of high water slack. There are as well several examples of lesser peaks in concentration near the low water stages but these are of limited significance where transport is concerned because of the minimal current speeds and diminutive flow sections

extant near low tide. Thus, there is evidence in many of the "high energy" runs (those with large prisms) that the maximum flow speeds are more than sufficient to place bottom sediment in suspension, effecting sharp peaks in the flux curves on either side of the high water stage (e.g., Run 1, 5/16/72).

Erodibility of Fine, Cohesive Bottom Sediments

Sediments on the marshes, and on the bottoms and side walls of marsh creeks are typically composed of fine-grained silts and clays, having a certain organic content, which, in bulk, may be generally described as cohesive soil. Unlike cohesionless sediments (sands and gravels), the erosional properties of cohesive sediments are determined by interparticle attractive forces as well as the hydrodynamic forces of the surrounding fluid. Thus, many of the concepts applied in studies of cohesionless sediment motion in fluids, both as bedload and as suspended load, are not applicable here.

As mentioned previously in the review of the literature, erosion of cohesive sediments begins to take place as flow rates increase to the point where the critical shear stress applied at the sediment-water interface is sufficient to break interparticle bonds and release the material directly into suspension (Partheniades, 1965). This view of the erosive process and the consequent transport of material in suspension does not involve any transport of material as

bedload.[3] Moreover, the minimum shear stresses required to initiate erosion in Partheniades' flume experiments were found to be independent of the shear strength of the bed and were accompanied by mean velocities slightly greater than those which would maintain the clay-sized material in suspension.

During the course of the present experiments, a special set of current profile measurements were made during an average tide at the mid-sections of the three bridges located on Little Fool Creek (shown in Figure 11). The object of this exercise was to determine the approximate bottom shear stress values, τ_o , that are realized at various locations between mouth and head of the creek, using the logarithmic distribution law for vertical velocities

$$\frac{\tau_o}{\rho} = ky \frac{d\bar{u}}{dy}$$

in which ρ = water density, y = distance above bottom, $\bar{u}$ = mean flow speed at y, and k = von Karman's constant. Integrating the equation yields

---

[3]Whether one wants to argue that a bedload composed of agglutinized particles (fecal pellets) and large pieces of organic flotsam exists is a moot point. Amid total suspended loads measured in metric tons, the significance of the latter in terms of mass transport is doubtful.

$$\ln (y + y_o) = \frac{k}{\sqrt{\tau_o/\rho}} \bar{u} + \ln y_o$$

where y_o = the roughness length (point at which $\bar{u} = 0$, a function of the height of the roughness elements on the bottom). Thus, the slope of the curve $\ln(y + y_o)$ versus $\bar{u}$ near the bottom can be used to obtain estimates of τ_o if k and ρ are known. Several such profiles for the three bridges during an ebb flow are shown in Figure 23. The maximum shear stress values for these runs were estimated using $k = 0.4$ and $\rho = 1.04$ and are given along with other pertinent data in Table 11.

TABLE 11

MAXIMUM SHEAR STRESS VALUES, τ_o,
OBSERVED DURING EBB TIDE, FEB. 21, 1973,
LITTLE FOOL CREEK
TIDAL RANGE: 1.2 to 0.0 m above MLW.

Bridge	τ_o (dynes/cm^2)	$\bar{u}$ (cm/sec)	Depth (cm)
1	9.46	28.0	132
2	1.84	18.8	151
3	21.36	30.4	110

The inference drawn from the results in Table 11 is that the shallower the depth, the greater the bottom shear stress and sediment transport capacity. This relationship was also mentioned by Partheniades and Paaswell (1970, p. 757). As a comparison to the magnitudes of τ_o in Table

Figure 23. Vertical velocity profiles measured Feb. 21, 1973, during flood phase at (a) Bridge 1, (b) Bridge 2, (c) Bridge 3. Bridge 1 is closest to the entrance of Little Fool Creek, Bridge 3 is closest to the head of the creek.

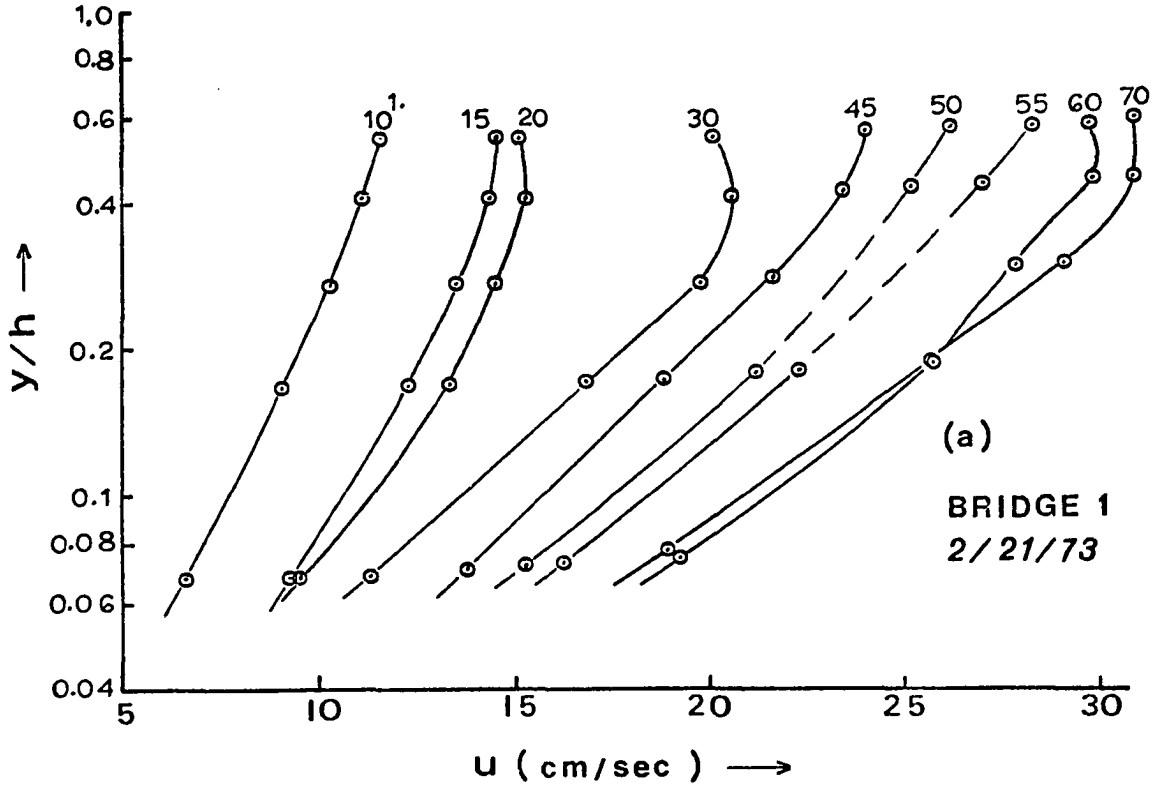

[1]minutes following start of ebb

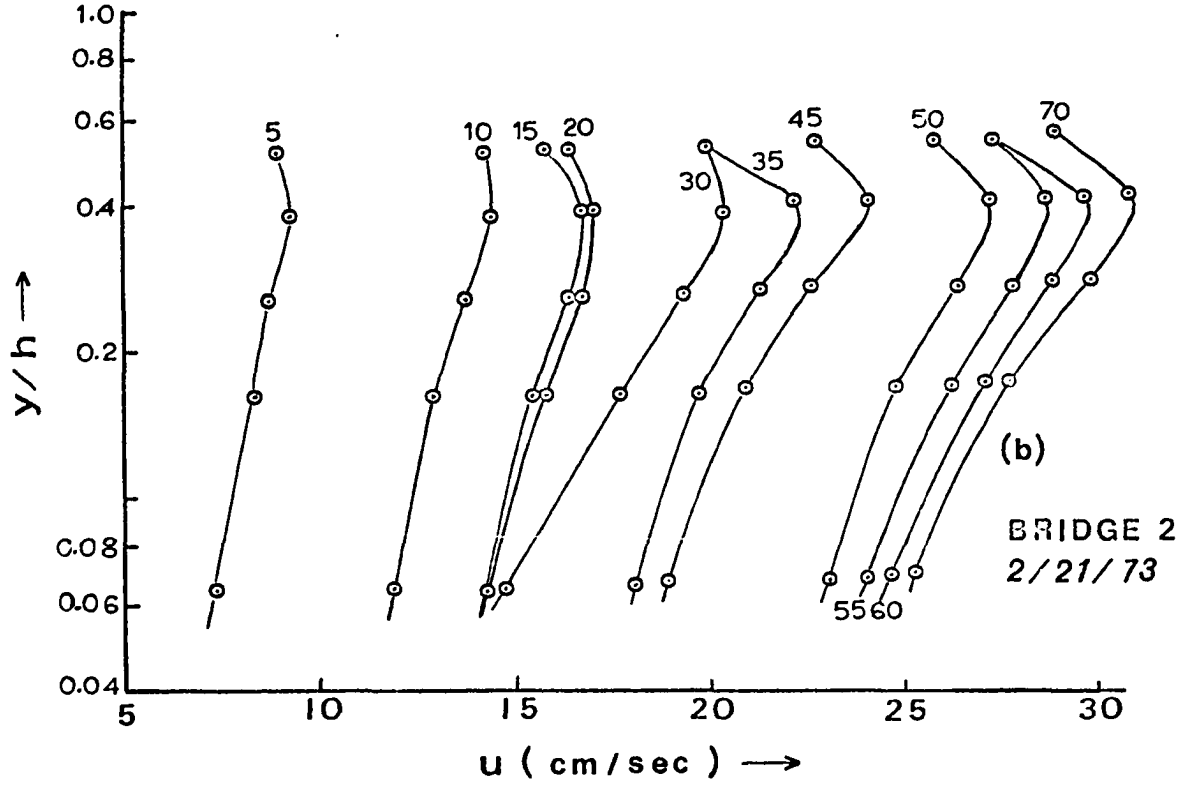

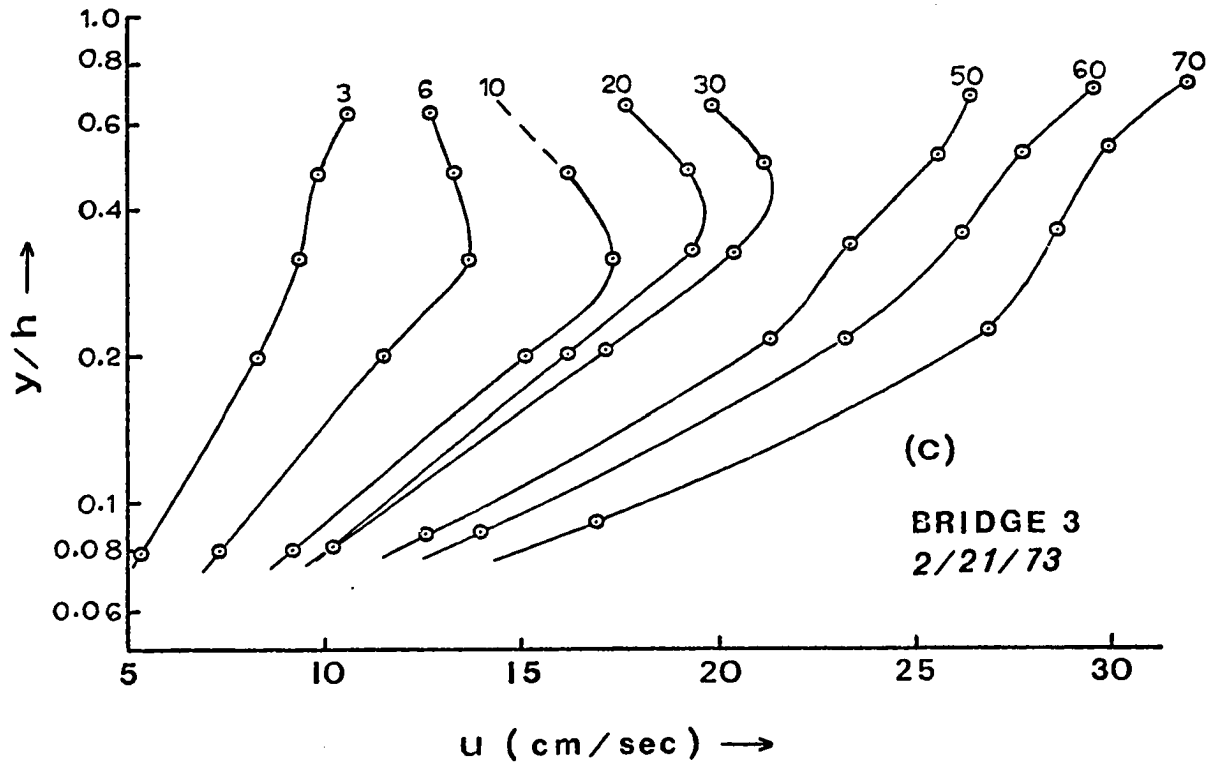

11, Partheniades (1965) reports a similar range of values for flume experiments in which τ_o = 1.10 dynes/cm^2 was taken to be the critical shear stress required to initiate scouring (the material used was San Francisco Bay mud in ocean water). Assuming the comparison to be valid, one might tentatively conclude that erosion and suspension of bottom material could occur at some point in time along most portions of the study creek during average tidal flows, particularly near the head of the main channel. There is at least one other factor which can easily modify this conclusion under certain conditions, however.

Concentration - Water Temperature

Grissinger (1966) in a laboratory study of the erodibility of cohesive soils noted that water temperature is a highly important factor. Among his findings was that erosion rates were almost halved when water temperature was decreased from 20°C to 5°C. Grissinger apparently links this effect to a change in the resistance of the soil to erosion at various temperatures since he reports no change in flow characteristics in his flume during those runs. Partheniades (1965, p. 129), citing work by Einstein and Huon-Li (1958), postulates that suspension of sediment in turbulent flows is dependent upon a periodically forming and disintegrating thin laminar sublayer at the bottom, the inference being that vertical exchange of water and sediment cannot occur through this layer but occurs instead when the sublayer breaks down and turbulence extends all the way to

the bottom. If one accepts this hypothesis, it is equally reasonable to assume that the effect of changing viscosity will have much to do with the thickness and relative permanence of the laminar sublayer.[4] Since the kinematic viscosity of normal seawater increases nearly 50% with a temperature change from 20° to 5°C, there is reason to suppose that temperature plays an important part in the erosion and suspension of cohesive sediments. Varying salinities also effect changes in viscosity, but to a much lesser extent. The effect of salinity in changing the erodibility of fine muds was mentioned by Migniot (1971).

Looking at the seasonal variation in overall concentration levels shown in Appendix A, the importance of temperature variation is unmistakable (mean water temperature is shown on the title page of each run). Figure 24 shows the variation in temperature through time during a number of the runs and reveals not only a seasonal difference but a difference over the tidal cycle which is clearly related to heat transfer processes in the upper reaches of the marsh. The author has observed no temperature stratification at Bridge 1, indicating that mixing is probably complete within the flow at this station. Of particular interest is the temperature profile for

---

[4]The thickness of an unseparated laminar boundary layer is proportional to $\sqrt{\nu}$, ν = kinematic viscosity (see Schlichting, 1960, p. 25).

Figure 24. Water temperature variations during selected runs at entrance to Little Fool Creek.

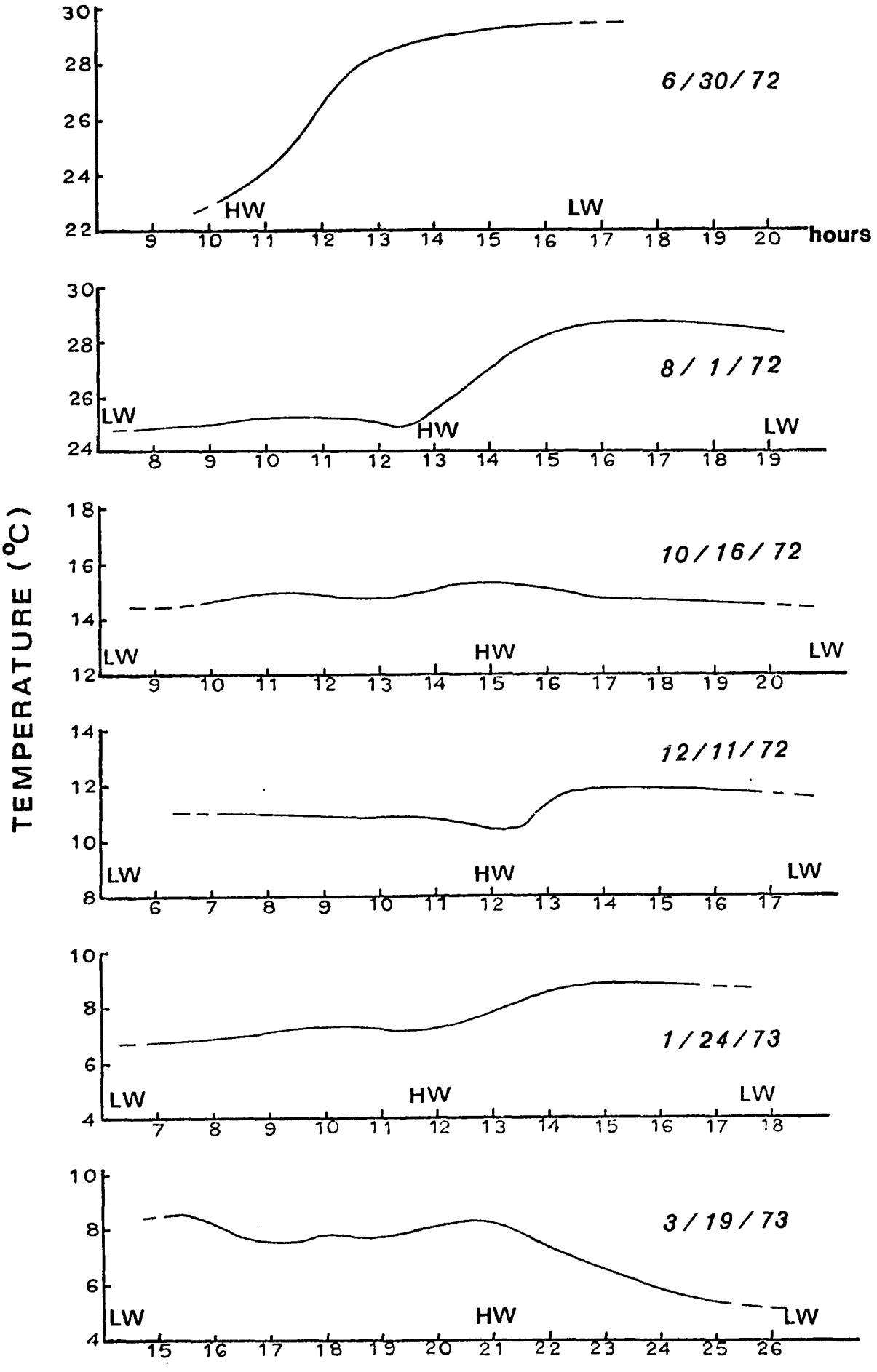

Run 11, 3/19/73, which indicates a heat loss during marsh flooding.

Advective - Dispersive Processes

Thus far, the process of sediment transport has been treated as a local phenomena; i.e., only the observed distributions of u and c in a given channel cross-section through time have received attention. Although these distributions are sufficient insofar as flux measurements are concerned, one cannot weigh the importance of the various processes contributing to the transport through local concentration change unless an additional dimension, longitudinal direction, is considered. This may be done using a one-dimensional mass balance equation

$$\frac{\partial C}{\partial t} = \frac{1}{A}\frac{\partial}{\partial x}\left(AE\frac{\partial C}{\partial x}\right) - U\frac{\partial C}{\partial x} + s \qquad (15)$$

in which

C = cross-sectional average concentration

U = cross-sectional average velocity

x = longitudinal coordinate

A = cross-sectional area

E = dispersion coefficient

s = local source term applying at the sediment-water boundary

In other words, the left side of Equation (15), the local time change (rate of change of the average concentration in the cross-section), equals the effect of

longitudinal diffusion and dispersion minus the effect of advection, plus local addition (s+) or removal (s-) of sediment in suspension via erosion or deposition at the channel boundaries. The dispersion coefficient, E, represents the combined effects of longitudinal turbulent diffusion and longitudinal dispersion, although dispersion, which results from vertical and transverse gradients in u and c is considered to be the more important of the two in estuarine flow (Holley, et al., 1970). However, in marsh channels the concentration of suspended sediment evidences relatively minor spatial variations in cross-section (p. 24), so that longitudinal diffusion and dispersion are probably insignificant in these systems.

Advection, on the other hand, may be quite significant whenever longitudinal concentration gradients exist in conjunction with longitudinal reversing currents. As an example, a horizontal concentration gradient may be established through the action of wind waves on bottom sediments in the shallow bays and mud flats adjacent to the marshes, the latter being less subject to wave action owing to the vegetation present. Sediment stirred up in the bay and flats areas will then be carried into the marshes on flood tide where it will encounter conditions more favorable to resuspension at the onset of ebb, a process which should result in a net transport of sediment into the marsh. This contribution due to advective transport must then be considered additional to the transport that occurs even on

calm days due to the turbulent action of tidal currents on bottom sediments within the marsh.

In an attempt to assess advective transport under ordinary conditions, two of the measurement runs presented in Appendix A (Run 3, 8/1/72 and Run 5, 10/16/72) were conducted with additional measurements being taken at Bridges 2 and 3 on Little Fool Creek (Figure 9; Bridge 3 is nearest the head of the creek). A lesser number of water samplers and current meters were used at the supplementary stations, otherwise the same methods as employed at Bridge 1 were in effect. No current data are shown for the extra stations during Run 5, however, due to neap tide conditions accompanied by minimal currents.

Generally, the additional stations do not reveal any horizontal concentration gradients that could not be explained by differential erosion and suspension along the channel, recalling from the results in Table 11 that bottom shear stresses apparently differ among stations having different water depths. The fact that most of the peaks in concentration occur in close proximity to peaks in current speed argues in favor of local turbulence in explaining the bulk of local concentration change. Additional experiments are needed to evaluate the advective contribution, however, inasmuch as the present ones were not operative during windy days which should be most conducive to the latter.

Transport of Particulate Organic Matter (POM)

An important question arises on separating the material found in suspension in marsh creeks into organic and inorganic fractions; i.e., do the two fractions evidence like or unlike behavior within the transport system? The view has been expressed that particulate organic matter is produced within the marsh through decay of plant and animal remains and thereafter experiences a net transport in the water column away from the marsh. There is no compelling reason to believe, however, that particulate inorganic matter (clays, etc.) should originate within a marsh, rather sedimentologists often argue that currents bring such material into the marsh where it accumulates due to entrapment by marsh vegetation. To examine this question more fully, a number of suspended sediment samples collected during transport measuring runs were subsequently analyzed in the laboratory to determine their organic content based on the amount of combustibles present. The procedures are given in the Instrumentation and Methods section.

The combustibles flux for one entire run is shown in the appendix for Run 1, 5/16/72. In this run, very similar shapes are observed in the two curves for total solids and combustibles flux, their residual transports differing by little more than 2%. Expressed as a percentage by weight of the total solids contained in each sample (g/100g), the fractional combustibles content appears to vary between 8 and 16%.

Figure 25 shows the frequency distribution of fractional combustibles content compiled for 166 samples. In this figure, a single modal point is dominant near the 10% combustibles level, with possible minor modes near 13.5 and 15.0%. The samples in the 9.5-11.0% group are fairly evenly distributed as regards their time of collection during the cycle, with some tendency to cluster near the points of maximum discharge. Among the 15.0-15.5% group, five of six samples occur at the onset of ebb tide; among the 13.0-14.0% group, eleven out of twenty samples occur near low tide. Although this may well reflect different types of organic matter being suspended at various stages of the tidal cycle, much more data is needed to be conclusive on this matter. The evidence from Run 1, however, is that suspended POM follows the variation in total suspended solids to a great extent and mirrors the transport characteristics of the latter. A number of samples chosen at random from some of the other runs were also analyzed and these results are shown in Table 12, including a random sampling from Run 1.

The information given in Table 12 reveals a fairly narrow range insofar as the combustibles content of the samples is concerned. All but the 6/30/72 run, in fact, have confidence intervals that overlap with at least one other run. Based on these results, the conclusion which must be reached is that the POM content of suspended sediments is fairly consistent, allowing for a certain

Figure 25. Frequency distribution of fractional combustibles content in samples of suspended sediment collected during Run 1, 5/16/72.

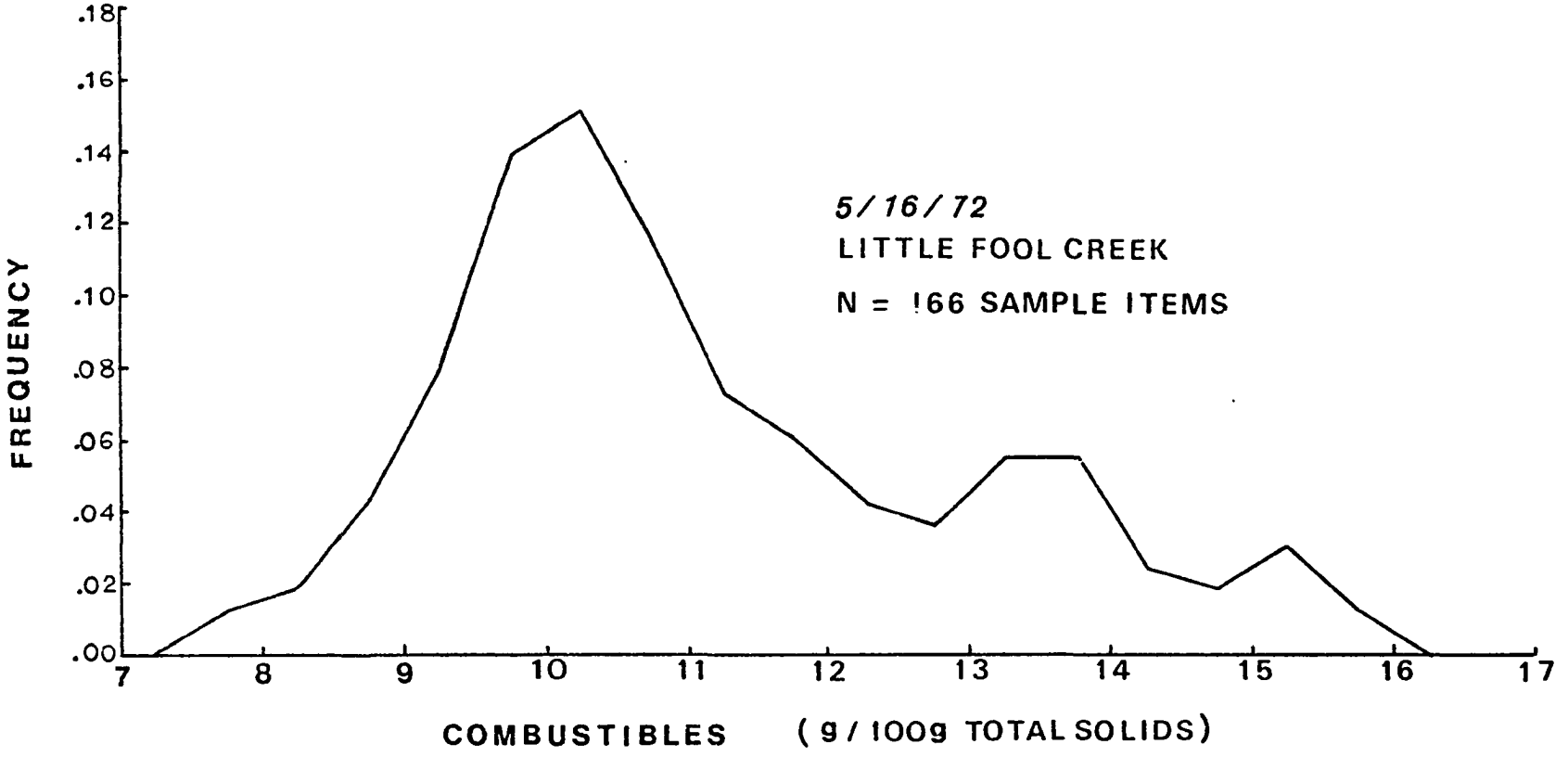

amount of variance in individual samples. If this conclusion is correct, then the transport of POM in suspension will be linked to that of the total suspended solids in marsh channels.

TABLE 12

% COMBUSTIBLES (g/100g TOTAL SOLIDS IN SAMPLE), LITTLE FOOL CREEK

Date	Mean	Confidence Limits[6]	High	Low	No. Samples
5/16/72	11.58	± 0.86	15.66	7.95	25
6/30/72	8.95	± 0.75	13.19	5.26	25
8/31/72	11.58	± 0.67	13.27	8.85	23
12/11/72	10.65	± 0.57	13.11	8.83	25
1/24/73	13.48	± 1.15	18.42	8.70	25

[6]Confidence limits expressed as $S_{\bar{x}}\ t_{.05}$, where $S_{\bar{x}}$ is the standard deviation of the mean and $t_{.05}$ is student's t at the 5% level.

SOME REMARKS ON MARSH EVOLUTION

From the data on hand, there is at least an indication that suspended sediment transport in the marsh drainage system under study will favor a residual ebb transport during much of the year. The complexity of marsh drainage systems is such, however, that firm conclusions about the sediment balance during any given year will require extended research on a large scale. At this stage, the wisest course would seem to be to form a tentative hypothesis and to examine the factors that affirm or deny it.

The hypothesis which the author puts forward is as follows: Stratigraphic evidence shows clearly that marshes grow vertically through sediment entrapment in keeping their highest levels on a par with the secular rise in mean high water. The channel networks draining a given area of marsh are net erosive features, however, and are removing sediments and consequently extending themselves at the heads of the first order channels. This pattern of simultaneous growth in both the channels and the marsh surface constitutes an apparent enigma, unless other processes are at work. Considering the lateral growth of the marshes onto the tidal flats areas, as demonstrated by Redfield (1965) and Pestrong (1970), there may be as well a transport via

sheetflow during flooding across this interface at the higher tide levels. Marsh grasses would be very effective in baffling this type of flow and effecting the entrapment of sediments. To an extent, this entrapment occurs as well along the banks of the main creek body where overbank flows during spring tides commonly encounter the thickest accumulations of Spartina alterniflora (the so-called tall form of the species) and where raised channel levees are to be seen (Figure 14). Nevertheless, the net conveyance of sediment entering and leaving the marsh via the channel network is directed seaward.

The present study concentrates only on one part of the total system, namely, the low-order channels which handle most of the marsh drainage. The initial question which the author considered was, "Do the low-order channels convey a net quantity of sediment to inner marsh areas by some process akin to any of the various 'lag' phenomena described by Netherlands researchers (Postma, 1954, 1961; Van Straaten and Kuenen, 1957; Groen, 1967)?" Groen, in particular, has shown mathematically that a distorted curve of current velocity could enhance the transport efficiency of the flood phase in the higher-order tidal flat channels. But, as the present work has shown, the distortion of both the discharge and velocity curves in marsh channels is such that the efficiency of the ebb phase should be increased. The theory is that, because maximum ebb velocity is closely preceded by the maximum flood velocity, more sediment is likely to be

placed in suspension with less time to settle prior to the beginning of ebb; this creates relatively higher concentration levels at the time of maximum ebb. This idealized process of Groen's is seemingly borne out by the field data collected at Little Fool Creek, the only difference being that the phases are reversed here as compared to the distorted curves which Groen describes for tidal flat channels in the Wadden Sea.

Groen, however, did not consider advective processes in his work. The present author considered that advection may be quite important during windy periods because bay and tidal flat sediments are much more subject to wind wave action than are the marsh and marsh channel sediments. Such an effect could establish pronounced horizontal concentration gradients which would in turn favor enhanced flood transport of sediment in suspension toward the marshes. This type of gradient was never well-observed in the field, due in part to the difficulty of conducting experiments at those times when wind effects are most severe. Thus, the advective process cannot be ruled out, but if and when it becomes dominant, the chances are that it belongs in the domain of storm-related events which so often cause a great amount of change in a short amount of time in beach environments. The reader will appreciate that experiments are difficult to set up in advance of the "weather" and even more difficult to carry out with meaningful results.

Perhaps the most interesting set of factors discussed in this work is that of seasonal variation in the tidal prisms entering and leaving the marsh and seasonal variation in water temperatures. The month of January, 1973, contained very few tides producing a large prism and local water clarity seemed high during most of the month in which water temperatures were uniformly low (Michael Castagna, personal communication). There is little doubt that these factors in combination held sediment movements to a minimum during January and probably most of the other winter months as well. March, 1973, marked a sharp increase in suspended sediment levels which coincided with a reversal in heat exchange patterns in the study marsh (Figure 24), cooler ebb waters being observed for the first time, accompanied by the first significant flood residual for suspended sediment transport.

With the exception of March and possibly April, the months of significant transport activity as evidenced by the measurement runs and the associated factors of demonstrated importance would appear to be those of the summer and fall seasons. It is tentatively held that the latter periods are also conducive of ebb residual transports on the whole, so that the long range tendency of the marsh drainage system in the study area is to remove sediment.

The above conclusion is made in relation to the sediment balance in the drainage system as a whole. Within the marsh, there are sites locally which evidence either

deposition or erosion. The most obvious example of erosion is found near the heads of the creeks. These areas are characterized by a pear-shaped apron of gentle slope surrounding the first-order channel segments. These segments appear without exception as deep and narrow grooves of the type cited by Partheniades (1965) as the focal point of erosion in his flume studies. In some places, the author has observed the tips of these segments cutting through the rhizome layer of dead Spartina growth. Within the apron itself, vegetation is generally sparce, increasing gradually towards the apron's outer edge. Unlike the firm ground of the marsh proper, the surfaces of the apron are soft and difficult to walk on, having little plant material to bind the soil.

The local sites of deposition appear to be confined to the levees about the higher-order channels. Rules placed in the soil on transects parallel to these channels were read before and after a seventy-day period (8/18/72 - 10/27/72). The results showed accumulations of as much as three centimeters one meter from the channel edge, tapering off to a half centimeter or less at 8 meters distance. These data are not sufficient to predict long-term accumulation rates and are mentioned only in support of the fact that some local deposition does occur along the channel levees.

The question of the exact nature of marsh evolution has many facets, some of which have been treated in this work

while others remain for future investigations. For example, if marsh channels of the type studied in this work are indeed growing at the expense of the inner marsh areas, one must ask whether or not this process has a limit in the form of a maximum drainage density, taking drainage density to be the sum of the lengths of all channel segments included within a unit area of marsh. The most obvious factor which could act to limit drainage density would be the reduction in drainage area associated with any one channel network as more and more channels cut through the marsh. Each channel system would then convey a smaller tidal prism to and from its effective drainage area with a probable loss in its capacity to transport sediments. Possibly such circumstances would lead to the closing of older stream networks and renewed deposition in portions of the marsh. Perhaps, on the other hand, lateral growth of the marsh at its interface with tidal mud flats and shallow bays represents a redistribution of marsh acreage in a continuously changing pattern which tends to offset maximum drainage configurations in the marsh-lagoon complex.

A very significant question must also be asked concerning the effect of man-made channels through the marsh. Wherever such channels are dredged, there is not only the matter of spoil deposits which may cause local damage to actively growing marshes, but the possibility exists that tidal flow characteristics in many adjacent natural channels may be dramatically changed, causing a

sudden redirection in erosional and depositional patterns over a wide area. This is certainly a question deserving of future research.

SUMMARY AND CONCLUSIONS

In the preceding pages, the author has sought to examine the numerous processes which affect the transport of water and materials in suspension into and out of a typical marsh area via the channel network comprising the marsh drainage system. Among the most important processes, as ascertained in this and in other works, are:

1. Tidal characteristics, most notably the deformation of the tide curve by shallow-water tides.
2. Marsh topography in terms of water surface area-height relationships. These in turn relate to the tidal prism and the time-varying discharge at a cross-section when coupled with a suitable model of the tide.
3. Frictional and wind stress effects.
4. Bottom shear stresses induced by channel flow and their ability to erode and suspend cohesive sediments.
5. Temperature effects in terms of cohesive soils resistance to erosion and possible modification of boundary flow characteristics.
6. Advective processes acting between marshes and adjacent bays and tidal flats.

A combination of modeling efforts and a detailed program of field measurements over a period of a year has been aimed at reducing the lack of knowledge which surrounds many if not all of these processes in the marsh environment.

With regard to area-height relationships, it has been shown that tidal prisms can be accurately modeled using a variation of Strahler's hypsometric formula in combination with tidal data. Using available tidal data, it was found that a well-known seasonal cycle in mean high water level exerts a strong seasonal influence on the distribution of tidal prisms. Viewing the prism as a discharge; i.e., the volume of flow per semidiurnal time period, the frequency of discharge at a given level of magnitude is found to be significantly higher in September and October but significantly lower during January and February as compared to the remainder of the year. On a quarterly basis, the mean and median discharge both show a progressive increase between the first quarter (January-March) and the final quarter (October-December). These trends in level of discharge have obvious implications regarding seasonal flushing characteristics and the capacity for transport in marshes.

An equally important seasonal factor, in terms of the observed level of suspended sediment concentration, is that of water temperature. It is apparent that the resistance to erosion exhibited by cohesive bottom sediments is enhanced by cooler temperatures. A change in flow characteristics near the channel boundaries may also be an important consequence of varying seasonal temperatures. As a result, markedly lower levels of concentration are normally observed in winter (except during spells of

wind-generated turbulence) as opposed to the other seasons. A final temperature effect may be that of differential heat transfer on marshes which was observed in all three modes at the study creek (warmer water going in, warmer water coming out, and no change). In all of the flux measurement runs involving significant suspended sediment loads, the heaviest concentrations were observed in association with the tidal phase having the warmest effluent.

On balance, the marsh drainage network is considered to be an erosive feature, removing more sediment from the inner marsh than it brings in. This is a very tentative conclusion, owing to the complexity of the system under consideration which shows a variable pattern of residual sediment transport. Broken into seasonal components, the residual transport may be characterized as heavy and ebb-oriented during summer and fall months, light and variable during winter months, heavy and flood oriented during early spring. Further field experiments are needed to confirm or refute this interpretation in its broad application to the present as well as other similar marsh environments.

The impact of these findings may be disturbing to coastal geomorphologists who rightly view marshes as sedimentary features that have evolved through a process of sediment accumulation. The proof of the above comes mainly from stratigraphic evidence. In attempting to discover the dynamic processes at work which build marshes, the source of

the sediments within them, etc., the path the investigator must follow is not so simple. The most popular approach in this direction has been the advocation of various types of "lag" phenomena in sediment-bearing tidal flows. A drawback to this approach is that the motions of the individual particles are usually considered in a highly idealized flow field. In nature, transport processes are considerably more complex.

The present study has been limited to a definable subsystem, the marsh drainage network featuring channels which end on the marsh. From the point of view of open-channel hydraulic processes, the factors which affect transport have been examined. The conclusions reached do not support a net conveyance of sediment to the marshes via the low-order drainage channels. Consequently, other avenues of transport must be called upon to account for sediment accumulations within the marsh.

APPENDIX A

MEASUREMENT DATA

RUN 1

5/16/72

Wind 5-10 mph S to SSW, gusts, overcast

Mean air temp..... 23°C

Mean water temp..... 20°C

Tidal range..... 1.61 m

Mean water level..... 0.72 m

Duration of run: 16.8 to 29.5 hrs.

L.F.1 5/16/72 DISCHARGE (CU.M./SEC.)

INTEGRATED VALUES
FLOOD= 44660.5782
EBB= -45979.2969
RESIDUAL= -1318.7189 PGA= 2.90

TS1=16.75 TS2=23.55 TS3=29.50

INTERPOLATIVE VALUES

TIME(HRS)	DISCHARGE (CU.M./SEC.)
16.750	0.0000
17.000	0.0320
17.250	0.1252
17.500	0.2304
17.750	0.2878
18.000	0.3066
18.250	0.3158
18.500	0.3565
18.750	0.4485
19.000	0.5176
19.250	0.5053
19.500	0.5124
19.750	0.6730
20.000	1.0298
20.250	1.5557
20.500	2.2351
20.750	3.0576
21.000	3.9391
21.250	4.7384
21.500	5.2829
21.750	5.3333
22.000	4.7160
22.250	3.8103
22.500	3.1622
22.750	2.7186
23.000	2.1613
23.250	1.3246
23.500	0.2419
23.750	-1.0308
24.000	-2.3699
24.250	-3.6232
24.500	-4.6656
24.750	-5.4007
25.000	-5.8368
25.250	-6.0622
25.500	-6.0359
25.750	-5.4257
26.000	-4.1381
26.250	-2.7000
26.500	-1.6061
26.750	-0.8873
27.000	-0.4587
27.250	-0.2352
27.500	-0.1397
27.750	-0.1133
28.000	-0.1037
28.250	-0.0898
28.500	-0.0650
28.750	-0.0381
29.000	-0.0320
29.250	-0.0237
29.500	0.0000

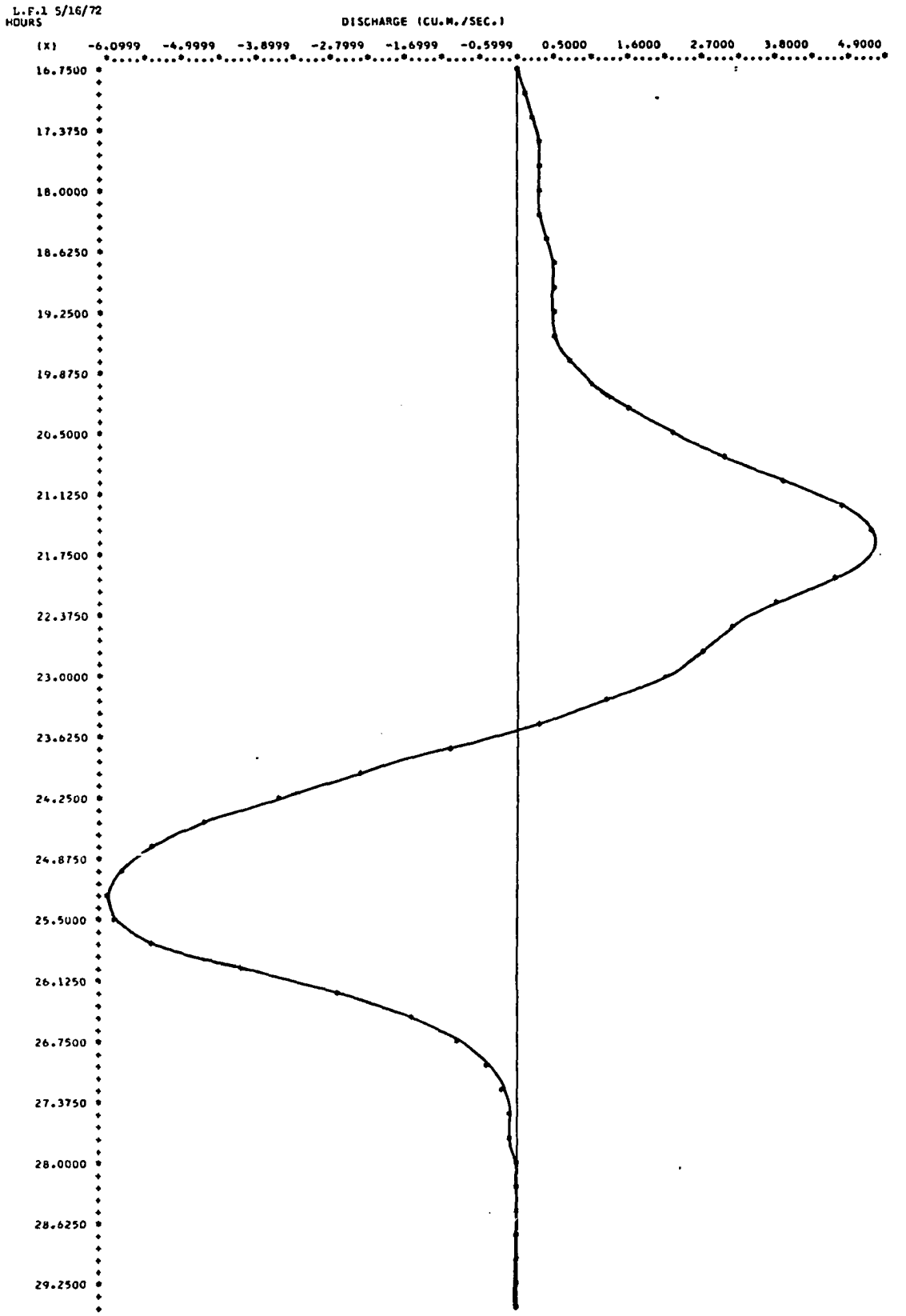

L.F.1 5/16/72 S.S. FLUX(KG./SEC.)

INTEGRATED VALUES

FLUGD= 2119.0517

FBB= -3573.6845

RESIDUAL= -1454.6330 PGA= 51.10

TS1=16.75 TS2=23.55 TS3=29.50

INTERPOLATIVE VALUES

TIME(HRS)	S.S. FLUX(KG./SEC.)
16.750	0.0000
17.000	0.0022
17.250	0.0037
17.500	0.0062
17.750	0.0109
18.000	0.0150
18.250	0.0156
18.500	0.0147
18.750	0.0147
19.000	0.0155
19.250	0.0165
19.500	0.0182
19.750	0.0216
20.000	0.0332
20.250	0.0634
20.500	0.1147
20.750	0.1832
21.000	0.2550
21.250	0.3083
21.500	0.3258
21.750	0.2995
22.000	0.2275
22.250	0.1441
22.500	0.0931
22.750	0.0706
23.000	0.0512
23.250	0.0252
23.500	0.0029
23.750	-0.0078
24.000	-0.0291
24.250	-0.0933
24.500	-0.1892
24.750	-0.2751
25.000	-0.3456
25.250	-0.4242
25.500	-0.5116
25.750	-0.5561
26.000	-0.5232
26.250	-0.4319
26.500	-0.3086
26.750	-0.1797
27.000	-0.0715
27.250	-0.0103
27.500	0.0000
27.750	-0.0023
28.000	-0.0034
28.250	-0.0025
28.500	-0.0015
28.750	-0.0011
29.000	-0.0010
29.250	-0.0007
29.500	0.0000

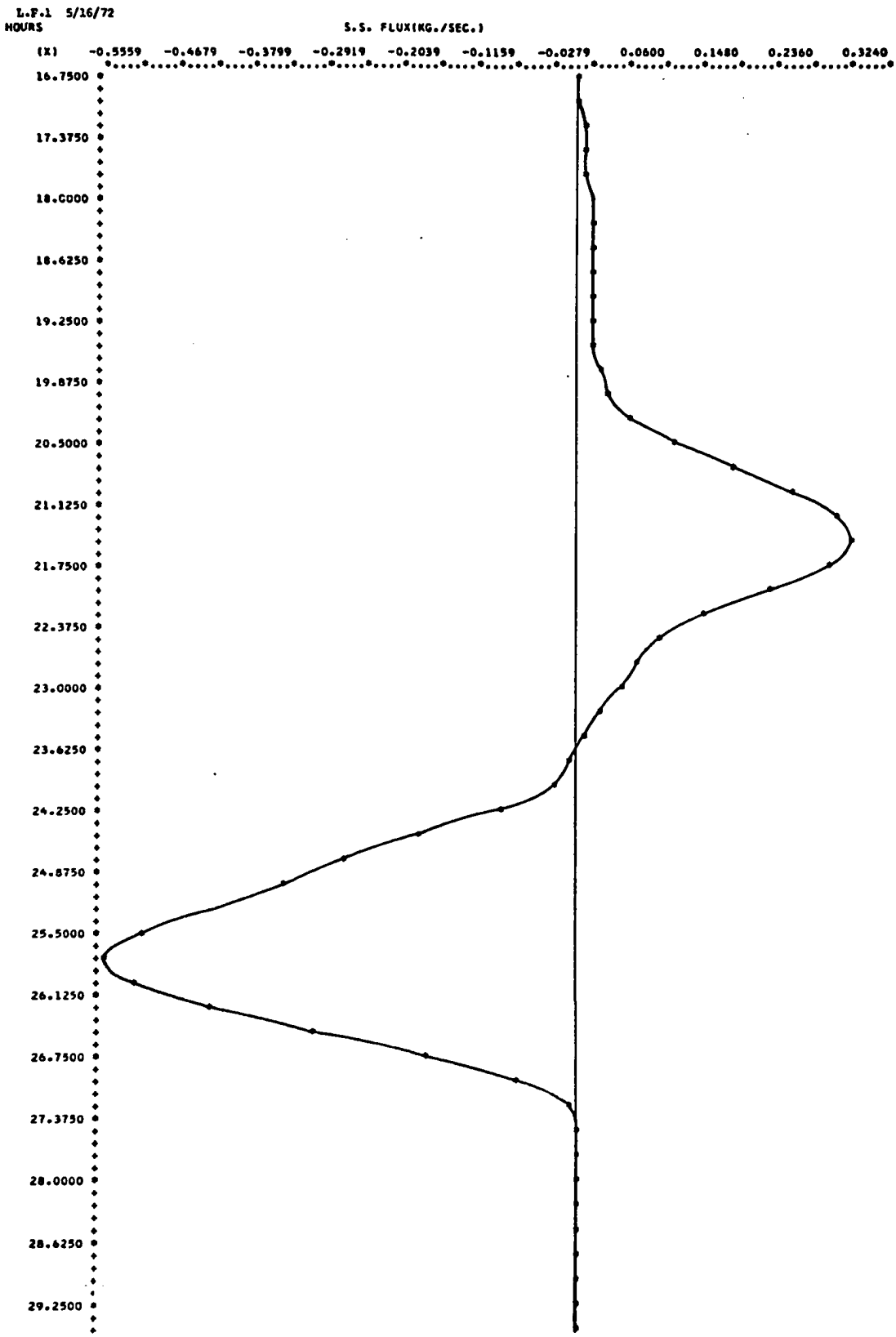

L.F. 1 5/16/72 COMB. FLUX(KG./SEC.)

INTEGRATED VALUES

FLOOD= 229.1974

EBB= -376.2055

RESIDUAL= -147.0081 PGA= 48.56

TS1=16.75 TS2=23.55 TS3=29.50

INTERPOLATIVE VALUES

TIME(HRS)	COMB. FLUX(KG./SEC.)
16.750	0.0000
17.000	0.0002
17.250	0.0005
17.500	0.0008
17.750	0.0012
18.000	0.0016
18.250	0.0017
18.500	0.0017
18.750	0.0018
19.000	0.0019
19.250	0.0018
19.500	0.0019
19.750	0.0026
20.000	0.0043
20.250	0.0075
20.500	0.0127
20.750	0.0200
21.000	0.0279
21.250	0.0332
21.500	0.0338
21.750	0.0300
22.000	0.0226
22.250	0.0147
22.500	0.0102
22.750	0.0082
23.000	0.0063
23.250	0.0034
23.500	0.0004
23.750	-0.0017
24.000	-0.0047
24.250	-0.0109
24.500	-0.0194
24.750	-0.0264
25.000	-0.0324
25.250	-0.0409
25.500	-0.0523
25.750	-0.0593
26.000	-0.0570
26.250	-0.0476
26.500	-0.0342
26.750	-0.0199
27.000	-0.0078
27.250	-0.0010
27.500	0.0000
27.750	-0.0003
28.000	-0.0004
28.250	-0.0003
28.500	-0.0001
28.750	-0.0001
29.000	-0.0001
29.250	-0.0001
29.500	0.0000

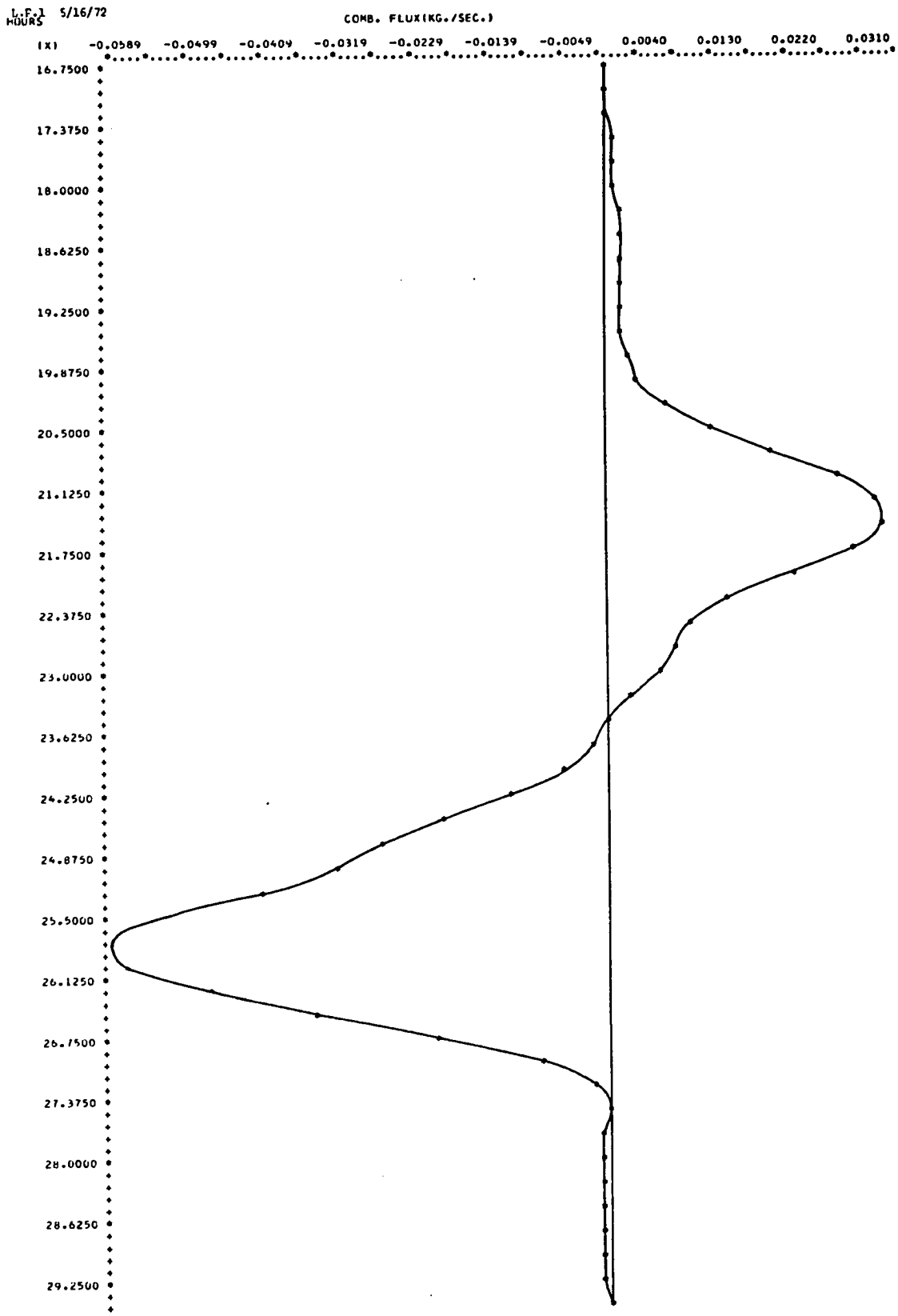

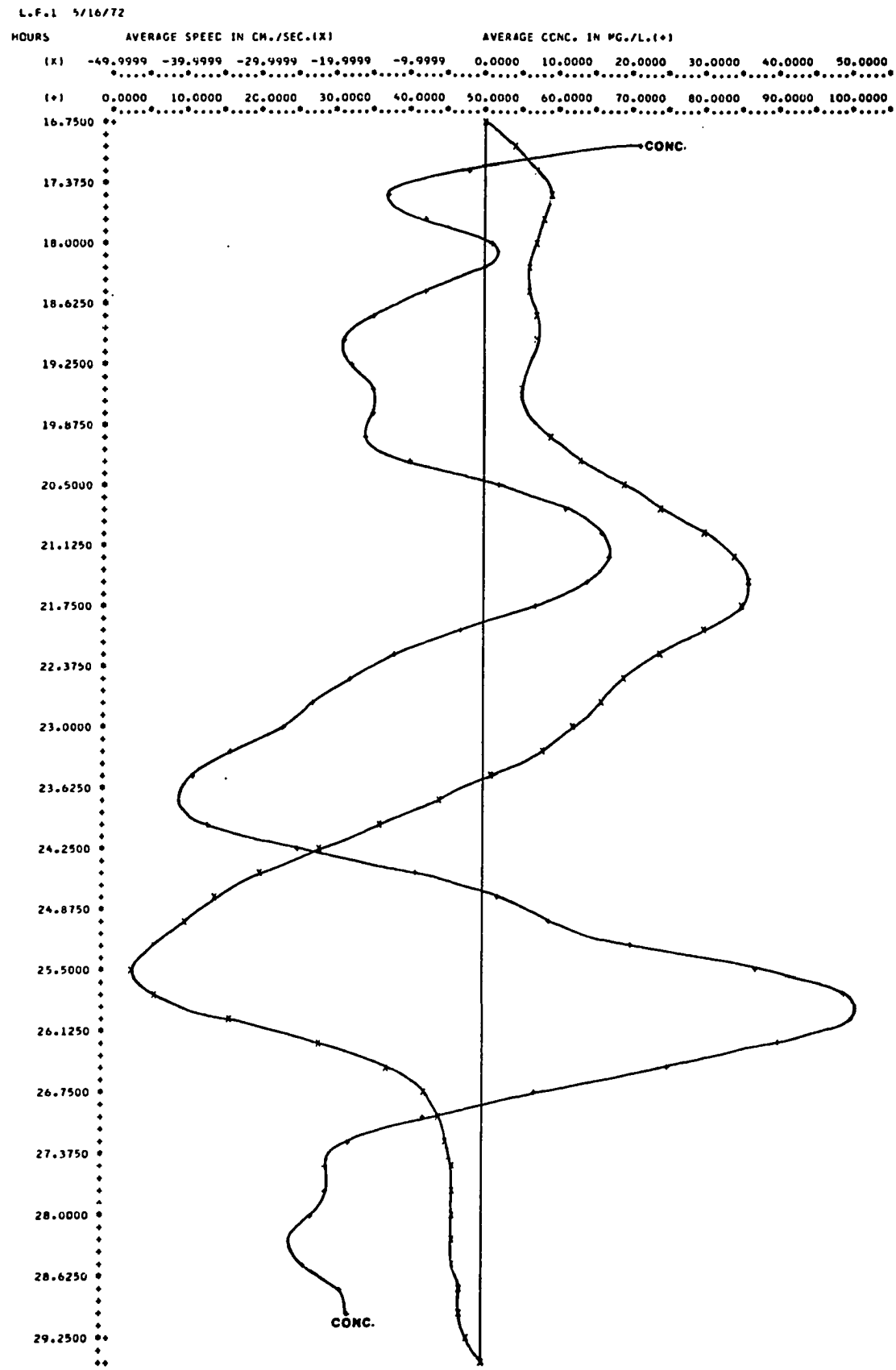

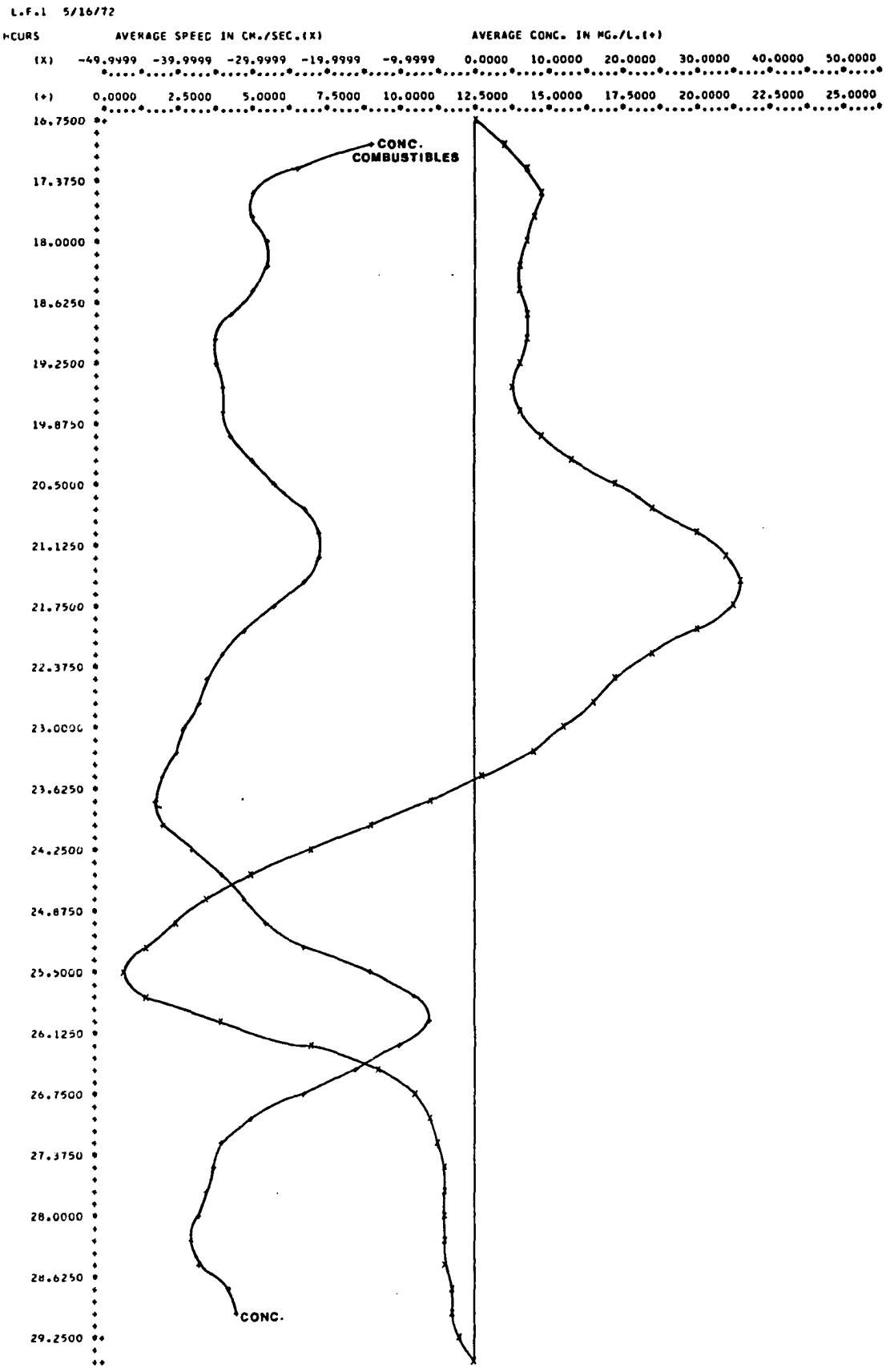

RUN 2

6/30/72

Wind 5-10 mph WSW, clear sky

Mean air temp..... 26°C

Mean water temp..... 27°C

Tidal range..... 1.16 m

Mean water level..... 0.70 m

Duration of run: 4.7 to 16.7 hrs.

L.F.1 6/30/72 DISCHARGE(CU.M./SEC.)

INTEGRATED VALUES
FLOOD= 27671.5039
EBB= -29982.5703
RESIDUAL= -2111.0669 PGA= 7.29

TS1= 4.70 TS2=10.55 TS3=16.65

INTERPOLATIVE VALUES

TIME(HRS)	DISCHARGE(CU.M./SEC.)
4.500	0.0000
4.750	0.0214
5.000	0.1261
5.250	0.2201
5.500	0.2948
5.750	0.3412
6.000	0.3538
6.250	0.3512
6.500	0.3620
6.750	0.3943
7.000	0.4289
7.250	0.4612
7.500	0.5531
7.750	0.7765
8.000	1.1780
8.250	1.7856
8.500	2.4443
8.750	2.9240
9.000	3.2552
9.250	3.5208
9.500	3.5996
9.750	3.2714
10.000	2.5459
10.250	1.4954
10.500	0.2548
10.750	-0.9990
11.000	-2.1346
11.250	-3.0644
11.500	-3.7956
11.750	-4.3509
12.000	-4.6379
12.250	-4.4771
12.500	-3.7080
12.750	-2.2396
13.000	-0.7742
13.250	-0.2859
13.500	-0.4118
13.750	-0.4852
14.000	-0.3628
14.250	-0.2900
14.500	-0.3178
14.750	-0.3401
15.000	-0.2904
15.250	-0.2001
15.500	-0.1069
15.750	-0.0327
16.000	0.0030
16.250	0.0031
16.500	-0.0011
16.750	0.0000

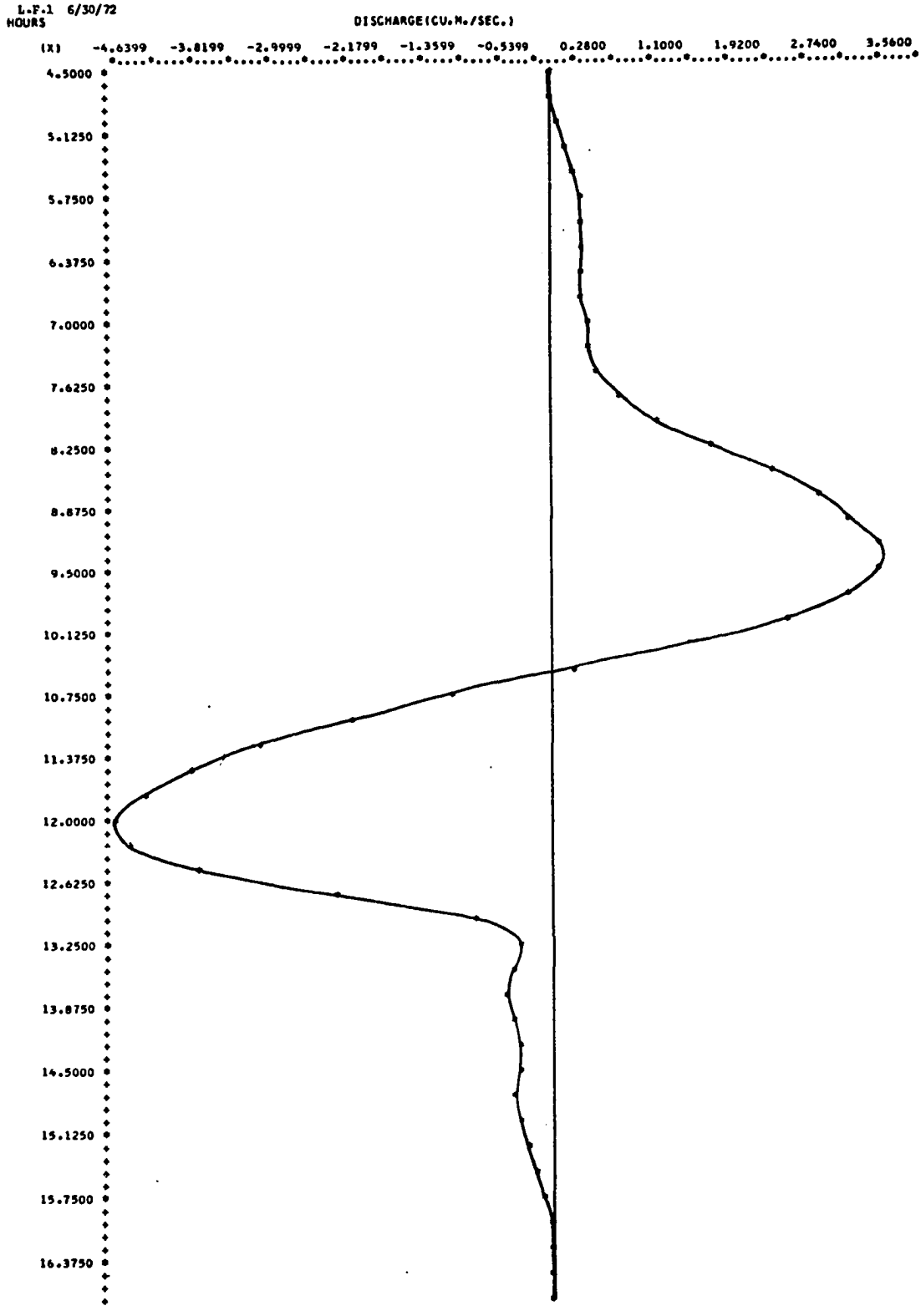

L.F.1 6/30/72 S.S. FLUX(KG./SEC.)

INTEGRATED VALUES

FLOOD= 690.4399

EBB= -2174.0376

RESIDUAL= -1283.5974 PGA= 33.77

TS1= 4.70 TS2=10.55 TS3=16.65

INTERPOLATIVE VALUES

TIME(HRS)	S.S. FLUX(KG./SEC.)
4.500	0.0000
4.750	0.0007
5.000	0.0041
5.250	0.0072
5.500	0.0097
5.750	0.0112
6.000	0.0115
6.250	0.0111
6.500	0.0106
6.750	0.0104
7.000	0.0108
7.250	0.0119
7.500	0.0139
7.750	0.0176
8.000	0.0282
8.250	0.0504
8.500	0.0776
8.750	0.0974
9.000	0.1136
9.250	0.1324
9.500	0.1395
9.750	0.1138
10.000	0.0700
10.250	0.0308
10.500	0.0041
10.750	-0.0155
11.000	-0.0488
11.250	-0.1182
11.500	-0.2265
11.750	-0.3673
12.000	-0.4794
12.250	-0.4658
12.500	-0.3330
12.750	-0.1669
13.000	-0.0422
13.250	-0.0030
13.500	-0.0140
13.750	-0.0222
14.000	-0.0157
14.250	-0.0129
14.500	-0.0172
14.750	-0.0198
15.000	-0.0159
15.250	-0.0102
15.500	-0.0067
15.750	-0.0049
16.000	-0.0039
16.250	-0.0029
16.500	-0.0010
16.750	0.0000

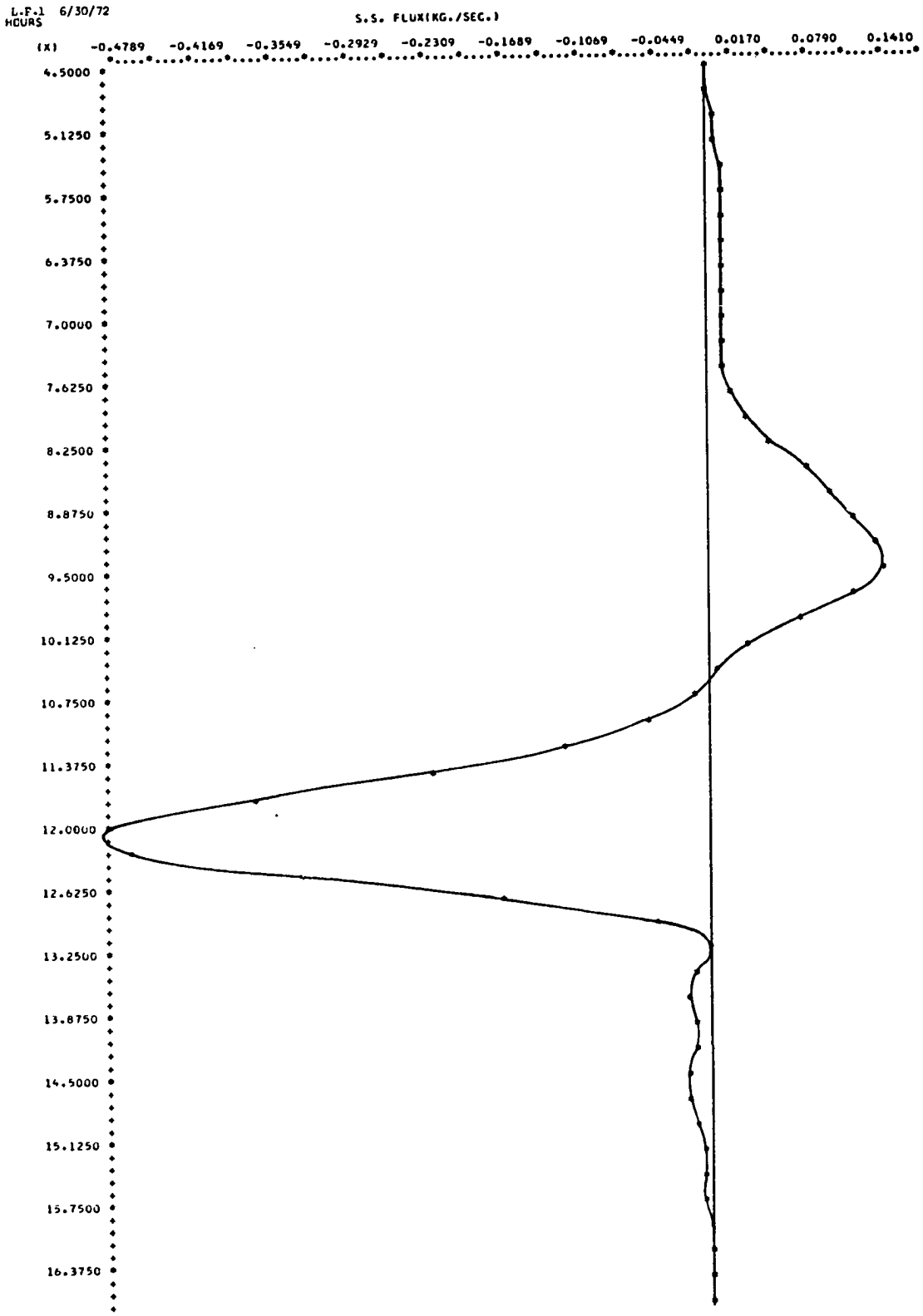

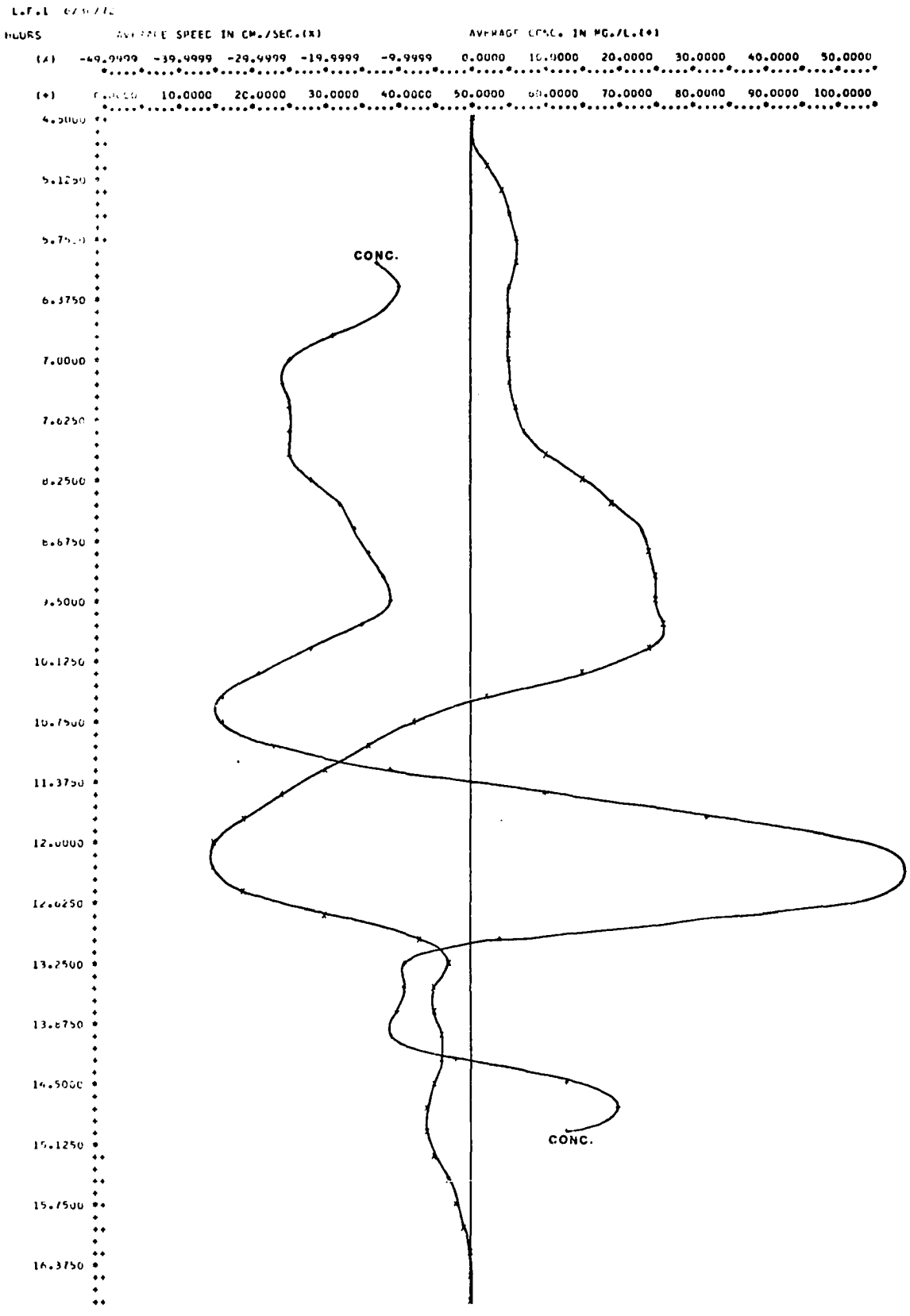

RUN 3*

8/1/72

Wind 0-5 mph & variable, partly cloudy

Mean air temp..... 28°C

Mean water temp..... 27°C

Tidal range..... 1.46 m

Mean water level..... 0.70 m

Duration of run: 6.6 to 19.2 hrs.

*Three bridge run

L.F.1 8/1/72 DISCHARGE(CU.M./SEC.)

INTEGRATED VALUES
FLOOD= 40623.8907
EBB= -42269.3829
RESIDUAL= -1645.4924 PGA= 3.97

TS1= 6.55 TS2=13.00 TS3=19.20

INTERPOLATIVE VALUES

TIME(HRS)	DISCHARGE(CU.M./SEC.)
6.500	0.0000
6.750	0.0931
7.000	0.2023
7.250	0.2946
7.500	0.3607
7.750	0.3912
8.000	0.3778
8.250	0.3586
8.500	0.4281
8.750	0.5632
9.000	0.5829
9.250	0.3957
9.500	0.3123
9.750	0.6240
10.000	1.1452
10.250	1.6644
10.500	2.3455
10.750	3.3291
11.000	4.2884
11.250	4.8603
11.500	5.0051
11.750	4.7771
12.000	4.2863
12.250	3.6557
12.500	2.8918
12.750	1.7410
13.000	0.0000
13.250	-1.9380
13.500	-3.5325
13.750	-4.4316
14.000	-4.9099
14.250	-5.3200
14.500	-5.7026
14.750	-5.9254
15.000	-5.4791
15.250	-3.8395
15.500	-1.6764
15.750	-0.4884
16.000	-0.4535
16.250	-0.7160
16.500	-0.6994
16.750	-0.5100
17.000	-0.3432
17.250	-0.2776
17.500	-0.2397
17.750	-0.1671
18.000	-0.0832
18.250	-0.0304
18.500	-0.0150
18.750	-0.0156
19.000	-0.0101
19.250	0.0000

L.F.2 8/1/72 DISCHARGE(CU.M./SEC.)

INTEGRATED VALUES
FLOOD= 21401.2422
EBB= -23161.8047
RESIDUAL= -1760.5627 PGA= 7.90

TS1= 6.55 TS2=13.00 TS3=19.20

INTERPOLATIVE VALUES

TIME(HRS)	DISCHARGE(CU.M./SEC.)
6.500	0.0000
6.750	0.0182
7.000	0.0407
7.250	0.0620
7.500	0.0817
7.750	0.0990
8.000	0.1133
8.250	0.1236
8.500	0.1255
8.750	0.1181
9.000	0.1259
9.250	0.1737
9.500	0.2642
9.750	0.3918
10.000	0.5184
10.250	0.5975
10.500	0.8308
10.750	1.5663
11.000	2.4814
11.250	2.9214
11.500	2.9732
11.750	2.8949
12.000	2.6840
12.250	2.1968
12.500	1.5231
12.750	0.7855
13.000	0.0000
13.250	-0.8308
13.500	-1.6505
13.750	-2.3889
14.000	-2.9763
14.250	-3.3764
14.500	-3.6890
14.750	-3.9108
15.000	-3.4915
15.250	-2.0706
15.500	-0.5962
15.750	-0.0294
16.000	-0.0757
16.250	-0.1552
16.500	-0.1143
16.750	-0.0915
17.000	-0.0916
17.250	-0.0836
17.500	-0.0442
17.750	-0.0063
18.000	0.0087
18.250	0.0084
18.500	0.0010
18.750	-0.0051
19.000	-0.0027
19.250	0.0000

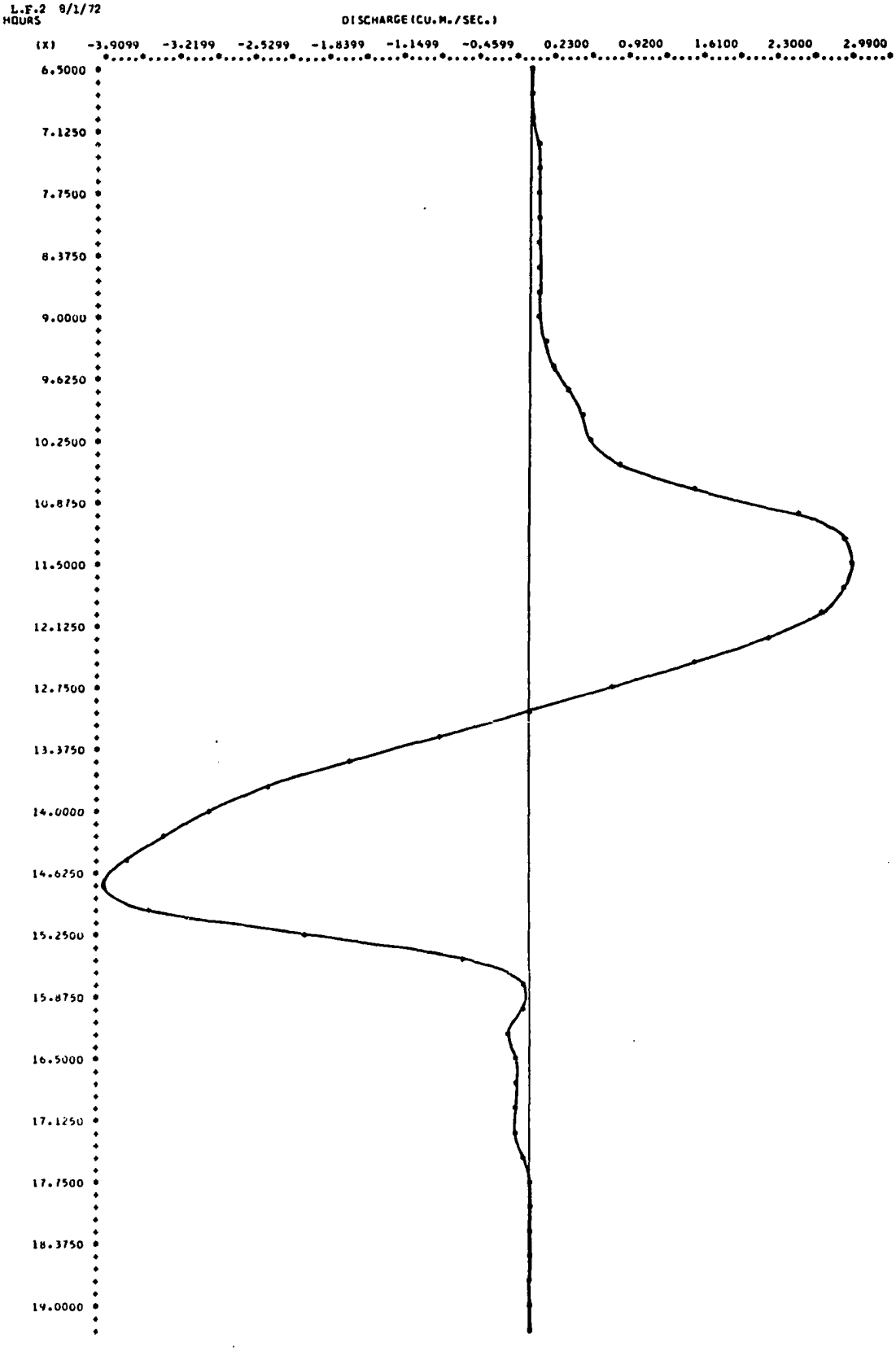

L.F. 3 8/1/72 DISCHARGE(CU.M./SEC.)

INTEGRATED VALUES
FLOOD= 15310.5195
EBB= -16803.0742
RESIDUAL= -1492.5529 PGA= 9.29

TS1= 6.55 TS2=13.00 TS3=19.20

INTERPOLATIVE VALUES

TIME(HRS)	DISCHARGE(CU.M./SEC.)
6.500	0.0000
6.750	0.0080
7.000	0.0187
7.250	0.0307
7.500	0.0450
7.750	0.0607
8.000	0.0719
8.250	0.0733
8.500	0.0706
8.750	0.0707
9.000	0.0776
9.250	0.0959
9.500	0.1385
9.750	0.2252
10.000	0.3981
10.250	0.6941
10.500	1.1097
10.750	1.5970
11.000	1.9744
11.250	2.0902
11.500	2.0475
11.750	1.9590
12.000	1.7222
12.250	1.2517
12.500	0.7477
12.750	0.3910
13.000	0.0000
13.250	-0.5758
13.500	-1.1164
13.750	-1.5455
14.000	-1.8712
14.250	-2.1912
14.500	-2.5490
14.750	-2.8759
15.000	-2.7249
15.250	-1.7927
15.500	-0.7305
15.750	-0.2183
16.000	-0.0998
16.250	-0.0671
16.500	-0.0460
16.750	-0.0251
17.000	-0.0135
17.250	-0.0199
17.500	-0.0326
17.750	-0.0378
18.000	-0.0351
18.250	-0.0275
18.500	-0.0180
18.750	-0.0093
19.000	-0.0040
19.250	0.0000

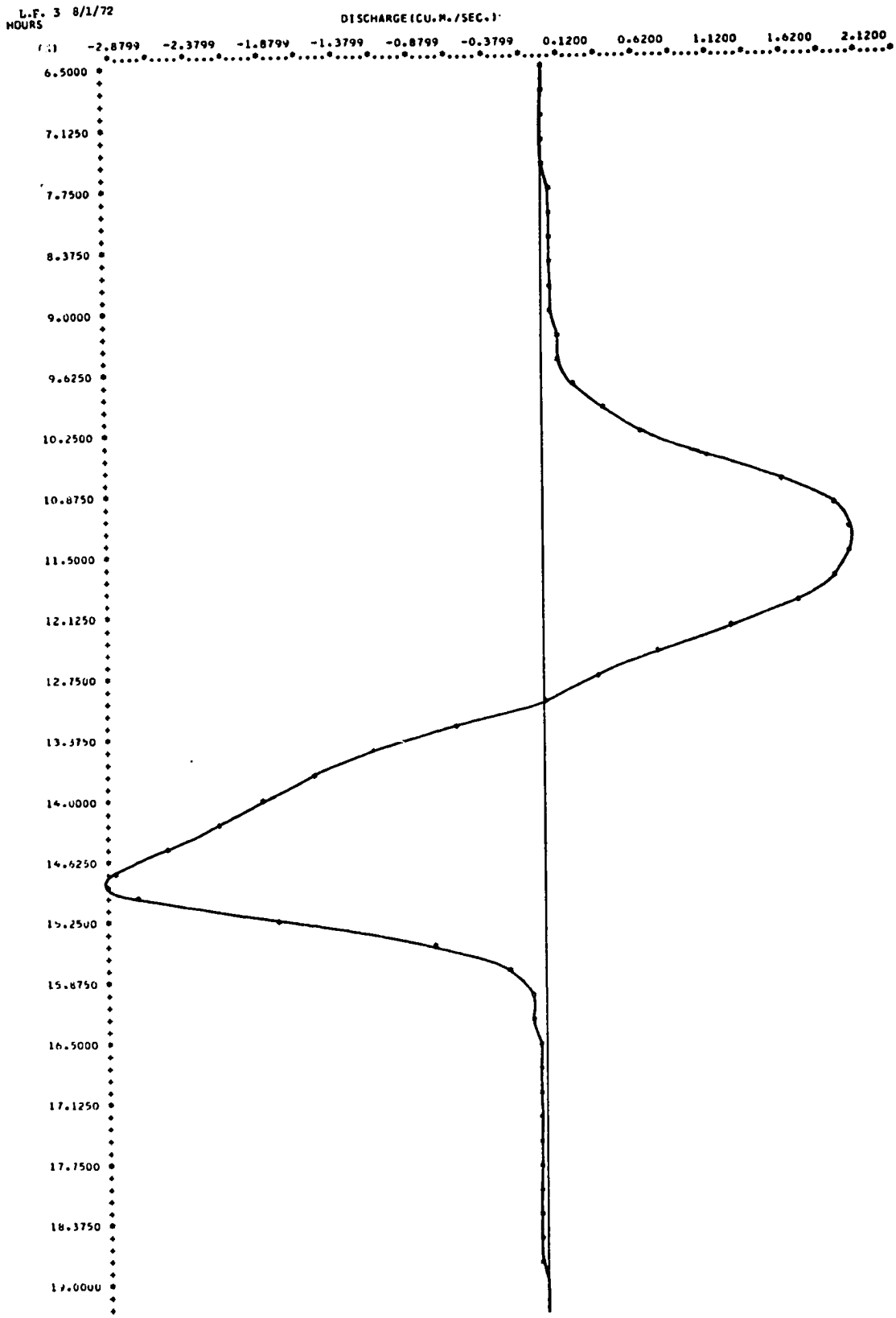

L.F.1 8/1/72 S.S. FLUX(KG./SEC.)

INTEGRATED VALUES

FLOOD= 2064.8335

EBB= -2820.6757

RESIDUAL= -755.8424 PGA= 30.94

TS1= 6.55 TS2=13.00 TS3=19.20

INTERPOLATIVE VALUES

TIME(HRS)	S.S. FLUX(KG./SEC.)
6.500	0.0000
6.750	0.0070
7.000	0.0150
7.250	0.0213
7.500	0.0250
7.750	0.0249
8.000	0.0204
8.250	0.0159
8.500	0.0223
8.750	0.0379
9.000	0.0437
9.250	0.0278
9.500	0.0128
9.750	0.0205
10.000	0.0366
10.250	0.0455
10.500	0.0649
10.750	0.1143
11.000	0.1885
11.250	0.2705
11.500	0.3244
11.750	0.3194
12.000	0.2684
12.250	0.1947
12.500	0.1180
12.750	0.0500
13.000	0.0000
13.250	-0.0385
13.500	-0.0917
13.750	-0.1797
14.000	-0.2842
14.250	-0.3816
14.500	-0.4692
14.750	-0.5364
15.000	-0.5229
15.250	-0.3652
15.500	-0.1368
15.750	-0.0074
16.000	0.0000
16.250	-0.0254
16.500	-0.0290
16.750	-0.0182
17.000	-0.0081
17.250	-0.0056
17.500	-0.0065
17.750	-0.0068
18.000	-0.0061
18.250	-0.0048
18.500	-0.0032
18.750	-0.0018
19.000	-0.0007
19.250	0.0000

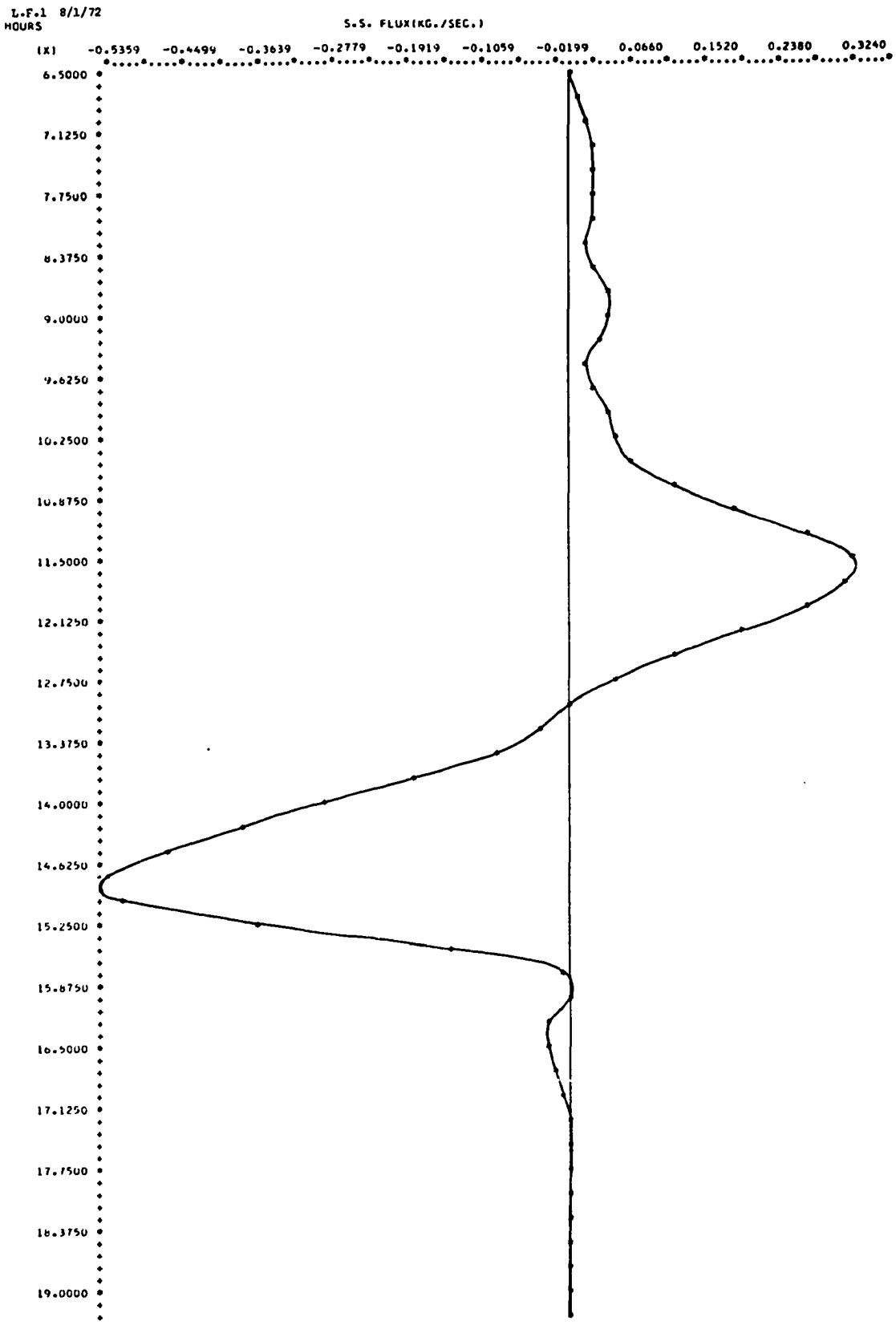

L.F.2 8/1/72 S.S. FLUX(KG./SEC.)

INTEGRATED VALUES

FLOOD= 1262.1762

EBB= -1525.5866

RESIDUAL= -263.4104 PGA= 18.89

TS1= 6.55 TS2=13.00 TS3=19.20

INTERPOLATIVE VALUES

TIME(HRS)	S.S. FLUX(KG./SEC.)
6.500	0.0000
6.750	0.0004
7.000	0.0011
7.250	0.0019
7.500	0.0029
7.750	0.0041
8.000	0.0054
8.250	0.0067
8.500	0.0074
8.750	0.0069
9.000	0.0061
9.250	0.0061
9.500	0.0087
9.750	0.0149
10.000	0.0199
10.250	0.0158
10.500	0.0220
10.750	0.0751
11.000	0.1554
11.250	0.2105
11.500	0.2312
11.750	0.2194
12.000	0.1785
12.250	0.1163
12.500	0.0570
12.750	0.0210
13.000	0.0000
13.250	-0.0196
13.500	-0.0435
13.750	-0.0750
14.000	-0.1177
14.250	-0.1764
14.500	-0.2625
14.750	-0.3640
15.000	-0.3721
15.250	-0.2111
15.500	-0.0382
15.750	0.0000
16.000	-0.0019
16.250	-0.0040
16.500	-0.0028
16.750	-0.0001
17.000	0.0005
17.250	-0.0034
17.500	-0.0015
17.750	0.0014
18.000	0.0022
18.250	0.0017
18.500	0.0006
18.750	-0.0002
19.000	-0.0001
19.250	0.0000

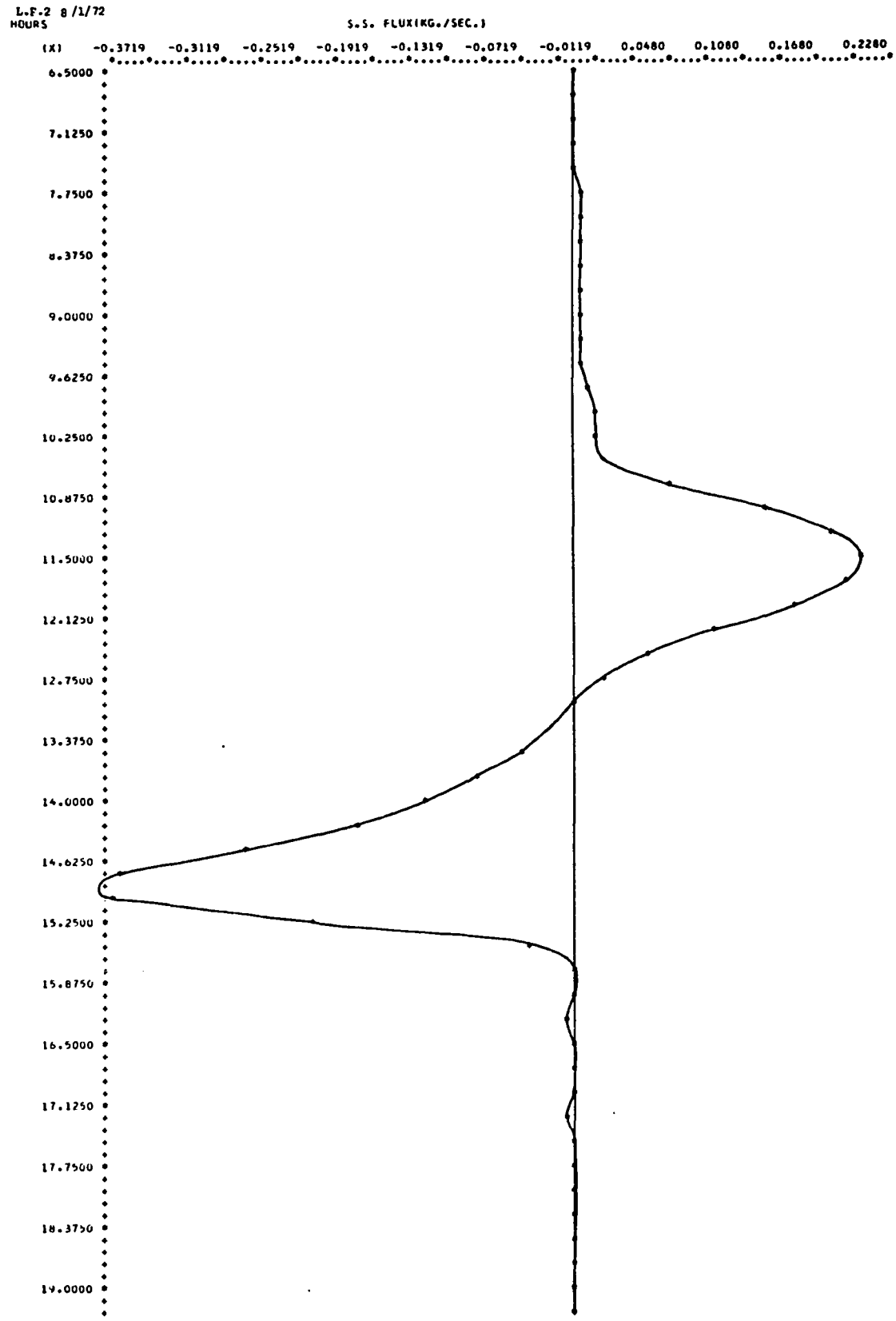

L.F.3 8/1/72 S.S. FLUX(KG./SEC.)

INTEGRATED VALUES

FLOOD= 779.4184

EBB= -738.2299

RESIDUAL= 41.1884 PGA= 5.42

TS1= 6.55 TS2=13.00 TS3=19.20

INTERPOLATIVE VALUES

TIME(HRS)	S.S. FLUX(KG./SEC.)
6.500	0.0000
6.750	0.0002
7.000	0.0006
7.250	0.0011
7.500	0.0018
7.750	0.0027
8.000	0.0032
8.250	0.0031
8.500	0.0028
8.750	0.0030
9.000	0.0034
9.250	0.0039
9.500	0.0050
9.750	0.0079
10.000	0.0145
10.250	0.0267
10.500	0.0467
10.750	0.0750
11.000	0.1056
11.250	0.1302
11.500	0.1369
11.750	0.1175
12.000	0.0838
12.250	0.0504
12.500	0.0255
12.750	0.0121
13.000	0.0000
13.250	-0.0185
13.500	-0.0343
13.750	-0.0460
14.000	-0.0559
14.250	-0.0710
14.500	-0.1014
14.750	-0.1469
15.000	-0.1616
15.250	-0.1100
15.500	-0.0410
15.750	-0.0089
16.000	-0.0034
16.250	-0.0024
16.500	-0.0016
16.750	-0.0013
17.000	-0.0014
17.250	-0.0019
17.500	-0.0023
17.750	-0.0023
18.000	-0.0021
18.250	-0.0016
18.500	-0.0011
18.750	-0.0006
19.000	-0.0002
19.250	0.0000

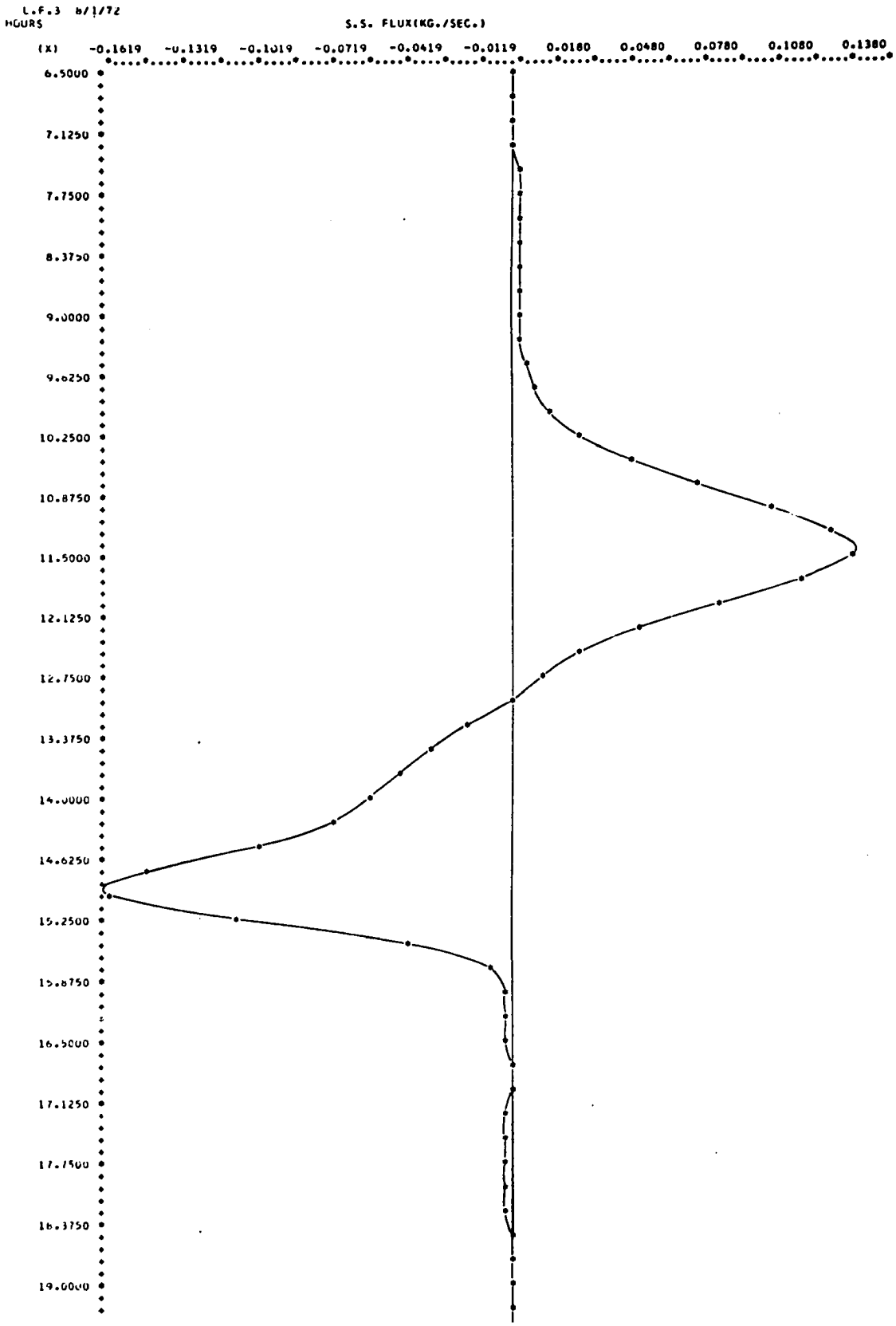

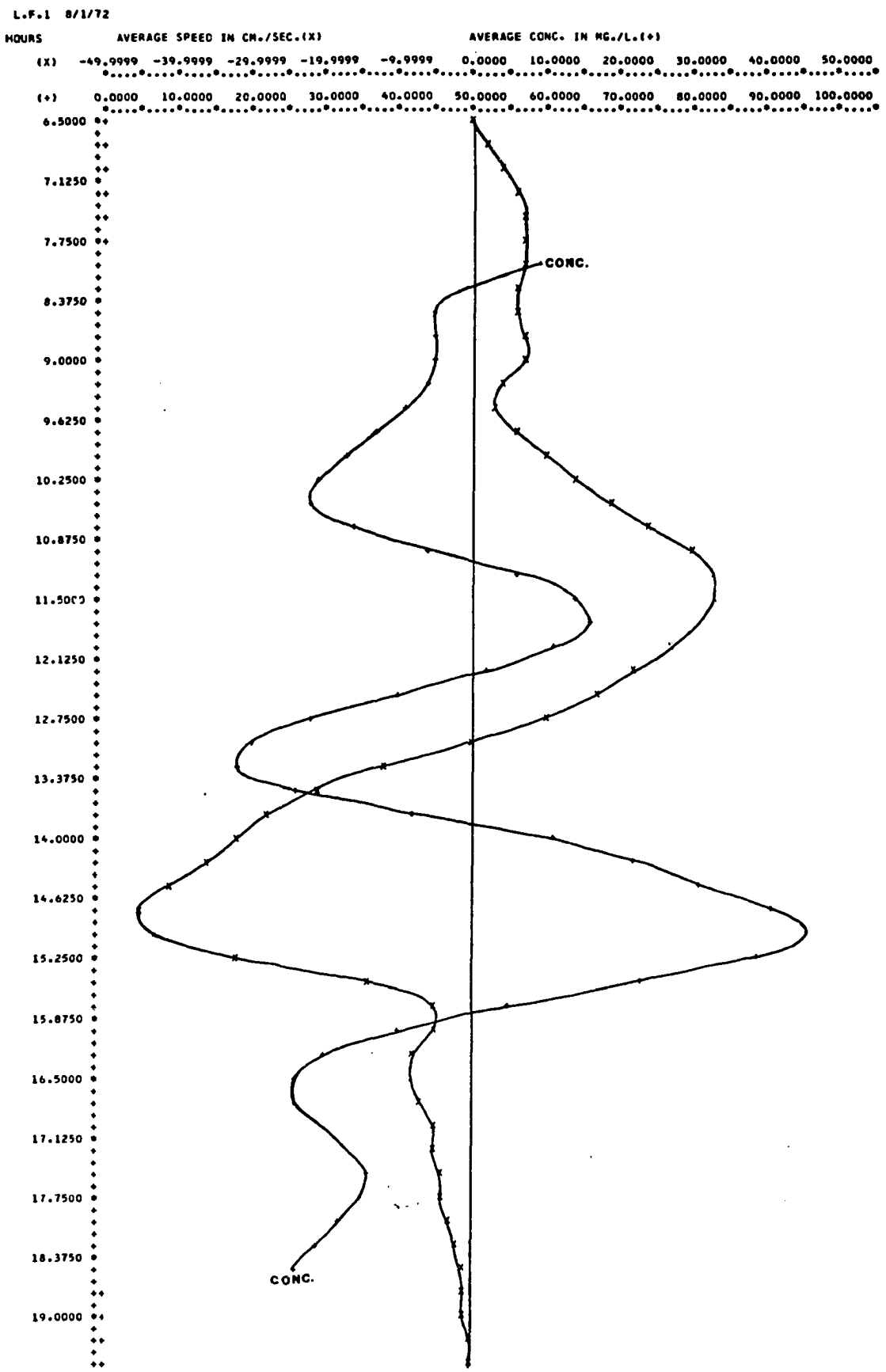

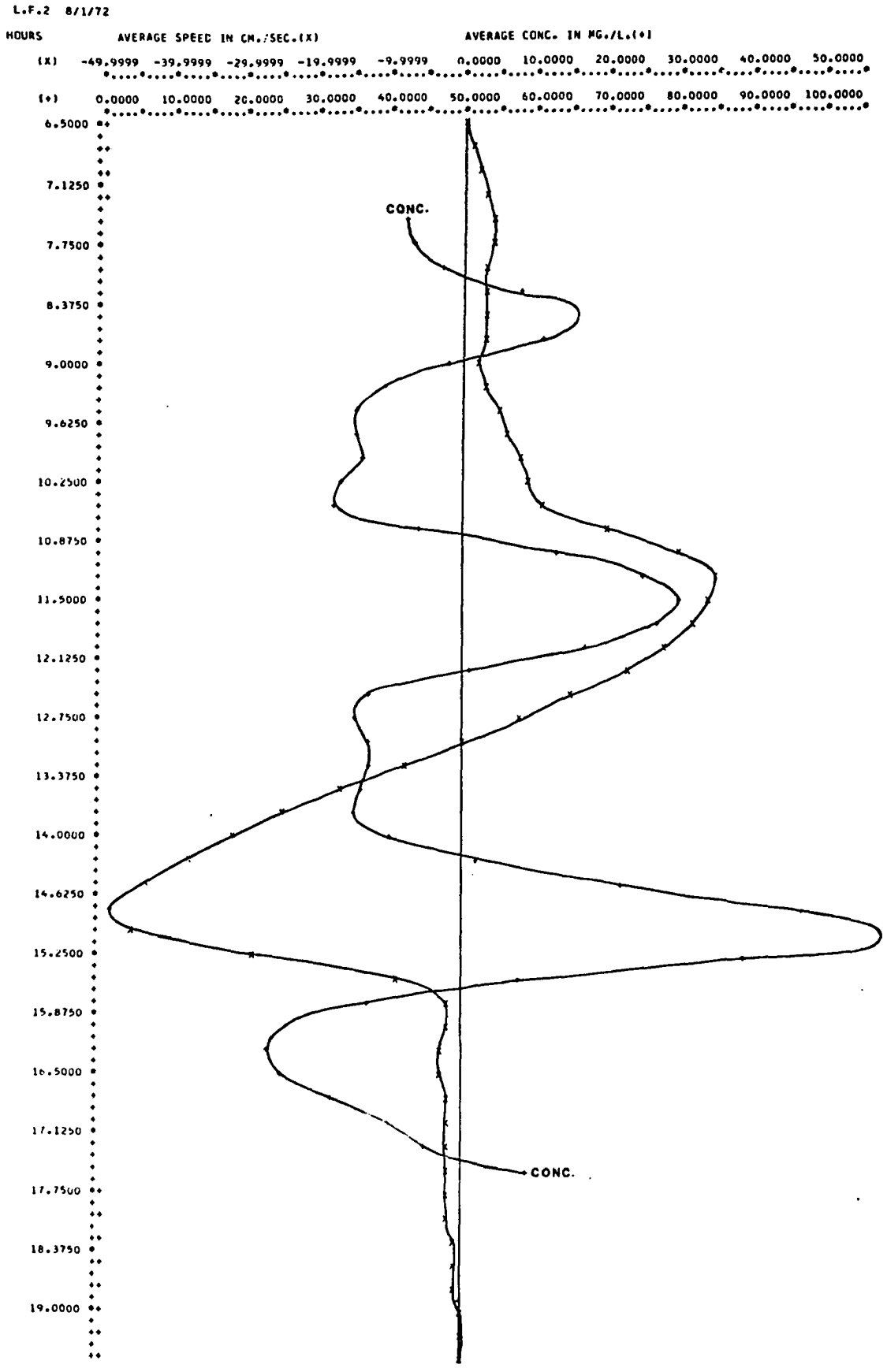

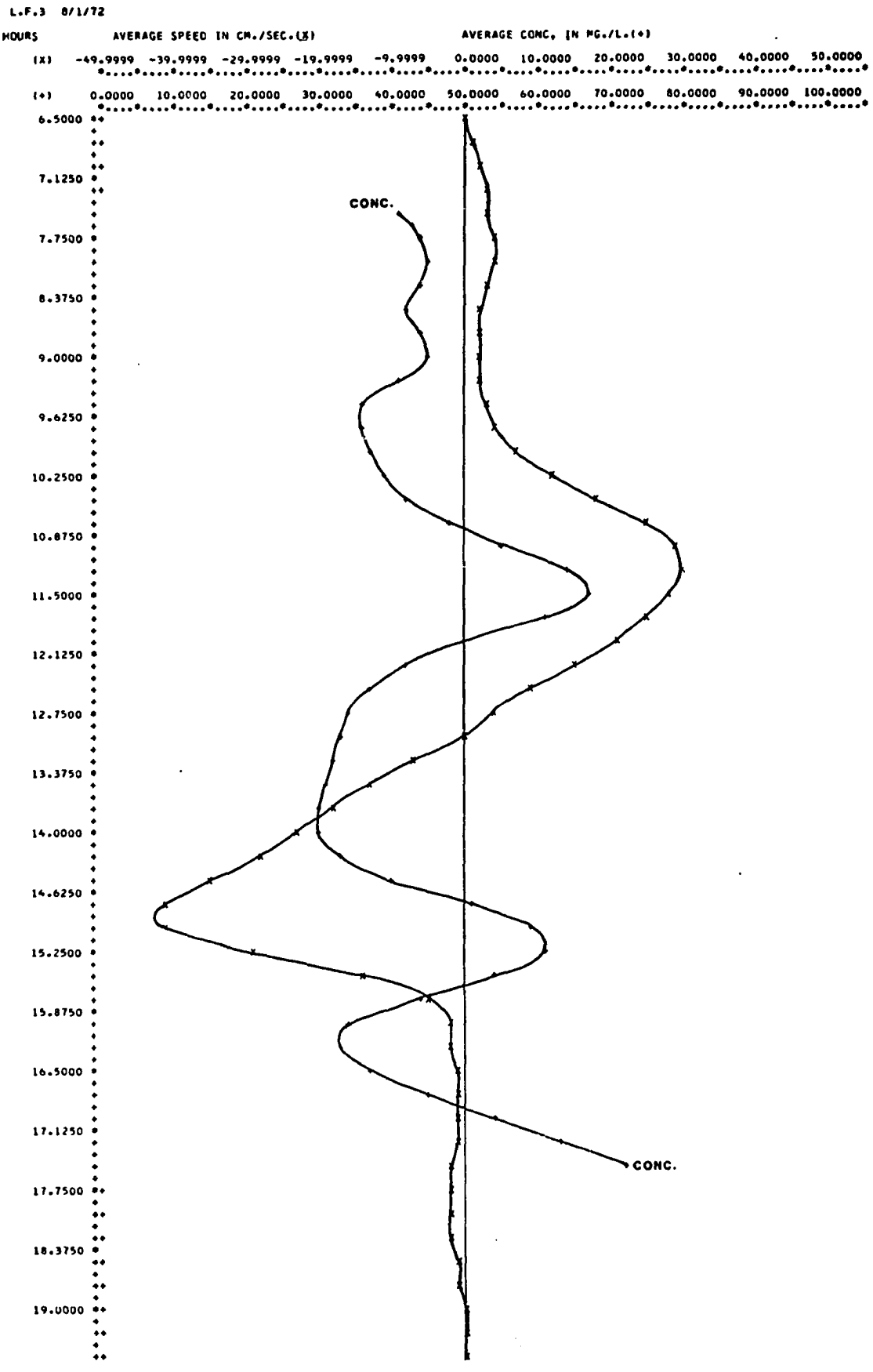

RUN 4

8/31/72

Wind 10-15 mph ENE, partly cloudy

Mean air temp..... 26°C

Mean water temp..... 23°C

Tidal range..... 1.03 m

Mean water level..... 0.68 m

Duration of run: 20.0 to 31.9 hrs.

L.F.1 8/31/72 DISCHARGE(CU.M./SEC.)

INTEGRATED VALUES

FLOOD= 21432.6484

EBB= -22542.0312

RESIDUAL= -1109.3830 PGA= 5.04

TS1=20.00 TS2=25.80 TS3=31.90

INTERPOLATIVE VALUES

TIME(HRS)	DISCHARGE(CU.M./SEC.)
20.000	0.0000
20.250	0.0589
20.500	0.1128
20.750	0.1566
21.000	0.1878
21.250	0.2221
21.500	0.2838
21.750	0.3926
22.000	0.5021
22.250	0.5153
22.500	0.4114
22.750	0.3428
23.000	0.4815
23.250	0.8664
23.500	1.3625
23.750	1.8237
24.000	2.1637
24.250	2.4308
24.500	2.6875
24.750	2.8649
25.000	2.7224
25.250	2.0375
25.500	1.0207
25.750	0.1618
26.000	-0.7567
26.250	-1.7974
26.500	-2.6879
26.750	-3.2710
27.000	-3.5412
27.250	-3.4882
27.500	-3.0440
27.750	-2.1984
28.000	-1.2321
28.250	-0.4976
28.500	-0.1893
28.750	-0.1492
29.000	-0.1883
29.250	-0.2409
29.500	-0.2964
29.750	-0.3440
30.000	-0.3629
30.250	-0.3253
30.500	-0.2145
30.750	-0.0984
31.000	-0.0444
31.250	-0.0328
31.500	-0.0324
31.750	-0.0128
32.000	0.0000

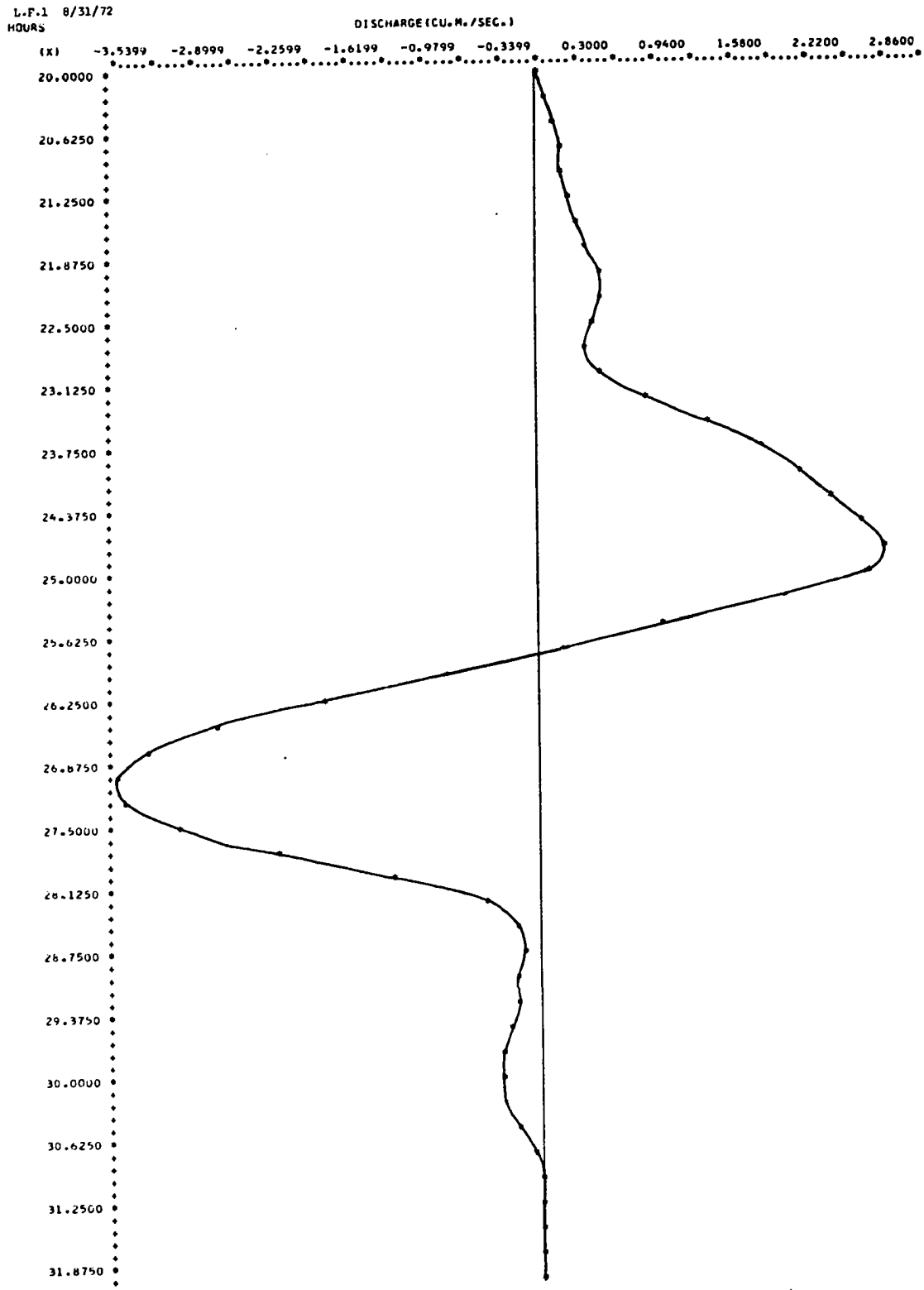

L.F.I 8/31/72 S.S. FLUX(KG./SEC.)
INTEGRATED VALUES
FLOOD= 792.7691
EBB= -1043.0773
RESIDUAL= -250.3081 PGA= 27.26

TS1=20.00 TS2=25.80 TS3=31.90

INTERPOLATIVE VALUES

TIME(HRS)	S.S. FLUX(KG./SEC.)
20.000	0.0000
20.250	0.0030
20.500	0.0059
20.750	0.0082
21.000	0.0098
21.250	0.0112
21.500	0.0134
21.750	0.0169
22.000	0.0202
22.250	0.0197
22.500	0.0147
22.750	0.0114
23.000	0.0164
23.250	0.0314
23.500	0.0511
23.750	0.0699
24.000	0.0841
24.250	0.0943
24.500	0.1015
24.750	0.1035
25.000	0.0936
25.250	0.0659
25.500	0.0295
25.750	0.0036
26.000	-0.0140
26.250	-0.0398
26.500	-0.0888
26.750	-0.1552
27.000	-0.2064
27.250	-0.2152
27.500	-0.1832
27.750	-0.1221
28.000	-0.0559
28.250	-0.0112
28.500	0.0000
28.750	-0.0027
29.000	-0.0060
29.250	-0.0073
29.500	-0.0079
29.750	-0.0091
30.000	-0.0105
30.250	-0.0102
30.500	-0.0067
30.750	-0.0027
31.000	-0.0010
31.250	-0.0007
31.500	-0.0009
31.750	-0.0003
32.000	0.0000

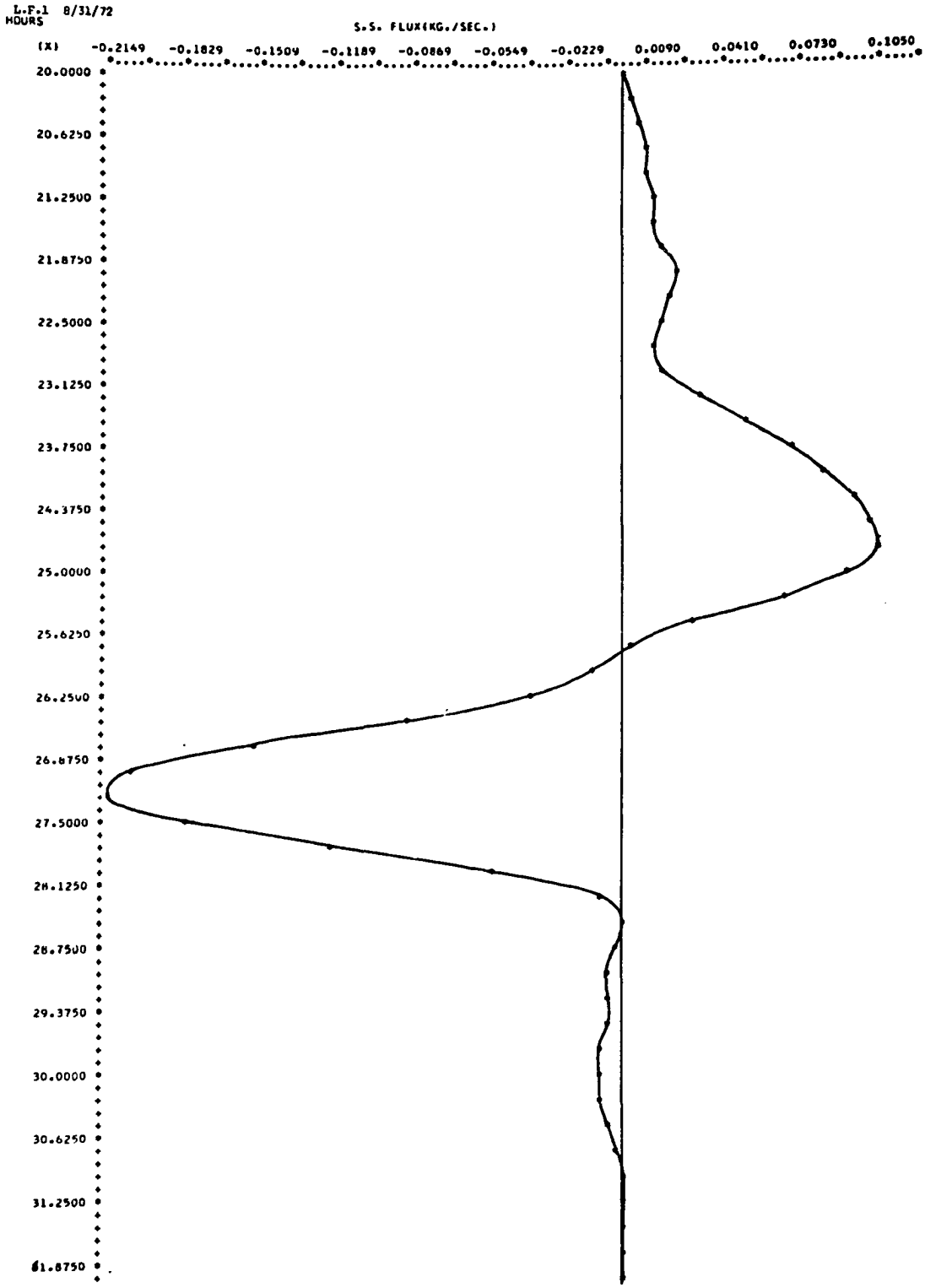

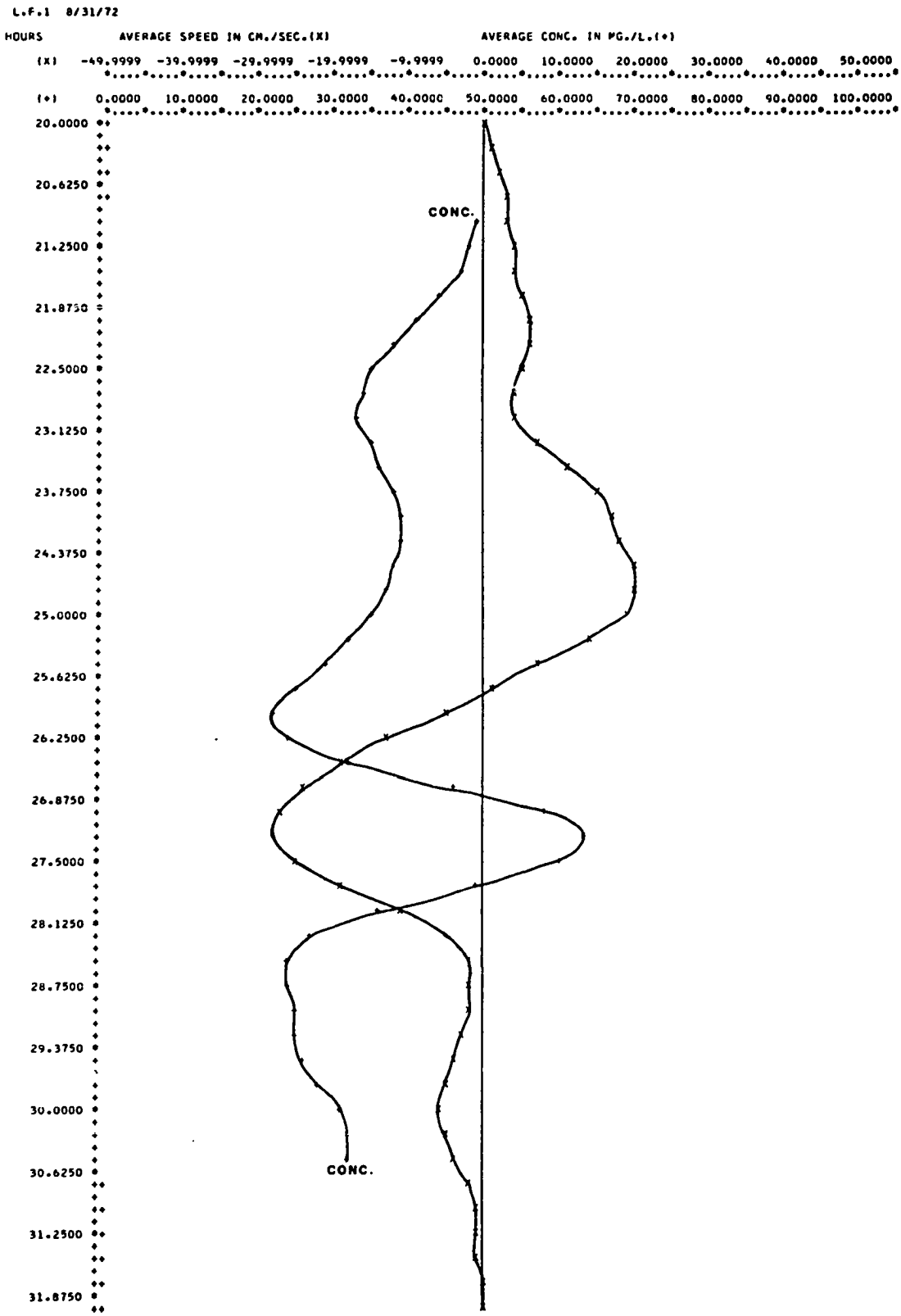

RUN 5*

10/16/72

Wind 10-15 mph SSW, gusts, overcast

Mean air temp..... 16°C

Mean water temp..... 15°C

Tidal range..... 0.82 m

Mean water level..... 0.56 m

Duration of run: 8.2 to 21.0 hrs.

*Three bridge run; minimal current speeds, not reported for L.F.2 and L.F.3.

L.F.1 10/16/72 DISCHARGE(CU.M./SEC.)

INTEGRATED VALUES
FLOOD= 7164.0859
EBB= -7347.0058
RESIDUAL= -182.9199 PGA= 2.24

TS1= 6.20 TS2=15.00 TS3=21.00

INTERPOLATIVE VALUES

TIME(HRS)	DISCHARGE(CU.M./SEC.)
8.000	0.0000
8.250	0.0107
8.500	0.0650
8.750	0.1216
9.000	0.1826
9.250	0.2500
9.500	0.3158
9.750	0.3334
10.000	0.2764
10.250	0.1864
10.500	0.1143
10.750	0.0992
11.000	0.1345
11.250	0.2016
11.500	0.2765
11.750	0.3310
12.000	0.3478
12.250	0.3331
12.500	0.2978
12.750	0.2606
13.000	0.2441
13.250	0.2659
13.500	0.3255
13.750	0.4175
14.000	0.5340
14.250	0.6648
14.500	0.7441
14.750	0.5824
15.000	0.0000
15.250	-0.5509
15.500	-0.8427
15.750	-0.9446
16.000	-0.8939
16.250	-0.7074
16.500	-0.4632
16.750	-0.2870
17.000	-0.2456
17.250	-0.2719
17.500	-0.3015
17.750	-0.3150
18.000	-0.3000
18.250	-0.2609
18.500	-0.2245
18.750	-0.2118
19.000	-0.2165
19.250	-0.2251
19.500	-0.2245
19.750	-0.2044
20.000	-0.1687
20.250	-0.1243
20.500	-0.0782
20.750	-0.0374
21.000	0.0000
21.250	0.0000

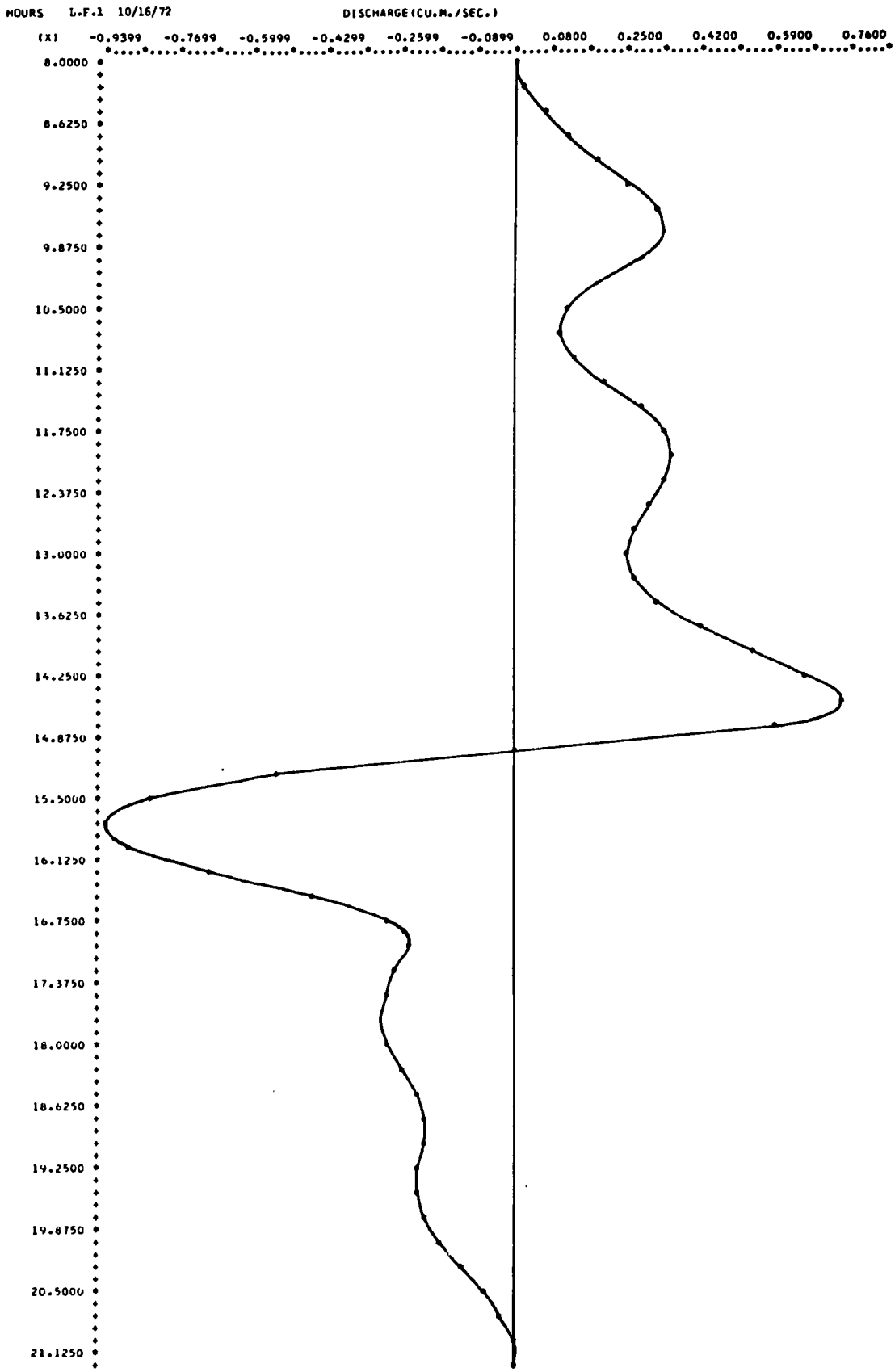

L.F.1 10/16/72 S.S. FLUX(KG./SEC.)

INTEGRATED VALUES

FLOOD= 276.0084

EBB= -230.0614

RESIDUAL= 45.9470 PGA= 18.15

TS1= 8.20 TS2=15.00 TS3=21.00

INTERPOLATIVE VALUES

TIME(HRS)	S.S. FLUX(KG./SEC.)
8.000	0.0000
8.250	0.0004
8.500	0.0027
8.750	0.0049
9.000	0.0070
9.250	0.0089
9.500	0.0105
9.750	0.0105
10.000	0.0085
10.250	0.0057
10.500	0.0032
10.750	0.0022
11.000	0.0031
11.250	0.0058
11.500	0.0096
11.750	0.0126
12.000	0.0137
12.250	0.0132
12.500	0.0118
12.750	0.0102
13.000	0.0095
13.250	0.0105
13.500	0.0128
13.750	0.0161
14.000	0.0205
14.250	0.0272
14.500	0.0334
14.750	0.0278
15.000	0.0000
15.250	-0.0170
15.500	-0.0252
15.750	-0.0291
16.000	-0.0280
16.250	-0.0223
16.500	-0.0147
16.750	-0.0091
17.000	-0.0077
17.250	-0.0085
17.500	-0.0095
17.750	-0.0101
18.000	-0.0101
18.250	-0.0094
18.500	-0.0085
18.750	-0.0077
19.000	-0.0072
19.250	-0.0066
19.500	-0.0060
19.750	-0.0051
20.000	-0.0041
20.250	-0.0031
20.500	-0.0020
20.750	-0.0010
21.000	0.0000
21.250	0.0000

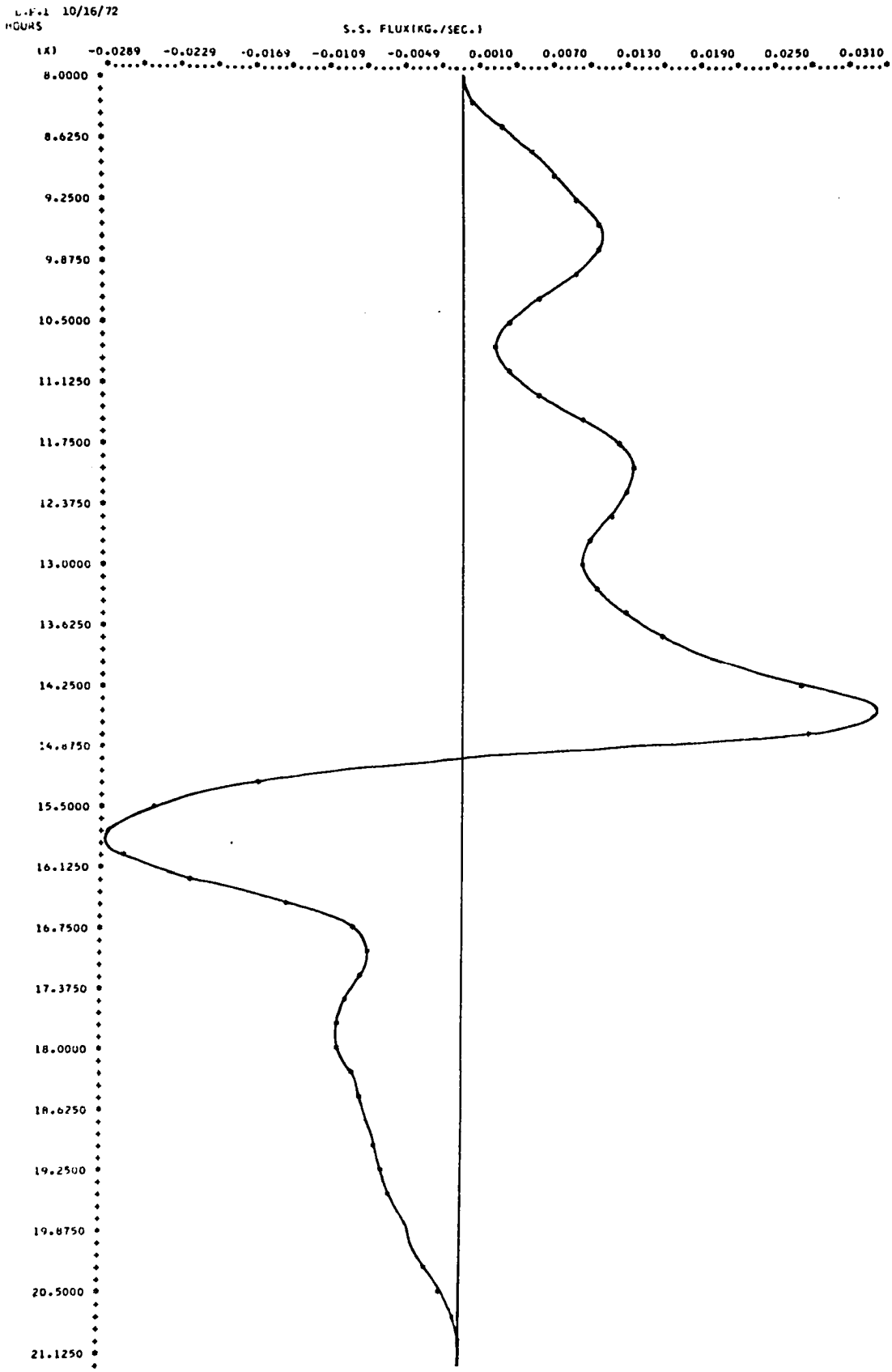

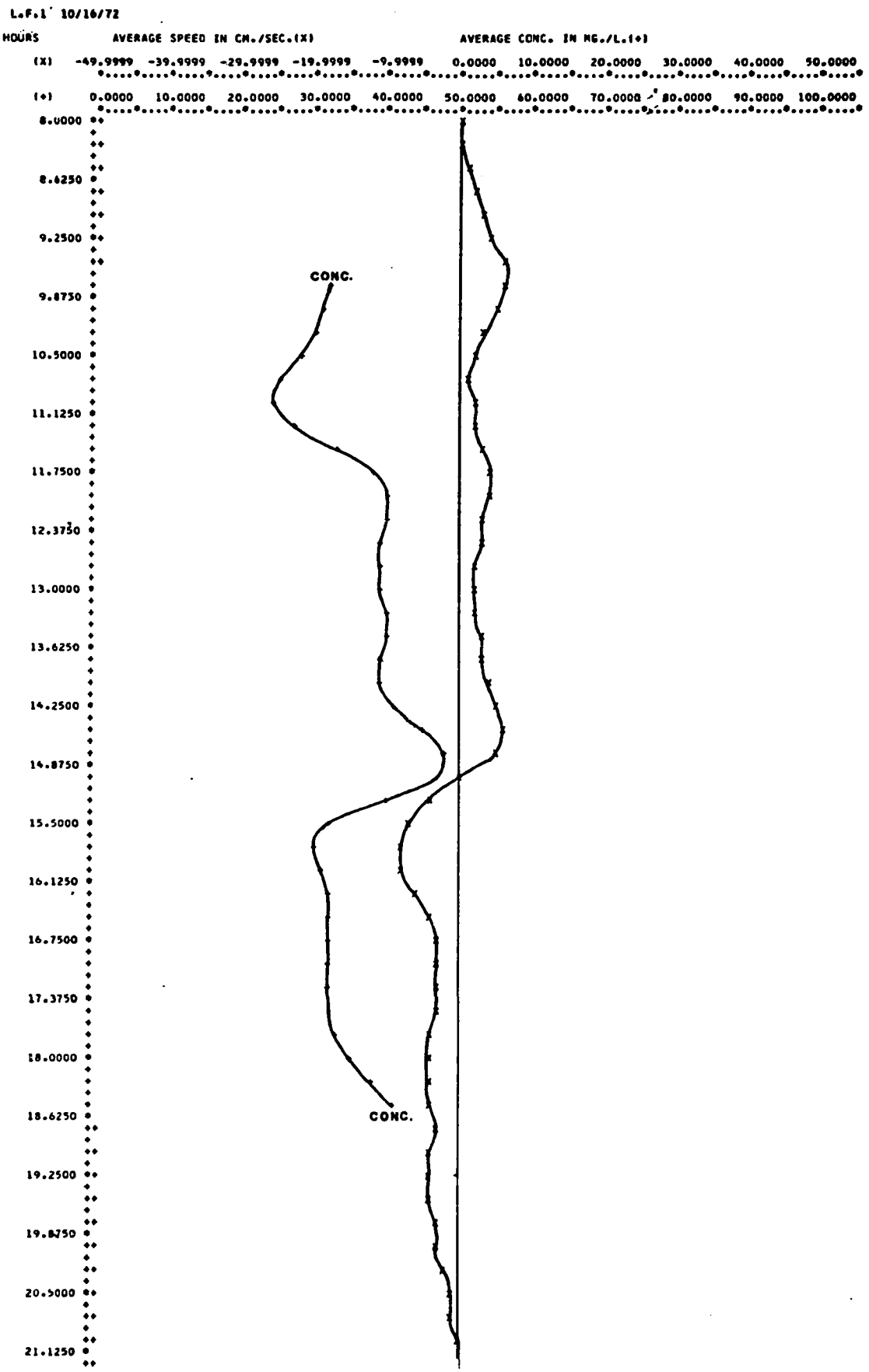

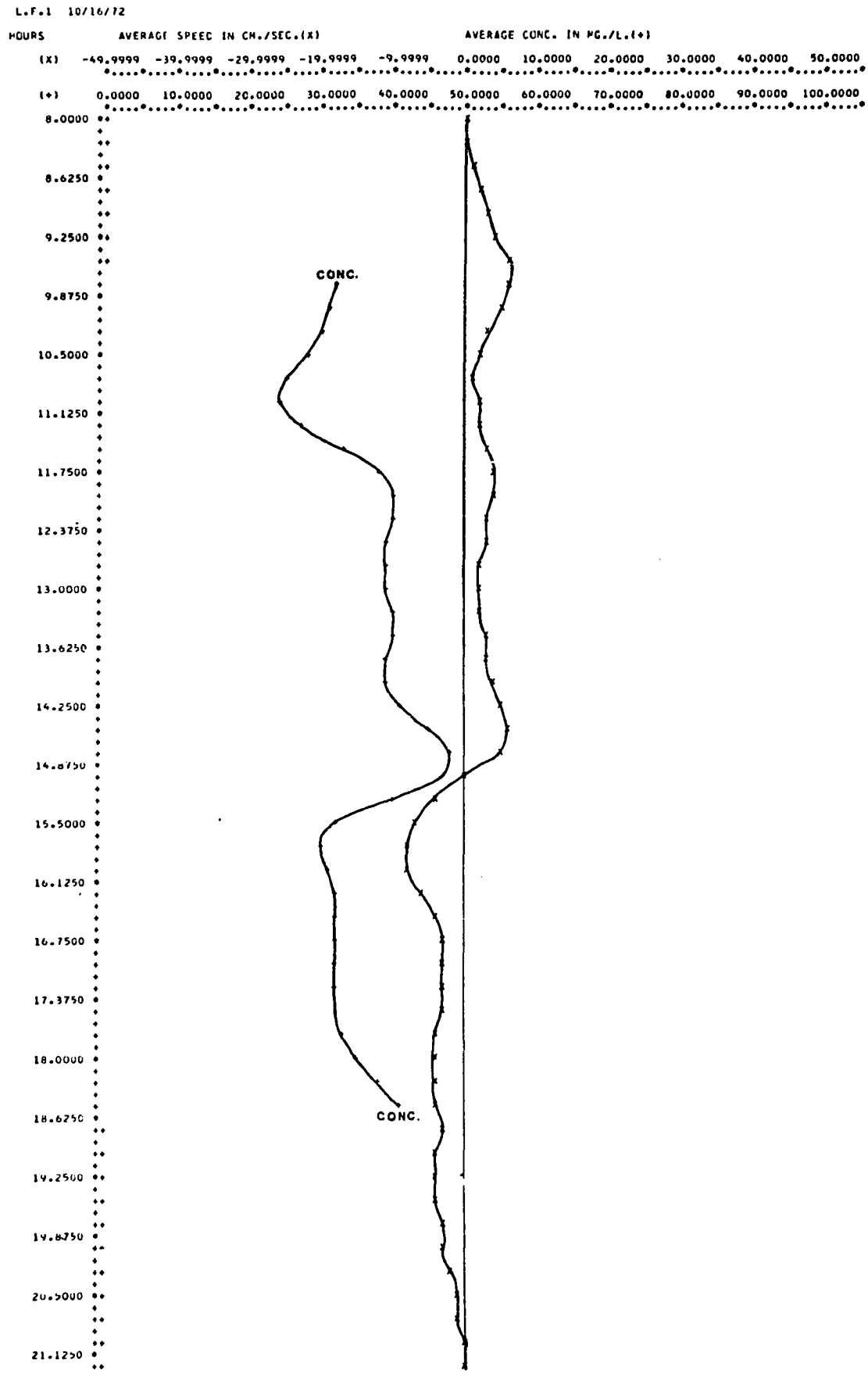

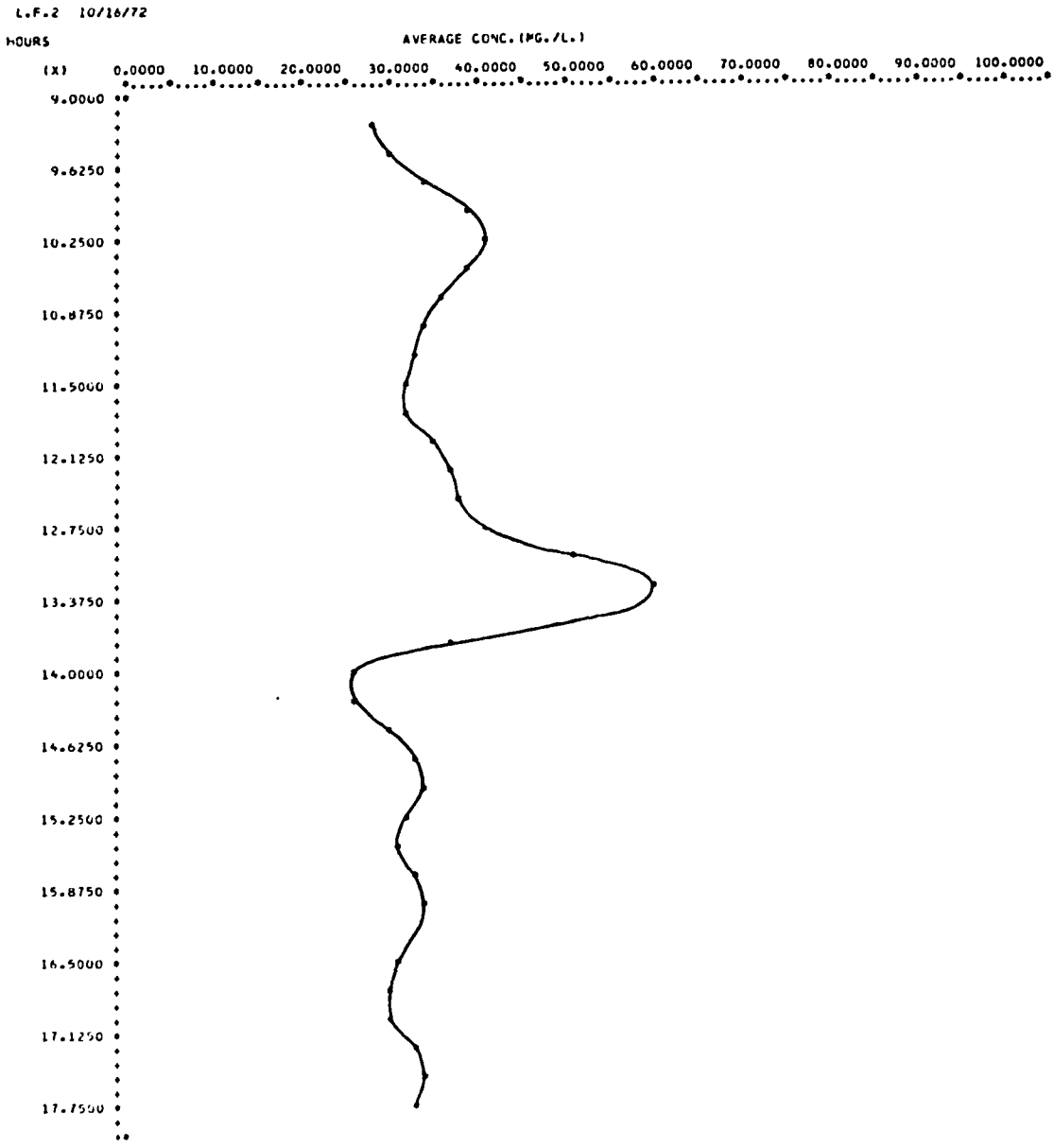

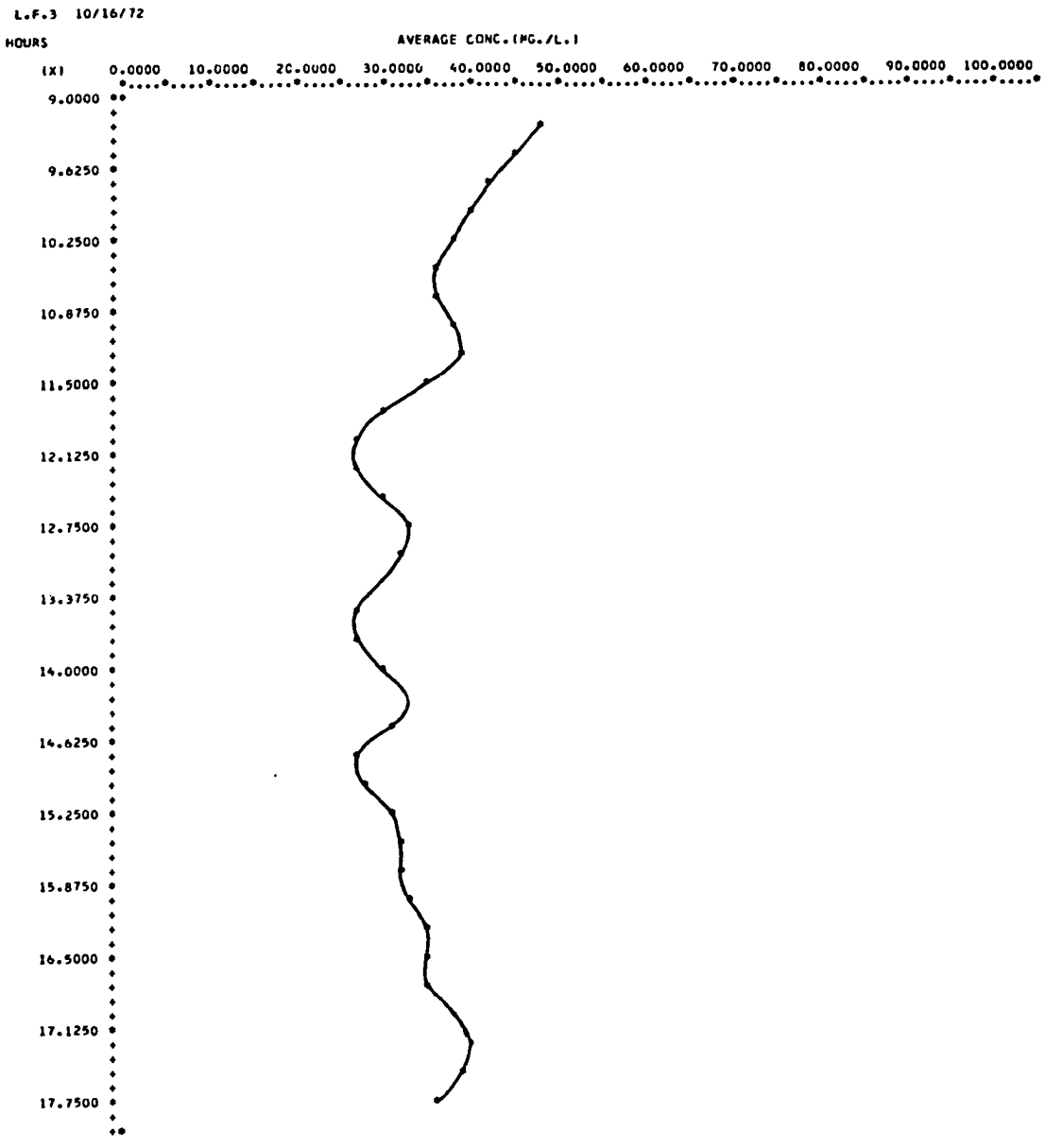

RUN 6

11/12/72

Wind 0-5 mph & variable, clear sky

Mean air temp..... ****

Mean water temp..... 12°C

Tidal range..... 0.99 m

Mean water level..... 0.94 m

Duration of run: 6.0 to 18.5 hrs.

NOTE: This run contains data compiled using two different sampling intervals; viz. 15 minutes and 30 minutes.

L.F.1 11/12/72 15MIN DISCHARGE(CU.M./SEC.)
INTEGRATED VALUES
FLOOD= 37302.5391
EBB= -38582.8516
RESIDUAL= -1280.3127 PGA= 3.37

TS1= 6.00 TS2=12.50 TS3=18.50

INTERPOLATIVE VALUES

TIME(HRS)	DISCHARGE(CU.M./SEC.)
6.000	0.0000
6.250	0.1828
6.500	0.3430
6.750	0.4579
7.000	0.5049
7.250	0.4615
7.500	0.3410
7.750	0.2678
8.000	0.4072
8.250	0.6984
8.500	1.1401
8.750	1.1683
9.000	1.6683
9.250	1.9826
9.500	2.6212
9.750	3.1436
10.000	3.6456
10.250	3.7372
10.500	3.6773
10.750	3.3099
11.000	2.9421
11.250	2.3853
11.500	2.1047
11.750	1.5965
12.000	1.4798
12.250	1.0588
12.500	0.0000
12.750	-1.1466
13.000	-1.6360
13.250	-2.4649
13.500	-3.2041
13.750	-3.7039
14.000	-3.6720
14.250	-3.9521
14.500	-4.0079
14.750	-4.3251
15.000	-4.2138
15.250	-3.7921
15.500	-2.7536
15.750	-1.0938
16.000	-0.6858
16.250	-0.5073
16.500	-0.2656
16.750	-0.3600
17.000	-0.1829
17.250	-0.2133
17.500	-0.2381
17.750	-0.1880
18.000	-0.1078
18.250	-0.0426
18.500	0.0000

L.F.1 11/12/72 30MIN DISCHARGE(CU.M./SEC.)
INTEGRATED VALUES
FLOOD= 37287.7657
FBB= -37678.8047
RESIDUAL= -391.0391 PGA= 1.04

TS1= 6.00 TS2=12.50 TS3=18.50

INTERPOLATIVE VALUES

TIME(HRS)	DISCHARGE(CU.M./SEC.)
6.000	0.0000
6.250	0.1035
6.500	0.1990
6.750	0.2785
7.000	0.3340
7.250	0.3575
7.500	0.3410
7.750	0.3078
8.000	0.4072
8.250	0.7463
8.500	1.1401
8.750	1.4065
9.000	1.6683
9.250	2.0803
9.500	2.6212
9.750	3.2025
10.000	3.6456
10.250	3.7947
10.500	3.6773
10.750	3.3671
11.000	2.9421
11.250	2.4863
11.500	2.1047
11.750	1.8417
12.000	1.4798
12.250	0.8198
12.500	0.0000
12.750	-0.8080
13.000	-1.6360
13.250	-2.5065
13.500	-3.2041
13.750	-3.5399
14.000	-3.6720
14.250	-3.8080
14.500	-4.0079
14.750	-4.2347
15.000	-4.2138
15.250	-3.6934
15.500	-2.7538
15.750	-1.6101
16.000	-0.6858
16.250	-0.3147
16.500	-0.2656
16.750	-0.2332
17.000	-0.1829
17.250	-0.1411
17.500	-0.1095
17.750	-0.0836
18.000	-0.0587
18.250	-0.0304
18.500	0.0000

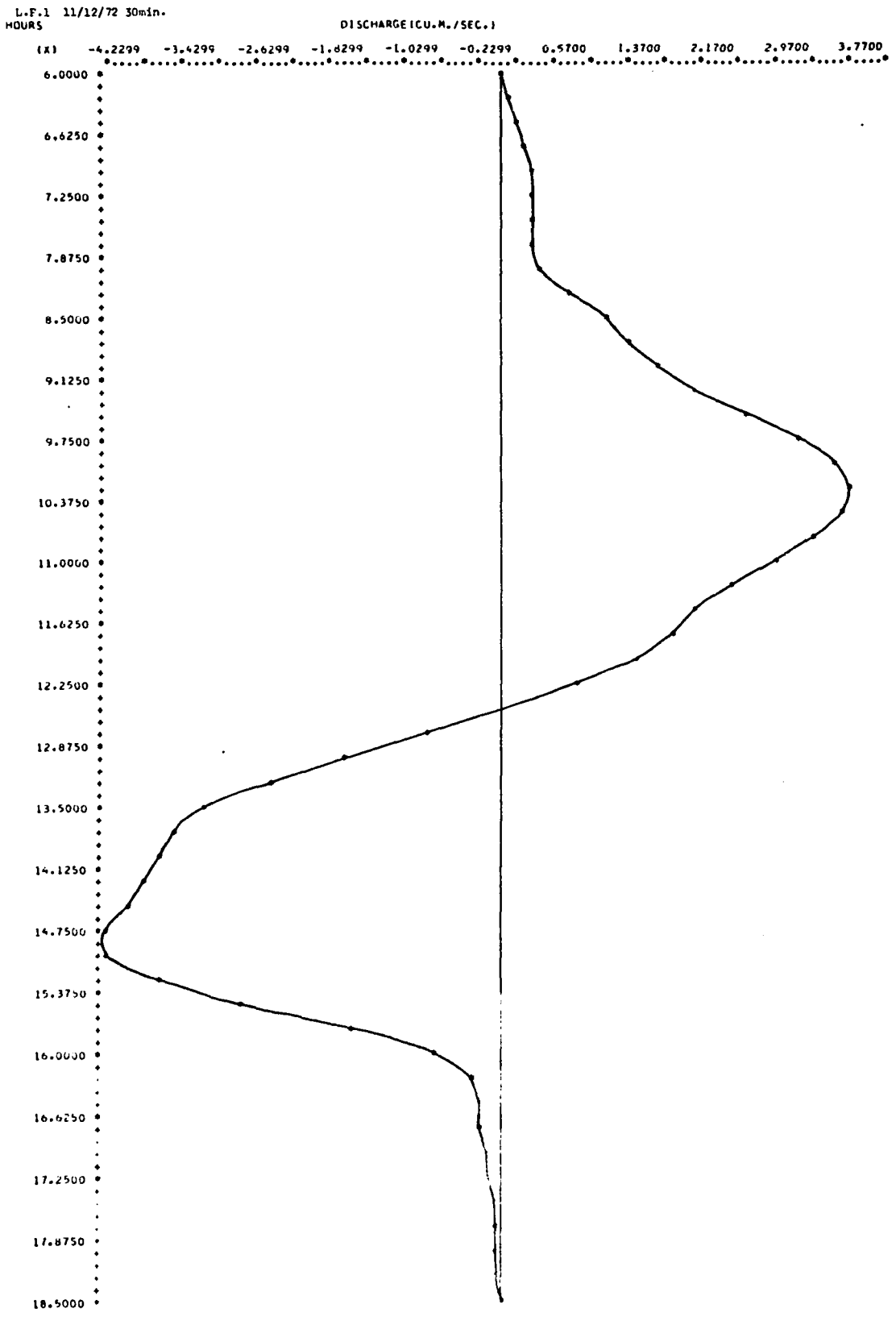

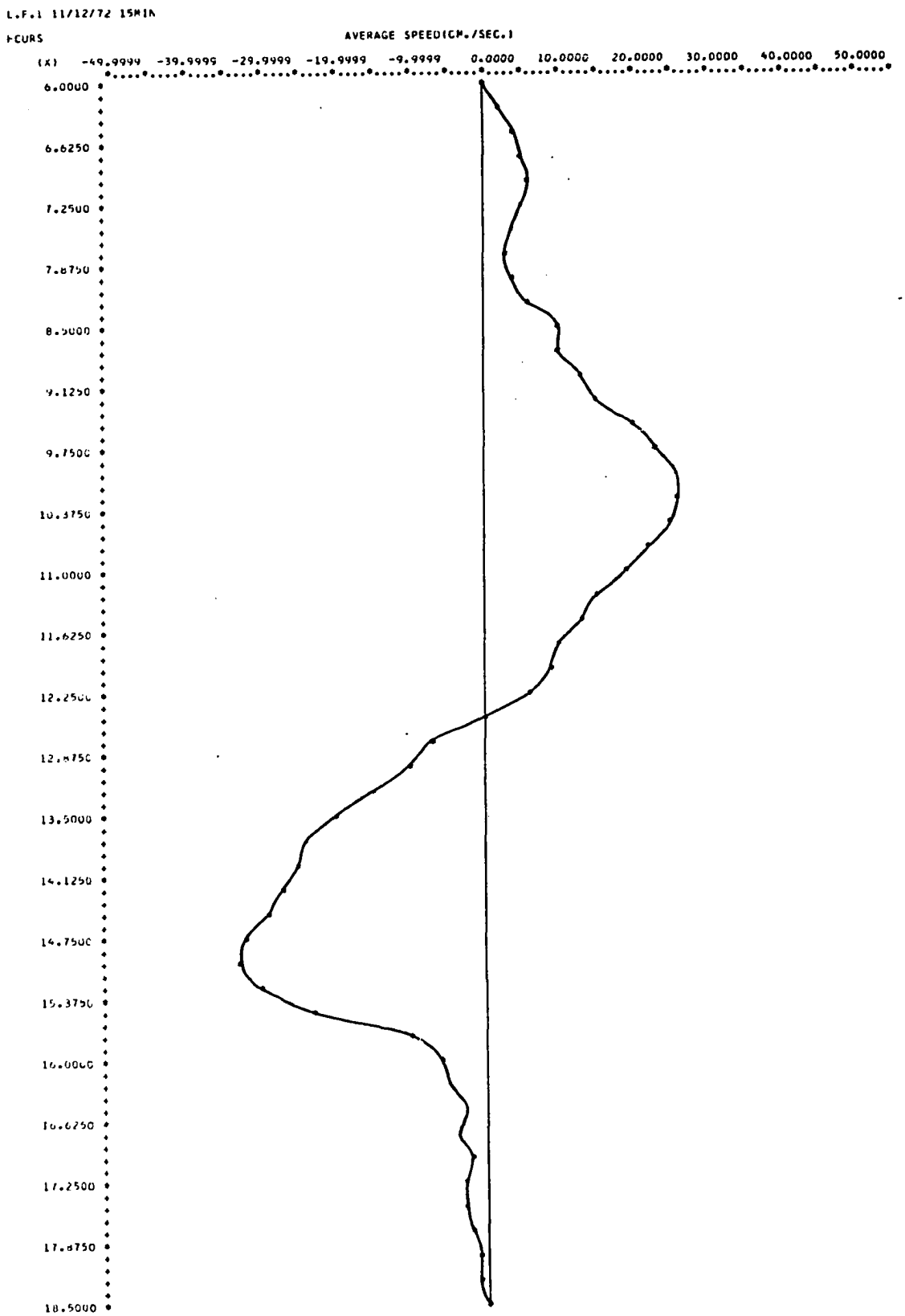

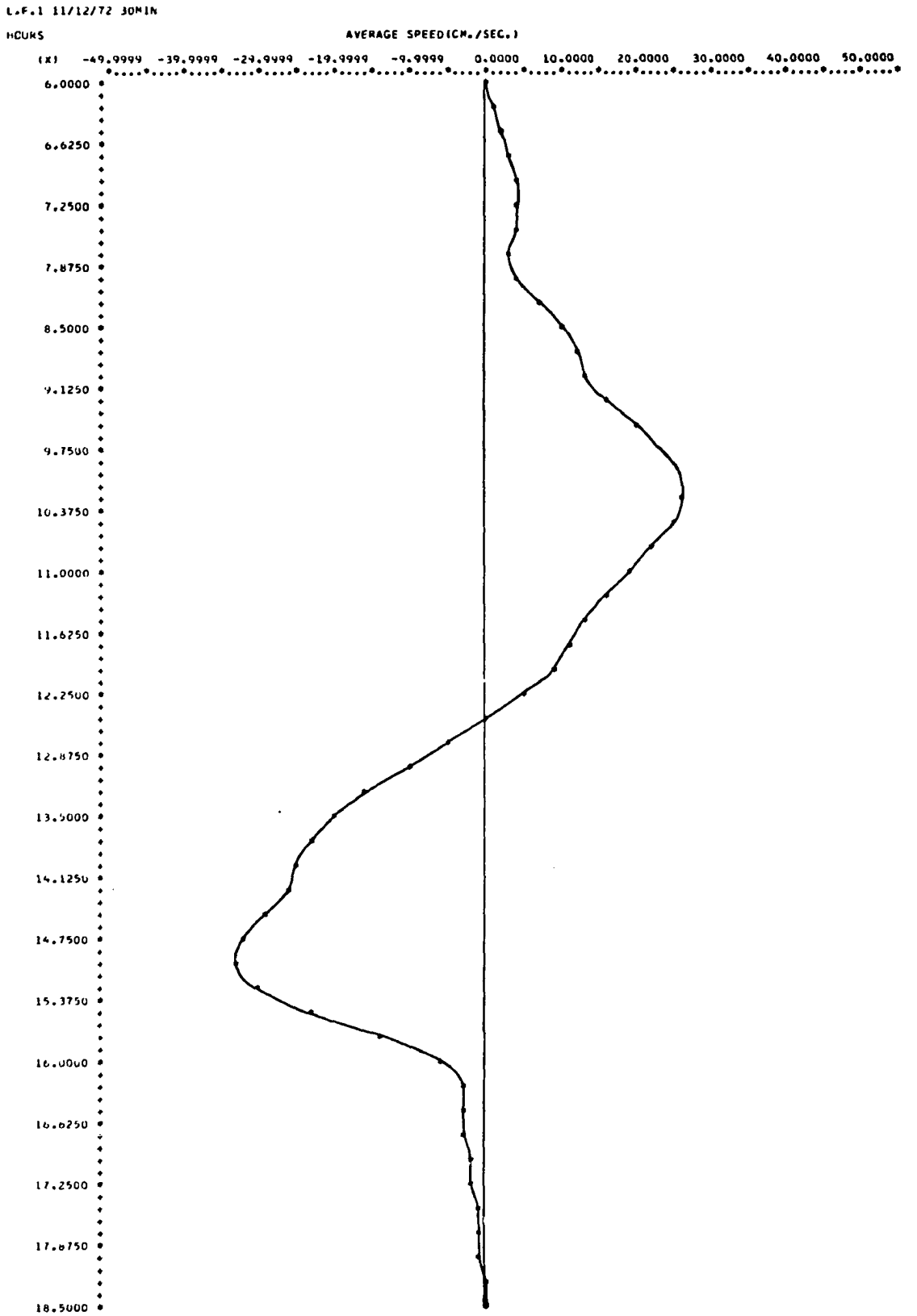

RUN 7

11/30/72

Wind 10-15 mph NE to NNW, light rain

Mean air temp..... 10°C

Mean water temp..... 12°C

Tidal range..... 1.03 m

Mean water level..... 0.81 m

Duration of run: 9.9 to 22.2 hrs.

L.F.1 11/30/72 DISCHARGE(CU.M./SEC.)

INTEGRATED VALUES

FLOOD= 30201.0078

EBB= -32232.4063

RESIDUAL= -2031.3986 PGA= 6.50

TS1= 9.90 TS2=16.70 TS3=22.20

INTERPOLATIVE VALUES

TIME(HRS)	DISCHARGE(CU.M./SEC.)
9.750	0.0000
10.000	0.0601
10.250	0.1994
10.500	0.3023
10.750	0.3427
11.000	0.2960
11.250	0.1965
11.500	0.1550
11.750	0.2495
12.000	0.4084
12.250	0.5198
12.500	0.4635
12.750	0.2162
13.000	0.1541
13.250	0.5733
13.500	1.0525
13.750	1.1770
14.000	1.2775
14.250	1.7177
14.500	2.2509
14.750	2.5930
15.000	2.9240
15.250	3.3998
15.500	3.6184
15.750	3.2281
16.000	2.6390
16.250	2.2101
16.500	1.3360
16.750	-0.3385
17.000	-1.7123
17.250	-2.3924
17.500	-2.7492
17.750	-3.4116
18.000	-4.1897
18.250	-4.7129
18.500	-4.7209
18.750	-4.0643
19.000	-2.9282
19.250	-1.6220
19.500	-0.6208
19.750	-0.2807
20.000	-0.3190
20.250	-0.3690
20.500	-0.3682
20.750	-0.3298
21.000	-0.2670
21.250	-0.1932
21.500	-0.1216
21.750	-0.0655
22.000	-0.0307
22.250	0.0000

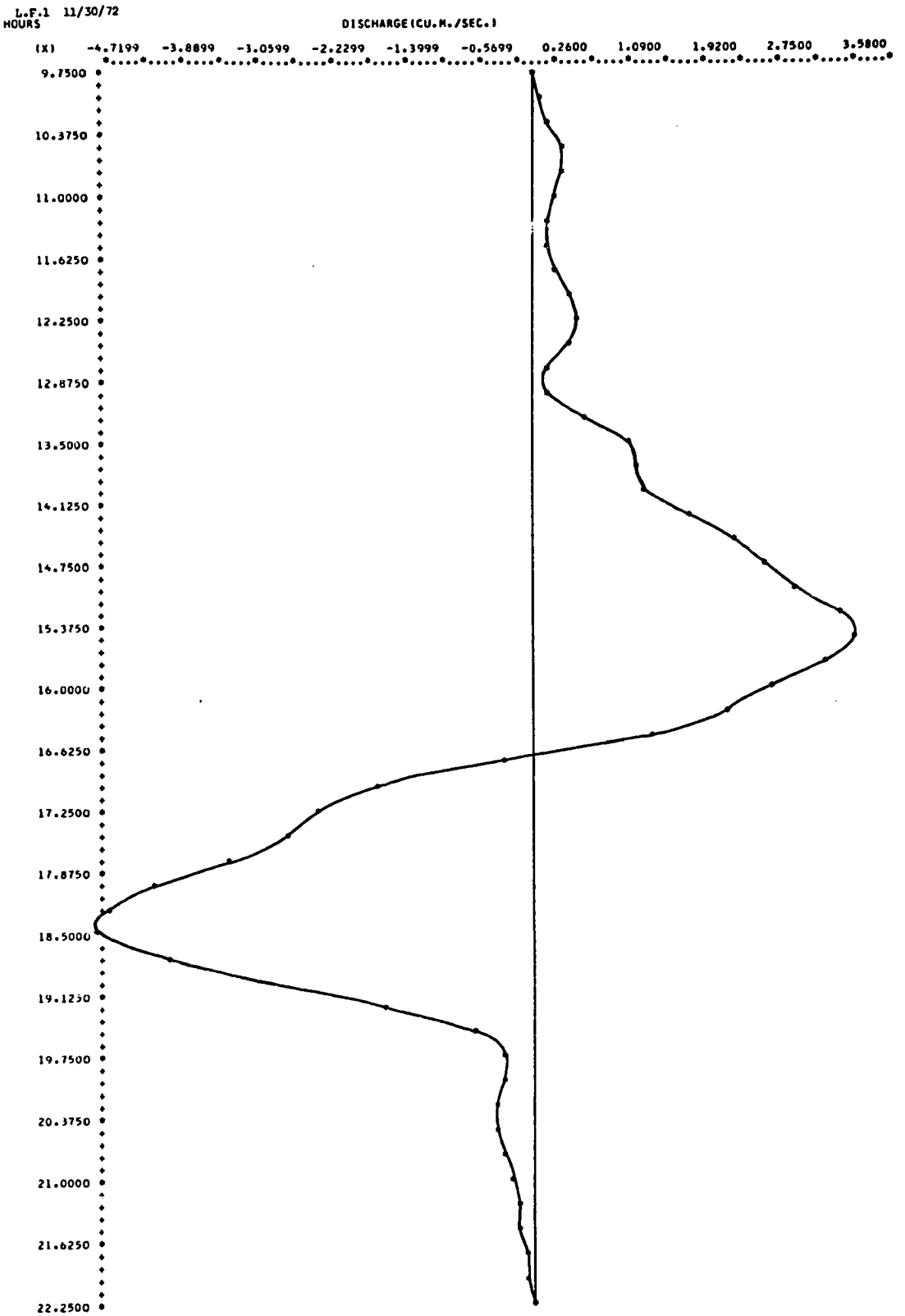

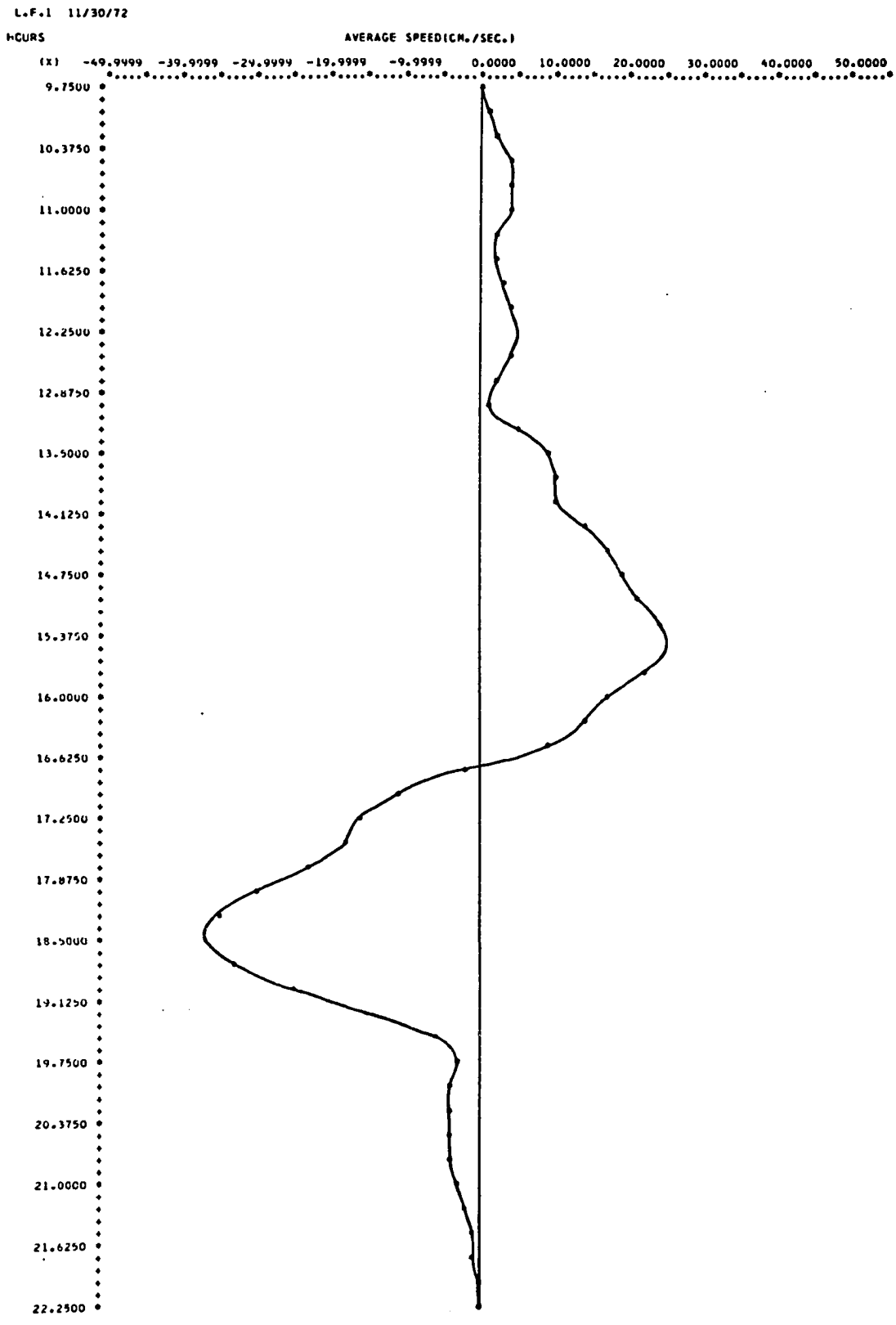

RUN 8

12/11/72

Wind 0-5 mph N, clear sky

Mean air temp..... 6°C

Mean water temp..... 11°C

Tidal range..... 1.10 m

Mean water level..... 0.68 m

Duration of run: 5.2 to 17.5 hrs.

L.F.1 12/11/72 DISCHARGE(CU.M./SEC.)

INTEGRATED VALUES
FLOOD= 24530.0469
EBB= -24047.7891
RESIDUAL= 482.2578 PGA= 1.98

TS1= 5.15 TS2=11.95 TS3=17.50

INTERPOLATIVE VALUES

TIME(HRS)	DISCHARGE(CU.M./SEC.)
5.000	0.0000
5.250	0.0240
5.500	0.0807
5.750	0.1261
6.000	0.1519
6.250	0.1500
6.500	0.1183
6.750	0.0788
7.000	0.0597
7.250	0.0890
7.500	0.1937
7.750	0.3604
8.000	0.5233
8.250	0.6213
8.500	0.6278
8.750	0.5354
9.000	0.4963
9.250	0.7841
9.500	1.4696
9.750	2.1633
10.000	2.5738
10.250	2.7682
10.500	2.8486
10.750	2.8183
11.000	2.6365
11.250	2.2761
11.500	1.7282
11.750	0.9428
12.000	-0.2929
12.250	-1.5665
12.500	-2.3608
12.750	-3.1468
13.000	-3.9600
13.250	-4.4644
13.500	-4.2665
13.750	-3.0220
14.000	-1.3047
14.250	-0.3242
14.500	-0.2521
14.750	-0.4476
15.000	-0.4664
15.250	-0.3489
15.500	-0.2010
15.750	-0.1066
16.000	-0.0613
16.250	-0.0394
16.500	-0.0273
16.750	-0.0209
17.000	-0.0162
17.250	-0.0090
17.500	0.0000

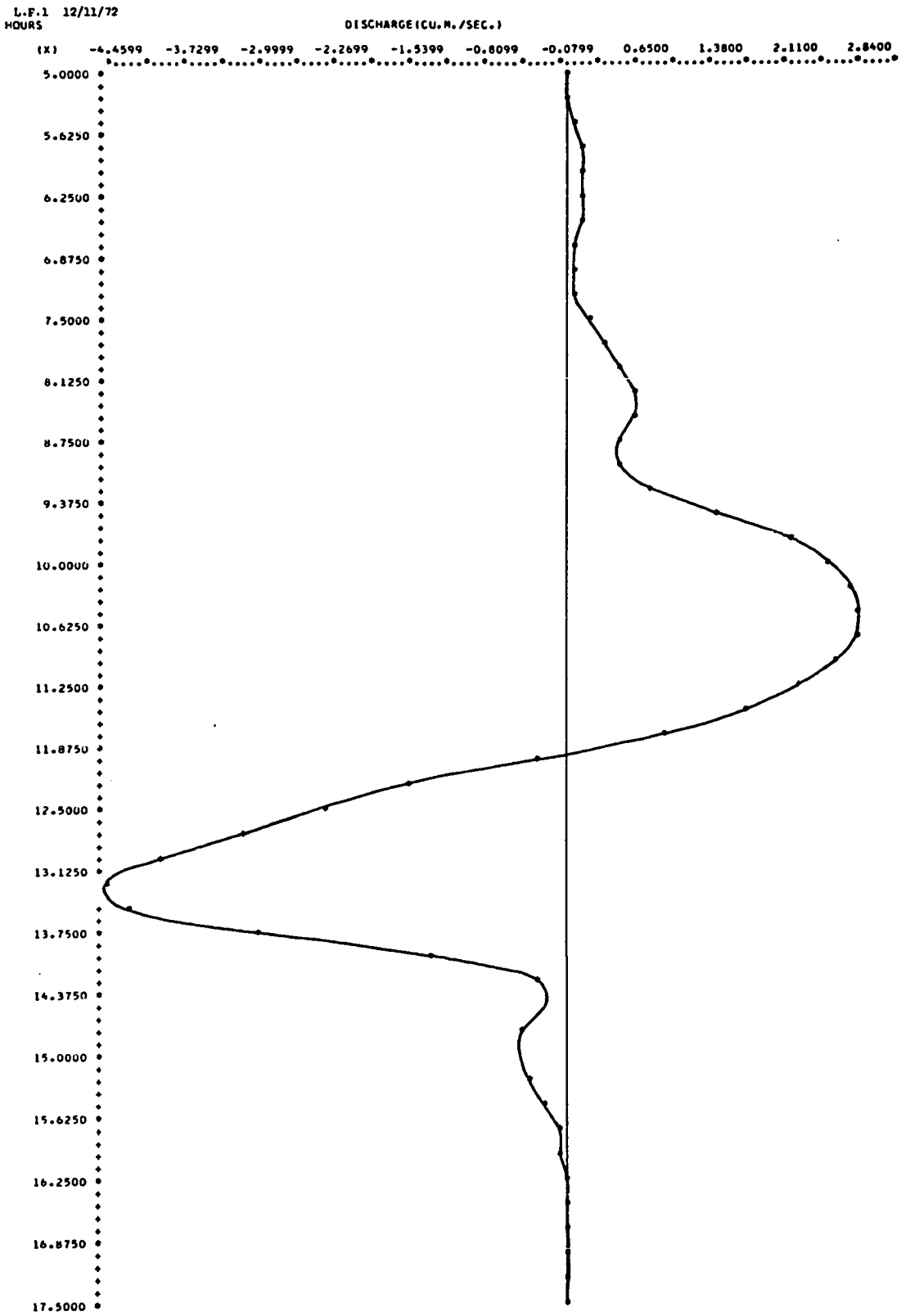

L.I.1 12/11/72 S.S. FLUX(KG./SEC.)

INTEGRATED VALUES

FLOOD= 723.0202

EBB= -548.3155

RESIDUAL= 174.7047 PGA= 27.48

TS1= 5.15 TS2=11.95 TS3=17.50

INTERPOLATIVE VALUES

TIME(HRS)	S.S. FLUX(KG./SEC.)
5.000	0.0000
5.250	0.0001
5.500	0.0006
5.750	0.0011
6.000	0.0016
6.250	0.0020
6.500	0.0022
6.750	0.0022
7.000	0.0016
7.250	0.0014
7.500	0.0037
7.750	0.0088
8.000	0.0139
8.250	0.0167
8.500	0.0171
8.750	0.0155
9.000	0.0148
9.250	0.0198
9.500	0.0333
9.750	0.0537
10.000	0.0769
10.250	0.0948
10.500	0.1000
10.750	0.0943
11.000	0.0831
11.250	0.0689
11.500	0.0497
11.750	0.0239
12.000	-0.0062
12.250	-0.0278
12.500	-0.0372
12.750	-0.0544
13.000	-0.0844
13.250	-0.1167
13.500	-0.1269
13.750	-0.0905
14.000	-0.0306
14.250	-0.0034
14.500	-0.0052
14.750	-0.0069
15.000	-0.0064
15.250	-0.0047
15.500	-0.0028
15.750	-0.0016
16.000	-0.0009
16.250	-0.0005
16.500	-0.0003
16.750	-0.0002
17.000	-0.0002
17.250	-0.0001
17.500	0.0000

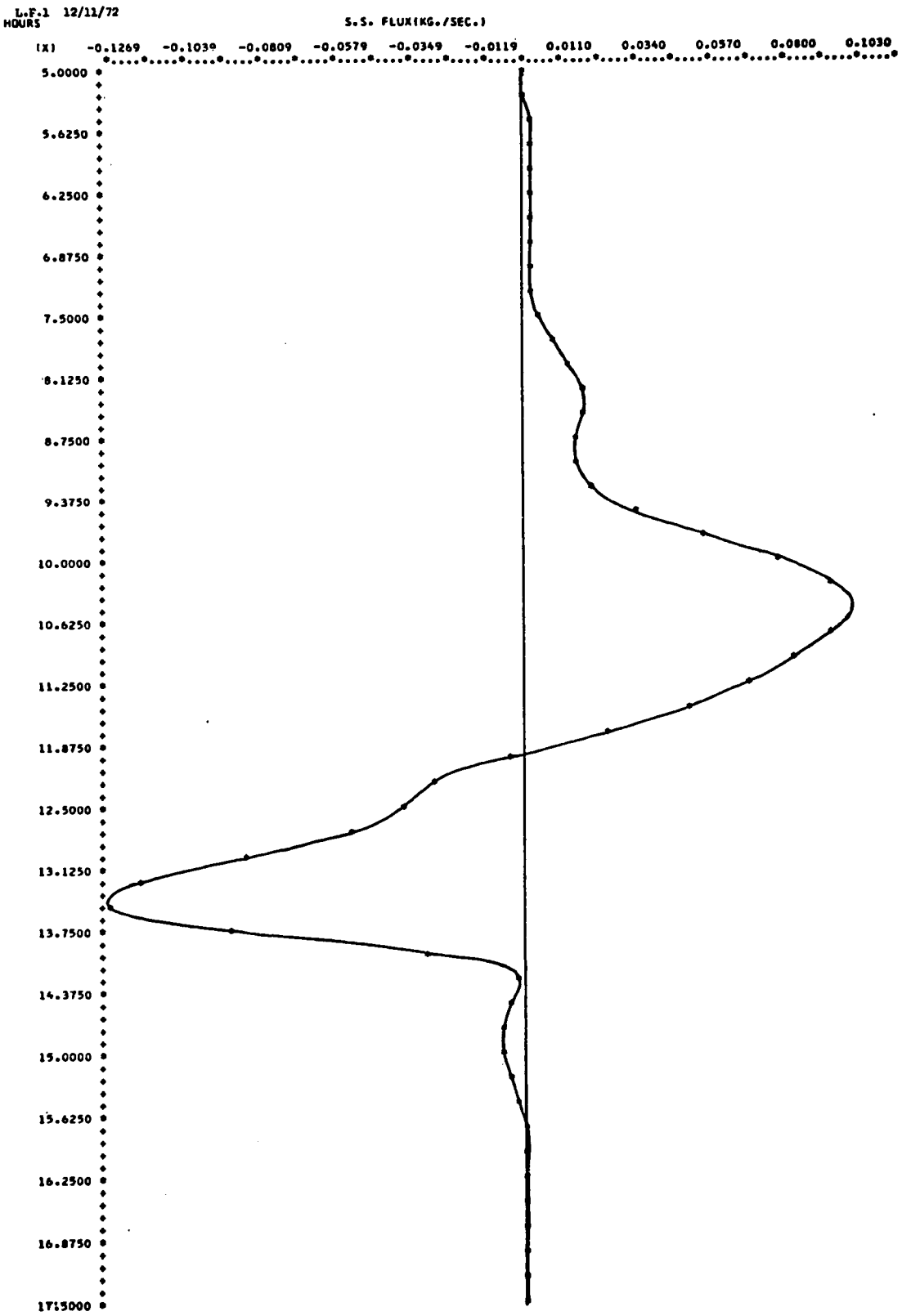

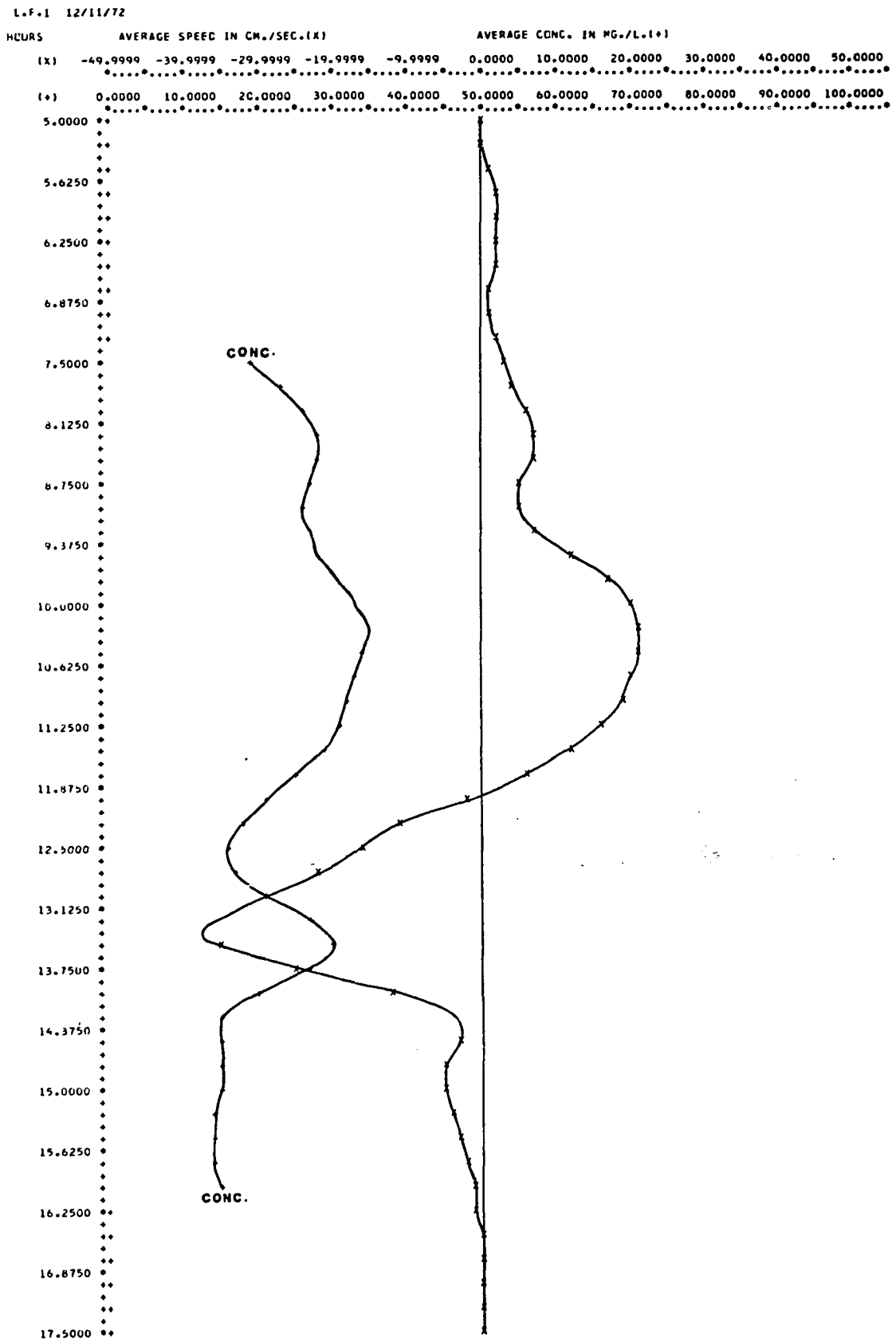

RUN 9

12/20/72

Wind 5-10 mph WSW, partly cloudy

Mean air temp..... 15°C

Mean water temp..... 6°C

Tidal range..... 1.88 m

Mean water level..... 0.60 m

Duration of run: 1.2 to 14.2 hrs.

L.F.1 12/20/72 DISCHARGE(CU.M./SEC.)

INTEGRATED VALUES

FLOOD= 41986.3125

FBB= -44962.4844

RESIDUAL= -2976.1723 PGA= 6.84

TS1= 1.20 TS2= 8.30 TS3=14.20

INTERPOLATIVE VALUES

TIME(HRS)	DISCHARGE(CU.M./SEC.)
1.000	0.0000
1.250	-0.0007
1.500	-0.0039
1.750	-0.0049
2.000	-0.0017
2.250	0.0074
2.500	0.0244
2.750	0.0512
3.000	0.0895
3.250	0.1414
3.500	0.2087
3.750	0.2889
4.000	0.3631
4.250	0.4121
4.500	0.4352
4.750	0.4791
5.000	0.7653
5.250	1.4742
5.500	2.4483
5.750	3.4683
6.000	4.4075
6.250	5.1386
6.500	5.4422
6.750	5.1603
7.000	4.4749
7.250	3.6560
7.500	2.9869
7.750	2.5774
8.000	1.8321
8.250	0.3218
8.500	-1.1375
8.750	-2.3171
9.000	-3.3711
9.250	-4.3795
9.500	-5.1589
9.750	-5.5561
10.000	-5.8034
10.250	-6.0414
10.500	-5.6604
10.750	-4.1811
11.000	-2.3989
11.250	-1.2042
11.500	-0.5958
11.750	-0.3595
12.000	-0.3243
12.250	-0.3450
12.500	-0.3396
12.750	-0.2663
13.000	-0.1824
13.250	-0.1294
13.500	-0.0963
13.750	-0.0686
14.000	-0.0322
14.250	0.0000

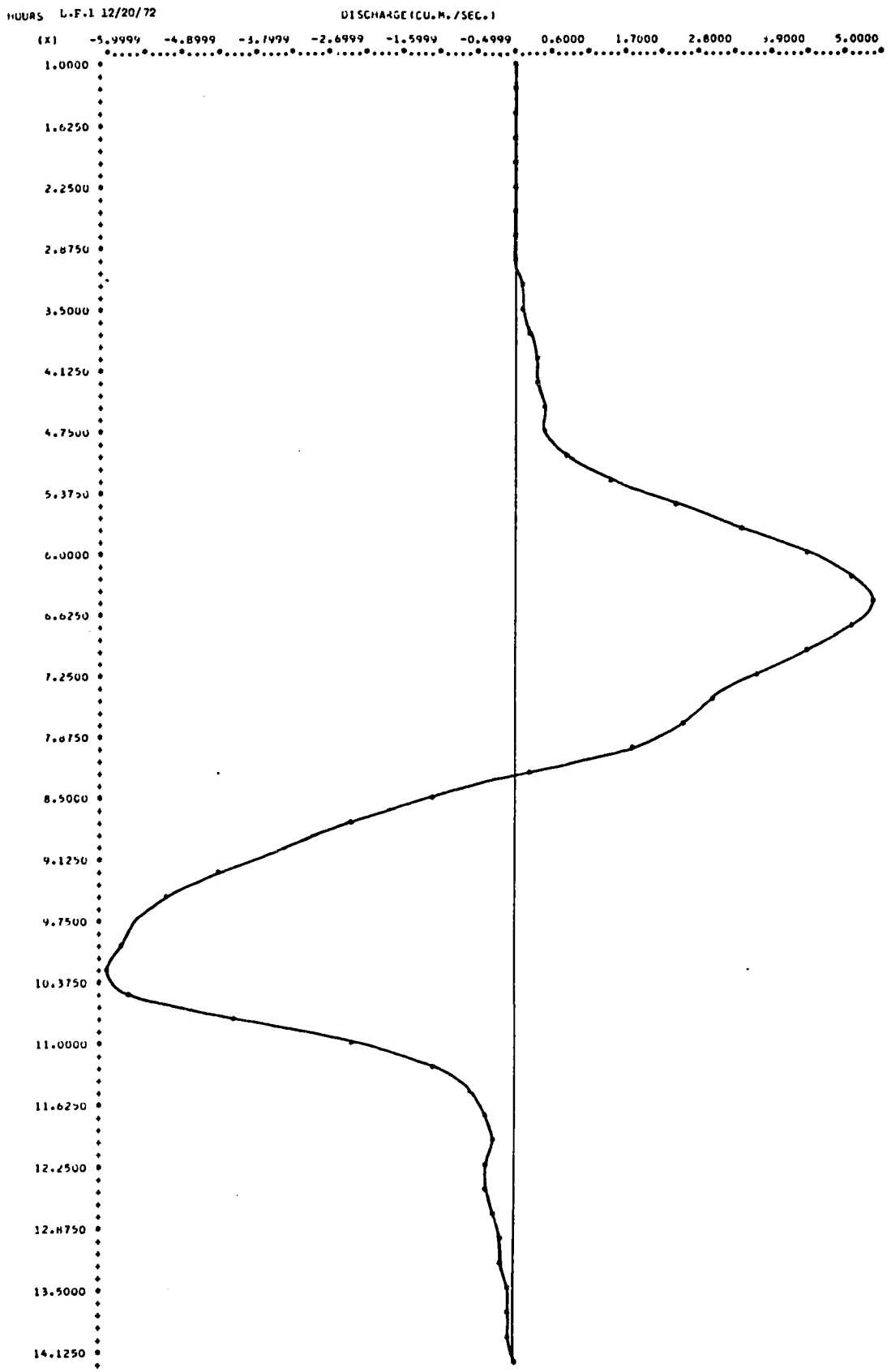

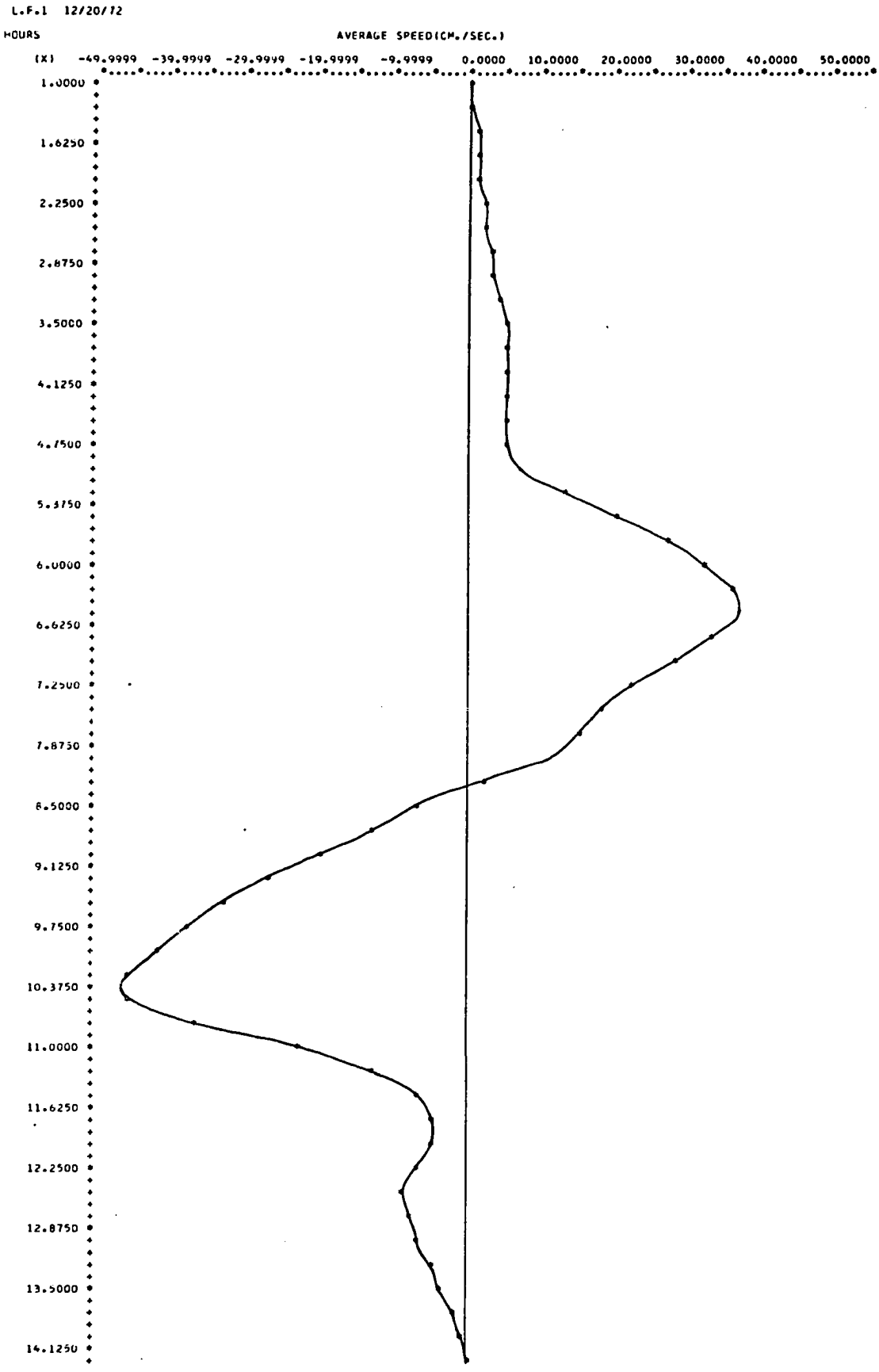

RUN 10

1/24/73

Wind 5-10 mph NNW, clear sky

Mean air temp..... 7°C

Mean water temp..... 7°C

Tidal range..... 1.00 m

Mean water level..... 0.44 m

Duration of run: 6.4 to 17.7 hrs.

L.F.1 1/24/73 DISCHARGE (CU.M./SEC.)

INTEGRATED VALUES
FLOOD= 6200.8945
EBB= -6991.8437
RESIDUAL= -790.9493 PGA= 11.99

TS1= 6.40 TS2=11.80 TS3=17.70

INTERPOLATIVE VALUES

TIME(HRS)	DISCHARGE (CU.M./SEC.)
6.250	0.0000
6.500	0.0276
6.750	0.0950
7.000	0.1568
7.250	0.2087
7.500	0.2470
7.750	0.2740
8.000	0.3000
8.250	0.3300
8.500	0.3459
8.750	0.3331
9.000	0.3167
9.250	0.3191
9.500	0.3132
9.750	0.2821
10.000	0.3006
10.250	0.4302
10.500	0.5905
10.750	0.6769
11.000	0.6327
11.250	0.4440
11.500	0.2229
11.750	0.0451
12.000	-0.2449
12.250	-0.5953
12.500	-0.8301
12.750	-0.8383
13.000	-0.7703
13.250	-0.7787
13.500	-0.7644
13.750	-0.6161
14.000	-0.4265
14.250	-0.3109
14.500	-0.2742
14.750	-0.2872
15.000	-0.2989
15.250	-0.2526
15.500	-0.1395
15.750	-0.0577
16.000	-0.0645
16.250	-0.0943
16.500	-0.0771
16.750	-0.0309
17.000	-0.0066
17.250	-0.0051
17.500	-0.0052
17.750	0.0000

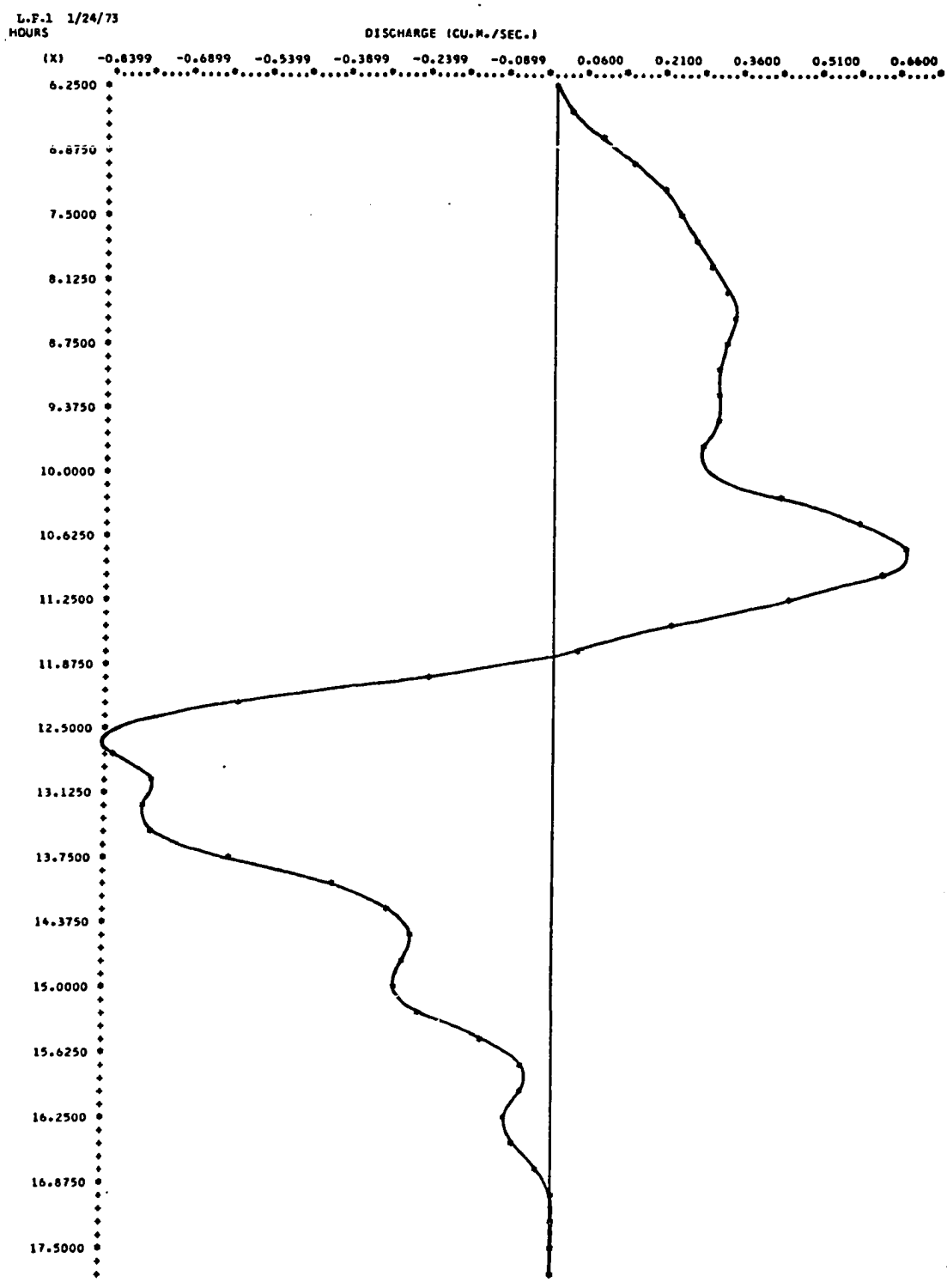

L.F.1 1/24/73 S.S. FLUX(KG./SEC.)

INTEGRATED VALUES

FLOOD= 100.7284

EBB= -62.1416

RESIDUAL= 38.5867 PGA= 47.38

TS1= 6.40 TS2=11.80 TS3=17.70

INTERPOLATIVE VALUES

TIME(HRS)	S.S. FLUX(KG./SEC.)
6.250	0.0000
6.500	0.0005
6.750	0.0017
7.000	0.0028
7.250	0.0035
7.500	0.0039
7.750	0.0041
8.000	0.0048
8.250	0.0063
8.500	0.0071
8.750	0.0063
9.000	0.0049
9.250	0.0043
9.500	0.0044
9.750	0.0045
10.000	0.0054
10.250	0.0077
10.500	0.0102
10.750	0.0111
11.000	0.0096
11.250	0.0056
11.500	0.0018
11.750	0.0003
12.000	-0.0021
12.250	-0.0055
12.500	-0.0077
12.750	-0.0075
13.000	-0.0064
13.250	-0.0064
13.500	-0.0063
13.750	-0.0050
14.000	-0.0033
14.250	-0.0024
14.500	-0.0023
14.750	-0.0026
15.000	-0.0028
15.250	-0.0025
15.500	-0.0015
15.750	-0.0007
16.000	-0.0009
16.250	-0.0012
16.500	-0.0008
16.750	-0.0002
17.000	0.0000
17.250	0.0000
17.500	-0.0000
17.750	0.0000

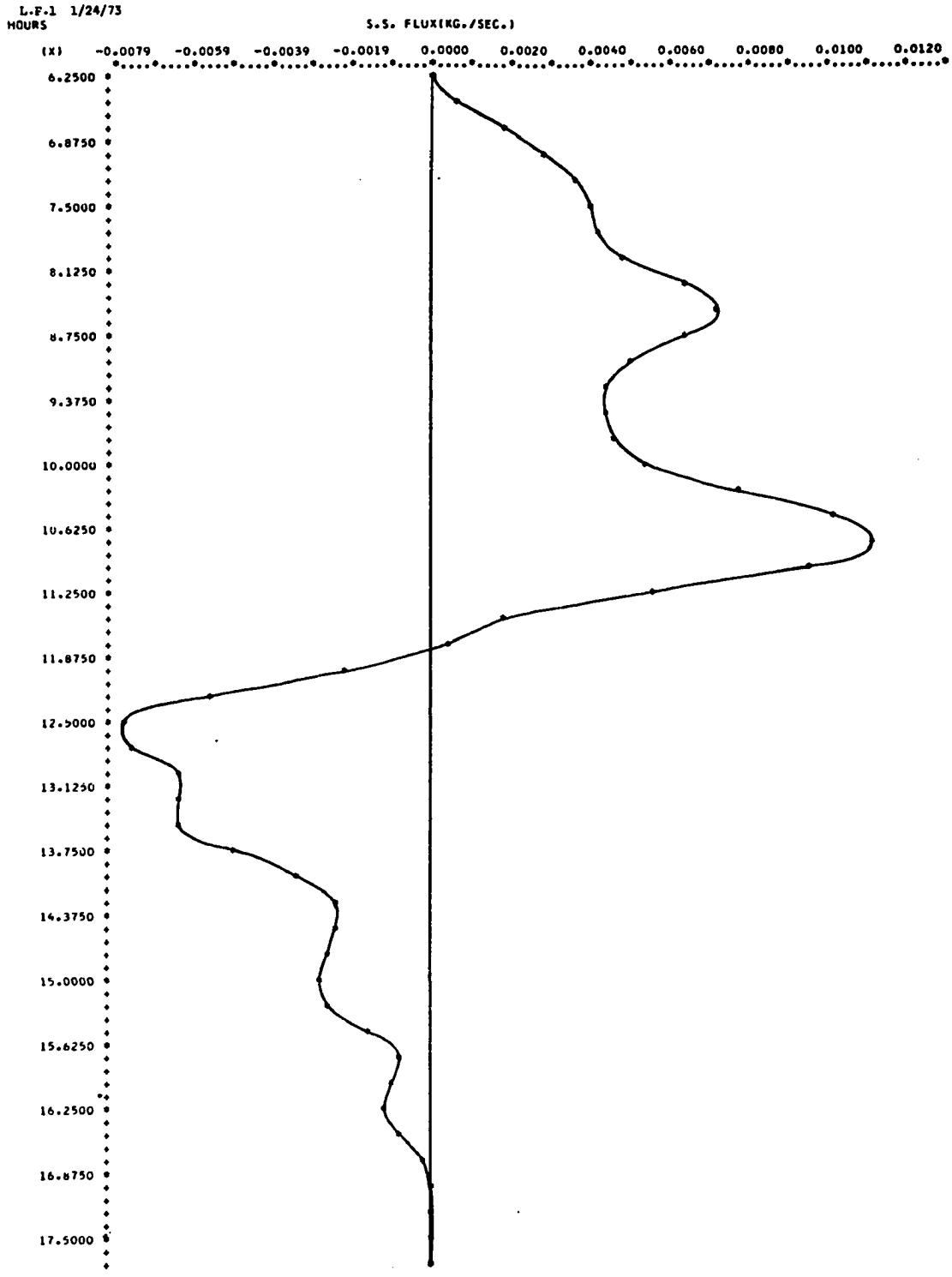

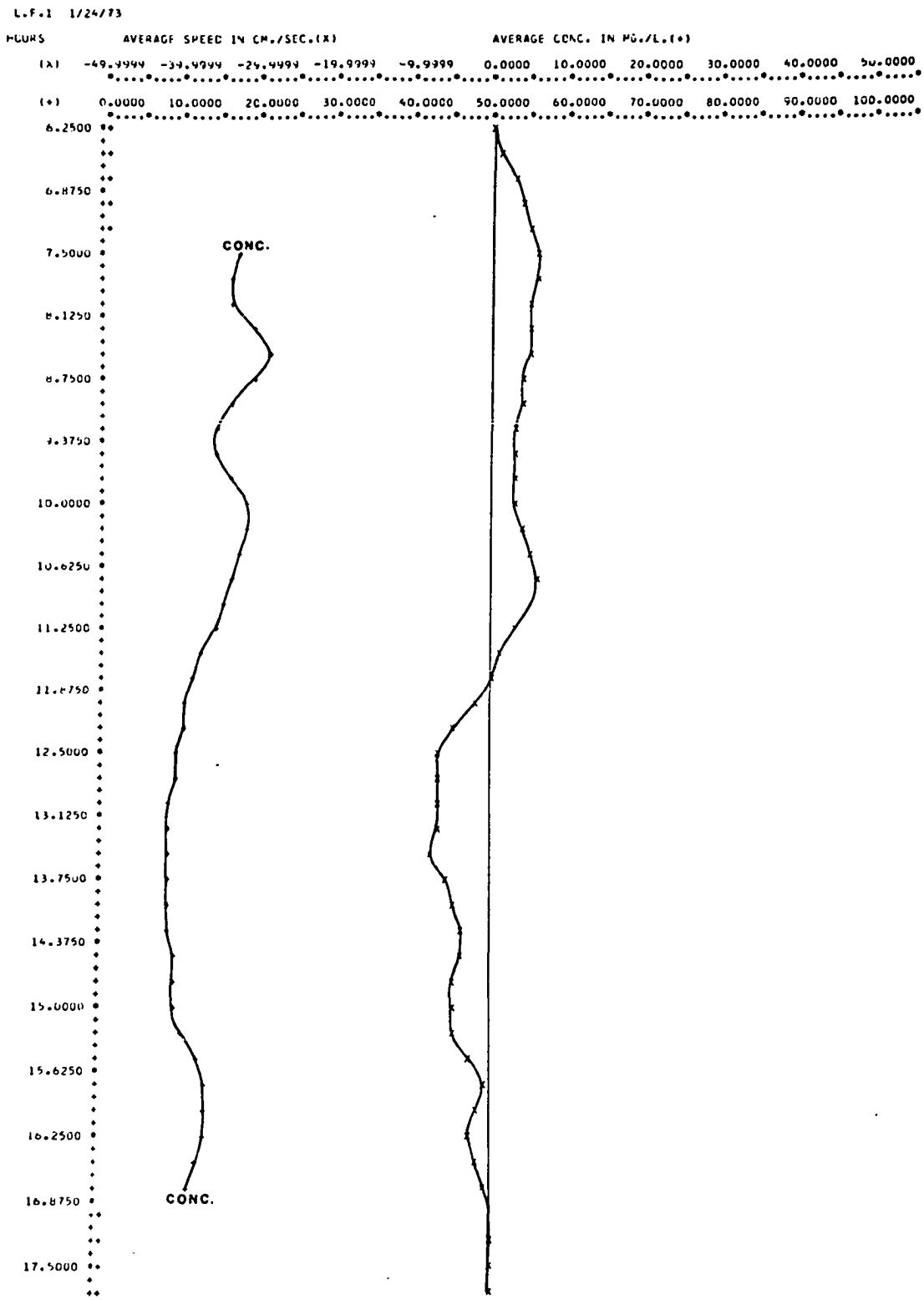

RUN 11

3/19/73

Wind 10-15 mph NNW, gusts, cloudy

Mean air temp..... 8°C

Mean water temp..... 7°C

Tidal range..... 1.54 m

Mean water level..... 0.53 m

Duration of run: 14.0 to 26.5 hrs.

```
 L.F.1 3/19/73          DISCHARGE(CU.M./SEC.)
INTEGRATED VALUES
FLOOD=      26274.9336
EBB=       -28404.6094
RESIDUAL=   -2129.6762   PGA=    7.78

TS1=14.00 TS2=21.00 TS3=26.50

INTERPOLATIVE VALUES
TIME(HRS)  DISCHARGE(CU.M./SEC.)
  14.000          0.0000
  14.250         -0.0145
  14.500         -0.0264
  14.750         -0.0332
  15.000         -0.0322
  15.250         -0.0208
  15.500          0.0035
  15.750          0.0434
  16.000          0.1016
  16.250          0.1804
  16.500          0.2717
  16.750          0.3435
  17.000          0.3683
  17.250          0.3754
  17.500          0.4149
  17.750          0.4999
  18.000          0.6271
  18.250          0.8128
  18.500          1.0980
  18.750          1.5228
  19.000          2.1165
  19.250          2.8902
  19.500          3.6177
  19.750          3.9108
  20.000          3.6763
  20.250          3.0515
  20.500          2.1732
  20.750          1.1297
  21.000          0.0000
  21.250         -0.9211
  21.500         -1.7864
  21.750         -2.9413
  22.000         -4.2152
  22.250         -5.0410
  22.500         -5.0497
  22.750         -4.3368
  23.000         -3.0869
  23.250         -1.6793
  23.500         -0.5805
  23.750         -0.1254
  24.000         -0.1215
  24.250         -0.2447
  24.500         -0.2806
  24.750         -0.2597
  25.000         -0.2279
  25.250         -0.1919
  25.500         -0.1533
  25.750         -0.1136
  26.000         -0.0743
  26.250         -0.0369
```

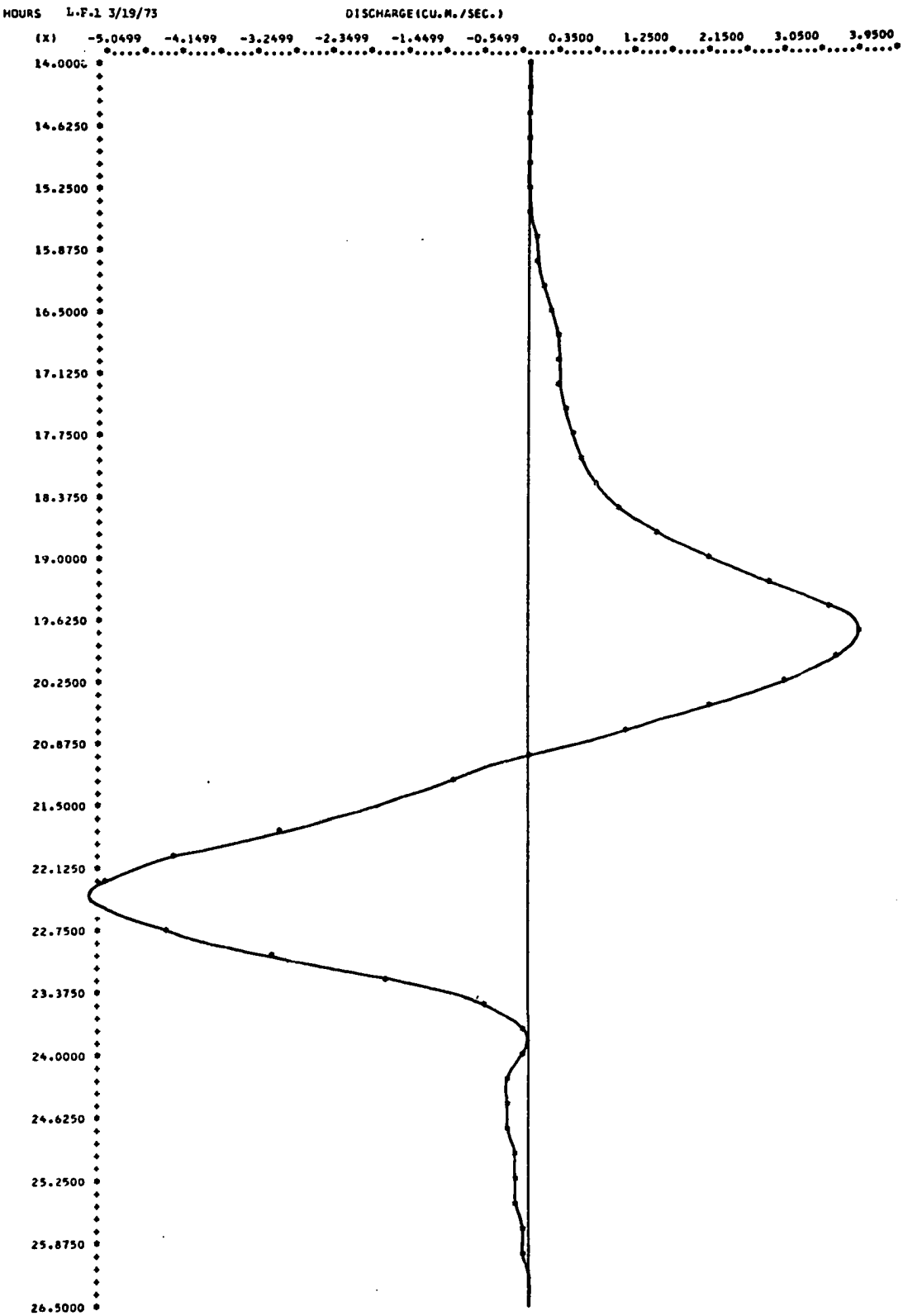

```
 L.F.1  3/19/73          S.S. FLUX(KG./SEC.)
INTEGRATED VALUES
FLCCD=      3053.6958
CBF=       -1617.2507
RESIDUAL=   1436.4450    PGA=  61.50

TS1=14.00 TS2=21.00 TS3=26.50

INTERPOLATIVE VALUES
TIME(HRS)  S.S. FLUX(KG./SEC.)
  14.000          0.0000
  14.250          0.0002
  14.500          0.0006
  14.750          0.0011
  15.000          0.0020
  15.250          0.0032
  15.500          0.0049
  15.750          0.0072
  16.000          0.0101
  16.250          0.0136
  16.500          0.0178
  16.750          0.0202
  17.000          0.0196
  17.250          0.0173
  17.500          0.0161
  17.750          0.0174
  18.000          0.0221
  18.250          0.0305
  18.500          0.0424
  18.750          0.0693
  19.000          0.1714
  19.250          0.4094
  19.500          0.6722
  19.750          0.7308
  20.000          0.5670
  20.250          0.3274
  20.500          0.1475
  20.750          0.0480
  21.000          0.0000
  21.250          0.0000
  21.500         -0.0173
  21.750         -0.1390
  22.000         -0.3235
  22.250         -0.4307
  22.500         -0.3849
  22.750         -0.2596
  23.000         -0.1412
  23.250         -0.0579
  23.500         -0.0123
  23.750         -0.0010
  24.000         -0.0015
  24.250         -0.0039
  24.500         -0.0046
  24.750         -0.0042
  25.000         -0.0036
  25.250         -0.0030
  25.500         -0.0024
  25.750         -0.0018
  26.000         -0.0012
  26.250         -0.0006
  26.500          0.0000
```

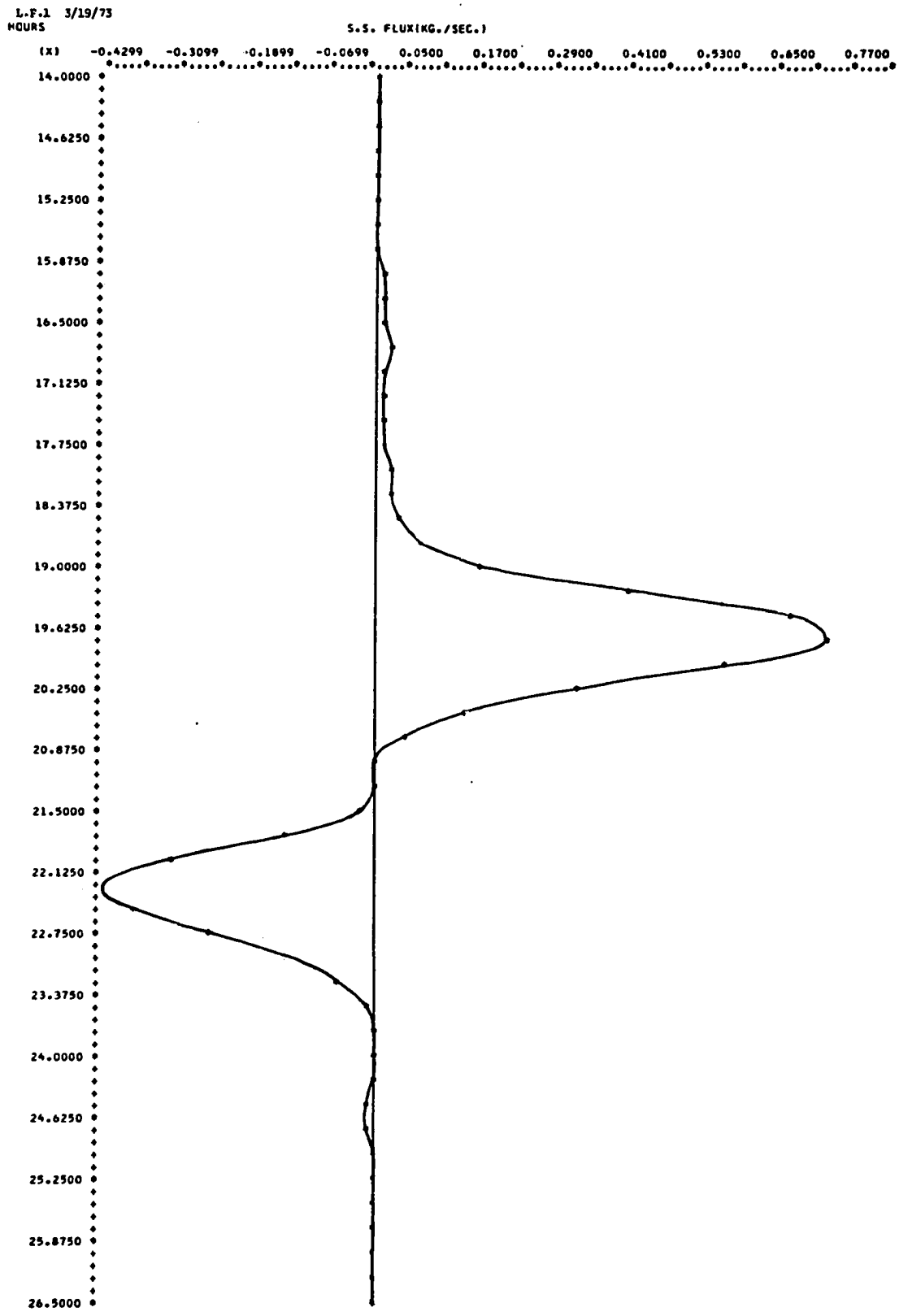

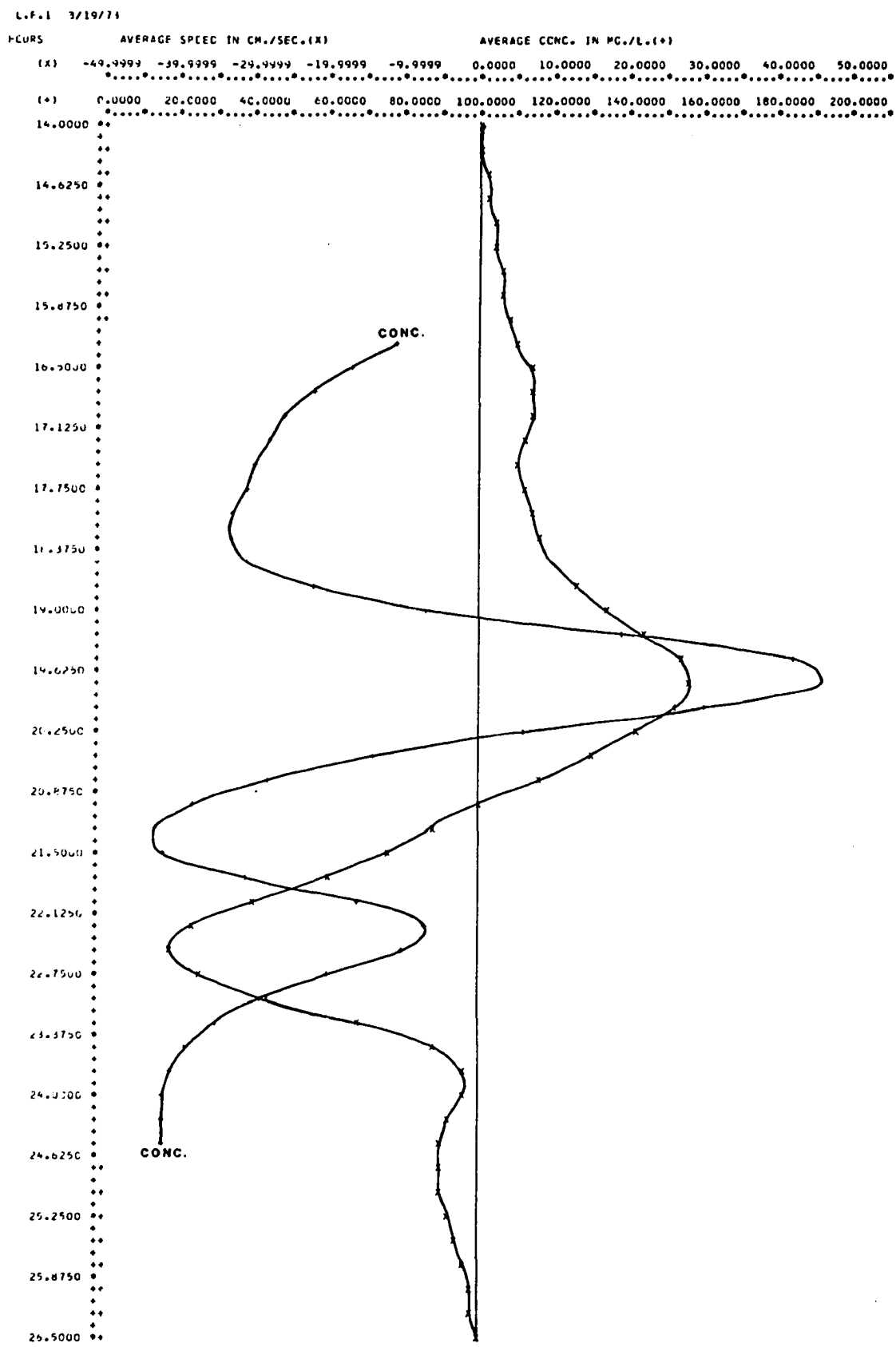

APPENDIX B

COMPUTER PROGRAMS

PROGRAM INTEFIT

PROGRAM INTEFIT

I. DESCRIPTION

Program INTEFIT is a general purpose program for computation of tidal transport in open channel systems in which slack waters occur at or near the extremes of tidal stage. The input data consist of a time variable and a rate variable, the latter being an approximation of the flux of material past a channel cross-section at the time stated. Times are expressed as hours, tenths, and hundredths, 0.00 to 23.99 hours in one day, except that measurements covering parts of two days must use consecutive hours; e.g., a series starting 8 p.m., 5/16/72, and ending 8 a.m., 5/17/72, would be written 5/16/72: 20.00-32.00 hours. Rates may be either mass or volume transport per unit time; e.g., kg/sec, etc. Graphically, flood rates are taken as positive, ebb rates as negative ordinate values, while corresponding times are taken as the abscissa values.

Given a set of rate values with corresponding time values, program INTEFIT utilizes the spline fit method to (1) fit a smooth curve to the data points, (2) numerically integrate the area under the curve, and (3) interpolate between given data points at regularly spaced intervals of time (0.25 hour). The integrated values represent total

III. INSTRUCTIONS FOR USE

A. Program INTEFIT is designed to process a set of measurements taken over a complete tidal cycle from low water slack to low water slack. Therefore, the first and last data cards must contain low water time values (approximate) and zero rate values. The time of high water slack should be carefully determined and entered with zero rate value at the appropriate intermediate position in the data deck.

B. The program deck may be followed by any number of data decks, each beginning with a title card. The computer will continue processing data sets automatically until a blank card is encountered in lieu of a title card at which point the program terminates.

IV. OUTPUT

A. Integrated values

1. Total transport for flood, ebb phases
2. Flood-ebb residual transport
3. PGA, residual expressed as a percentage of the gross average for flood and ebb transports

B. Times of slack water

1. TS1= time of first slack (low)
2. TS2= time of second slack (high)
3. TS3= time of third slack (low)

C. Interpolative values

1. Listing of times and rates interpolated at 0.25 hour intervals
2. Graphic plot of interpolative values

```
*********   V.I.M.S. COMPUTER CENTER   *********



C PROGRAM INTEFIT
C GENERAL PURPOSE PROGRAM FOR CURVE FITTING, INTERPOLATION, AND
C INTEGRATION USING SPLINE FIT SUBROUTINES SPLIC AND SPLIN
C ABSCISSA VALUES ARE TIMES IN HOURS,TENTHS,HUNDREDTHS
C ORDINATE VALUES ARE RATES(CU.M./SEC.,KG./SEC.,M./SEC.,ETC.)
C J.D. BOON, VIMS, 1972
      DIMENSION X(   ),Y(   ),Q(   ),C(4,   ),XIN(56),YIN(56)
C*************************************
C READ TITLE CARDS
C*************************************
   60 READ(2,1) NC,TI,TLE,SO,FOR,TH
    1 FORMAT(I3,5A4)
      READ(2,12) OR,DI,XA,TE,AX,XS,TS2,ISHF
   12 FORMAT(6A4,F4.2,2X,I2)
      IF(NC)75,75,76
C*********************
C READ DATA CARDS
C*********************
   76 DO 13 I=1,NC
      READ(2,2) X(I),Y(I),ISN
    2 FORMAT(F4.2,F5.4,I3)
      Y(I)=ISN*Y(I)*10.0**ISHF
   13 CONTINUE
      NF=NC-1
      NE=NC+1
      X(NE)=X(NC)
      Y(NE)=Y(NC)
      X(NC)=(X(NE)-X(NF))*0.8+X(NF)
      Y(NC)=Y(NF)-(Y(NF)-Y(NE))*0.8
      NC=NC+1
C*****************************
C CALL SUBROUTINE SPLIC
C COMPUTE AREA UNDER CURVE
C*****************************
      CALL SPLIC(X,Y,NC,C)
      QP=0.0
      QN=0.0
      NP=NC-1
      DO 3 I=1,NP
      X1=X(I+1)-X(I)
      X2=X1*X1
      X4=X2*X2
      Q(I)=0.25*X4*(C(1,I)+C(2,I))+0.5*X2*(C(3,I)+C(4,I))
      IF(Q(I))15,6,6
   15 QN=QN+Q(I)
      GO TO 3
    6 QP=QP+Q(I)
```

```
PAGE   2

     3 CONTINUE
       QP=QP*3600.
       QN=QN*3600.
       QR=QP+QN
       PGA=(QR/(QP-QN))*200.
       PGA=ABS(PGA)
C**************************************
C PRINT TITLE, INTEGRATED VALUES
C**************************************
       WRITE(5,5) TI,TLE,SO,FOR,TH,OR,DI,XA,TE,AX,XS
     5 FORMAT(////////////1X,5A4,3X,6A4)
       WRITE(5,4) QP,QN,QR,PGA,X(1),TS2,X(NC),OR,DI,XA,TE,AX,XS
     4 FORMAT(1X,'INTEGRATED VALUES',/1X,'FLOOD= ',F14.4,/1X,'EBB= ',F16.
      14,/1X,'RESIDUAL= ',F11.4,3X,'PGA= ',F6.2,//1X,'TS1=',F5.2,1X,'TS2=
      2',F5.2,1X,'TS3=',F5.2,//1X,'INTERPOLATIVE VALUES',/1X,'TIME(HRS)',
      32X,6A4)
C*********************************************************
C CALL SUBROUTINE SPLIN
C COMPUTE INTERPOLATIVE VALUES AT 0.25-HR. INTERVALS
C*********************************************************
       NOR=X(1)
       XMIN=FLOAT(NOR)
    17 IF(XMIN-X(1)+0.25)9,9,10
     9 XMIN=XMIN+0.25
       GO TO 17
    10 XIN(1)=XMIN
       NOR=X(NC)
       XMAX=FLOAT(NOR)
     8 IF(XMAX-X(NC)+0.25)19,20,20
    19 XMAX=XMAX+0.25
       GO TO 8
    20 XMAX=XMAX+0.25
       JT=(XMAX-XIN(1))/0.25-0.9
       JE=JT+2
       XIN(JE)=XMAX
       DO 7 I=1,JT
       XIN(I+1)=XIN(I)+0.25
     7 CONTINUE
       DO 11 I=1,JE
       XIT=XIN(I)
       CALL SPLIN(X,Y,NC,C,XIT,YIT)
       YIN(I)=YIT
    11 CONTINUE
C*********************************************************
C PRINT INTERPOLATIVE VALUES, PLOT INTERPOLATIVE VALUES
C*********************************************************
       WRITE(5,16) (XIN(I),YIN(I), I=1,JE)
    16 FORMAT(3X,F6.3,4X,F10.4)
       WRITE(5,14) OR,DI,XA,TE,AX,XS
    14 FORMAT(////////////1X,'HOURS',40X,6A4)
       CALL PLOT2(JE,YIN,YIN,XIN,0.0,0.0,0.0,0.0,XMIN,0.125)
C
C
```

```
PAGE    3

C*************************************************
C ENTER NEXT DATA SET, PUSH START
C OR ENTER BLANK CARD, PUSH START, TO EXIT
C*************************************************
      GO TO 60
   75 CALL EXIT
      END
```

SUBROUTINES SPLIC AND SPLIN

SUBROUTINES SPLIC AND SPLIN

For:

(1) Curve fitting through plotted points by spline fit method (50 points maximum)

(2) Interpolation between plotted points

(3) Integration of fitted curve to obtain area over specified abscissa interval

I. Introduction

Engineers often draw a smooth curve through a number of plotted points using a flexible draftsman's spline. The expert does this in such a way that not only the curve itself, but the slope and curvature are continuous functions. Interpolation is done by picking off points from the curve and integration is accomplished by planimetering the area under the curve.

A computer subroutine has been written which fits a third-order polynomial, Y= f(X), to plotted points in such a way that the second derivative, Y", i.e., the curvature, varies linearly from point to point. After specifying boundary conditions at the end points, the coefficients for this polynomial are expressed as unknowns in a system of simultaneous equations and are obtained in a unique solution (ref: Pennington, 1965, pp. 404-411).

II. The spline fit

The equation of the fitted polynomial is:

$$Y= C_{1,k}(X_{k+1}-X)^3 + C_{2,k}(X-X_k)^3 + C_{3,k}(X_{k+1}-X) + C_{4,k}(X-X_k)$$

where

Y = desired ordinate value

X = selected abscissa value between X_k and X_{k+1}

X_k = kth plotted point

X_{k+1} = k+1th plotted point

$C_{1,k}$ = 1st coefficient for kth point

$C_{2,k}$ = 2nd coefficient for kth point

$C_{3,k}$ = 3rd coefficient for kth point

$C_{4,k}$ = 4th coefficient for kth point

Given NC plotted points, not necessarily equally spaced but in ascending order, subroutine SPLIC will compute all of the coefficients as an array, C(I,K) I= 1,4 & K= 1,NC where NC≤ 50. Subroutine SPLIN uses these coefficients to compute Y values via the polynomial equation.

III. Interpolation

The following steps are taken in the main program:

(1) Store plotted points as subscripted variables, X(k), Y(k), k= 1,NC
(2) Call SPLIC(X,Y,NC,C)
(3) Define XINT (X value at point of interpolation)
(4) Call SPLIN(X,Y,NC,C,XINT,YINT)
(5) Y value of interpolation point returned as YINT

IV. Integration

Steps (1) and (2) are accomplished as above, then the following statements are incorporated:

```
      QI= 0.0
      NN= NC-1
      DO 20 K=1,NN
      X1= x(K+1)-X(K)
      X2= X1*X1
      X4= X2*X2
      Q(K)= 0.25*X4*(C(1,K)+C(2,K))+0.5*X2*(C(3,K)
      + C(4,K))
   20 QI=QI+Q(K)
```

QI is then the area for the interval X(1) to X(NC)

REFERENCE

Pennington, R. H., 1965, Introductory computer methods and numerical analysis: Macmillan Co., N. Y., 452 p.

********* V.I.M.S. COMPUTER CENTER *********

```
      SUBROUTINE SPLIC(X,Y,M,C)
      DIMENSION X(1),Y(1),P(50),E(50),B(50),Z(50),D(50)
      DIMENSION C(4,1),A(50,3)
    1 MM=M-1
      DO 2 K=1,MM
      D(K)=X(K+1)-X(K)
      P(K)=C(K)/6.
    2 E(K)=(Y(K+1)-Y(K))/D(K)
      DO 3 K=2,MM
    3 B(K)=E(K)-E(K-1)
      A(1,2)=0.0
      A(1,3)=0.0
      A(2,3)=P(2)-P(1)*A(1,3)
      A(2,2)=2.*(P(1)+P(2))-P(1)*A(1,2)
      A(2,3)=A(2,3)/A(2,2)
      B(2)=B(2)/A(2,2)
      DO 4 K=3,MM
      A(K,2)=2.*(P(K-1)+P(K))-P(K-1)*A(K-1,3)
      B(K)=B(K)-P(K-1)*B(K-1)
      A(K,3)=P(K)/A(K,2)
    4 B(K)=B(K)/A(K,2)
      Q=C(M-2)/C(M-1)
      A(M,1)=A(M-2,3)
      A(M,2)=C(M-2)-A(M,1)*A(M-1,3)
      B(M)=B(M-2)-A(M,1)*B(M-1)
      Z(M)=B(M)/A(M,2)
      MN=M-2
      DO 6 I=1,MN
      K=M-I
    6 Z(K)=B(K)-A(K,3)*Z(K+1)
      Z(1)=-A(1,2)*Z(2)-A(1,3)*Z(3)
      DO 7 K=1,MM
      Q=1./(6.*D(K))
      C(1,K)=Z(K)*Q
      C(2,K)=Z(K+1)*Q
      C(3,K)=Y(K)/D(K)-Z(K)*P(K)
    7 C(4,K)=Y(K+1)/D(K)-Z(K+1)*P(K)
      RETURN
      END
```

********* V.I.M.S. COMPUTER CENTER *********

```
      SUBROUTINE SPLIN(X,Y,M,C,XINT,YINT)
      DIMENSION X(1),Y(1),C(4,1)
      IF(XINT-X(1))7,1,2
    1 YINT=Y(1)
      RETURN
    2 K=1
    3 IF(XINT-X(K+1))6,4,5
    4 YINT=Y(K+1)
      RETURN
    5 K=K+1
      IF(M-K)7,7,3
    6 FAC1=X(K+1)-XINT
      FAC2=XINT-X(K)
      FAC3=FAC1*FAC1
      FAC4=FAC2*FAC2
      YINT=FAC1*(C(1,K)*FAC3+C(3,K))
      YINT=YINT+FAC2*(C(2,K)*FAC4+C(4,K))
      RETURN
    7 YINT=0.0
      RETURN
      END
```

PROGRAM HYPSOPRISM

********* V.I.M.S. COMPUTER CENTER *********

```
C PROGRAM HYPSOPRISM
C COMPUTES FLOOD AND EBB TIDAL PRISMS IN BASINS
C DESCRIBED BY HYPSOMETRIC FORMULA.
C PARAMETER INPUT CONSISTS OF FORMULA CONSTANTS, R AND Z,
C PLUS HEIGHT AND AREA EXTREMA FOR THE DRAINAGE BASIN.
C DATA INPUT CONSISTS OF HEIGHT EXTREMA DURING A GIVEN TIDAL
C CYCLE, BEGINNING WITH LOW WATER.
C SUBROUTINE SPLIC REQUIRED
      DIMENSION X(50),Y(50),A(50),C(4,50)
      FORM(HP)=R*(1.-(1.-HP)**Z)/(R+((1.-HP)**Z)*(1.-R))
      TRAN(H)=(H-HMIN)/(HMAX-HMIN)
C************************
C READ PARAMETERS
C************************
      READ(2,25) HMAX,HMIN,AMAX,AMIN,Z,R
   25 FORMAT(F3.2,1X,F3.2,1X,F6.0,1X,F4.0,1X,F3.2,1X,F4.3)
      Z=1./Z
C*****************
C READ DATA
C*****************
  100 READ(2,1) XLW1,HW,XLW2,DA,TE
    1 FORMAT(F3.2,1X,F3.2,1X,F3.2,1X,2A4)
      IF(HW)50,50,51
C************************************
C TRANSFORM TO DIMENSIONLESS HEIGHTS
C************************************
   51 HP1=TRAN(XLW1)
      HP2=TRAN(HW)
      HP3=TRAN(XLW2)
      OBNK=0.0
      IF(HP1)2,2,3
    2 HP1=0.02
    3 IF(HP2-1.0)4,4,5
C*******************************
C COMPUTE OVERBANK VOLUME
C*******************************
    5 OBNK=((HMAX-HMIN)*(AMAX-AMIN)+AMIN*(HMAX-HMIN))*(HP2-1.0)
      HP2=1.0
    4 IF(HP3)6,6,7
    6 HP3=0.02
    7 CONTINUE
      X(1)=HP1
      DHP1=HP2-HP1
      N=DHP1/.02
      DO 8 I=1,N
      X(I+1)=X(I)+.02
    8 CONTINUE
```

PAGE 2

```
      N=N+1
      X(N)=HP2
      NCUT=0
      DO 9 I=1,N
      HP=X(I)
      Y(I)=FORM(HP)
    9 CONTINUE
C*************************************************
C CALL SUBROUTINE SPLIC, COMPUTE CHANNEL VOLUMES
C*************************************************
      CALL SPLIC(X,Y,N,C)
      EPA=0.0
      NP=N-1
      DO 10 I=1,NP
      X1=X(I+1)-X(I)
      X2=X1*X1
      X4=X2*X2
      A(I)=0.25*X4*(C(1,I)+C(2,I))+0.5*X2*(C(3,I)+C(4,I))
      EPA=EPA+A(I)
   10 CONTINUE
      IF(NCUT)13,13,14
   13 FPA=EPA
      X(1)=HP3
      DHP2=HP2-HP3
      N=DHP2/.02
      DO 11 I=1,N
      X(I+1)=X(I)+.02
   11 CONTINUE
      N=N+1
      X(N)=HP2
      DO 12 I=1,N
      HP=X(I)
      Y(I)=FORM(HP)
   12 CONTINUE
      NCUT=1
      GO TO 9
C***********************
C PRINT RESULTS
C***********************
   14 FPA=FPA*(AMAX-AMIN)*(HMAX-HMIN)+AMIN*(HMAX-HMIN)*DHP1+OBNK
      EPA=EPA*(AMAX-AMIN)*(HMAX-HMIN)+AMIN*(HMAX-HMIN)*DHP2+OBNK
      RES=FPA-EPA
      PGA=200.*ABS(RES)/(FPA+EPA)
      WRITE(5,15) DA,TE,FPA,EPA,RES,PGA,XLW1,HW,XLW2
   15 FORMAT(//1X,2A4,1X,'FLOOD= ',F10.3,1X,'EBB= ',F10.3,/10X,'RESIDU
     1= ',F10.3,1X,'PGA= ',F8.3,/10X,'LW1= ',F5.2,1X,'HW= ',F5.2,1X,'L
     2= ',F5.2)
      GO TO 100
   50 CALL EXIT
      END
```

PROGRAM SATIDE

********* V.I.M.S. COMPUTER CENTER *********

```
C PROGRAM SATIDE
C FOR SPECTRAL ANALYSIS OF TIME SEQUENTIAL TIDAL HEIGHTS
C PROGRAM OPERATES ON DATA VECTOR OF LENGTH 2*2**M, 3<M<20
C PROGRAM FORMS VECTOR OF TIME SEQUENTIAL DATA BY QUEUING COLUMNS OF
C ONE OR MORE INPUT ARRAYS, A(45,9), FORMAT (9F4.2)
C INPUT IS TIDAL HEIGHT IN FEET,TENTHS,HUNDREDS, OUTPUT IS METRIC(CM)
C THE PROGRAM REQUIRES SYSTEM/360 SSP RHARM AND HARM SUBROUTINES
C ST,AT,C,X= STATION NAME(4A4)
C MO1=STARTING MONTH(I2),NDA1=STARTING DAY(I2),NYR1=STARTING YEAR(I2)
C ITM1=STARTING TIME, HRS*10(I3)
C MO2=ENDING MONTH(I2),NDA2=ENDING DAY(I2),NYR2=ENDING YEAR(I2)
C ITM2=ENDING TIME,HRS*10(I3)
C NSI=SAMPLING INTERVAL,HRS*10(I2)
C INDA=INCLUSIVE NO. DAYS(I3)
C M=RHARM DATA VECTOR SIZE PAR.(I2)
C NP=NO. NON-ZERO RAW DATA POINTS FOR INPUT(I4)
C NBANS= NO. OF FREQ. BANDS DESIRED FOR OUTPUT(I3)
C WHERE NBANS*BANDWIDTH FACTOR= 2**M
C BANDWIDTH FACTOR= NO. DISCRETE HARMONIC COMPONENTS IN EACH BAND
      DIMENSION A(3000),INV(300),S(300),Q(300,2),P(300),R(1500)
      N=5
      L=6
C*****************************
C READ TITLE CARD
C*****************************
      READ(N,1) ST,AT,C,X,MO1,NDA1,NYR1,ITM1,MO2,NDA2,NYR2,ITM2,NSI,INDA
     1,M,NP,NBANS
    1 FORMAT(4A4,2(1X,3I2,1X,I3),1X,I2,1X,I3,1X,I2,1X,I4,1X,I3)
C************************************
C TEST INPUT FOR CONTINUITY
C************************************
      NET=((INDA-1)*24)*(10/NSI)+(ITM2-ITM1)/NSI+1
      IF(NP-NET)2,3,2
    3 IF(NBANS-(2*2**M+2)/8)61,61,100
C****************************************
C READ RAW DATA, CONVERT TO METRIC
C****************************************
   61 NET=(NP-1)/405+1
      DO 4 J=1,NET
      K=(J-1)*405
      DO 5 I=1,45
      I1=I+K
      I2=45+I+K
      I3=2*45+I+K
      I4=3*45+I+K
      I5=4*45+I+K
      I6=5*45+I+K
      I7=6*45+I+K
```

```
      I8=7*45+I+K
      I9=8*45+I+K
      READ(N,6) A(I1),A(I2),A(I3),A(I4),A(I5),A(I6),A(I7),A(I8),A(I9)
    6 FORMAT(9F4.2)
    5 CONTINUE
    4 CONTINUE
      NET=(NP-1)*NSI/10
      DO 90 I=1,NP
      A(I)=A(I)*30.48
   90 CONTINUE
C*****************************************************
C REMOVE LINEAR TREND, ADJUST DATA TO MEAN ZERO
C*****************************************************
      SX=0.
      SX2=0.
      SY=0.
      SXY=0.
      DO 7 I=1,NP
      SX=SX+I
      SX2=SX2+I*I
      SY=SY+A(I)
      SXY=SXY+I*A(I)
    7 CONTINUE
      XBAR=SX/NP
      YBAR=SY/NP
      SXY=SXY-XBAR*SY
      SX2=SX2-XBAR*SX
      B=SXY/SX2
      C=YBAR-B*XBAR
      DO 8 I=1,NP
      A(I)=A(I)-B*I-C
    8 CONTINUE
C*****************************************************
C APPLY DATA WINDOW, ADD ZEROES,COMPUTE VARIANCE
C*****************************************************
      J=NP/10
      K=NP-J
      DO 9 I=1,J
      ARG1=3.1415927*I/J
      ARG2=3.1415927*(NP-I-K)/J
      A(I)=A(I)*.5*(1.-COS(ARG1))
      IN=I+K
      A(IN)=A(IN)*.5*(1.-COS(ARG2))
    9 CONTINUE
      NT=2*(2**M)
      NZ1=NT-NP
      NZ2=NZ1-NZ1/2
      NZ1=NZ1-NZ2
      NZ2=NP+NZ1+1
      SA=0.
      SA2=0.
      DO 11 I=1,NP
      IN=NZ2-I
```

```
      IC=NP-I+1
      A(IN)=A(IC)
      SA=SA+A(IN)
      SA2=SA2+A(IN)**2
   11 CONTINUE
      VAR=(SA2-SA**2/NT)/NT
      DO 12 I=1,NZ1
      A(I)=0.
   12 CONTINUE
      DO 13 I=NZ2,NT
      A(I)=0.
   13 CONTINUE
C**************************************
C CALL RHARM, COMPUTE POWER SPECTRA
C**************************************
      CALL RHARM(A,M,INV,S,IFERR)
      IF(IFERR)100,93,100
   93 J=1
      SVAR=0.
      DO 15 I=1,NT,2
      R(J)=A(I+2)**2+A(I+3)**2
      R(J)=R(J)/2.
      SVAR=SVAR+R(J)
      J=J+1
   15 CONTINUE
      NT=NT/2
   43 NIB=NT/NBANS
      K=1
      DO 16 I=1,NBANS
      POW=0.
      DO 17 J=1,NIB
      POW=POW+R(K)
      K=K+1
   17 CONTINUE
      P(I)=POW
      S(I)=I*NIB*5.0/(NT*NSI)
   16 CONTINUE
C**********************************
C PRINT RESULTS
C**********************************
      WRITE(L,21) ST,AT,C,X,MO1,NDA1,NYR1,ITM1,MO2,NDA2,NYR2,ITM2,NSI,NE
     1T,VAR,NIB
   21 FORMAT(//1X,'PROGRAM SATICE OUTPUT ',/1X,'STATION NAME= ',4A4,/1X,
     1'STARTING DATE= ',I2,'/',I2,'/',I2,3X,'HRS*10= ',I3,/1X,'ENDING DA
     2TE= ',I2,'/',I2,'/',I2,3X,'HRS*10= ',I3,/1X,'SAMPLING INTERVAL(HRS
     3*10)= ',I2,/1X,'SERIES LENGTH(HRS)=     ',I5,/1X,'VARIANCE OF SERIE
     4S(SQ.CM.)= ',F15.5,//1X,'BANDWIDTH FACTOR= ',I3,//1X,'FREQUENCY(CP
     5H)',3X,'PERIOD(HRS)',2X,'VARIANCE(SQ.CM.)',2X,'PERCENT OF TOTAL',/
     61X)
      DO 22 I=1,NBANS
      PRD=1./S(I)
      PC=P(I)/SVAR*100.
      WRITE(L,23) S(I),PRD,P(I),PC
```

```
   23 FORMAT(2X,F9.7,8X,F8.4,5X,F9.4,8X,F8.5)
      P(I)=ALOG(P(I))
   22 CONTINUE
      WRITE(L,24) SVAR
   24 FORMAT(/1X,'TOTAL VARIANCE FOR ALL FREQUENCIES= ',F15.5)
      WRITE(L,33)
   33 FORMAT(///1X,'FREQ.(CPH)',35X,'LOG VARIANCE (SQ.CM.)')
      CALL PLOT2(NBANS,P,P,S,0.0,0.0,0.0,0.0,0.0,0.0)
C*********************************************************
C READ ADDITIONAL NBANS SPECIFICATION DESIRED
C FOR DISCRETE HARMONIC OUTPUT, SET NBANS=2**M
C*********************************************************
      READ(N,42) NBANS
   42 FORMAT(I4)
      IF(NBANS)100,100,44
   44 IF(NBANS-2**M)43,25,25
    2 WRITE(L,26)
   26 FORMAT(/1X,'INPUT DATA ARE NOT CONTINUOUS',/1X,'PROGRAM CANCELLED'
     1)
      GO TO 100
C*********************************************
C PRINT DISCRETE HARMONIC DATA
C*********************************************
   25 NIB=1
      J=1
      WRITE(L,102)
  102 FORMAT(//1X,'LISTING OF DISCRETE HARMONIC DATA',//1X,'PERIOD(HRS)'
     1,3X,'VARIANCE',3X,'PERCENT OF TOTAL',6X,'AM',6X,'BM',8X,'PHI')
      IF(NBANS-350)103,103,104
  104 NBANS=350
  103 DO 101 I=1,NBANS
      PRD=NT*NSI/(I*NIB*5.0)
      PC=R(I)/SVAR*100.0
      AC=A(J+2)
      BC=A(J+3)
      ARG=-BC/AC
      PHI=ATAN(ARG)
      J=J+2
      WRITE(L,105) PRD,R(I),PC,AC,BC,PHI
  105 FORMAT(/2X,F9.4,4X,F9.4,5X,F8.5,8X,2F8.3,3X,F7.4)
  101 CONTINUE
  100 CALL EXIT
      END
```

REFERENCES

Bendat, J. S., and A. G. Piersol. Random data: analysis and measurement procedures: Wiley Interscience, New York, 407 p., 1971.

Bingham, C., M. D. Godfrey, and J. W. Tukey. Modern techniques of power spectrum estimation: IEEE Trans. on Audio and Electroacoustics, Vol. AV-15, No. 2, pp. 56-66, 1967.

Boon, J. D. Optimum sampling intervals for measurement of discharge and suspended sediment transport in a low-order tidal stream typical of salt marsh drainage systems: Chesapeake Res. Consortium, Inc., Annual Report, pp. 186-215, 1972.

_____, and M. P. Lynch. Tidal datum planes and tidal boundaries and their use as legal boundaries: Special Report No. 22, Virginia Institute of Marine Science, 61 p., 1972.

Byrne, R. J., and J. D. Boon. An inexpensive, fast response current speed indicator: Chesapeake Sci., Vol. 14, No. 3, pp. 217-219, 1973.

Chapman, V. J. Salt marshes and salt deserts of the world: Interscience Publishers, N. Y., 392 p., 1960.

Defant, A. Ebb and flow, the tides of earth, air, and water: University of Michigan Press, 121 p., 1958.

Doodson, A. T., and H. D. Warburg. Admiralty manual of tides: Admiralty Hydrographic Office, London, 270 p., 1941.

De La Cruz, A. A. A study of particulate organic detritus in a Georgia salt marsh-estuarine ecosystem: Ph.D. dissertation, Univ. of Georgia, 110 p., 1965.

Eaton, J. S., G. E. Likens, and F. H. Bormann. Use of membrane filters in gravimetric analysis of particulate matter in natural waters: Water Resources Res., Vol. 5, No. 5, pp. 1151-1156, 1969.

Einstein, H. A., and Huon-Li. Secondary currents in straight channels: Trans., Am. Geophysical Union, Vol. 39, No. 6, pp. 1085-1088, 1958.

Gilbert, G. K. Hydraulic mining debris in the Sierra Nevada: U. S. Geol. Survey Prof. Paper 105, 154 p., 1917.

Graf, W. H. Hydraulics of sediment transport: McGraw-Hill, N. Y., 513 p., 1971.

Grissinger, E. H. Resistance of selected clay systems to erosion by water: Water Resources Research, Vol. 2, No. 1, pp. 131-138, 1966.

Groen, P. On the residual transport of suspended matter by an alternating tidal current: Netherlands J. Sea Res., Vol. 3, No. 4, pp. 564-574, 1965.

Harrison, W., R. J. Malloy, G. A. Rusnak, and J. Terasmae. Possible late Pleistocene uplift, Chesapeake Bay entrance: J. Geol., Vol. 73, No. 2, pp. 201-229, 1965.

Henderson, F. M. Open channel flow: Macmillan Co., N. Y., 522 p., 1966.

Hicks, S. D., and W. Shofnos. Yearly sea level variations for the United States: J. Hydraulics Div., ASCE, Vol. 91, No. HY5, pp. 23-32, 1965.

Holley, E. R., D. R. F. Harleman, and H. B. Fischer. Dispersion in homogeneous estuary flow: J. Hydraulics Div., ASCE, Vol. 96, No. HY8, pp. 1691-1709, 1970.

Horton, R. E. Erosional development of streams and their drainage basins; hydrophysical approach to quantitative morphology: Geol. Soc. Am. Bull., Vol. 56, pp. 275-370, 1945.

Jenkins, G. M., and D. G. Watts. Spectral analysis and its applications: Holden-Day, Inc., San Francisco, 525 p., 1968.

Langbein, W. B. The hydraulic geometry of a shallow estuary: Bull. Int. Assoc. Sci. Hydrology, Sept., pp. 84-94, 1963.

_____. Geometry of river channels: J. Hydraulics Div., ASCE, Vol. 90, No. HY2, Mar., pp. 301-312, 1964.

Leopold, L. B., and T. Maddock. The hydraulic geometry of stream channels and some physiographic implications: U. S. Geol. Survey Prof. Paper 252, 57 p., 1953.

Marmer, H. A. Tidal datum planes: U. S. Coast and Geodetic Survey Special Pub. No. 135, revised ed., 142 p., 1951.

Migniot, C. A study of the physical properties of various forms of very fine sediment and their behavior under hydrodynamic action: La Houile Blanche, No. 7, pp. 591-619, 1968.

Mota Olivera, I. B. Tidal prism in large lagoons: 14th Congress, Int. Assoc. for Hydraulic Research, Paris, France, pp. D3-1 to D3-10, 1971.

Myrick, R. M., and L. B. Leopold. Hydraulic geometry of a small tidal estuary: U. S. Geol. Survey Prof. Paper 422-B, 18 p., 1963.

Newman, W. S., and G. A. Rusnak. Holocene submergence of the Eastern Shore of Virginia: Science, Vol. 148, pp. 1464-1466, 1965.

_____, and C. A. Munsart. Holocene geology of the Wachapreague lagoon, Eastern Shore peninsula, Virginia: Mar. Geol., Vol. 6, pp. 487-491, 1968.

Partheniades, E. Erosion and deposition of cohesive soils: J. Hydraulics Div., ASCE, Vol. 91, No. HY1, pp. 105-139, 1965.

_____, and R. E. Paaswell. Erodibility of channels with cohesive boundary: J. Hydraulics Div., ASCE, Vol. 96, No. HY3, pp. 755-771, 1970.

_____, and A. J. Mehta. Rates of deposition of fine cohesive sediments in turbulent flows: Int. Assoc. for Hydraulic Research, 14th Congress, Paris, France, pp. D3-1, D3-8, 1971.

Pattullo, J., W. Munk, R. Revelle, and E. Strong. The seasonal oscillation in sea level: J. Mar. Res., Vol. 14, No. 1, pp. 88-155, 1955.

Pestrong, R. The development of drainage patterns on tidal marshes: Ph.D. dissertation, Stanford Univ., 87 p., 1965.

_____. Tidal flat sedimentation at Cooley Landing, S.W. San Francisco Bay: ONR Tech. Report, Stanford Univ., 55 p., 1970.

Pomeroy, L. R., R. D. Shenton, R. D. H. Jones, and R. J. Reimold. Nutrient flux in estuaries: Am. Soc. Limn. and Oceanog., Special Symposia, Vol. 1, pp. 274-291, 1972.

Postma, H. Hydrography of the Dutch Wadden Sea: Arch. Neerl. Zool., Vol. 10, pp. 405-511, 1954.

_____. Suspended matter and Secchi Disc visibility in coastal waters: Neth. Jour. Sea Res., Vol. 1, pp. 359-390, 1961.

_____. Sediment transport and sedimentation in the estuarine environment: Estuaries (G. Lauff, ed.), Pub. No. 83, AAAS, pp. 158-179, 1967.

Ragotzkie, R. A., and R. A. Bryson. Hydrography of the Duplin River, Sapelo Island, Georgia: Bull. Mar. Sci. Gulf and Caribbean, Vol. 5, No. 4, pp. 297-314, 1955.

Redfield, A. C. Ontogeny of a salt marsh estuary: Science, Vol. 147, No. 3653, pp. 22-28, 1965.

Schlichting, H. Boundary layer theory, 4th ed.: McGraw-Hill, Inc., New York, 635 p., 1960.

Steers, J. A. The coastline of England and Wales. Cambridge Univ. Press, Cambridge, G. B., 750 p., 1964.

Strahler, A. N. Hypsometric (area-altitude) analysis of erosional topography: Bull. Geol. Soc. Am., Vol. 63, pp. 1117-1142, 1952.

Swift, D. J. P., J. R. Schubel, and R. W. Sheldon. Size analysis of fine-grained suspended sediments: a review. J. Sed. Pet., Vol. 42, No. 1, pp. 122-134, 1972.

Troskolansky, A. T. Hydrometry: Pergamon Press, N. Y., 684 p, 1960.

Van Straaten, L. M. J. U., and P. H. Kuenen. Accumulation of fine-grained sediments in the Dutch Wadden Sea: Geologie Mijnb., Vol. 19, pp. 329-354, 1957.

Wolman, M. G., and J. P. Miller. Magnitude and frequency of forces in geomorphic processes: J. Geol., Vol. 68, No. 1, pp. 54-74, 1960.

VITA

John Daniel Boon, III

Born in Austin, Texas, January 29, 1940. Graduated from Arlington High School, Arlington, Texas, June 1958 and from Rice University, Houston, Texas, June 1962 (B.A., Geology). Attended University of Washington as a graduate student in oceanography, 1962-1963; received the M.A. degree in marine science at the Virginia Institute of Marine Science through the College of William and Mary, June, 1968.

The author served in the Commissioned Corps of the United States Coast and Geodetic Survey (presently the National Ocean Survey, National Oceanic and Atmospheric Administration) from 1963-1969; resigned in April 1969 at the rank of Lieutenant Commander to accept position of assistant marine scientist at the Virginia Institute of Marine Science.